ESCOLA POLITÉCNICA DA UNIVERSIDADE DE SÃO PAULO

ARTHUR KOJI NISHIKAWA

Structural Design of an Industrial Building with a Crane of 15 tons

A Comparison between Brazilian and German Design Codes

ESCOLA
POLITÉCNICA
DA USP

São Paulo
2017

ESCOLA POLITÉCNICA DA UNIVERSIDADE DE SÃO PAULO

ARTHUR KOJI NISHIKAWA

Structural Design of an Industrial Building with a Crane of 15 tons

A Comparison between Brazilian and German Design Codes

Trabalho de Formatura apresentado à
Escola Politécnica da Universidade de São
Paulo para obtenção da Graduação em
Engenharia Civil.

Área de Concentração: Engenharia Civil

Orientadores: Prof. Dr. Henrique Campelo Gomes
Prof. Dr.-Ing. Jörg Lange

ESCOLA
POLITÉCNICA
DA USP

São Paulo
2017

Catalogação-na-publicação

Nishikawa, Arthur Koji
Structural design of an industrial building with a crane of 15 tons A comparison between Brazilian and German design codes / A. K. Nishikawa -- São Paulo, 2017.
238 p.

Trabalho de Formatura - Escola Politécnica da Universidade de São Paulo. Departamento de Engenharia de Estruturas e Geotécnica.

1.ESTRUTURAS DE AÇO 2.NORMAS TÉCNICAS [COMPARAÇÃO] 3.PONTE ROLANTE I.Universidade de São Paulo. Escola Politécnica. Departamento de Engenharia de Estruturas e Geotécnica II.t.

Catalogação-na-publicação

Nishikawa, Arthur Koji
Structural design of an industrial building with a crane of 15 tons A comparison between Brazilian and German design codes / A. K. Nishikawa -- São Paulo, 2017.
238 p.

Trabalho de Formatura - Escola Politécnica da Universidade de São Paulo. Departamento de Engenharia de Estruturas e Geotécnica.

1.ESTRUTURAS DE AÇO 2.NORMAS TÉCNICAS [COMPARAÇÃO] 3.PONTE ROLANTE I.Universidade de São Paulo. Escola Politécnica. Departamento de Engenharia de Estruturas e Geotécnica II.t.

Acknowledgments

I would like to thank my supervisors, Professor Dr. Henrique Campelo Gomes and Professor Dr.-Ing. Jörg Lange, for having accepted me and for having offered all the support and assistance necessary for this project. I would also like to thank my family, who are the ones that were and will always be there for me.

Abstract

The focus of this project was to develop, from an already existing industrial steel hall with a crane, a study that would create models of two different structures from the existing one. This study involved dimensioning the structure according to two different design codes [the Brazilian code NBR (Norma Brasileira) by the ABNT (Associação Brasileira de Normas Técnicas – Brazilian Association for Technical Norms) and the German Norm DIN (Deutsches Institut für Normung e.V. – German Institute for Standardization)] using the software RSTAB from Dlubal. Both halls were modeled, each according to its respective Norm, and inspected in order to verify if they would still be statically stable, withstanding all of the loads applied to them. In the end, a critical analysis and comparison between both, Brazilian and German norms, was performed.

Keywords: Steel Industrial Structure; Comparison; Brazilian and German Norms; Crane

TABLE OF CONTENTS

1. INTRODUCTION

Engineering is a worldwide prestigious career. In every corner of the world, in every continent, in every country, engineering will always be one of the most important occupations. Of all the branches of this field, one that will never get old or surpassed is the civil engineering. There will always be a demand for civil engineers, being for their expertise in construction, planning or any of the other great capabilities they possess. Wherever a bridge must be made, whenever a highway must be planned, civil engineers are the ones to be sought. And it is because of this that every time a third-world country has the need to grow, these professionals are the first to be pursued.

Having this in mind, the Brazilian scenario emerges. A third-world country that has all the potential to arise as one of the most powerful nations in the world. A country that, not so long ago, was seen as one of the best countries to invest in, one that would grow exponentially in some years. As any undeveloped country, it has an immense lack of infrastructure. In spite of that, Brazil still continues to have an enormous potential and that is the reason why the pursuit for more industries and new and better technologies should never stop.

On the other side of the Atlantic lies Germany, a first-world country that has made progress in every part of science. From the electric industry to the automobile industry, Germany has achieved many technological breakthroughs. And one of the great technologies that Germany has to offer is its advancements in steel constructions.

The first building to use skeleton frame construction, as reported by Steel Business Briefing[1], the Home Insurance Building, was completed in 1883. This building had 10 floors and was the first iron-framed skyscraper. The first all-steel frame building was the Rand McNally building, erected a few years later. It also had 10 stories. Both skyscrapers were located in Chicago. Their constructions were particularly influenced by the Englishman Henry Bessemer, whose discovery of the Bessemer's Process[2] in 1856 provided an inexpensive industrial process for mass production of steel. Germany, with the Ruhr Valley[3] in the 1850s-1940s and Brazil, with the Carajás Mine[4] (the largest iron ore mine in the world), had/have excellent locations for the mining and production of iron and steel. Nowadays, Brazil is the 3rd largest iron ore producer in the world (428 million tons in 2015 – only after China and Australia) while Germany ranks at 32nd (450 thousand tons in 2015)[5]. For the production of raw steel, Brazil produces 34 million tons against 44 million from Germany (in 2015)[6]. This only proves that since Bessemer, steel productions, and in consequence steel constructions, have boomed in every part of the globe.

For decades, steel constructions have played an important role in developing societies. Not only do these constructions offer an aesthetically beautiful, strong and resistant structure, they also provide great benefits for the economy and society. Their use is broad and varied: sport halls and stadiums (leisure), bridges (effective transportation), skyscrapers (architecture and economy). In particular, the evolution of industrial steel buildings is especially noteworthy. As technology expanded at an accelerated pace, so did

[1] (Steel Business Briefing) – (01.02.2017)
[2] (Wikipedia 7) – (01.02.2017)
[3] (Wikipedia 4) – (01.02.2017)
[4] (Wikipedia 8) – (01.02.2017)
[5] (USGS - United States Geological Survey 2, 2016) and (Wikipedia 5) – (01.02.2017)
[6] (USGS - United States Geological Survey 1, 2016) – (01.02.2017)

the perception of this emerging field. Concomitantly with the technology boom, the minds of young architects and engineers blossomed with creativity and many steel constructions were built, that today are very famous and known all over the world. One of the most remarkable ones was the tower built by the French civil engineer and architect, Gustave Eiffel, presented at the 1889 World's Fair[7]. To this day, it is still regarded as one of the most memorable and fascinating monuments that still exist and it is known all over the globe. Two other very glamorous constructions that use steel that are not only alluring but also socially and economically interesting are the Allianz Arena[8] in Munich (FC Bayern München's Stadium) and the Allianz Parque[9] in São Paulo (SE Palmeiras' Stadium) which can have soccer matches as well as great concerts. Besides both having their naming rights belonging to the same company and being very charming, both are huge soccer stadiums that can not only accommodate more than 40,000 people (the Arena can admit almost double the amount: 75,000 people) but can endure the load (even from the jumping during the scoring of a goal) of all these people together. This is the true definition of usefulness and pleasure combined.

As steel becomes more interesting and more popular, so does the number of constructions around the world. Concomitantly, so must the regulations that control it. With the intention to prevent misfortunes, like the West Berlin Congress Hall Collapse in West Berlin, 1980 (due to a poor structural design that failed to address corrosion prevention) [10], the Magic Mart Roof Collapse in Bolivar, USA in 1983 (due to a severe weather event with a heavy rainfall, not common for the area, along with improper addition of roofing materials)[11] and the Bad Reichenhall Ice Rink Roof Collapse in Bad Reichenhall in the region of Bavaria, Germany in 2006 (due to heavy snowfall on its roof built in the 1970s)[12], specific Norms for the design and construction of steel buildings have been created and improved over time. The examples mentioned before include failures from corrosion, wind and rain, and snow. Another famous construction failure in Germany happened in Halstenbeck, when the sports hall "Knick-Ei"[13] collapsed twice: the first during severe weather in its construction phase and the second after it had already been built. This proves that not only must engineers be cautious of the actions that the constructions may suffer during its life-span, but also during its construction phase, when strong winds may damage the unfinished building. And even after countless modifications and improvements made on the Norms along the years, many failures and tragedies still occur to this day, like the Česká Třebová Sport Hall Collapse in the city of Česká Třebová, Czech Republic, on January 14, 2017 (with the causes being yet unknown[14] – but having a 25-cm of layer of snow on the roof before the accident, even though the arena designer affirmed that it was not the cause of the destruction)[15]. Contrary to some old collapses in the past, the wrecking of the roof was able to be caught on video and can be seen easily on the internet[16]. Although recently opened (the same month), the hall clearly had flaws. Figure 1, Figure 2 and Figure 3 show the moment when the players flee the court, when the roof gives in and a photo of the hall from the outside after the roof had collapsed. This is an indication that once again, even though Norms can be very strict, other variables must be taken into account, like imperfections

[7] (Mairie de Paris) – (01.02.2017)
[8] (Allianz Arena) – (01.02.2017)
[9] (Allianz Parque) – (01.02.2017)
[10] (Wiki Spaces 1) – (01.02.2017)
[11] (Wiki Spaces 2) – (01.02.2017)
[12] (Wikipedia 6) – (01.02.2017)
[13] (Wikipedia 3) – (01.02.2017)
[14] on February 1st, 2017
[15] (Telegraph) – (01.02.2017)
[16] (YouTube) – (01.02.2017)

of the manufactured beams or even human-fault (when the design and project are well done but the construction is done incorrectly).

Figure 1: Moment When Players Flee the Sports Hall in Česká Třebová[17]

Figure 2: Moment of the Roof Collapsing in Česká Třebová Sports Hall[18]

[17] (Telegraph) – (01.02.2017)

Figure 3: Česká Třebová Sports Hall After the Collapse of the Roof[19]

The best way to prevent such situations is to correctly dimension and build a hall. For most halls, the main component of the whole structure is the frame (a 2D model, meaning the transversal section of the hall). As Portal Met@lica[20] best describes, there are two basic types of frames for the halls generally used: with solid section or framework. The space between the columns and the distance between the frames are decisive factors for the choice of frame. Shorter distances between the frames will reduce the loads on each frame, but in turn will increase the number of frames and consequently the number of foundations. Longer distances will increase the secondary elements (like purlins) and decrease the number of foundations. The projects using solid sections are visually "cleaner", with fewer elements, have easier manufacturing, have faster assembly, have simpler maintenance but need more steel. This greatly impacts on the viability of a project, since the budget is normally the most important factor for the decision to build or not to build. However, it also has much less costs with execution, having the total costs close to the costs for the framework type for small and medium-sized halls. Withal, the hall should be adjusted in order to obtain a structure that best attends the specific conditions of the project. The original hall for this study had a frameworked type of hall.

Halls with cranes are an even more special type of hall. Although being more complex, since it requires supports along the hall for the wheels of the crane (at the end truck), it is commonly used in small and big industrial halls. The heaviest load is now the crane load, which must be resisted by the frames and also have its maximum deformations under the limit for the operation of the crane. The most frequent columns for a hall with crane(s) are: columns with console (a welded element on the column which will sustain the

[18] (Telegraph) – (01.02.2017)
[19] (Telegraph) – (01.02.2017)
[20] (Portal Met@lica Construção Civil) – (01.02.2017)

runway girder, also known as the beam under the crane rail) – for light loads, columns with different cross-sections (under the crane, the cross-section will be much bigger) – for medium loads and/or bigger heights, and a double-column, having them both attached by framework – for heavy loads. These types of halls are usually built for industrial purposes, in view of the heavy weight-lifting and transporting of machinery or other items. Frequent industries that require crane operations are shipyards, mining and even construction (for example: manufacture of steel beams).

Contemplating the aforementioned precautions engineers and architects must take during the development of the project, this study was elaborated with the purpose of investigating possible actions that would act upon an industrial steel hall with a crane operation according to two different Norms and critically analyze and compare how the actions would affect the building. In addition, there was also the desire of triggering the interest as to how different or similar would the two Norms be. The Norms were the Brazilian code NBR (Norma Brasileira) by the ABNT (Associação Brasileira de Normas Técnicas – Brazilian Association for Technical Norms) and the German Norm DIN (Deutsches Institut für Normung e.V. – German Institute for Standardization). In this context, this comparison could even lead to observations for improvement, pointing out strengths and weaknesses of the sections of the Norms.

1.1 Objectives

In a globalized world, exchange of information is inevitable and essential to everyone. In view of this, and with the knowledge that the search for different and better technologies should be continuous, this project seeks to compare and analyze the dimensioning methods between the Brazilian Norm NBR (Norma Brasileira) by the ABNT (Associação Brasileira de Normas Técnicas – Brazilian Association for Technical Norms) and the German Norm DIN (Deutsches Institut für Normung e.V. – German Institute for Standardization). The object of the study will be an industrial steel hall with a crane.

As a starting point, an existing industrial steel hall was taken as a model/reference (seen in Figure 7 and Figure 8). From this model, 2 new models were elaborated and an analysis of the main structural components according to both, the Brazilian and German Design Codes, was performed. This analysis included verifications such as computing the loads and their combinations according to each of the mentioned design codes. The numerical model and verifications were performed by the RSTAB software (see Section 1.2 Software RSTAB) from the company Dlubal. Further, the member's section sizes should be chosen according to each country's commercial standardization.

The intention of this project was to identify similarities and discrepancies in a building designed using the Brazilian or the German design codes. In addition, there is a special interest on the reasons that can lead to some differences on the final result.

Furthermore, it is expected, throughout this process, to enhance the knowledge on a subject that is particularly very interesting to, not only the author, but also any other structural engineer involved in the area of steel constructions. At the end, a critical analysis regarding the norms and their comparison was also realized.

1.2 Software RSTAB

The program that was used for the simulation of the structure of the industrial steel hall and the load forces that act upon it is called RSTAB. RSTAB is a software developed by the company Dlubal that can create three dimensional models of structures and input loads on them. These structures can be from different materials, such as steel (see Figure 5), timber (see Figure 6) and concrete. Additionally, the software already includes standard commercial cross-sections from many different norms worldwide (example seen in Figure 4). The loads can be not only input, but also the Wind and the Snow Loads can be calculated by the German Norm according to the structure presented.

After the structure and loads are modeled, the program can be run and the structure's deformations (also depicted in Figure 5) and points of failure can be found. Subsequently, if there is a necessity of remodeling the structure, it can be done and when all required changes are made, the program would be run again. This process can be done until the best solution for the respective structure is achieved.

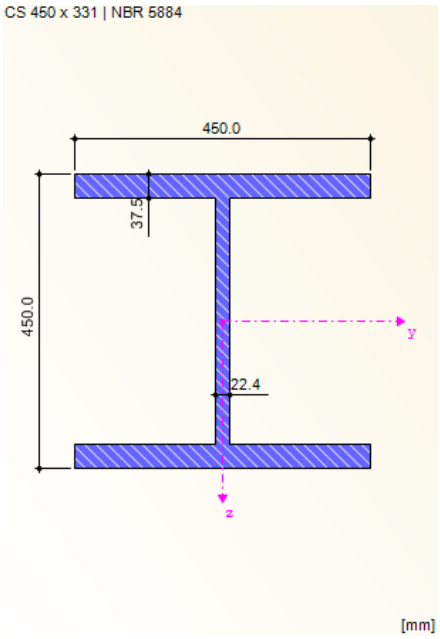

Figure 4: Example of a Steel Cross-Section (CS 450 x 311) from the NBR included in the Software RSTAB

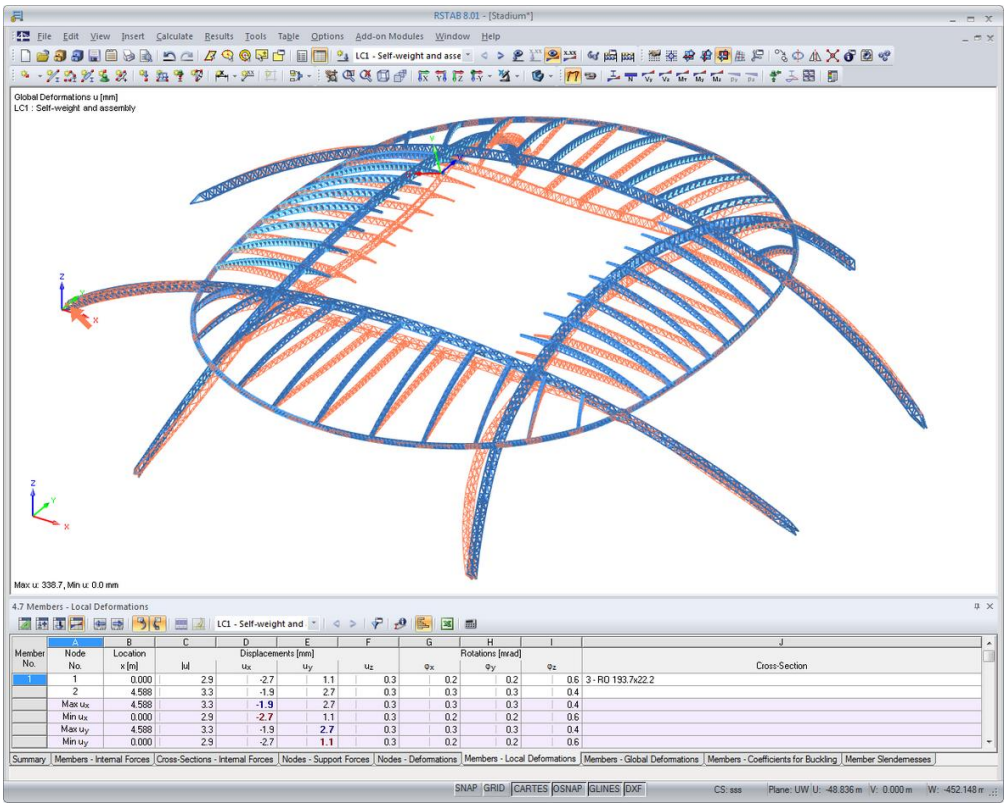

Figure 5: Example of a Steel Construction modeled by the Software RSTAB[21]

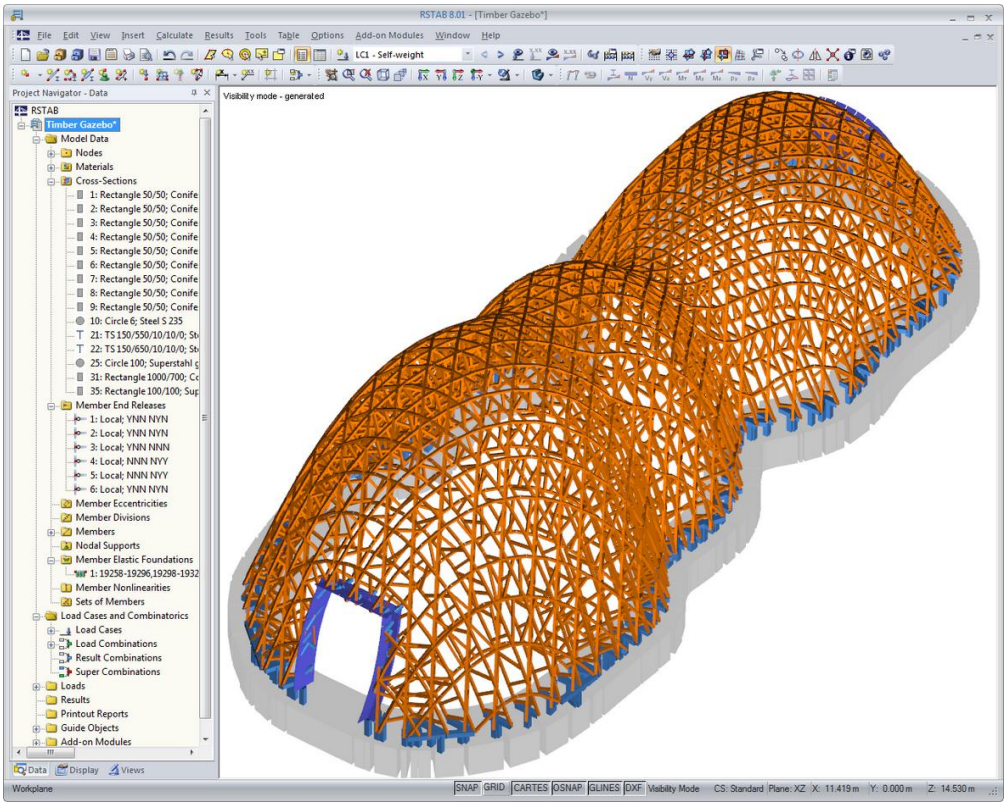

Figure 6: Example of a Timber Construction modeled by the Software RSTAB [22]

[21] (Dlubal) – (01.02.2017)
[22] (Dlubal) – (01.02.2017)

1.3 Literature Research

The discovery of the Bessemer process made it possible for the steel to be produced in mass quantities at an inexpensive cost, in comparison to how it was made at the time. From this process, the steel industry flourished. From pans to buildings, steel revolutionized the modern age for its unique characteristics. The development of techniques and methods of construction offered new options and different styles of structures, in contrast to the traditional ones. Even for halls typically used for industries, there are different manners of building them, although they are frequently very similar to one another, since aesthetics is not the main focus of this kind of project.

As Ackermann[23] presents in "*Industriebau*" (1984), industrial construction has a vast history and many different types of structures are often used in the design of industrial buildings. Models – in 2D (represented by the frames) and 3D – are made from these designs in order to better understand and work with them. The steel halls have many uses and offer a variety of advantages, which include: extensive, column-free space; simple corrosion protection (usually); fast assembly and disassembly capacity; extensive recovery of the steel after expiration of the utilization period; low transport volume and relative simple assembly possibilities (in comparison to reinforced concrete); lightweight design; high material resistance that allows dynamic stresses; high adaptability, in comparison to other construction methods, especially with concrete; and that after the assembly of the building and also during its usage, alterations in the structural concept may be implemented at relatively low cost. These reasons show how beneficial constructing with steel can be.

There were two sites that provided updated information for the weather loads. The site for the "*Deutsches Insitut für Bautechnik (DIBt)*"[24] (2015) provides Excel tables for the wind zones and snow zones in Germany. These tables contain data for each state and, in the case of the snow zone for Hesse, a classification for each city. This site from Schmidt[25] is extracted from the 21st edition of the book *Bautabellen für Ingenieure - mit Berechnungshinweisen und Beispielen*. It is the entire section on wind loads, which was used to generate the diagrams and tables for the determination of the wind's influence.

In "*Praxisbeispiele für Einwirkungen nach neuen Normen*" (2007), Bucak, Seiler, Seeßelberg et al.[26] present examples of the influence of the actions of loads according to the new Norm (ex: DIN 1055). Examples include those from wind and snow loads to crane loads, and structures from steel halls to the construction of roads. The loads, especially the Additional Dead Load and the Crane Loads were determined with the aid of this book.

In Buttner & Stenker's[27] book "*Stahlhallen: Entwurf und Konstruktion*" (1986), there are many details on construction and elaboration of the static systems of the frames and halls, stabilization, frame design due to cranes, with its examples (with graphics) and structural designs of existing steel hall projects. Also, "*Stahltragwerke im Industriebau*" (2010) from Pasternak[28] offered similar ideas for the static system to be used. Furthermore, details for the crane and for the dimensioning of the runway girder can be found in the

[23] (ACKERMANN, 1984)
[24] (Bautechnik, 2015)
[25] (SCHMIDT, 2014)
[26] (BUCAK, SEILER, GEBHARD, HAUSSER, MAINZ, & SEEßELBERG, 2007)
[27] (BÜTTNER & STENKER, 1986)
[28] (PASTERNAK, HOCH, & FÜG, 2010)

book. These concepts offered a deep understanding of the importance of how a correct static system must be chosen for the objective of a project and how the choice affects the whole realization of the project.

Literally a must for engineers who wish to build a steel hall in Brazil, Drehmer, Mesacasa Júnior & Pravia's[29] "*Manual de Construção em Aço: Galpões para Usos Gerais*" (2010) gives an introduction to each component of a steel hall to which then becomes, as its title would suggest, a manual on how to build a steel hall for general use. This step-by-step was essencial for the elaboration of the Brazilian part of the project, since the example given in the manual must undergo the (almost all of the same) verifications as the one in study. Even though the halls very different (dimensions, wind speeds, type of frames etc) the step-by-step was, along with the NBR 6123 and the NBR 8800, fundamental for the conclusion of the thesis.

The article "*Hallen aus Stahl: Planungsleitfaden*" (2015) from Grimm & Kocker[30] describes numerous structures already built and their designs. In addition, there are explanations for the differences between frames and support-girder systems (*Stützen-Bindern-System*), with many examples, and reasons in favor of a construction of this type. Since the original construction was made of a column and a truss system, it was interesting to learn that there are many different variations to the 2 basic forms of the frame.

"*Stahl- und Verbundkonstruktionen*" (2012) was a very inspirational book. In it, Kindmann & Krahwinkel[31] detailed how to design and construct a steel hall. The information ranged from how many and how to layout wall rails (*Wandriegeln*) and purlins through to which types of frames and frame corners to use. Moreover, specifications for the construction of framework, cross sections, frame stanchions, gables, wall and roof bracings (*Wand- und Dachverbände*) and runway girders and consoles were also included.

In "*Musterstatik: 15 x 60 x 5 m³ Stahlhallenkonstruktion aus warm gewalzten Profilen*" (2012) from Kocker[32], the usual loads from the German Norm that would be applied to a hall were introduced and a model hall (using the software RSTAB) was designed and calculated. The results were also available. In addition, there were verifications for the connections and the foundation.

"*Baukonstruktionslehre 5: Sanierungen, Ferigteilbau und Fassaden, Industriehallen*" (2012) from Riccabona & Mezera[33] presented some static systems, details about different systems and details for designs of the frame corner. There were also some details about different types of roofs, to comprehend if the choice of the German roof was acceptable. Likewise, the article "*Dach- und Wandkonstruktionen aus Stahl*"[34] (2015) contains information about roof and wall constructions made of steel. It provided support for selecting the steel profiles and also more details about composite (sandwich) elements. An example of how the planning and execution should be conducted is also included. Both assisted in the choice for the roofing.

It is no surprise that the Brazilian Norm is very similar to the American Norm. The Brazilian Norm is an adaptation of the American Norm, and that is the reason why they are not only very similar but almost identical. For a better understanding of structures made of steel and their behavior, "*Steel Structures Design and Behavior*" (2009) from Salmon, Johnson & Malhas[35] is a most recommended book on the

[29] (DREHMER, MESACASA JÚNIOR, & PRAVIA, 2010)
[30] (GRIMM & KOCKER, 2011 (Aktualisierte Ausgabe 2015))
[31] (KINDMANN & KRAHWINKEL, 2012)
[32] (KOCKER, Musterstatik: 15 x 60 x 5 m³ Stahlhallenkonstruktion aus warm gewalzten Profilen, 2014)
[33] (RICCABONA & MEZERA, 2012)
[34] (TICHELMANN, WELLAN, & WERKMEISTER, 2015)
[35] (SALMON, JOHNSON, & MALHAS, 2009)

subject. It is elaborated in such a way to facilitate its readers' comprehension on a not so simple theme. The book aided in the assimilation of specific technical terms (vocabulary) and to better interpret the brazilian norm which, as most of the norms worldwide, is not easy to understand.

Ruga's[36] article "*Sporthallen aus Stahl: Planungsleitfaden*" (2013) contained explanations of how and why a sport hall should be planned. From the beginning, it informs which aspects are to be taken into account, such as the production (*Fertigung*) and assembly (*Montage*). It does not, however, take into account the loads deriving from the crane. It was an exceptional way for better understanding how a sport hall project differs from an industrial hall and how very important subjects like production and assembly of the elements (beams, purlins etc) affect the project. Although these informations were not correlated to the objective of the study, it was important to realize how other features of the project may affect more than only the total weight of the hall.

The site "*Exercício Cargas na Estruturas*" (2015) from Santiago[37] summarizes how loads would affect and influence structures. There are definitions of the different types of loads and from these definitions, the information that the snow loads are not included in the Brazilian norm NBR from ABNT was confirmed.

The book "*Kranbahnen: Bemessung und konstruktive Gestaltung*" (2005) by Seeßelberg[38] encompasses detailed explanations about everything related to cranes. For example, it includes the selection of the type of crane, the dimensioning of the hall and crane according to the loads, and influences of the construction on the entire crane system. In this study, the information of the crane was already given by the original project. Nonetheless, this book allowed a gain of knowledge on how a hall should be pre-dimensioned depending on the weight of the lifting load and the dimensions. His article "*Zum Entwurf von Kranbahnträgern für Laufkrane*"[39] (2005) can also be read since it is a simplified and shorter version of the book. Along with Seeßelberg, Von Berg's[40] book "*Krane und Kranbahnen: Berechnung, Konstruktion und Ausführung*" (1989) also had theoretical explanations about the selection of the appropriate type of crane for the designated type of industrial hall observed in this project. Furthermore, it presents the formulation of the influences due to the crane and its analysis. However, its analysis and verifications are all in accordance to the old norm. Both books were very educational.

[36] (RUGA, 2010 (erweiterte Ausgabe 2013))
[37] (SANTIAGO, 2015)
[38] (SEEßELBERG, Kranbahnen: Bemessung und konstruktive Gestaltung, 2005)
[39] (SEEßELBERG, Zum Entwurf von Kranbahnträgern für Laufkrane, 2005)
[40] (VON BERG, 1989)

2. PREMISES

2.1 Dimensions of the Hall

The building has nine single bay frames spaced by 6 meters each, resulting in 48.0 meters on its longitudinal direction (see Figure 8). On the transversal direction, the spam between columns is 19.80 meter long (see Figure 7). The columns have different cross sections along its height (10.40 m until eave), being stiffer up to the runway girder level (6.064 m). The roof, in turn, is supported by a truss type structure.

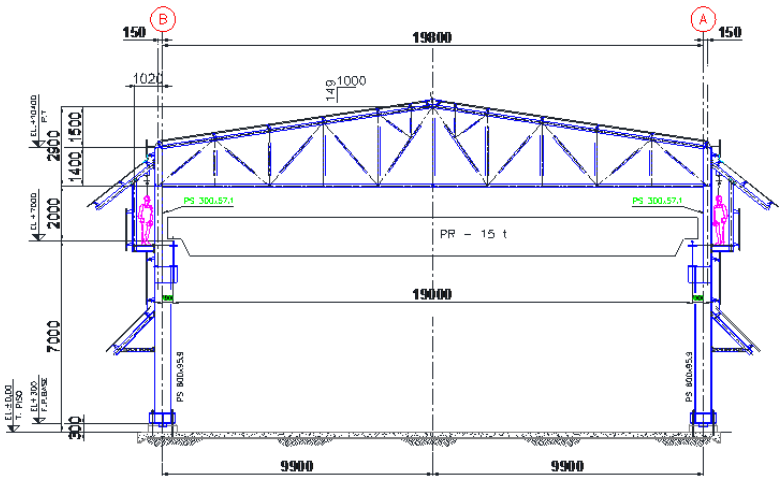

Figure 7: Design of the Existing Industrial Hall (Front)

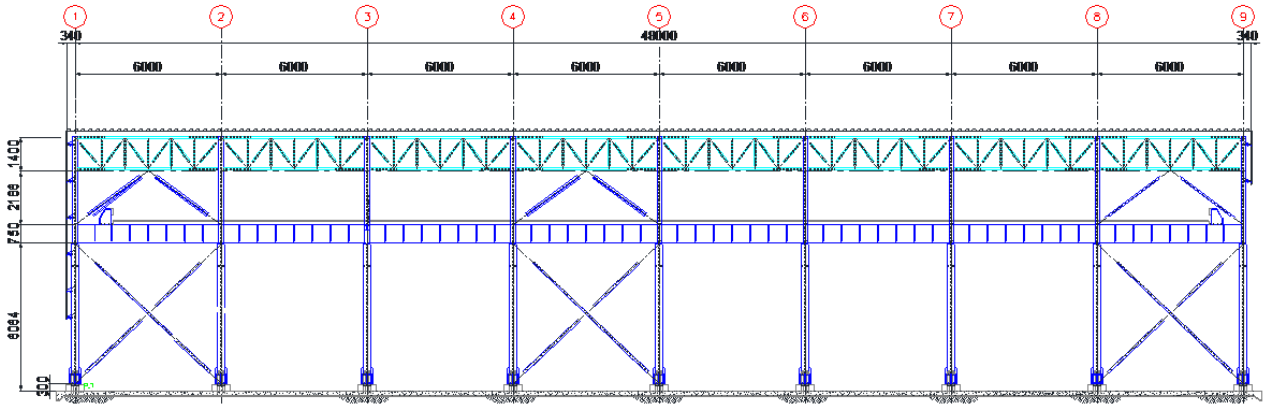

Figure 8: Design of the Existing Industrial Hall (Side)

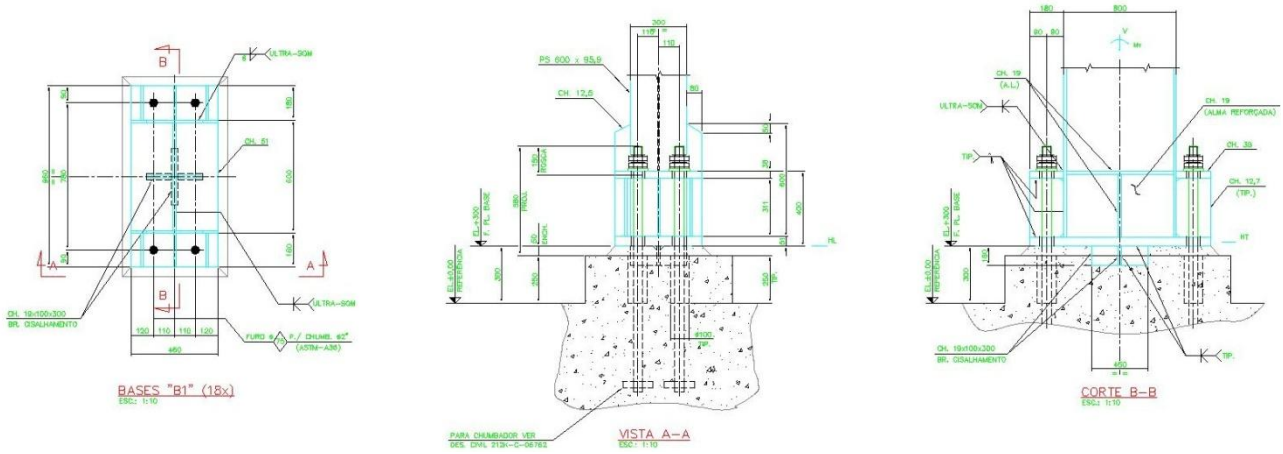

Figure 9: Details of the Connection between the Columns and the Foundations

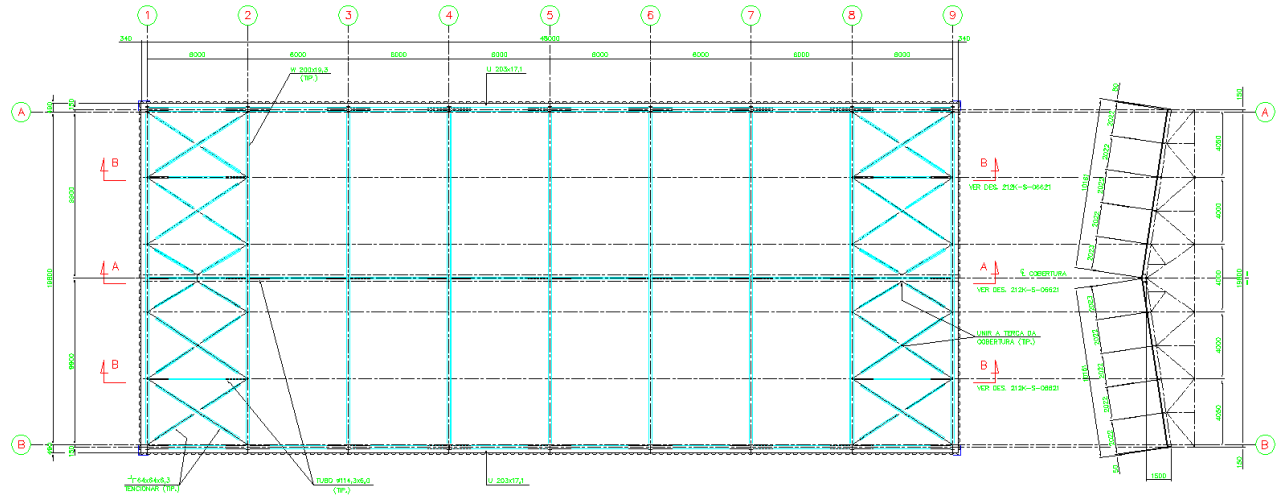

Figure 10: Upper Part of the Truss System (Connected to Purlins)

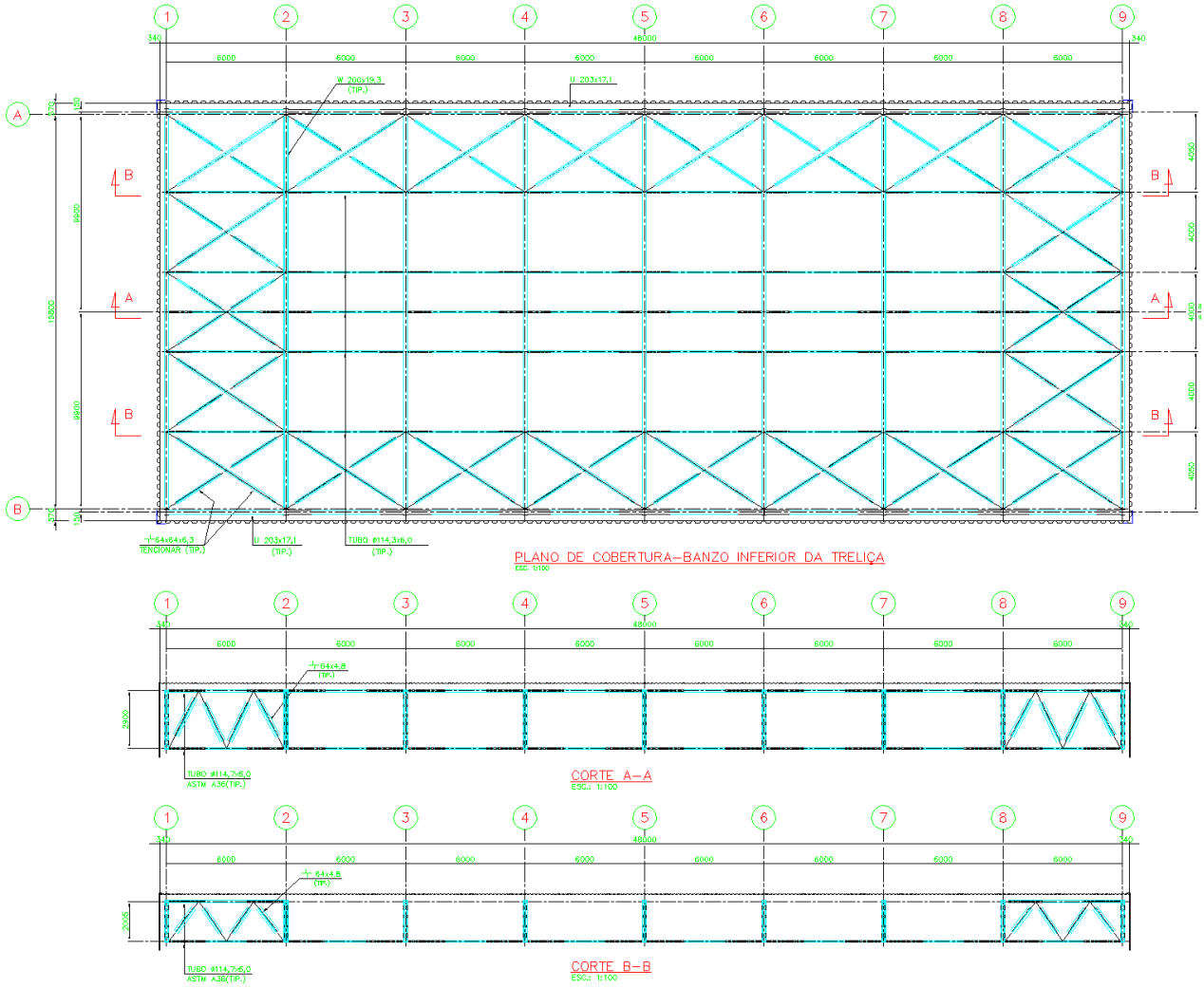

Figure 11: Lower Part of the Truss System

2.2 Location

2.2.1 Brazilian Location

The location of the aforementioned structure is São Luís, Maranhão, Brazil (Figure 12 and Figure 13). The city of São Luís is the largest city of the state of Maranhão and is also the capital of that same state. It is located on the Ilha de São Luís (Saint Louis' Island) in the Baía de São Marcos (Saint Mark's Bay). The exact coordinates for the construction site are 2°35'54.61'' south and 44°19'5.247'' west. According to a 2016 IBGE estimate, the city has a population of 1,082,935 people, whereas the metropolitan area has 1,605,305 people, ranking the 15th largest city in Brazil[41].

The construction site is located in an industrial area on the outskirts of the city.

Figure 12: Location of the city of São Luís in the state of Maranhão, Brazil [42]

[41] All data from this paragraph retrieved from (Wikipedia 1) and (Wikipedia 2) – (01.02.2017)
[42] (Wikipedia 2) – (01.02.2017)

Figure 13: Zoomed in location of the city of São Luís [43]

2.2.2 German Location

For the calculations of the German design codes, the structure was presumed to be situated in Darmstadt, Hesse, Germany. The area would also be an industrial one.

Figure 14: Location of Darmstadt on the map of Germany[44]

[43] (Weather Forecast) – (01.02.2017)

Figure 15: Location of Darmstadt on a map of Hessen[45]

2.3 Construction State Calculations

For our modeling and analysis purposes, the structure was studied in its final state, not during its assembly state. Since the incidence and value of some of the loads could vary and thus modifying the main purpose of the case in study, it was determined that the analysis would be based solely on the calculations on the final state.

2.4 Seismic Loads

Since São Luís is located in an earthquake free zone, seismic activity is not considered to be a substantial threat and its addition to the calculation could be neglected[46]. Further, Darmstadt is also not located in a seismic area, indicating that the earthquake calculations could also be disregarded.

[44] (Türkiye Rehberi) – (01.02.2017) (Adapted)
[45] (Wikimedia Commons) – (01.02.2017)
[46] (G1 Globo, 2017) – Although neglected, a 4.7 (Richter Scale) magnitude tremor was felt in the state of Maranhão on January 3rd, 2017. Nonetheless, these tremors are rare and do not pose great threat to infrastructure, as stated in the site.

2.5 Column Foundation

The foundations of the columns were all originally rigid (transversal) in the X-Direction (or XZ plane – transversal direction of the hall) and articulated (longitudinal) in the Y-Direction (or YZ plane – longitudinal direction of the hall) and were so considered and none of the connections between the columns and the foundations were to be verified (not in the scope of this project).

2.6 Material and its Characteristics

In line with the assignment, the material used was steel. The resistance of the steel (or yield stress) was designated as 23.5 kN/cm² (S 235) or 35.5 kN/cm² (S 355 N) for the German design code and as 25 kN/cm² (ASTM A-36) or 34.5 kN/cm² (ASTM A-572) for the Brazilian design code (however, the software RSTAB does not have the ASTM A-36 or the ASTM A-572 material, and therefore, the material MR250 and G-35 were used as substitutes, due to the their similar values of resistance, respectively). Since the resistances are approximate, the comparison was found to be plausible. This difference would affect the final result, but this factor would be remembered. From this, the German material properties[47] were obtained:

- **Yield Resistance (or Yield Strength):**
  - For S235:
    - For width $t \leq 40\ mm$: f_y = 235 N/mm²
    - For width $40\ mm < t \leq 80\ mm$: f_y = 215 N/mm²
  - For S355 N:
    - For width $t \leq 16\ mm$: f_y = 355 N/mm²
    - For width $16\ mm < t \leq 40\ mm$: f_y = 345 N/mm²
    - For width $40\ mm < t \leq 63\ mm$: f_y = 335 N/mm²
- **Tensile Strength (or Tensile Resistance):**
  - For S235:
    - f_u = 360 N/mm²
  - For S355 N:
    - f_u = 470 N/mm²
- **Modulus of Elasticity (or Young's Modulus):** E = 210.000 N/mm²
- **Poisson's Ratio:** ν = 0.30
- **Shear Modulus (or Modulus of Rigidity):** $G = \frac{E}{2(1+\nu)} = 81.000$ N/mm²
- **Density:** ρ = 7850 kg/m³
- **Coefficient of Thermal Expansion:** α_T = 0.000012 K^{-1} (for $T \leq 100\ °C$)

[47] (SCHNEIDER, 2012) – Table 3.4a and Table 8.4b

The Brazilian material properties[48] were very similar to the German:

- **Yield Resistance (or Yield Strength):**
  - For width $t \leq 200\ mm$[49]: f_y = 250 N/mm² (ASTM A-36)
  - For width $t_f \leq 37.5\ mm$[50]: f_y = 345 N/mm² (ASTM A-572)
- **Tensile Strength (or Tensile Resistance):** f_u = 400 - 550 N/mm² (ASTM A-36) and 450 N/mm² (ASTM A-572)
- **Modulus of Elasticity (or Young's Modulus):** E = 200.000 N/mm²
- **Poisson's Ratio:** ν = 0.30
- **Shear Modulus (or Modulus of Rigidity):** $G = \frac{E}{2(1+\nu)} = 77.000$ N/mm²
- **Density:** ρ = 7850 kg/m³
- **Coefficient of Thermal Expansion:** α_T = 0.000012 K^{-1} (for $T \leq 100\ °C$)

[48] (ABNT NBR 8800, 2008) – Section 4.5.2.9 Page 13
[49] (ABNT NBR 8800, 2008) – Table A.2 Page 109
[50] (ABNT NBR 8800, 2008) – Table A.2 Page 109

3. ANALYSIS OF LOADS

For the conception of the load forces for halls with cranes, it is usual to consider three actions. The first are the permanent (dead) loads:

- Self-Weight of the structure, which in this case is specifically only made of steel.
- Additional Dead Loads

Second, there are the non-permanent forces, which comprise:

- Wind
- Snow
- Live Loads (including the "*Ação Acidental*")

As a European Norm, the DIN EN takes into account the Snow Load [Remark: the ABNT applied norm NBR used in Brazil only examines the Wind action and has no reference for Snow Loads[51]]. For wind, many variables have to be taken into account, such as the geometry of the building, location of the construction site, etc.

Third, the actions resulting from imperfections must be studied. Any manufactured steel product has a slight probability of having an imperfection due to deformations. For example, a beam may not always be totally straight as it is planned to be and this imperfection is considered during the calculation of the forces that influence each member of the structure. These imperfections are important, on account of the Second Order Theory. The First Order Theory states that a straight and untwisted bar without deformations will be considered approximately as a beam element and the forces balance themselves. The Non-Linear Theory (or Second Order Theory) affirms that a deformed bar is considered as a beam element, however the mathematical model is to be linearized. It is necessary to solve stability problems, when compression on the beam occurs. Due to the deformation (pre-existing or after the assembly), the pressure on the beam can cause unwanted extra deformation and, ultimately, lead to the failure of the member, causing it to break down. The imperfections are given in more detail in the Section 5.6.5, Section 6.1.2 and Section 6.2.2.

Lastly, some considerations were to be taken into account. The hall was considered to be enclosed by walls and a roof. There were openings on the sides that could affect how the wind would influence the structure, and a front and a back door. The wind would have an impact (originating from the external wind pressure and from the internal wind pressure) on the walls and the roof (pressure and suction, see Section 3.1.4.3.1 b) External Pressure Coefficient) that would then act upon the steel construction by the means of linear loads (only on the purlins – from roof – and columns – from walls). Despite the fact that the hall would have some windows, these do not interfere with the calculations and determinations of the other loads. Another point to be recognized was that since the hall had openings, it could not be temperature-controlled, which in this case would prevent temperature-induced deformations[52] (due to great temperature variation) and subsequent generated loads. These deformations and resultant loads occur particularly when the column supports are rigid. However, since the location of the original project does not take this into account (the average temperature does not vary much – see Section 9.1), these possible occurring loads were neglected. In spite of the steel hall having articulated supports in the longitudinal

[51] (SANTIAGO, 2015)
[52] (PASTERNAK, HOCH, & FÜG, 2010) – Figures 3.8 – 3.10 and Pages 78 – 80

direction and the forces provoked also being greatly reduced in this direction, they are always an important factor to be considered, when designing steel constructions.

3.1 German Design Codes

3.1.1 Self-Weight

The program RSTAB determines the dead weight (or own weight) of the structure on its own, in agreement with whichever beams were utilized for its construction in the program. Additionally, it does not consider some components. These components may include the weight of the painting, of the corrosion protection, of the pieces used for the connections between the beams and even the weight of the pieces for the connection of the beams with the seating. Such pieces consist of screws, bolts or even a cap plate.

Therefore, the dead weight factor of the structure was amplified by 10%[53], modified from 1.00 factor to a 1.10 factor (on the Z-axis – the "floor-to-sky" axis).

3.1.2 Additional Dead Load

The additional dead load is also considered to be a permanent self-weight load. This additional load is composed of the roof covering: beddings – for example trapezoidal profiles, coatings (such as heat insulation, vapor barrier etc) and any other secondary finishing. In the case studied, however, since the RSTAB model did not include the models of these additional self-load components, their weight (in other words, of the whole roof) was represented by a linear load along the purlins.

Insomuch as the inclination of the roof is approximately 8.6°, a single-skinned insulated steel trapezoidal sheeting roof with sealing was chosen. To simplify the calculations, the following weights were assumed:

- 2 layers of sealing: 0.14 kN/m²
- 10 cm of rigid foam: 10 cm * 0.01 kN/m²/cm = 0.10 kN/m²
- Vapor barrier: 0.07 kN/m²
- Trapezoidal sheet T 50.1 with t = 0.88 mm: 0.09 kN/m²

The sum of the roof covering was 0.40 kN/m².

Because the coating of the wall has a very low self-weight (example: a sandwich wall product "Hoesch Isowand vario", from the manufacturer Hoesch Bausysteme GmbH, with a width of 10 cm, is only 0.14 kN/m²) in relation to the other vertical forces (dead load of the steel constructions) and that generally, this weight is transferred directly to the ground, the additional dead load of the wall was not considered for the construction of the model.

[53] For truss-type structures it is common to add 10% and in solid sections, 7%.

Similarly, the forces caused by lighting, which would eventually illuminate the hall's interior, as well as wires used for electricity were not considered in the modeling, due to their low self-weight in comparison to the other aforementioned additional dead loads.

3.1.3 Live Loads

The live loads involve mainly the traffic of people and of the crane. In keeping with the project aims, for the calculations of the final state, the loads concerning the traffic of people were not included, due to the fact that there would be no forces created by people along the roof or along the columns. In cases of maintenance, these forces are usually also not considered, because the snow loads are already larger than any traffic load, caused by persons, which would occasionally appear. Since our study does not have any snow load (see Section 3.1.5), an additional load "*Ação Acidental*"[54] can be applied to the roof (0.50 kN/m²) – see Section 3.2.3.

3.1.4 Wind Loads

According to Schneider[55], common residential, commercial or industrial buildings with a height lower than 25 m and constructions that are similar in form are considered to be not susceptible to oscillation (by the wind). In this case, the calculation of the oscillation factor will not be considered, since the building has a height of 11.9 m (lower than 25 m).

3.1.4.1 Velocity Pressure ("Geschwindigkeitsdruck") – Dynamic Pressure

According to the DIN Norm[56] (see also Schneider[57]), the city of Darmstadt, located in the state of Hesse, Germany, is positioned inside the wind zone number 1 (see also Figure 16). To be exact, the DIBt (Deutsches Institut für Bautechnik) internet site[58] was consulted and the wind zone checked in the downloadable table for "Windzonen". Part of this table can be seen in Table 1. In addition, the terrain category was defined as category III, as can be confirmed in Figure 17. Terrain Category III includes the suburbs, trade and industry locations – exactly where the site for the hall was planned to be, – as well as forests.

[54] In the original Project, the load "Ação Acidental" was considered for the dimensioning of the hall
[55] (SCHNEIDER, 2012) – Section 4 Page 3.23
[56] (DIN EN 1991-1-4 NA, 2010) – Annex NA-A Page 14
[57] (SCHNEIDER, 2012) – Table 3.24a
[58] (Bautechnik, 2015)

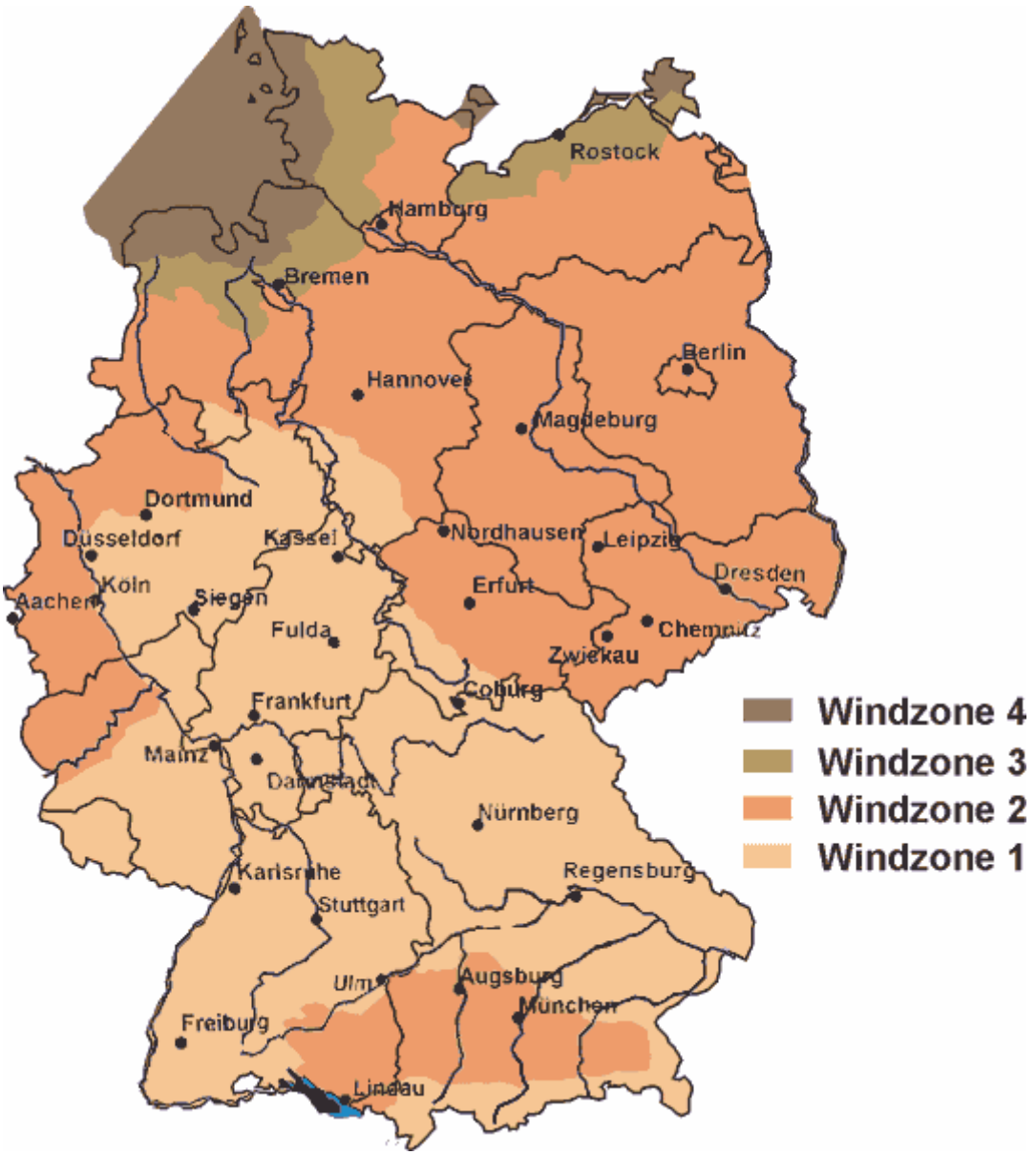

Figure 16: Map of Germany[59] representing the Areas of each Wind Zone (1 to 4) in conformity with DIN Norm Annex[60]

	6 Hessen		
6.1	**Hessen**	Windzone 1	alle Gemeinden

Table 1: Table for the Wind Zone for the Cities in the State of Hesse[61]

[59] (Renewable Energy Concepts)
[60] (DIN EN 1991-1-4 NA, 2010) – Annex NA-A Page 14
[61] Table downloadable at: (Bautechnik, 2015)

Figure 17: Terrain Category according to DIN Norm Annex[62]

[62] (DIN EN 1991-1-4 NA, 2010) – Annex NA-B Page 15

As a fixed value, the norm offers:

$$v_{b,0} = 22.5\frac{m}{s}$$

where $v_{b,o}$ is the basis wind speed. These numbers were empirically calculated as the middle values for a 10 meter high plane, over an open terrain, in a period of 10 minutes, with a yearly excess probability of 0.02.

Other factors taken into consideration for the estimate of the wind are:

- C_{dir} : Direction Factor, which in the NA is equal to 1.0.
- C_{season} : Seasonal Coefficient, which in the NA is equal to 1.0.

As such, the equation for the new basis wind speed v_b is the simple product of all three:

$$v_b = C_{dir} * C_{season} * v_{b,0} = 22.5\frac{m}{s}$$

The next variable to be calculated is the basis pressure speed q_b :

$$q_b = \frac{1}{2} * \rho * {v_b}^2 * 10^{-3}$$

with ρ being the density of the air in kg/m³ (ρ = 1.25 kg/m³ at a 1013 h Pa air pressure and a temperature of 10 °C at sea level).

From this equation, the basis pressure speed is (for buildings with height between 7m and 50m[63]):

$$q_b = 0.3164\frac{kN}{m^2}$$

$$\mathrm{q_p} = 1.7 * \mathrm{q_b} * \left(\frac{z}{10}\right)^{0.37} = 1.7 * 0.3164 * \left(\frac{11.9}{10}\right)^{0.37} = 0.5736\frac{kN}{m^2}$$

Since the height of the hall is lower than 25 meters and between 10m and 18m, the basis pressure speed (or velocity pressure, according to Schneider[64]) could have been facilitated into only one value for the velocity pressure:

$$q_p = 0.65\frac{kN}{m^2}$$

However, since the Brazilian Norm had a wind velocity pressure (dynamic pressure) result of 0.4856 kN/m² (see Section 3.2.4.3), and the software calculated this pressure as 0.53 kN/m² (see Section 5.3.2), for a better comparison (the closest values), the smallest of all 3 velocity pressure values (of all 3 calculated by the German norm) was kept:

$$q_p = 0.53\frac{kN}{m^2}$$

[63] (SCHNEIDER, 2012) – Table 3.26a
[64] (SCHNEIDER, 2012) – Section 5.3 and Table 3.25 Page 3.25

3.1.4.2 External and Internal Pressure from Wind

First, the external pressure (Schneider[65]) was calculated. Later, the internal pressure (see Section 3.1.4.4) was calculated.

As shown in Figure 7 and Figure 8 in Section 2.1 Dimensions of the Hall, the columns have a height of h = 10.40 meters until the eave (at the top of the ridge, h = 11.90 meters) and a width of d = 19.80 meters, while the length is b = 48 meters. The total height of the structure was considered during calculations to be the highest, until its top point in the middle, 11.90 meters. The angle between the columns and the roof is approximately α = 8.6°.

According to Schneider[66], the wind pressures w_e and w_i, external pressure and internal pressure, respectively, are calculated by:

$$w_e = q_p * c_{pe}$$

$$w_i = q_p * c_{pi}$$

with c_{pe} as the aerodynamic coefficient for the external pressure and c_{pi} as the aerodynamic coefficient for the internal pressure.

3.1.4.3 Influence of the External Pressure

3.1.4.3.1 Vertical Walls with Rectangular Layout of the Building

a) Direction θ of Influence of the External Pressure

The directions of the wind are divided into 2 categories:

1. the θ = 0° or θ = 180°;
2. the θ = 90°

where θ indicates the angle of incidence of the wind on the walls of the building. It is determined that when θ = 0° or when θ = 180° the wind is acting directly upon the side where the length of the hall is shorter. In this case, when θ = 0° or θ = 180°, b = 19.8 meters, as seen in Figure 18. Subsequently, when θ = 90°, b = 48 meters, as seen in Figure 19. The sides where the wind is not acting directly upon them were considered to have the length d.

[65] (SCHNEIDER, 2012) - Section 7.2 Page 3.28
[66] (SCHNEIDER, 2012) - Table 3.28a

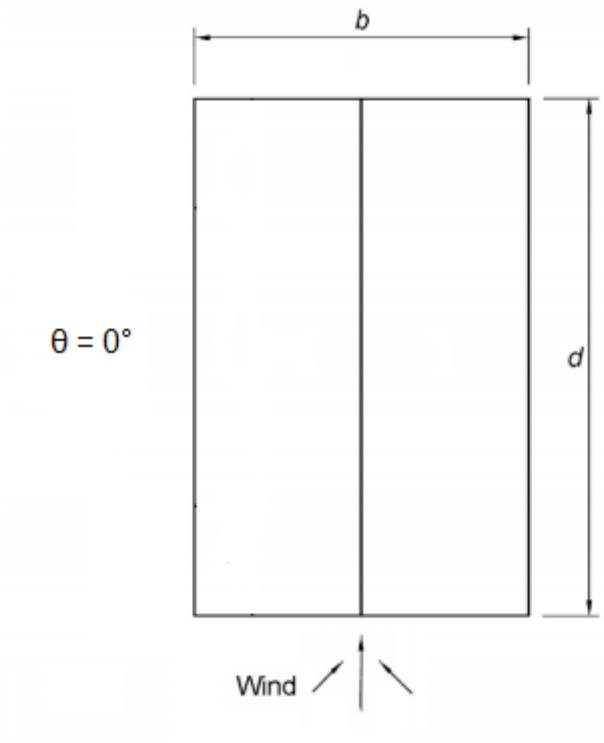

Figure 18: Angle of Incidence of θ = 0° of the Wind on the Structure

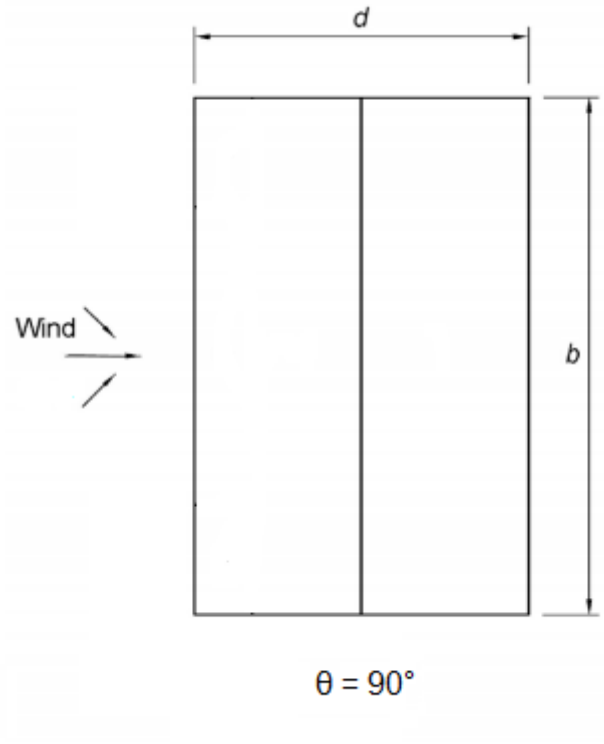

Figure 19: Angle of Incidence of θ = 90° of the Wind on the Structure

b) External Pressure Coefficient

As stated in Schneider[67] Table 3.28b, the external pressure coefficient c_{pe} is determined by the areas of Influence of the wind pressure:

If $A \leq 1\ m^2$, then $c_{pe} = c_{pe,1}$

If $1\ m^2 < A \leq 10\ m^2$ then $c_{pe} = c_{pe,1} - (c_{pe,1} - c_{pe,10}) * \log A$

If $A > 10\ m^2$ then $c_{pe} = c_{pe,10}$

Due to the fact that the whole structure is being measured, the external pressure coefficient c_{pe} will be $c_{pe} = c_{pe,10}$ where $c_{pe,10}$ is the coefficient of external pressure on areas of 10m² or more.

The sign of the external pressure coefficient is important for understanding in which direction the force will act. Pressure is determined as positive while suction is determined as negative. In Figure 20 it is possible to see the overlap and determination of the sign from the external and internal pressure.

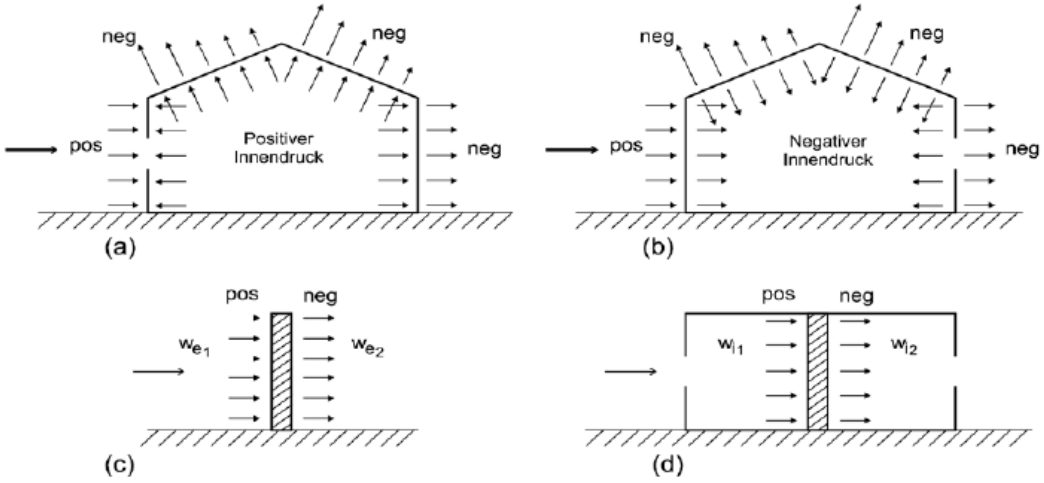

Figure 20: Overlap and Determination of the Sign from External and Internal Pressure[68]

c) Velocity Pressure Line

The hall has a height h of 11.90 meters and a length (or width) of 48 meters (or 19.80 meters). Therefore, the height will always be smaller than the length (or width): $h \leq b$. In Figure 21 below, from Schneider[69] Figure 3.29a, the velocity pressure will be uniform from bottom to top (first picture, on the upper left):

[67] (SCHNEIDER, 2012) - Table 3.28b
[68] (SCHNEIDER, 2012) – Figure 3.28a
[69] (SCHNEIDER, 2012) - Figure 3.29a

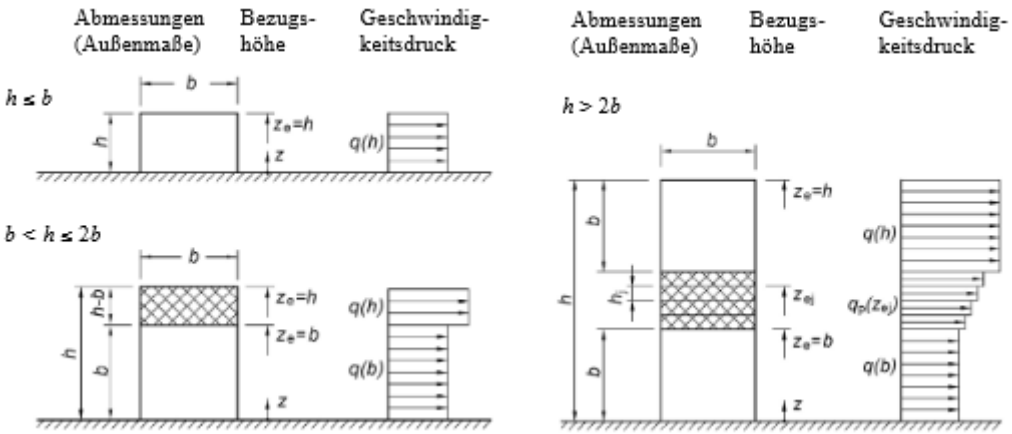

Figure 21: Velocity Pressure Line and Reference Height z_e for Vertical Walls subject to the Building Height h and Width

d) Division by Area of External Pressure Coefficient

- Value of when e when θ = 0° or when θ = 90°

To analyze the external pressure on the wall, the value of e must be found:

$$e = b \text{ or}$$
$$e = 2h$$

The value of e will be the lowest. Given that:

$$2h = 2 * 11.9\ m = 23.8\ m \text{ and}$$

$$b = \{19.8\ m, 48\ m\}$$

the values of e are now:

$$e_{\theta 0^\circ} = 19.8\ m$$

Because:

$$2h = 23.8\ m \geq 19.8\ m = b$$

θ =	0°	
h =	11.90	[m]
e_1 = b =	19.80	[m]
e_2 = 2h =	23.80	[m]
$e_{\theta 0^\circ}$ =	19.80	[m]
d =	48.00	[m]

Table 2: Values of the Dimensions for θ = 0°

And:

$$e_{\theta 90^\circ} = 23.8\ m$$

Because:

$$2h = 23.8\ m \leq 48\ m = b$$

θ =	90°	
h =	11.90	[m]
e_1 = b =	48.00	[m]
e_2 = 2h =	23.80	[m]
$e_{\theta 90^\circ}$ =	23.80	[m]
d =	19.80	[m]

Table 3: Values of the Dimensions for θ = 90°

- Length of each Division Area when θ = 0°

According to Schneider[70], Figure 22 below demonstrates the arrangement of the areas of the vertical walls (when $e < d$) when the layout of the building is rectangular (Figure 23):

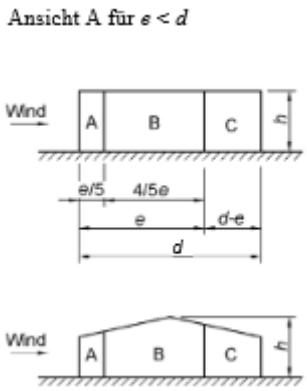

Figure 22: Arrangement of the Areas of the Vertical Walls when $e < d$ [71]

[70] (SCHNEIDER, 2012) - Figure 3.29b
[71] (SCHNEIDER, 2012) – Figure 3.29b

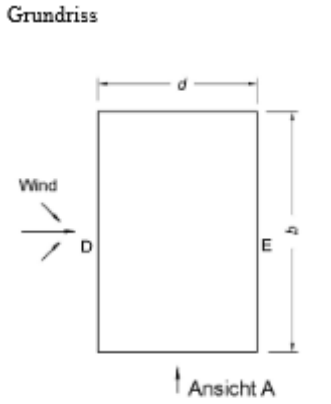

Figure 23: Layout of the Rectangular Building[72]

When $e = e_{\theta 0^\circ} = 19.8\,m < 48\,m = \ d$, there are 3 divisions (A, B and C). The length of each area is as follows:

$$\text{A: } \frac{e}{5} = \frac{e_{\theta 0^\circ}}{5} = \frac{19.8}{5} = 3.96\,m$$

$$\text{B: } \frac{4*e}{5} = \frac{4*e_{\theta 0^\circ}}{5} = \frac{4*19.8}{5} = 15.84\,m$$

$$\text{C: } d - e = d - e_{\theta 0^\circ} = 48 - 19.8 = 28.2\,m$$

θ =	0°	
A:	3.96	[m]
B:	15.84	[m]
C:	28.20	[m]

Table 4: Values of the Length of each Division (A, B and C) for θ = 0°

- Length of each Division Area when θ = 90°

Similarly, when the wind is blowing on the longer side:

$$e = e_{\theta 90^\circ} = 23.8\,m \geq 19.8\,m \ = \ d$$

[72] (SCHNEIDER, 2012) – Figure 3.29b

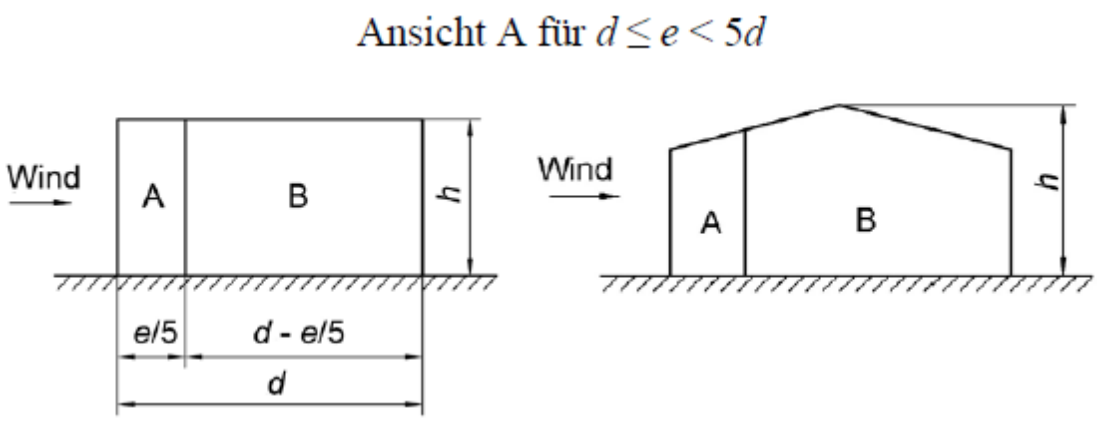

Figure 24: Arrangement of the Areas of the Vertical Walls when $d < e < 5d$ [73]

And in accordance, again, with Figure 24 above:

For the wind that falls on the longer side (when θ = 90°), the division is as follows:

$$\text{A: } \frac{e}{5} = \frac{e_{\theta 90°}}{5} = \frac{23.8}{5} = 4.76\ m$$

$$\text{B: } d - \frac{e}{5} = d - \frac{e_{\theta 90°}}{5} = 19.8 - \frac{23.8}{5} = 15.04\ m$$

θ =	90°	
A:	4.76	[m]
B:	15.04	[m]

Table 5: Values of the Length of each Division (A and B) for θ = 90°

e) External Pressure Coefficient by Area

- When θ = 90°

Considering that, in this case (for θ = 90°) the relation between the height h and the length d of the wall that is not affected by the wind is:

$$\frac{h}{d} = \frac{11.9}{19.8} = 0.6010$$

In agreement with Schneider[74], seen in Table 6 below, there is no value for the $c_{pe,10}$ when the relation between h and d is 0.6010. Since the relationship between h and d is between 0.25 and 1, the values of all divisions will be the linearly interpolated (see below in Table 6).

[73] (SCHNEIDER, 2012) – Figure 3.29b
[74] (SCHNEIDER, 2012) - Table 3.29

Bereich	A		B		C		D		E	
h/d	$c_{pe,10}$	$c_{pe,1}$	$c_{pe,10}$	$c_{pe,1}$	$c_{pe,10}$	$c_{pe,1}$	$c_{pe,10}$	$c_{pe,1}$	$c_{pe,10}$	$c_{pe,1}$
= 5	–1,4	–1,7	–0,8	–1,1	–0,5	–0,7	+0,8	+1,0	–0,5	–0,7
1	–1,2	–1,4	–0,8	–1,1	–0,5		+0,8	+1,0	–0,5	
≤ 0,25	–1,2	–1,4	–0,8	–1,1	–0,5		+0,7	+1,0	–0,3	–0,5
Für einzeln in offenem Gelände stehende Gebäude können im Sogbereich auch größere Sogkräfte auftreten. Zwischenwerte dürfen linear interpoliert werden. Für Gebäude mit *h/d* > 5 ist die Gesamtwindlast anhand der Kraftbeiwerte aus DIN EN 1991-1-4, Abschnitte 7.6 bis 7.8 und 7.9.2 (vgl. a. Abschn. 8 in diesem Beitrag) zu ermitteln.										

Table 6: Values of the External Pressure Coefficients for Vertical Walls of the Buildings with Rectangular Outline[75]

The interpolated values for each division are given in Table 7 below:

	$c_{pe,10} = c_{pe}$			
h/d	**A**	**B**	**D**	**E**
1.0000	-1.2	-0.8	0.8	-0.5
0.6010	-1.2	-0.8	0.7468	-0.3936
0.2500	-1.2	-0.8	0.7	-0.3

Table 7: Interpolated Values for the External Pressure Coefficient c_{pe} for each Division for θ = 90° when h/d = 0.6010

Following calculation of the coefficient c_{pe}, the wind pressure was determined. Table 8 provides the value for each area of division.

	A	**B**	**D**	**E**
W_e [kN/m²]	-0.636	-0.424	0.396	-0.209

Table 8: Values of the External Wind Pressure for θ = 90°

- When θ = 0°

The relation for θ = 0° is:

$$\frac{h}{d} = \frac{11.9}{48} = 0.2479$$

In agreement with Schneider[76], seen in Table 6 above, there is no value for the $c_{pe,10}$ when the relation between h and d is 0.2479. Since the relation between h and d is less than 0.25, the values of all divisions will be the same as for when the relation is 0.25 (see above in Table 6). The values for each division are shown in Table 9 below:

[75] (SCHNEIDER, 2012) – Table 3.29
[76] (SCHNEIDER, 2012) - Table 3.29

	$c_{pe,10} = c_{pe}$				
h/d	**A**	**B**	**C**	**D**	**E**
0.247917	-1.2	-0.8	-0.5	0.7	-0.3

Table 9: Values for the External Pressure Coefficient c_{pe} for each Division for θ = 90° when h/d = 0.2479

Similar to when θ = 90°, the wind pressure was calculated with the newly determined wind pressure coefficients c_{pe} for each area of division in Table 10 below.

	A	**B**	**C**	**D**	**E**
W_e [kN/m²]	-0.636	-0.424	-0.265	0.371	-0.159

Table 10: Values of the External Wind Pressure for θ = 0°

3.1.4.3.2 Saddle Roof

The angle α between the roof and the horizontal line at the top of the wall is approximately +8.6°. As it is more than 5° the roof cannot be considered as a flat roof and will be considered as a saddle roof.

a) Division by Area of External Pressure Coefficient

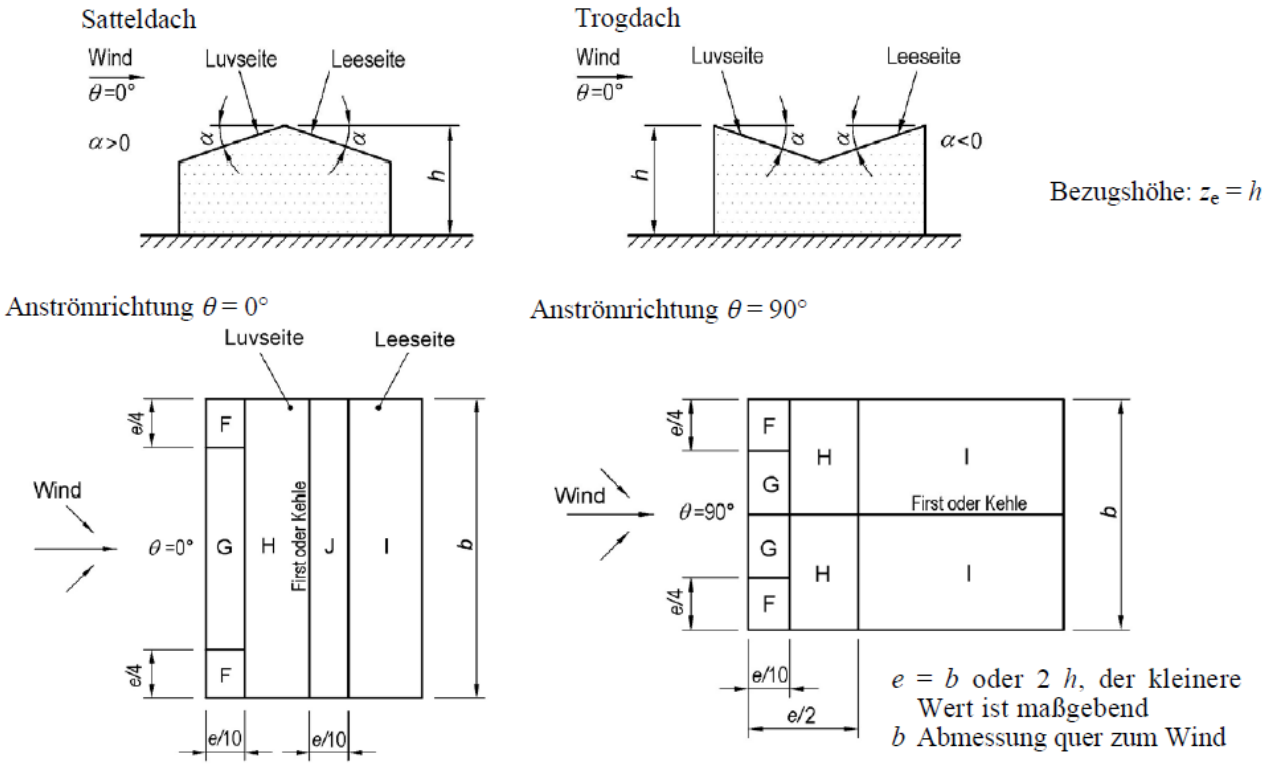

Figure 25: Allocation of the Areas of the Saddle Roof[77]

[77] (SCHNEIDER, 2012) – Figure 3.32

Similar to the calculations of the vertical wall, the variables e and b were calculated accordingly. Where b is always the length of the side perpendicular to the direction of the wind and e = b or e = 2h, being the smallest value between both.

- When b = 48 m (θ = 90°)

When b = 48 m, d = 19.8 m and e is calculated by:

$$e = b = 48\,m \text{ or}$$

$$e = 2 * h = 2 * 11.9\,m = \ 23.8\,m$$

The value of e is the smallest, thus:

$$e = \ 23.8\,m$$

The areas of each division are:

$$\text{F: } \frac{e}{10} * \frac{e}{4} = \frac{23.8}{10} * \frac{23.8}{4} = 2.38 * 5.95 = \ 14.16\,m^2$$

$$\text{G: } \frac{e}{10} * \left(b - \frac{e}{2}\right) = \frac{23.8}{10} * \frac{23.8}{2} = 2.38 * 36.1 = \ 85.92\,m^2$$

$$\text{H: } \left(\frac{d}{2} - \frac{e}{10}\right) * b = \left(\frac{19.8}{2} - \frac{23.8}{10}\right) * \ 48 = 7.52 * 48 = \ 360.96\,m^2$$

$$\text{I: } \left(\frac{d}{2} - \frac{e}{10}\right) * b = \left(\frac{19.8}{2} - \frac{23.8}{10}\right) * \ 48 = 7.52 * 48 = \ 360.96\,m^2$$

$$\text{J: } \frac{e}{10} * b = \frac{23.8}{10} * \ 48 = 2.38 * 48 = \ 114.24\,m^2$$

All values are shown in Table 11:

	d [m]	b [m]	A [m²]
F:	2.38	5.95	14.16
G:	2.38	36.1	85.92
H:	7.52	48	360.96
I:	7.52	48	360.96
J:	2.38	48	114.24

Table 11: Values for each Division of Area when the Wind focuses on the side with L = 48 m (θ = 90°)

- When b = 19.8 m (θ = 0°)

When b = 19.8 m, d = 48 m and e is calculated by:

$$e = b = 19.8\,m \text{ or}$$

$$e = 2 * h = 2 * 11.9\,m = 23.8\,m$$

Therefore:

$$e = 19.8\,m$$

when the wind focuses on the front of the structure.

The areas of each division are:

$$\text{F: } \frac{e}{10} * \frac{e}{4} = \frac{19.8}{10} * \frac{19.8}{4} = 1.98 * 4.95 = 9.80\,m^2$$

$$\text{G: } \frac{\frac{e}{10} * \left(b - \frac{e}{2}\right)}{2} = \frac{\frac{19.8}{10} * \left(23.8 - \frac{19.8}{2}\right)}{2} = 9.80\,m^2$$

$$\text{H: } \left(\frac{e}{2} - \frac{e}{10}\right) * \frac{b}{2} = \left(\frac{19.8}{2} - \frac{19.8}{10}\right) * \frac{19.8}{2} = 78.41\,m^2$$

$$\text{I: } \left(d - \frac{e}{2}\right) * \frac{b}{2} = \left(48 - \frac{19.8}{2}\right) * \frac{23.8}{2} = 377.19\,m^2$$

All values are shown in Table 12:

	d [m]	b [m]	A [m²]
F:	1.98	4.95	9.80
G:	1.98	4.95	9.80
H:	7.92	9.9	78.41
I:	38.1	9.9	377.19

Table 12: Values for each Division of Area when the Wind focuses on the side with L = 19.8 m (θ = 0°)

b) External Pressure Coefficient for Saddle Roof

Table 13 gives the external pressure coefficient for every division of the roof.

Neigungswinkel α [1]		Anströmrichtung $\theta = 0°$ [2]; Bereich									
		F		G		H		I		J	
		$c_{pe,10}$	$c_{pe,1}$	$c_{pe,10}$	$c_{pe,1}$	$c_{pe,10}$	$c_{pe,1}$	$c_{pe,10}$	$c_{pe,1}$	$c_{pe,10}$	$c_{pe,1}$
Trogdach	–45°	–0,6		–0,6		–0,8		–0,7		–1,0	–1,5
	–30°	–1,1	–2,0	–0,8	–1,5	–0,8		–0,6		–0,8	–1,4
	–15°	–2,5	–2,8	–1,3	–2,0	–0,9	–1,2	–0,5		–0,7	–1,2
	–5°	–2,3	–2,5	–1,2	–2,0	–0,8	–1,2	+0,2		+0,2	
								–0,6		–0,6	
Satteldach	5°	–1,7	–2,5	–1,2	–2,0	–0,6	–1,2	–0,6		+0,2	
		+0,0		+0,0		+0,0				–0,6	
	15°	–0,9	–2,0	–0,8	–1,5	–0,3		–0,4		–1,0	–1,5
		+0,2		+0,2		+0,2		+0,0		+0,0	+0,0
	30°	–0,5	–1,5	–0,5	–1,5	–0,2		–0,4		–0,5	
		+0,7		+0,7		+0,4		+0,0		+0,0	
	45°	-0,0		-0,0		-0,0		–0,2		–0,3	
		+0,7		+0,7		+0,6		+0,0		+0,0	
	60°	+0,7		+0,7		+0,7		–0,2		–0,3	
	75°	+0,8		+0,8		+0,8		–0,2		–0,3	

Neigungswinkel α		Anströmrichtung $\theta = 90°$; Bereich							
		F		G		H		I	
		$c_{pe,10}$	$c_{pe,1}$	$c_{pe,10}$	$c_{pe,1}$	$c_{pe,10}$	$c_{pe,1}$	$c_{pe,10}$	$c_{pe,1}$
Trogdach	–45°	–1,4	–2,0	–1,2	–2,0	–1,0	–1,3	–0,9	–1,2
	–30°	–1,5	–2,1	–1,2	–2,0	–1,0	–1,3	–0,9	–1,2
	–15°	–1,9	–2,5	–1,2	–2,0	–0,8	–1,2	–0,8	–1,2
	–5°	–1,8	–2,5	–1,2	–2,0	–0,7	–1,2	–0,6	–1,2
Satteldach	5°	–1,6	–2,2	–1,3	–2,0	–0,7	–1,2	–0,6	
	15°	–1,3	–2,0	–1,3	–2,0	–0,6	–1,2	–0,5	
	30°	–1,1	–1,5	–1,4	–2,0	–0,8	–1,2	–0,5	
	45°	–1,1	–1,5	–1,4	–2,0	–0,9	–1,2	–0,5	
	60°, 75°	–1,1	–1,5	–1,2	–2,0	–0,8	–1,0	–0,5	

[2] Für Dachneigungen zwischen den angegebenen Werten darf linear interpoliert werden, sofern nicht das Vorzeichen der Druckbeiwerte wechselt. Zwischen den Werten $\alpha = +5°$ und $\alpha = -5°$ darf nicht interpoliert werden, stattdessen sind die Werte für Flachdächer zu benutzen. Wert 0,0 für Interpolation.

[1] Für die Anströmrichtung $\theta = 0°$ und Neigungswinkel von $\alpha = -5°$ bis $+45°$ ändert sich der Druck schnell zwischen positiven und negativen Werten; daher werden sowohl der positive als auch der negative Wert angegeben. Bei solchen Dächern sind vier Fälle zu berücksichtigen, bei denen jeweils der kleinste bzw. größte Wert für die Bereiche F, G und H mit den kleinsten bzw. größten Werten der Bereiche I und J kombiniert werden. Das Mischen von positiven und negativen Werten auf einer Dachfläche ist nicht zulässig.

Table 13: Values of the External Pressure Coefficients for every Division of the Roof[78]

As the structure has a roof angle of 8.6° and according to Table 13[79], the values of c_{pe} for each division are as follows:

- When θ = 90°:

  There were 4 different wind load cases (see explanation in Table 13) for the wind that is applied on the largest (longitudinal) side of the hall. This occurs when the angle of the roof is between -5° and +45°, due to the fact that the compression changes very fast between the positive and negative values. Therefore, both values should be combined between 2 groups. The first group was composed by the areas F, G and H and the second group by the areas I and J. These groups were combined for their maximum (+) and minimum (-) values. If the for a maximum value there was

[78] (SCHNEIDER, 2012) – Table 3.32

[79] IMPORTANT NOTE: Figure 25 and Table 13 define θ = 0° as the Wind being applied on the longer side – not front or back – and for standardization reasons between both Norms, θ = 0° was defined as the Wind being applied on the shorter side – front and back

only a negative value for the c_{pe}, 0.0 was attributed to it. In this combination, there were 4 load cases and the values of c_{pe} were interpolated for the angle of 8.6°:

- Group 1 Max, Group 2 Max (++):

++	$c_{pe,10} = c_{pe}$				
α [°]	F	G	H	I	J
5.0	0	0	0	0	0.2
8.6	0.072	0.072	0.072	0.000	0.128
15.0	0.2	0.2	0.2	0	0
	F	G	H	I	J
W_e [kN/m²]	0.038	0.038	0.038	0.000	0.068

Table 14: Values for the External Pressure Coefficient c_{pe} and External Wind Pressure W_e for the Saddle Roof for each Division for θ = 90° when α = 8.6° and Combination ++

- Group 1 Min, Group 2 Min (--):

--	$c_{pe,10} = c_{pe}$				
α [°]	F	G	H	I	J
5.0	-1.7	-1.2	-0.6	-0.6	-0.6
8.6	-1.411	-1.055	-0.492	-0.528	-0.745
15.0	-0.9	-0.8	-0.3	-0.4	-1
	F	G	H	I	J
W_e [kN/m²]	-0.748	-0.559	-0.261	-0.280	-0.395

Table 15: Values for the External Pressure Coefficient c_{pe} and External Wind Pressure W_e for the Saddle Roof for each Division for θ = 90° when α = 8.6° and Combination –

- Group 1 Min, Group 2 Max (-+):

-+	$c_{pe,10} = c_{pe}$				
α [°]	F	G	H	I	J
5.0	-1.7	-1.2	-0.6	0	0.2
8.6	-1.411	-1.055	-0.492	0.000	0.128
15.0	-0.9	-0.8	-0.3	0	0
	F	G	H	I	J
W_e [kN/m²]	-0.748	-0.559	-0.261	0.000	0.068

Table 16: Values for the External Pressure Coefficient c_{pe} and External Wind Pressure W_e for the Saddle Roof for each Division for θ = 90° when α = 8.6° and Combination -+

- Group 1 Max, Group 2 Min (+-):

+-	$c_{pe,10} = c_{pe}$				
α [°]	**F**	**G**	**H**	**I**	**J**
5.0	0	0	0	-0.6	-0.6
8.6	0.072	0.072	0.072	-0.528	-0.745
15.0	0.2	0.2	0.2	-0.4	-1
	F	**G**	**H**	**I**	**J**
W_e [kN/m²]	0.038	0.038	0.038	-0.280	-0.395

Table 17: Values for the External Pressure Coefficient c_{pe} and External Wind Pressure W_e for the Saddle Roof for each Division for θ = 90° when α = 8.6° and Combination +-

- When θ = 0°

There were 2 load cases and the value of c_{pe} also had to be interpolated:

-	$c_{pe,10} = c_{pe}$			
α [°]	**F**	**G**	**H**	**I**
5.0	-1.6	-1.3	-0.7	-0.6
8.6	-1.492	-1.300	-0.664	-0.564
15.0	-1.3	-1.3	-0.6	-0.5
	F	**G**	**H**	**I**
W_e [kN/m²]	-0.791	-0.689	-0.352	-0.299

Table 18: Values for the External Pressure Coefficient c_{pe} and External Wind Pressure W_e for the Saddle Roof for each Division for θ = 0° when α = 8.6°

The other load case would be when the c_{pe} was maximum. However, there are only negative values for the c_{pe} on Table 13. This meant that the maximum value of c_{pe} would be 0.0 and for the second load case, the wind would only affect the walls.

3.1.4.4 Influence of the Internal Pressure

According to Schneider[80], for the calculations of ULS, the doors and windows may be perceived as closed. Similar to the Brazilian Norm (Section 3.2.4.4), there will be a "dominant opening" criteria. This occurs if the area of an opening of a side is at least twice the size of the sum of all the other openings of the other sides. Given that only the lateral sides of the hall have openings (since front and back doors are considered as closed) and there openings are the same (120m²), there was no "dominant opening".

[80] (SCHNEIDER, 2012) – Section 7.2.9 Page 3.35

Gebäude, Bauteil			Innendruckbeiwert c_{pi}
Gebäude mit einer dominanten Seite [1]	Verhältnis Gesamtfläche der Öffnungen in der dominanten Seite zur Summe der Öffnungen in den restl. Seitenflächen [2]	≥ 3	$c_{pi} = 0{,}90 \times c_{pe}$ [3]
		2	$c_{pi} = 0{,}75 \times c_{pe}$ [3]
Gebäude ohne eine dominante Seite, d. h. gleichmäßig verteilte Öffnungen [4]			c_{pi} s. Skizze
Offene Silos und Schornsteine			$c_{pi} = -0{,}60$
Belüftete Tanks mit kleinen Öffnungen			$c_{pi} = -0{,}40$

[1] Als dominante Seite wird die Gebäudeseite bezeichnet, bei der die Gesamtfläche der Öffnungen mindestens doppelt so groß ist wie die Summe der Öffnungen in den restlichen Seitenflächen (gilt auch für einzelne Innenräume).

[2] Zwischenwerte dürfen linear interpoliert werden.

[3] c_{pe}-Wert = Außendruckbeiwert der dominanten Seite. Bei unterschiedlichen Außendruckbeiwerten auf der dominanten Seite ist ein mit den Öffnungsflächen gewichteter Mittelwert für c_{pe} zu ermitteln.

[4] Bei Gebäuden ohne eine dominante Seite ist der Innendruckbeiwert abhängig von der Höhe h und der Tiefe d des Gebäudes sowie vom Flächenparameter μ (s. Skizze)

$\mu = A_1/A$ A_1 Gesamtfläche der Öffnungen in den leeseitigen und windparallelen Flächen mit $c_{pe} \leq 0$

A Gesamtfläche aller Öffnungen

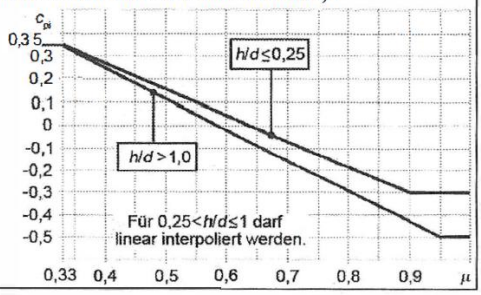

Table 19: Table for Determination of c_{pi} [81]

To determine the value of c_{pi}, A_1 and A were calculated:

- A_1: Sum of the Opening Areas in the wind-parallel sides and the side against the wind (with negative c_{pe})
- Sides: 120 m² (1.5m x 48m + 1m x 48m)
- A = $A_{OpenTot}$: 240 m² (2 * 120m²)

Thus, when wind was:

- 90°:

$$A_1 = 120\, m^2$$

$$\mu = \frac{A_1}{A} = \frac{120}{240} = 0.5$$

$$\frac{h}{d} = 0.601$$

And by interpolation:

$$c_{pi} = 0.1366 = 0.14$$

The new values for the Walls were:

	c_{pi}			
h/d	**A**	**B**	**D**	**E**
0.601	0.1366	0.1366	0.1366	0.1366

Table 20: Values for the Internal Pressure Coefficient c_{pi} for each Division for θ = 90° when h/d = 0.601

[81] (SCHNEIDER, 2012) – Table 3.35

And Wind Pressure of:

	A	B	D	E
W_i [kN/m²]	0.07	0.07	0.07	0.07

Table 21: Values of Internal Wind Pressure from on each Division when θ = 90°

- 0°:

$$A_1 = 120 + 120 = 240\ m^2$$

$$\mu = \frac{A_1}{A} = \frac{240}{240} = 1.0$$

$$\frac{h}{d} = 0.2479 = 0.25$$

$$c_{pi} = -0.3$$

The new values for the Walls were:

	c_{pi}				
h/d	A	B	C	D	E
0.25	-0.3	-0.3	-0.3	-0.3	-0.3

Table 22: Values for the Internal Pressure Coefficient c_{pi} for each Division for θ = 0° when h/d = 0.25

And Wind Pressure of:

	A	B	C	D	E
W_i [kN/m²]	-0.16	-0.16	-0.16	-0.16	-0.16

Table 23: Values of Internal Wind Pressure from on each Division when θ = 0°

It is important to notice that a negative pressure means suction and a positive pressure means overpressure.

3.1.5 Snow Loads

As mentioned in Chapter 3, European norms, such as the German DIN EN, must take snow loads into consideration, while the Brazilian norm NBR by the ABNT has no reference to it. However, the original building is located in Brazil and was built according to the NBR, which does not consider snow loads for the dimensioning of buildings. Thus, in order to achieve a better comparison between the Brazilian modeled structure and the German modeled structure, the snow load calculations were not taken into account. In its place, the Live Load ("*Ação Acidental*") would substitute it accordingly – see explanation in Section 3.1.3.

3.1.6 Crane Loads

3.1.6.1 Vertical Loads

The crane load was determined by the combined weight of the maximum lifting load (15 tons), self-weight of the cart and the self-weight of the crane. The method used in this project was to determine the wheel loads that would act upon the runway girder. The calculations for the loads analyzed in this Section are detailed in Section 3.2.6.1[82].

According to Seeßelberg's table[83], if the maximum forces of the crane are not given, the values in Table 24 can be considered. In view of the maximum wheel load R for a lifting load of 15 tons (approximate value of 16 tons) and a span length of 19 meters (approximate value is 18m) is 96 kN. In Section 3.2.6.1, the vertical load for the Brazilian design code (see Section 3.2.6.1) was 95.8 kN and thus, a maximum vertical wheel load (R) of 96 kN is proven plausible.

max. Radlast R	Spurmittenmaß l										
Tragfähigkeit	10 m	12 m	14 m	16 m	18 m	20 m	22 m	24 m	26 m	28 m	30 m
3,2 t	23	25	27	29	32	34	36	38	40	42	44
5 t	29	32	34	36	39	41	44	46	48	51	53
6,3 t	38	40	43	45	48	50	53	55	58	60	63
8 t	47	50	52	55	57	60	62	65	67	70	72
10 t	55	58	61	63	66	69	71	74	77	79	82
12,5 t	66	70	73	76	80	83	87	90	93	97	100
16 t	80	84	88	92	96	100	104	108	112	116	120
20 t	98	102	107	111	116	120	124	129	133	138	142

Table 24: Maximum Wheel Load R for Double-Girder Overhead Crane with no Walkways or Wheelhouse[84]

In this case, the vertical wheel load Q_r will be the sum of the wheel load of the self-weight of the crane (Q_c) and the wheel load from the lifting load (Q_h):

$$\text{MAX: } Q_c = Q_{SW} + Q_{Cart} = 0.9375 + 0.70658 = 1.64408\ tons = 16.44\ kN$$

$$\text{MIN: } Q_c = Q_{SW} + Q_{Cart} = 0.9375 + 0.04342 = 0.98092\ tons = 9.81\ kN$$

Q_h is given by:

$$\text{MAX: } Q_h = 7.06579\ tons = 70.66\ kN$$

$$\text{MIN: } Q_h = 0.43421\ tons = 4.34\ kN$$

And Q_r:

$$\text{MAX: } Q_r = Q_c + Q_h = 16.44 + 7.06579 = 8.70987\ tons = 87.1\ kN$$

$$\text{MIN: } Q_r = Q_c + Q_h = 9.81 + 0.43421 = 1.41513\ tons = 14.15\ kN$$

[82] For better comprehension of the origin of the loads from the crane and the lifting load see Section 3.2.6.1
[83] (SEEßELBERG, Kranbahnen: Bemessung und konstruktive Gestaltung, 2005) – Table 3-7 Page 64
[84] (SEEßELBERG, Kranbahnen: Bemessung und konstruktive Gestaltung, 2005) – Table 3-7 Page 64

φ_i	Berücksichtigter Einfluss	Anzuwenden auf	Definition der Schwingbeiwerte
φ_1	Schwingungsanregung des Krantragwerks infolge Anheben der Hublast vom Boden	Eigengewicht des Krans	$0{,}9 < \varphi_1 < 1{,}1$ 1,1 und 0,9 decken die unteren und oberen Werte des Schwingungsimpulses ab.
φ_2	Dynamische Wirkungen beim Anheben der Hublast vom Boden	Hublast	$\varphi_2 = \varphi_{2,min} + \beta_2 \cdot v_h$; v_h konstante Hubgeschwindigkeit in [m/s]; $\varphi_{2,min}$ und β_2 sind von der Hubklasse des Krans abhängig.

Hubklasse	β_2	$\varphi_{2,min}$
HC 1	0,17	1,05
HC 2	0,34	1,10
HC 3	0,51	1,15
HC 4	0,68	1,20

φ_3	Dynamische Wirkungen durch plötzliches Loslassen der Nutzlast bei Verwendung von Greifern und Magneten	Hublast	$\varphi_3 = 1 - \frac{\Delta m}{m} \cdot (1 + \beta_3)$ Δm der abgesetzte oder losgelassene Teil der gesamten Hublastmasse m $\beta_3 = 0{,}5$ bei Kranen mit Greifern oder ähnlichen Vorrichtungen für langsames Absetzen $\beta_3 = 1{,}0$ bei Kranen mit Magneten oder ähnlichen Vorrichtungen für schnelles Absetzen
φ_4	Dynamische Wirkungen, hervorgerufen durch Fahren auf Schienen o.Ä.	Eigengewicht von Kran und Hublast	$\varphi_4 = 1{,}0$, falls die in EN 1090-2 [71] spezifizierten Maßabw. für Kranschienen eingehalten werden. Sonst: siehe EN 13001-2
φ_5	Dynamische Wirkungen verursacht durch Antriebskräfte	Antriebskräfte	$\varphi_5 = 1{,}0$ für Fliehkräfte $1{,}0 \le \varphi_5 \le 1{,}5$ für Systeme mit stetiger Veränderung der Kräfte $1{,}5 \le \varphi_5 \le 2{,}0$ wenn plötzliche Veränderungen der Kräfte auftreten $\varphi_5 = 3{,}0$ bei Antrieben mit beträchtlichem Spiel
φ_6	Dynamische Wirkungen infolge einer Prüflast	Dyn. Prüflast 110 %	$\varphi_6 = 0{,}5\ (1 + \varphi_2)$, EC 1-3, Kap. 2.10 (4)
φ_7	Dynamische, elastische Wirkungen verursacht durch Pufferanprall	Pufferkräfte	$\varphi_7 = 1{,}25$ für $0 \le \xi \le 0{,}5$ $\varphi_7 = 1{,}25 + 0{,}7 \cdot (\xi - 0{,}5)$ für $0{,}5 \le \xi \le 1$ ξ ist von der Pufferkennlinie abhängig 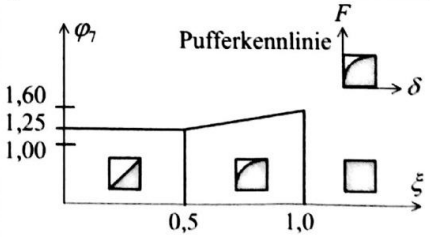

Table 25: Oscillation Coefficients According to EC 1-3, Tables 2.1, 2.4, 2.6 and 2.10[85]

[85] (SEEßELBERG, Kranbahnen: Bemessung und konstruktive Gestaltung, 2005) – Table 11-1 Page 257

Belastung	Bez. nach EC 1-3		Lastgruppen für Einwirkungskombinationen im GZT, im GZG und im Grenzzustand der Ermüdung samt Schwingbeiwerten													
	Symbol	Abschnitt	Grenzzustand der Tragfähigkeit (GZT)							GZT, Prüflast	GZT, außergewöhnl.		Grenzzustand der Gebrauchstaugl. d)			Ermüdung
			1	2	3	4	5	6	7	8 e)	9	10	11 b)	12 c)	13 c)	14
Eigengewicht des Krans	Q_C	2.6	φ_1	φ_1	1	φ_4	φ_4	φ_4	1	φ_1	1	1	1	1	1	$\varphi_{fat,1}$
Hublast	Q_h	2.6	φ_2	φ_3	—	φ_4	φ_4	φ_4	η a)	—	1	1	1	1	1	$\varphi_{fat,2}$
Anfahren/ Bremsen der Kranbrücke	H_L H_T	2.7	φ_5	φ_5	φ_5	φ_5	—	—	—	φ_5	—	—	—	—	1	—
Schräglauf der Kranbrücke	H_S	2.7	—	—	—	—	1	—	—	—	—	—	—	1	—	—
Anfahren/ Bremsen der Laufkatze oder des Hubwerks	$H_{T,3}$	2.7	—	—	—	—	—	1	—	—	—	—	—	—	—	—
Wind in Betrieb	F_W*	Anh. A.1	1	1	1	1	1	—	—	1	—	—	—	1	1	—
Kranprüflast	Q_T	2.10	—	—	—	—	—	—	—	φ_6	—	—	—	—	—	—
Pufferkraft	H_B	2.11	—	—	—	—	—	—	—	—	φ_7	—	—	—	—	—
Kippkraft	H_{TA}	2.11	—	—	—	—	—	—	—	—	—	1	—	—	—	—

Teilsicherheitsbeiwerte Einwirkungen γ_Q siehe Tab. 11-4,
Teilsicherheitsbeiwerte Widerstände γ_M siehe Abschnitt 12.1 und 13.1.3

a η ist der Anteil der Hublast, der nach Entfernen der Nutzlast verbleibt, jedoch nicht im Eigengewicht des Krans enthalten ist.
b Zur Bestimmung der vertikalen Durchbiegungen bzw. Verformungen.
c Zur Bestimmung der horizontalen Verformungen.
d NA zu EC 3-6, Kap. 4.1.
e Für Prüflasten gilt ein reduzierter Teilsicherheitsbeiwert, siehe Tab. 11-4.

Table 26: Load Groups for Measurement of the Runway Girder According to EC 1-3 Table 2.2[86]

[86] (SEEßELBERG, Kranbahnen: Bemessung und konstruktive Gestaltung, 2005) – Table 11-3 Page 260

According to Table 25, the oscillation coefficients were given by:

- $\varphi_1 = 1.1$ (normally, for bridge cranes $\varphi_1 = 1.1$[87])
- $\varphi_2 = 1.10 + 0.34 * \frac{4}{60} \frac{\frac{m}{\min}}{\frac{sec}{\min}} = 1.12$ (Class H2, Crane speed $v_h = 4 \frac{m}{min}$)
- $\varphi_3 = \varphi_4 = 1.0$
- $\varphi_5 = 1.5$ (system with constant alteration of the forces)

Typically, for the crane studied, the load groups (LG) 1 and 5, given in Table 26, are the critical ones. Therefore, the characteristic values of the vertical wheel loads were:

- LG 1: $F = F_1 = F_2 = \varphi_1 * Q_c + \varphi_2 * Q_h = 1.1 * 16.44 + 1.12 * 70.66 = 97.22\ kN$
- LG 5: $F = F_1 = F_2 = \varphi_4 * Q_c + \varphi_4 * Q_h = 1.0 * 16.44 + 1.0 * 70.66 = 87.1\ kN$

For the minimum wheel loads on the other side of the crane:

- LG 1: $F = F_1 = F_2 = \varphi_1 * Q_c + \varphi_2 * Q_h = 1.1 * 9.81 + 1.12 * 4.34 = 15.17\ kN$
- LG 5: $F = F_1 = F_2 = \varphi_4 * Q_c + \varphi_4 * Q_h = 1.0 * 9.81 + 1.0 * 4.34 = 14.15\ kN$

Is it important to notice that for both load groups, a Wind action could be considered in the calculations. However, since the crane is located inside the building, a wind or a snow influence is dismissible[88].

In view of the 97.22 kN and 15.17 kN (LG1) being larger than the 87.1 kN and 14.15 kN (LG5), the 97.22 kN and 15.17 kN loads were recognized as the crucial loads and applied to the model (in favor of security).

3.1.6.2 Horizontal Loads (Transversal)

The horizontal loads are composed of 3 different actions:

The first action is the tracking movements' loads that develop from the skewing of the wheels[89]. This load was given by the equations[90]:

$$H_1 = (S - H_S) = 30.375 - 4.245 = 26.13\ kN$$

$$H_2 = 0$$

With:

$$f = 0.30$$

$$H_{S,1,1,T} = f * \min Q_r = 0.3 * 14.15 = 4.245\ kN$$

$$H_{S,2,1,T} = f * \max Q_r = 0.3 * 87.1 = 26.13\ kN$$

[87] (SCHNEIDER, 2012) – Table 8.81 Page 8.81
[88] (DIN EN 1991-3, 2010) – Annex A.1 (7) Page 43
[89] Can also be calculated by DIN 4132
[90] (SCHNEIDER, 2012) – Section 3.2c Page 8.78

$$S = f * (\min Q_r + \max Q_r) = H_{S,1,1,T} + H_{S,2,1,T} = 4.245 + 26.13 = 30.375\ kN$$

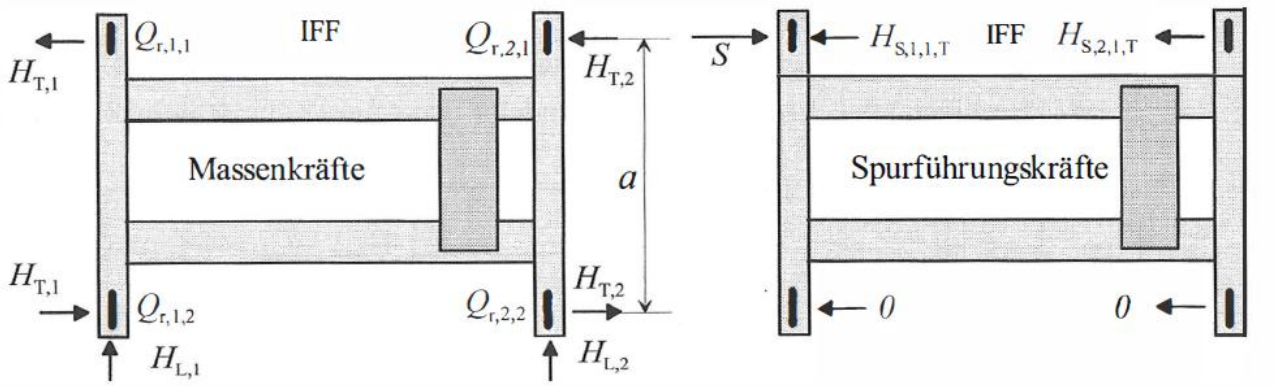

Figure 26: Horizontal Loads from Crane Service[91]

The second action derives from the inertia loads generated from the acceleration and/or braking of the bridge crane. There are two different loads: the load in the direction of the crane rail (index L) – longitudinal loads (see Section 3.1.6.3) – and the load perpendicular to the direction of the rail (index T). The latter originates when the propulsion load K does not act upon the center of mass of the crane-trolley system's lifting load.

Load Perpendicular to the Direction of the Crane H_T[92]:

$$H_{T,1} = \varphi_5 * \zeta_2 * \frac{M}{a}$$
$$H_{T,2} = \varphi_5 * \zeta_1 * \frac{M}{a}$$

With:

- $\Sigma Q_{r,max}$ = 2 * 70.66 kN = 141.32 kN[93] (Sum of the wheel loads on the side closest to the max lifting load)
- ΣQr,(max) = 2 * 4.34 kN = 8.68 kN[94] (Sum of the wheel loads on the side farthest to the max lifting load)
- $\Sigma Q_r = \Sigma Q_{r,max} + \Sigma Q_{r,(max)}$ = 141.32 + 8.68 = 150
- $\zeta_1 = \sum Q_{r,max} / \sum Q_r$ = 141.32 / 150 = 0.9421
- $\zeta_2 = 1 - \zeta_2 = 1 - 0.9421 = 0.0579$
- a = 3.6m (distance between the wheels on the same runway girder)
- l = 19m
- $l_s = (\zeta_1 - 0.5) * l = (0.9421 - 0.5) * 19 = 8.3999 = 8.4$m
- $M = K * l_s = 1.7 * 8.4 = 14.28$ kNm

[91] (SCHNEIDER, 2012) – Page 8.79
[92] (DIN EN 1991-3, 2010) – 2.7.2(3) Page 24
[93] (DIN EN 1991-3, 2010) – 2.5.2.1 Bild 2.1 Page 18
[94] (DIN EN 1991-3, 2010) – 2.5.2.1 Bild 2.1 Page 18

$$H_{T,1} = \varphi_5 * \zeta_2 * \frac{M}{a} = 1.5 * 0.0579 * \frac{14.28}{3.6} = 0.344505\ kN = 0.35\ kN$$
$$H_{T,2} = \varphi_5 * \zeta_1 * \frac{M}{a} = 1.5 * 0.9421 * \frac{14.28}{3.6} = 5.605495\ kN = 5.6\ kN$$

The direction of the load can be seen in Figure 27:

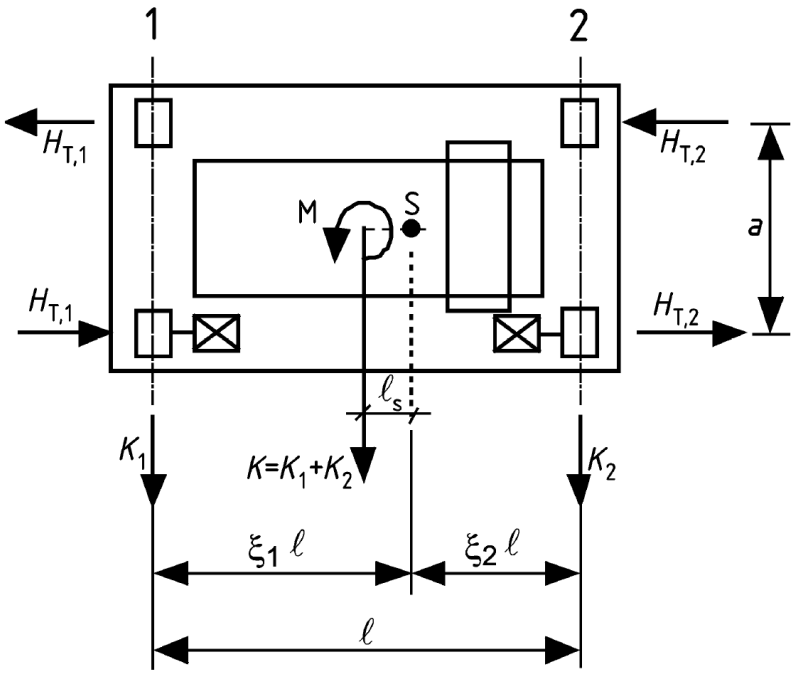

Legende

1 Schiene i = 1

2 Schiene i = 2

Figure 27: Horizontal Transversal Load $H_{T,i}$[95]

The third and last action derives from horizontal loads emerging from the acceleration and/or braking of the crane trolley. However, these loads do not need to be considered separately, because they are covered by the buffer forces from the collision of the trolley (exceptional influence).

Another load, deriving from the buffer will not be considered in this project.

The characteristic values of the horizontal wheel loads were calculated by:

- LG 1: $H_1 = -H_2 = \varphi_5 * H_{T,2} = 1.5 * 5.6 = 8.4\ kN$
- LG 5: $H_1 = 1 * (S - H_S) = 1.0 * 26.13 = 26.13\ kN; H_2 = 0\ kN$

[95] (DIN EN 1991-3, 2010) – Bild 2.6 Page 25

Since the horizontal load for the load group 5 (26.13 kN on one direction) was larger than that of the load group 1 (8.4 kN on each direction), the crucial load was identified as the 26.13 kN load (when applying to the 2D model).

3.1.6.3 Longitudinal Loads

Normally, the impact of the longitudinal loads is negligible for the calculation of the crane. It is used to dimension the braking bracings[96].

Load in the Direction of the Crane H_L[97]:

$$H_{L,i} = \varphi_5 * K * n_r$$

- $\varphi_5 = 1.5$
- $n_r = 2$ (2 runway girders)
- K[98]:

$$K = K_1 + K_2 = \mu * \Sigma Q^*_{r,min}$$

With:

- $\mu = 0.2$ (for steel over steel)
- $m_w = 2$ (2 independent electric-powered wheels)
- $\Sigma Q^*_{r,min} = m_w * Q_{r,min} = 2 * 4.245 = 8.49$ kN

$$K = K_1 + K_2 = \mu * \Sigma Q^*_{r,min} = 0.2 * 8.49 = 1.698 = 1.7\ kN$$

Therefore:

$$H_{L,i} = \varphi_5 * K * n_r = 1.5 * 1.7 * 2 = 5.1\ kN$$

The direction of the load can be seen in Figure 28:

[96] (SCHNEIDER, 2012) – Section 3.2b Page 8.79
[97] (DIN EN 1991-3, 2010) – 2.7.2(2) Page 23
[98] (DIN EN 1991-3, 2010) – 2.7.3 Page 26

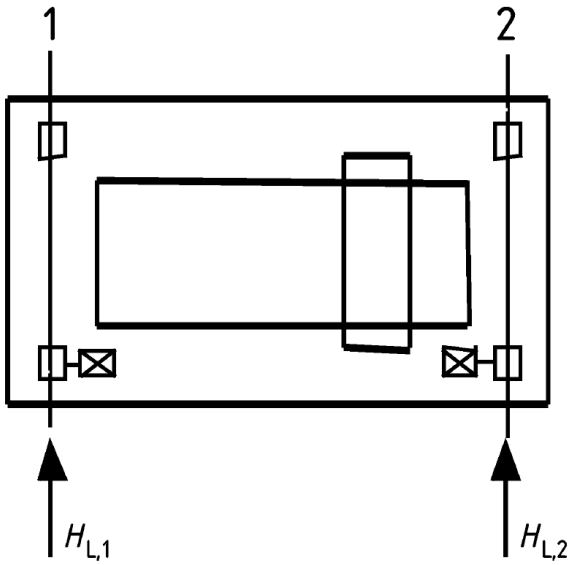

Legende

1 Schiene i = 1
2 Schiene i = 2

Figure 28: Horizontal Longitudinal Load $H_{L,i}$[99]

3.1.6.4 Moment Forces (Due to Eccentricities)

As a consequence of the horizontal transversal load H_T of a wheel (see Section 3.1.6.2), a moment force would be generated. Since this horizontal load is applied on the top part of the runway girder, this moment, due to the eccentricity of the cross section, would be the product of the H_T and the height of the beam. Yet, the runway girder is connected horizontally to a truss system that would prevent this moment from occurring, having the H_T being transferred to the truss system instead.

Another moment from the vertical load Q_r and the distance to the center of the column would appear and since the eccentricity of the loads are already taken into account during the modeling of the structure, the forces were already regarded and it was not necessary to duplicate the force (besides having the truss system also absorbing these forces).

[99] (DIN EN 1991-3, 2010) – Bild 2.5 Page 24

3.1.6.5 Modeling of the Runway Girder (Beam under the Crane Rail)

As seen in Table 34 (page 93), the profile of the runway girder is PS 750x128.7. To the program, the modeled cross-section used was the HEA 700, which was very similar to the original. The loads imposed on the beam were:

- Q_r = 97.2 kN (the largest value was used for both LGs in favor of security)
- For LG1: $H_{T,1}$ = 8.4 kN = – $H_{T,2}$
- For LG5: $H_{S,1}$ = 26.1 kN; $H_{S,2}$ = 0 kN
- H_L = 5.1 kN (for LG1, even though it is not necessary for this type of verification)

There were 4 load cases to be considered, 2 for each LG. For two load cases, the crane was imagined to be in the middle, where the maximum shear forces would occur (for a one-spanned beam). This middle meant that the wheels would have a distance of 1.2m from the edges of the beam and have a distance of 3.6m between them. Figure 29 and Figure 30 illustrate the modeling of the load cases.

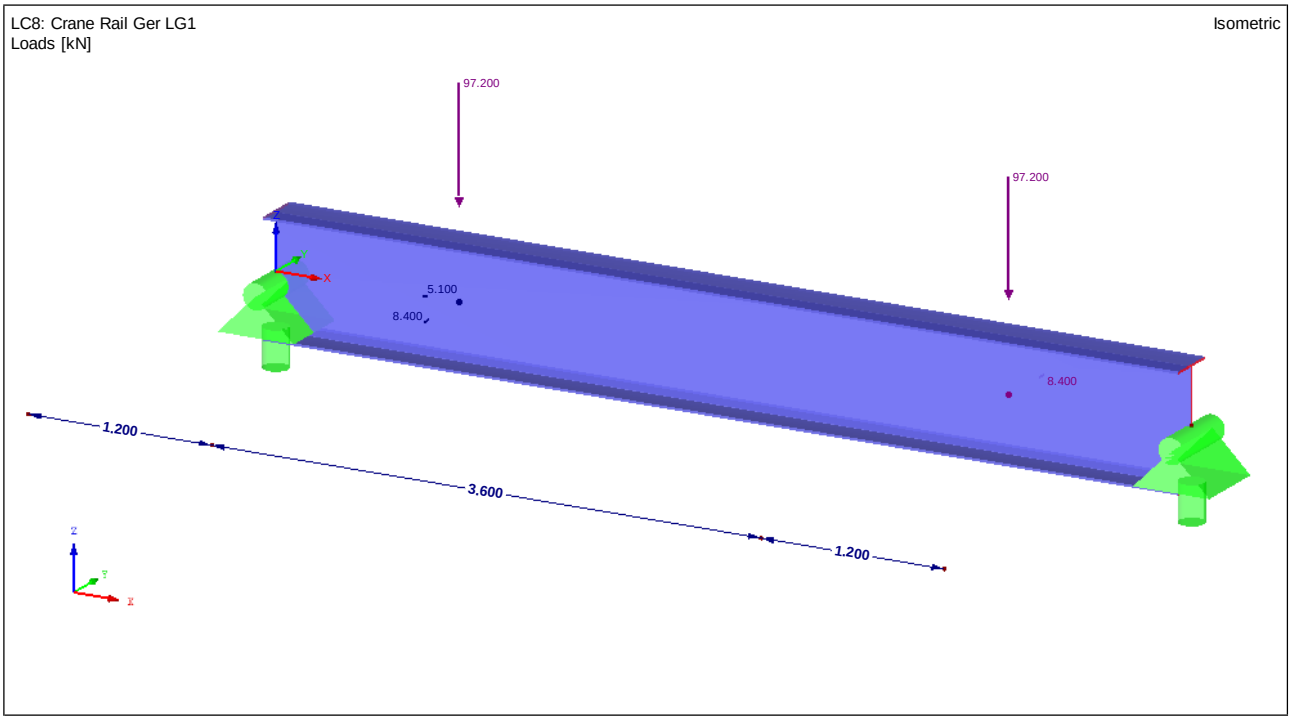

Figure 29: Runway Girder Modeling for LG1 (Crane Middle)

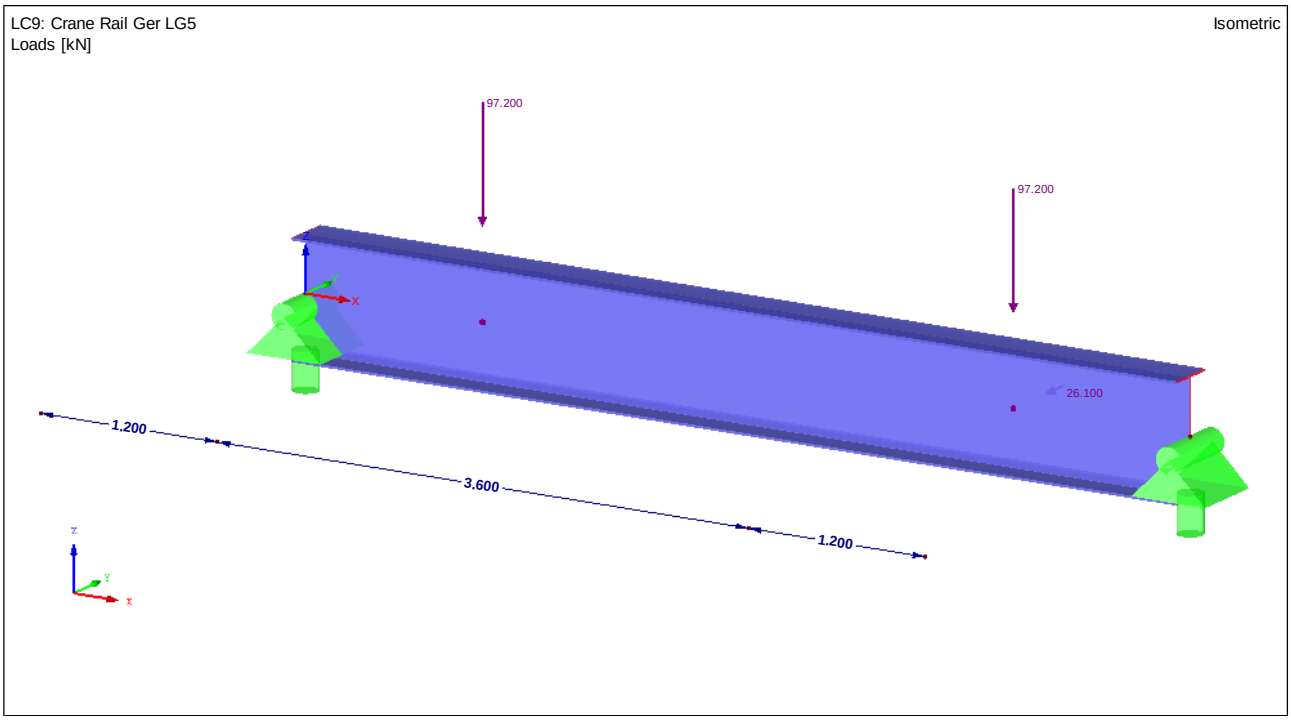

Figure 30: Runway Girder Modeling for LG5 (Crane Middle)

For the other two load cases, one of the crane wheels was imagined to be in the middle, where the maximum moment forces would occur (for a one-spanned beam). This middle meant that the wheel would have a distance of 3m from the edges of the beam and the other wheel being located on another beam (since the wheels have a distance of 3.6m between them). Figure 31 and Figure 32 illustrate the modeling of the load cases.

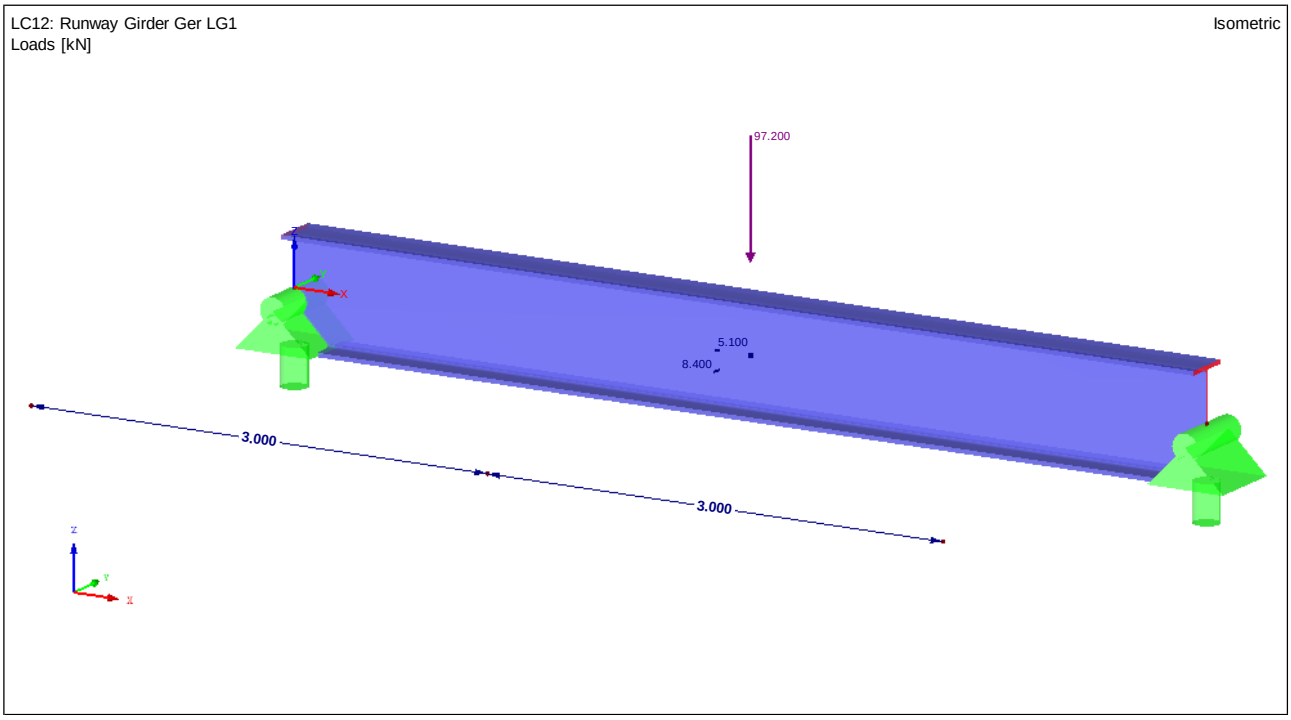

Figure 31: Runway Girder Modeling for LG1 (Wheel Middle)

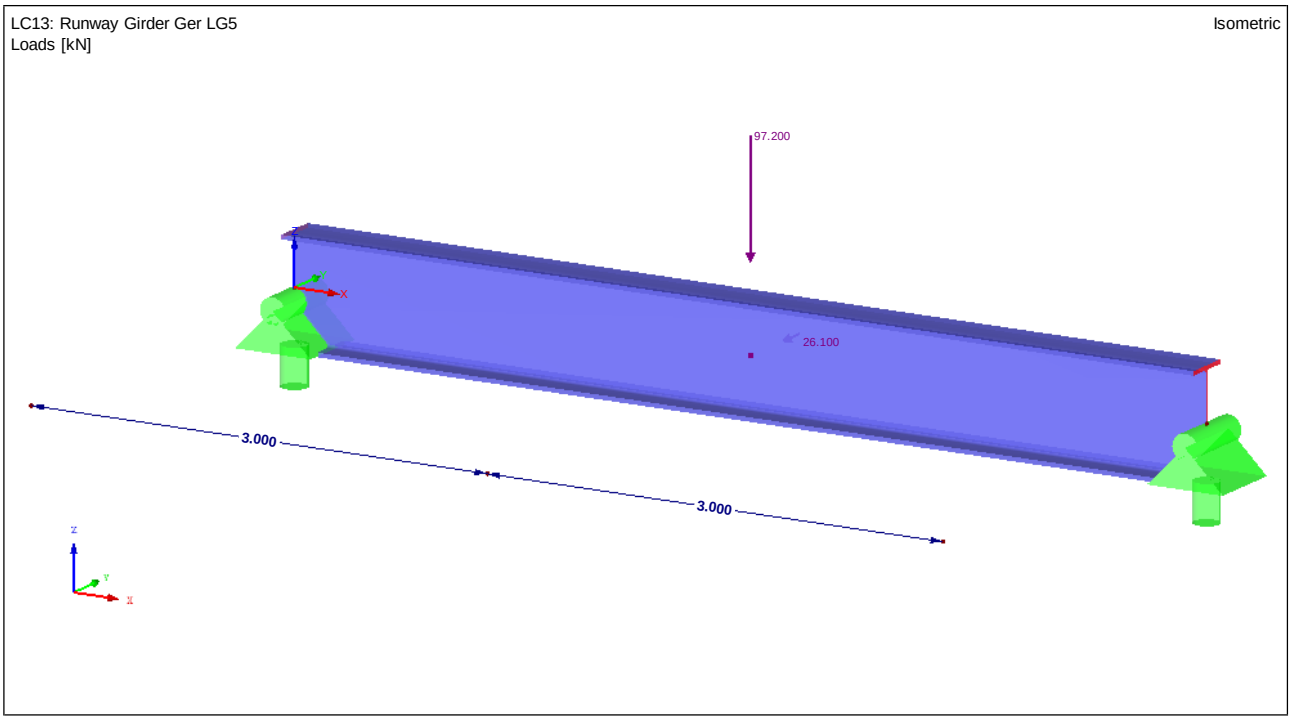

Figure 32: Runway Girder Modeling for LG5 (Wheel Middle)

For the results of the verification of the software, see Appendix 7, Appendix 8, Appendix 16, Appendix 17, Appendix 23, Appendix 24, Appendix 31 and Appendix 32. The Runway Girder cross-section was verified (see also Chapter 6 LOAD COMBINATIONS ULS (ELU OR GZT) AND SLS (ELS OR GZG) and Chapter 7 RESULTS).

3.2 Brazilian Design Codes

3.2.1 Self-Weight

Similarly to the German design codes, the self-weight for the Brazilian design codes were designed with a 1.10 factor (on the Z-Plane) – see Section 3.1.1.

3.2.2 Additional Dead Load

The additional dead load was calculated by:

- Metal Sheet Covering (Bedding): 0.10 kN/m²

The sum of the roof covering was 0.10kN/m². All the other considerations were similar to the German additional dead load (see Section 3.1.2).

3.2.3 Live Loads

The Live Loads, also known as "*Ações Acidentais*"[100], should be considered a minimum of 0.25kN/m². The original structure was calculated to sustain a live load of 0.50kN/m² and thus, this value was maintained.

The equivalent forces ("Forças Nocionais" [101]) derived from the imperfections of the elements were also calculated. Since the elements are determined to be of small or medium displacement (see Section 6.1.2.1, page 126), the horizontal shift between one end to the other end of the element would be L/333 meaning 0.3% of the gravitational load.

3.2.4 Wind Loads

3.2.4.1 Basic Velocity

According to the NBR[102], the Basic Velocity measured for the city of São Luís is 30m/s (see Figure 33). This velocity is the speed of a burst of wind of 3 seconds, which will be overcome in average only once in 50 years, at 10m above ground, in a plain and open field.

3.2.4.2 Characteristic Velocity

To determine the Characteristic Velocity of the Wind, 3 factors must be first analyzed.

3.2.4.2.1 Topographic Factor S_1

The Topographic Factor S_1[103] considers the great variations of the terrain's surface. Since the terrain was considered to be plain, $S_1 = 1$[104] (see Figure 34).

[100] (ABNT NBR 8800, 2008) – Annex B Page 112 (B.5.1)
[101] (ABNT NBR 8800, 2008) – Section 4.9.3.3 Page 25
[102] (ABNT NBR 6123, 1988) – Section 5.1 Page 5
[103] (ABNT NBR 6123, 1988) – Section 5.2 Page 5
[104] (ABNT NBR 6123, 1988) – Section 5.2a Page 5

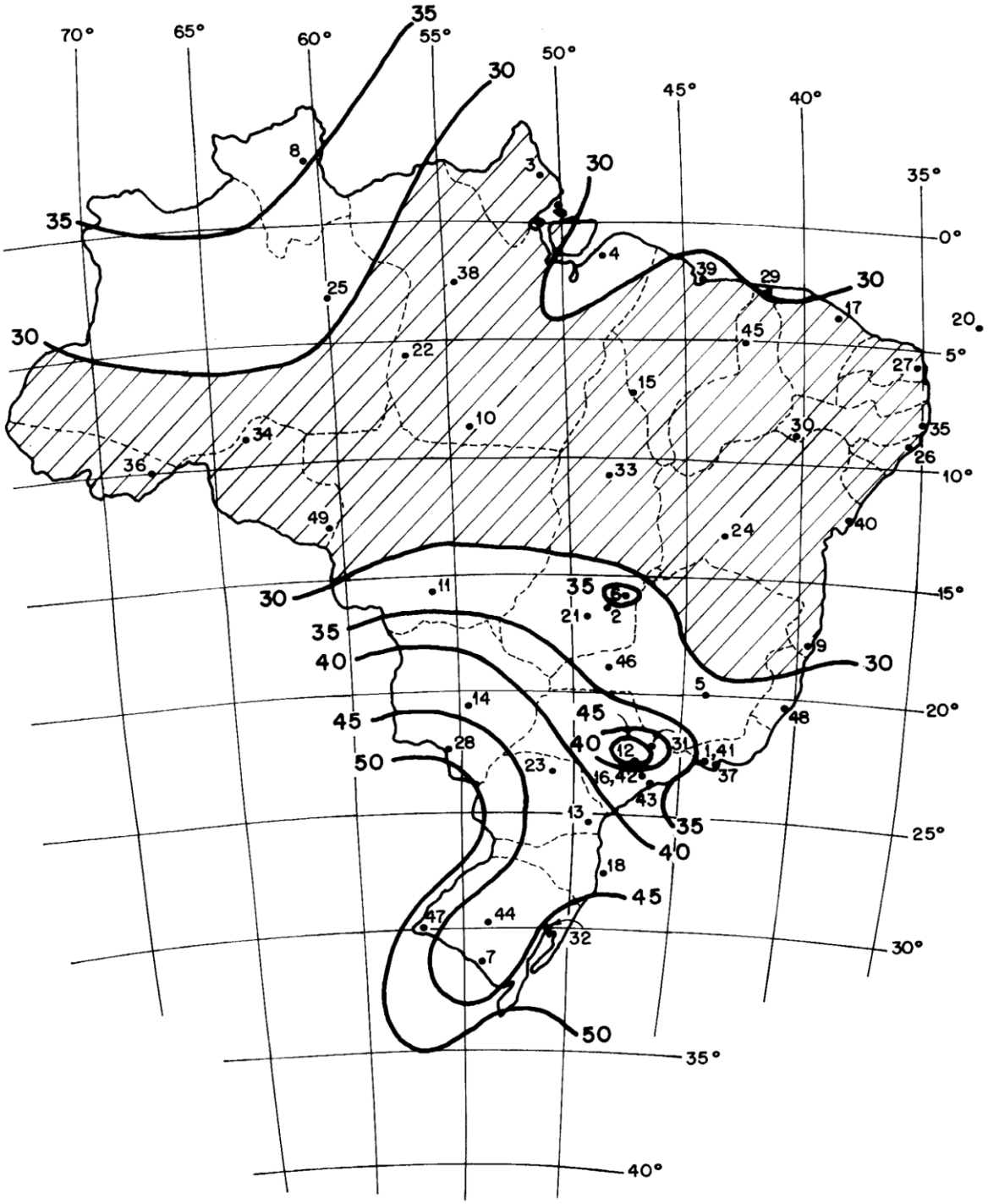

Figure 33: Map of Brazil's Basic Wind Velocity V_o [m/s][105]

[105] (ABNT NBR 6123, 1988) – Figure 1 Page 6

3.2.4.2.2 Terrain Roughness Factor S_2

The Terrain Roughness Factor S_2 is obtained by designating a category (terrain roughness) and a class (dimensions of the building). This factor is a combined effect of the roughness of the terrain, the variation of the speed of wind with the height above ground level and the dimensions of the building (or part of the building in question). During strong winds with neutral stability, the speed of the wind increases as the height of the building rises. This increment depends on the roughness of the terrain and the span of time considered in the determination of the speed. This period of time is related to the dimensions of the building, because smaller edifications and elements of the structure are more affected by short bursts than larger edifications. For these, it is more adequate to consider the average wind calculated with a longer period of time.

a) Roughness of the Terrain

There are five categories for the roughness of the terrain:

- Category I: smooth surface of great dimensions, having more than 5 km in extension in the direction of the wind. Examples: calm sea, lakes, rivers, and swamps with no vegetation.
- Category II: open country being plain (or almost plain) and having few obstacles, such as trees or small constructions. The average height of the obstacles is 1m or less. Examples: plain coastal zone, swamps with few vegetation, aviation fields, prairies, and farms (with no walls or hedges).
- Category III: plain or corrugated territory with obstacle, like walls and hedges, few wind barriers from trees, few small buildings. The average height of the obstacles is 3m. Examples: country houses, farms (with walls and/or hedges), and suburbs (far from center, with sparse small houses).
- Category IV: land covered with numerous obstacles, in a forest, industrial or urban zone. The average height for the obstacles is 10m. This category also includes zones with bigger obstacles that cannot be considered in Category V. Examples: park or wood zones with many trees, small cities and surroundings, densely built suburbs of big cities, and industrial areas (fully or partially developed).
- Category V: area covered with numerous big and tall obstacles and not very spaced. The average height for the obstacles is 25m or higher. Examples: forests with high trees and isolated treetops, centers of huge cities, and very developed industrial complexes.

The terrain category was determined as terrain Category III.

b) Dimensions of the Building

The speed of the wind varies continually, and its average value can be calculated to any period of time. It was verified that the shortest span of time of the usual measures (3s) corresponds to the gusts whose dimensions conveniently involve obstacles with up to 20m in the direction of the wind. The longer the span used to calculate the average speed, the longer the distance encompassed by the gust.

To define the parts of the building to be considered in the actions of the wind, it was necessary to consider structural characteristics that originate few or no structural continuity along the building.

Examples of these characteristics are buildings with joints that separate the structure in two or more independent structures, and buildings with low stiffness perpendicular to the direction of the wind (and because of that, low capacity to redistribute forces).

There are 3 Classes of Buildings:

- Class A: All sealing units, elements of fixation and individual pieces of structures without sealing. All edifications in which the largest horizontal or vertical dimension does not exceed 20m.
- Class B: All buildings or part of the buildings in which the largest horizontal or vertical dimension of the front surface is between 20m and 50m.
- Class C: All buildings or part of the buildings in which the largest horizontal or vertical dimension of the front surface exceeds 50m.

Since the hall's largest dimension is 48m, it was considered as Class B.

c) Factor S_2

The formula to calculate S_2 is as follows:

$$S_2 = b * F_r * \left(\frac{z}{10}\right)^p$$

- F_r is the gust of wind, always correspondent to Category II (see Table 28 below).
- Parameters b and p can also be found in Table 28 .
- Height z_g is the maximum height for z (considered for this project the maximum height of the hall, 11.9m).

In this case, due to the hall being defined as Category III and Class B:

- b = 0.94
- p = 0.105
- F_r = 0.98
- z_g = 350m
- z = 11.9m
  - z_1 = 10m → S_2 = 0.92
  - z_2 = 15m → S_2 = 0.96
  - z = 11.9m → S_2 = 0.9352 (by interpolation)

Thus, S_2 = 0.93818. In favor of security, S_2 was considered the same for the whole structure (from z = 0m to z = 11.9m)

3.2.4.2.3 Statistic Factor S_3

The Statistic Factor S_3 is based on statistics concepts and considers the level of safety required and the total life span of the building. As mentioned in 3.2.4.1, the basic velocity V_o is the speed of the wind with an average recurrence of 50 years. The probability that this velocity will be equaled or overcome in this period of time is 63%.

The level of probability (0.63) and the life span (50 years) assumed are considered adequate for normal buildings intended for housing, offices, hotels etc (Group 2 in Table 27). In case there are no other specific norms, the minimum values of S_3 shall be considered as seen in Table 27.

For the hall, $S_3 = 1.00$.

Grupo	Descrição	S_3
1	Edificações cuja ruína total ou parcial pode afetar a segurança ou possibilidade de socorro a pessoas após uma tempestade destrutiva (hospitais, quartéis de bombeiros e de forças de segurança, centrais de comunicação, etc.)	1,10
2	Edificações para hotéis e residências. Edificações para comércio e indústria com alto fator de ocupação	1,00
3	Edificações e instalações industriais com baixo fator de ocupação (depósitos, silos, construções rurais, etc.)	0,95
4	Vedações (telhas, vidros, painéis de vedação, etc.)	0,88
5	Edificações temporárias. Estruturas dos grupos 1 a 3 durante a construção	0,83

Table 27: Factor S_3[106]

[106] (ABNT NBR 6123, 1988) – Table 3 Page 10

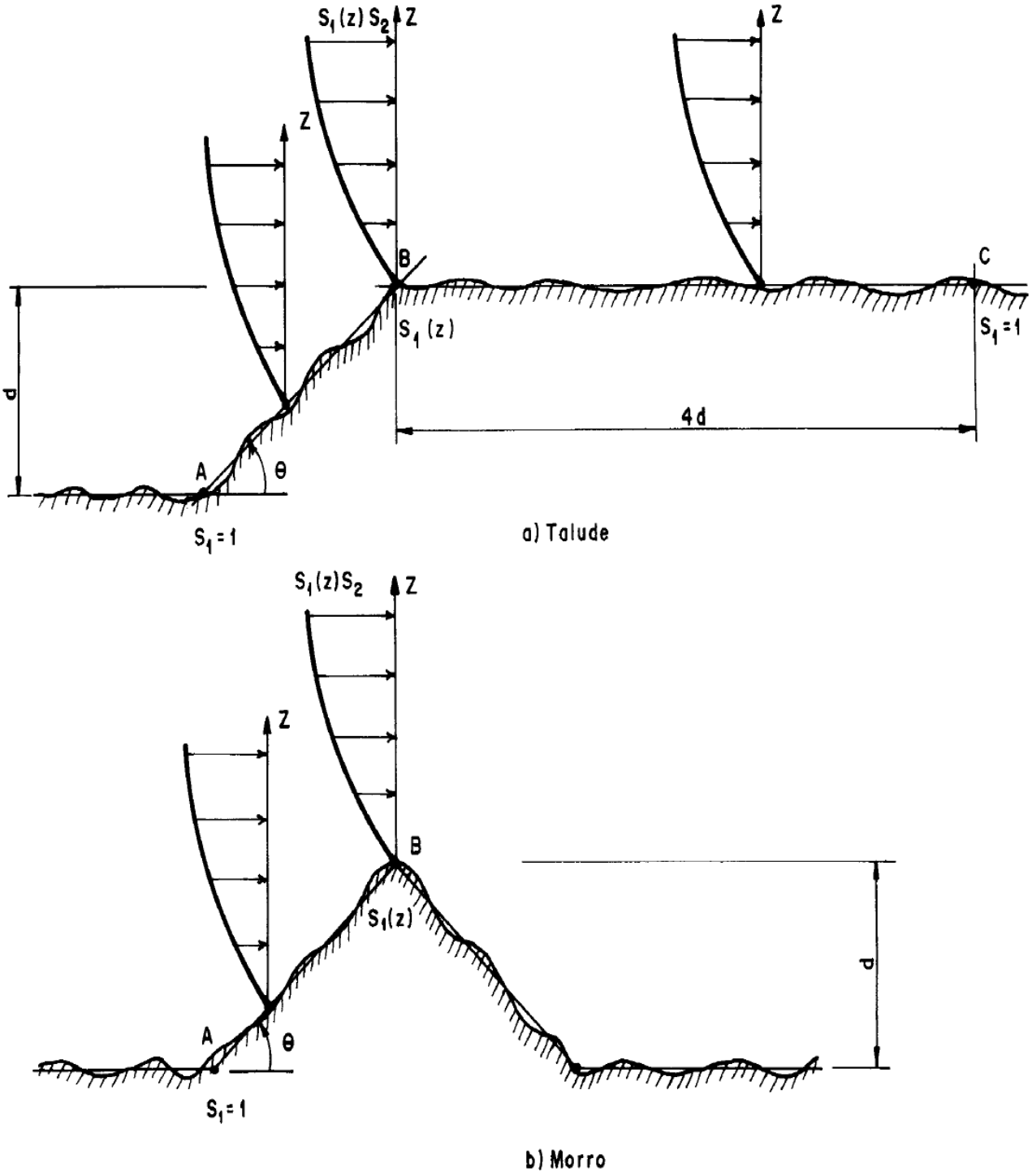

Figure 34: Illustration of the Determination of the S1 Factor[107]

[107] (ABNT NBR 6123, 1988) – Figure 2 Page 7

Categoria	z_g (m)	Parâmetro	Classes		
			A	B	C
I	250	b	1,10	1,11	1,12
		p	0,06	0,065	0,07
II	300	b	1,00	1,00	1,00
		F_r	1,00	0,98	0,95
		p	0,085	0,09	0,10
III	350	b	0,94	0,94	0,93
		p	0,10	0,105	0,115
IV	420	b	0,86	0,85	0,84
		p	0,12	0,125	0,135
V	500	b	0,74	0,73	0,71
		p	0,15	0,16	0,175

Table 28: Meteorological Parameters for S2[108]

z (m)	Categoria														
	I			II			III			IV			V		
	Classe			Classe			Classe			Classe			Classe		
	A	B	C	A	B	C	A	B	C	A	B	C	A	B	C
≤ 5	1,06	1,04	1,01	0,94	0,92	0,89	0,88	0,86	0,82	0,79	0,76	0,73	0,74	0,72	0,67
10	1,10	1,09	1,06	1,00	0,98	0,95	0,94	0,92	0,88	0,86	0,83	0,80	0,74	0,72	0,67
15	1,13	1,12	1,09	1,04	1,02	0,99	0,98	0,96	0,93	0,90	0,88	0,84	0,79	0,76	0,72
20	1,15	1,14	1,12	1,06	1,04	1,02	1,01	0,99	0,96	0,93	0,91	0,88	0,82	0,80	0,76
30	1,17	1,17	1,15	1,10	1,08	1,06	1,05	1,03	1,00	0,98	0,96	0,93	0,87	0,85	0,82
40	1,20	1,19	1,17	1,13	1,11	1,09	1,08	1,06	1,04	1,01	0,99	0,96	0,91	0,89	0,86
50	1,21	1,21	1,19	1,15	1,13	1,12	1,10	1,09	1,06	1,04	1,02	0,99	0,94	0,93	0,89
60	1,22	1,22	1,21	1,16	1,15	1,14	1,12	1,11	1,09	1,07	1,04	1,02	0,97	0,95	0,92
80	1,25	1,24	1,23	1,19	1,18	1,17	1,16	1,14	1,12	1,10	1,08	1,06	1,01	1,00	0,97
100	1,26	1,26	1,25	1,22	1,21	1,20	1,18	1,17	1,15	1,13	1,11	1,09	1,05	1,03	1,01
120	1,28	1,28	1,27	1,24	1,23	1,22	1,20	1,20	1,18	1,16	1,14	1,12	1,07	1,06	1,04
140	1,29	1,29	1,28	1,25	1,24	1,24	1,22	1,22	1,20	1,18	1,16	1,14	1,10	1,09	1,07
160	1,30	1,30	1,29	1,27	1,26	1,25	1,24	1,23	1,22	1,20	1,18	1,16	1,12	1,11	1,10
180	1,31	1,31	1,31	1,28	1,27	1,27	1,26	1,25	1,23	1,22	1,20	1,18	1,14	1,14	1,12
200	1,32	1,32	1,32	1,29	1,28	1,28	1,27	1,26	1,25	1,23	1,21	1,20	1,16	1,16	1,14
250	1,34	1,34	1,33	1,31	1,31	1,31	1,30	1,29	1,28	1,27	1,25	1,23	1,20	1,20	1,18
300	-	-	-	1,34	1,33	1,33	1,32	1,32	1,31	1,29	1,27	1,26	1,23	1,23	1,22
350	-	-	-	-	-	-	1,34	1,34	1,33	1,32	1,30	1,29	1,26	1,26	1,26
400	-	-	-	-	-	-	-	-	-	1,34	1,32	1,32	1,29	1,29	1,29
420	-	-	-	-	-	-	-	-	-	1,35	1,35	1,33	1,30	1,30	1,30
450	-	-	-	-	-	-	-	-	-	-	-	-	1,32	1,32	1,32
500	-	-	-	-	-	-	-	-	-	-	-	-	1,34	1,34	1,34

Table 29: Factor S2 from z[109]

[108] (ABNT NBR 6123, 1988) – Table 1 Page 9
[109] (ABNT NBR 6123, 1988) – Table 2 Page 10

3.2.4.2.4 Characteristic Velocity V_k

The Characteristic Velocity V_k is given by the formula:

$$V_k = V_o * S_1 * S_2 * S_3 = 30 * 1 * 1 * 0.93818 = 28.14541 \frac{m}{s}$$

3.2.4.3 Dynamic Pressure q

The Dynamic Pressure q is given by the expression:

$$q = 0.613 * V_k^2 = 0.613 * 28.14541^2 = 485.5967 \frac{N}{m^2} = 0.4856\ kN/m^2$$

3.2.4.4 Internal Pressure Coefficient c_{pi}

According to NBR[110], there will be a so-called "dominant opening" if the total area of an opening is equal to or more than the total area of all the other openings on the external surface of the building. The areas of the openings of each side are:

- Front: 53.4 m² (5.9m x 8m + 3.4m x 2m)
- Back: 76.45m² (13.9m x 5.5m)
- Sides: 120 m² (1.5m x 48m + 1m x 48m)

Therefore, the hall does not have a dominant opening.

In order to simplify and in favor of security, although the hall has openings on the roof, it was considered as closed, since the internal pressure would be smaller and its forces also smaller[111]. Moreover, the building was considered to have 4 equal permeable sides[112], meaning:

$$c_{pi} = -0.3\ or\ 0$$

The value used should be the most harmful.

It is important to notice that a negative pressure means suction and a positive pressure means overpressure.

[110] (ABNT NBR 6123, 1988) – Section 6.2.4 Page 12
[111] (ABNT NBR 6123, 1988) – Section 6.2.9 Page 13
[112] (ABNT NBR 6123, 1988) – Section 6.2.5b Page 13

3.2.4.5 External Pressure Coefficient c_{pe}

3.2.4.5.1 c_{pe} for Walls

To determine the External Pressure Coefficients c_{pe} indicated in Table 30, the necessary dimensions were (the same as the before, see Section 3.1.4.3):

- h = 11.9m
- a = 48m
- b = 19.8m
- θ = 8.6° (angle of roof)

Then, two calculations were made:

$$\frac{h}{b} = \frac{11.9}{19.8} = 0.601$$

a) $0.5 < \frac{h}{b} \leq 1.5$

$$\frac{a}{b} = \frac{48}{19.8} = 2.42$$

b) $2 \leq \frac{a}{b} \leq 4$

Therefore, the values for the c_{pe}, according to Table 30, for each section were determined as follows:

For α = 0°:

- A_1 and B_1 = -0.9
- A_2 and B_2 = -0.4
- A_3 and B_3 = -0.2
- C = 0.7
- D = -0.3

For α = 90°:

- A = 0.7
- B = -0.6
- C_1 and D_1 = -0.9
- C_2 and D_2 = -0.5

And the length for each section:

For α = 0°:

The length for A_1 and B_1 should be:

$$L = \max\left\{\frac{b}{3}, \frac{a}{4}\right\} \leq 2h$$

Meaning the largest between b/3 and a/4 but not surpassing 2h.

Since

$$\frac{b}{3} = 6.6 < \frac{a}{4} = 12$$

And

$$\frac{a}{4} = 12 < 2h = 23.8$$

- A_1 and B_1 = 12m
- A_2 and B_2 = 12m
- A_3 and B_3 = 24m
- C = 19.8m
- D = 19.8m

For α = 90°:

The length of C_1 and D_1 should be:

$$L = \min\left\{2h, \frac{b}{2}\right\}$$

Meaning the smallest between 2h and b/2.

Since

$$\frac{b}{2} = \frac{19.8}{2} = 9.9 < 2h = 23.8$$

- A = 48m
- B = 48m
- C_1 and D_1 = 9.9m
- C_2 and D_2 = 9.9m

The coefficients for external pressure on the walls and their distribution along the walls of the hall can be seen in Table 31, Figure 35 and Figure 36.

Altura relativa		Valores de C_e para								c_{pe} médio
		$\alpha = 0°$				$\alpha = 90°$				
		A_1 e B_1	A_2 e B_2	C	D	A	B	C_1 e D_1	C_2 e D_2	
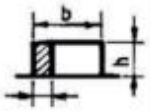 0,2 b ou h (o menor dos dois) $\frac{h}{b} \leq \frac{1}{2}$	$1 \leq \frac{a}{b} \leq \frac{3}{2}$	- 0,8	- 0,5	+ 0,7	- 0,4	+ 0,7	- 0,4	- 0,8	- 0,4	- 0,9
	$2 \leq \frac{a}{b} \leq 4$	- 0,8	- 0,4	+ 0,7	- 0,3	+ 0,7	- 0,5	- 0,9	- 0,5	- 1,0
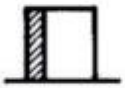 $\frac{1}{2} < \frac{h}{b} \leq \frac{3}{2}$	$1 \leq \frac{a}{b} \leq \frac{3}{2}$	- 0,9	- 0,5	+ 0,7	- 0,5	+ 0,7	- 0,5	- 0,9	- 0,5	- 1,1
	$2 \leq \frac{a}{b} \leq 4$	- 0,9	- 0,4	+ 0,7	- 0,3	+ 0,7	- 0,6	- 0,9	- 0,5	- 1,1
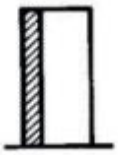 $\frac{3}{2} < \frac{h}{b} \leq 6$	$1 \leq \frac{a}{b} \leq \frac{3}{2}$	- 1,0	- 0,6	+ 0,8	- 0,6	+ 0,8	- 0,6	- 1,0	- 0,6	- 1,2
	$2 \leq \frac{a}{b} \leq 4$	- 1,0	- 0,5	+ 0,8	- 0,3	+ 0,8	- 0,6	- 1,0	- 0,6	- 1,2

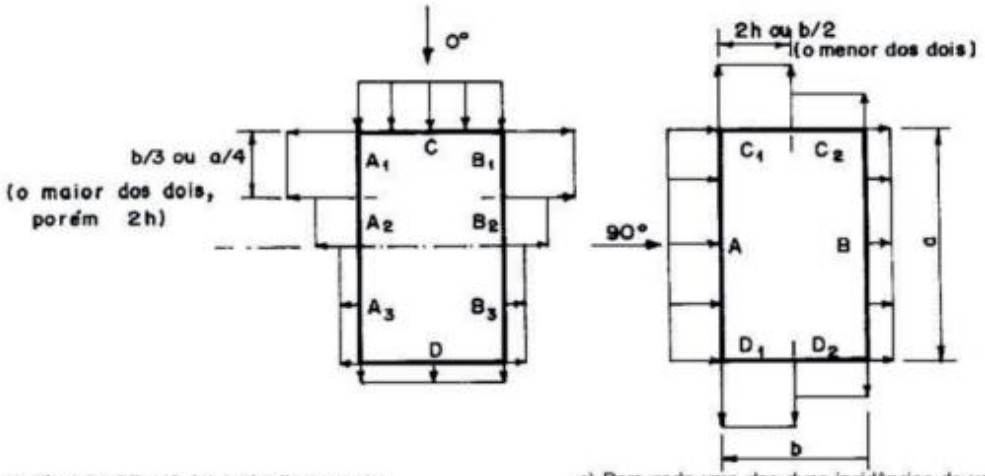

Notas: a) Para a/b entre 3/2 e 2, interpolar linearmente.

b) Para vento a 0°, nas partes A_3 e B_3, o coeficiente de forma C_e tem os seguintes valores:

- para a/b = 1: mesmo valor das partes A_2 e B_2;
- para a/b ≥ 2: C_e = - 0,2;
- para 1 < a/b < 2: interpolar linearmente.

c) Para cada uma das duas incidências do vento (0° ou 90°), o coeficiente de pressão médio externo c_{pe} médio, é aplicado à parte de barlavento das paredes paralelas ao vento, em uma distância igual a 0,2 b ou h, considerando-se o menor destes dois valores.

d) Para determinar o coeficiente de arrasto, C_a, deve ser usado o gráfico da Figura 4 (vento de baixa turbulência) ou da Figura 5 (vento de alta turbulência - ver 6.5.3).

Table 30: External Pressure Coefficient for Walls c_{pe}[113]

[113] (ABNT NBR 6123, 1988) – Table 4 Page 14

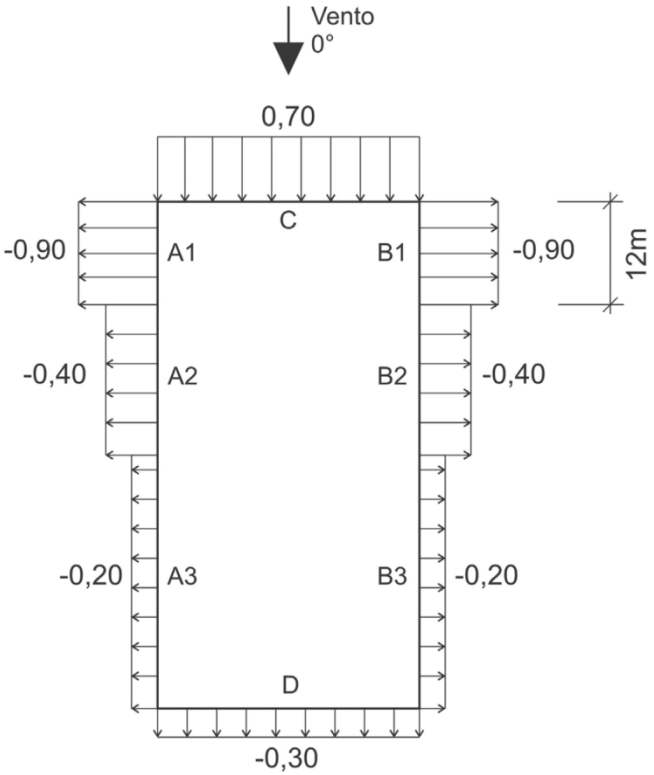

Figure 35: c_{pe} for Walls for Wind at 0°[114]

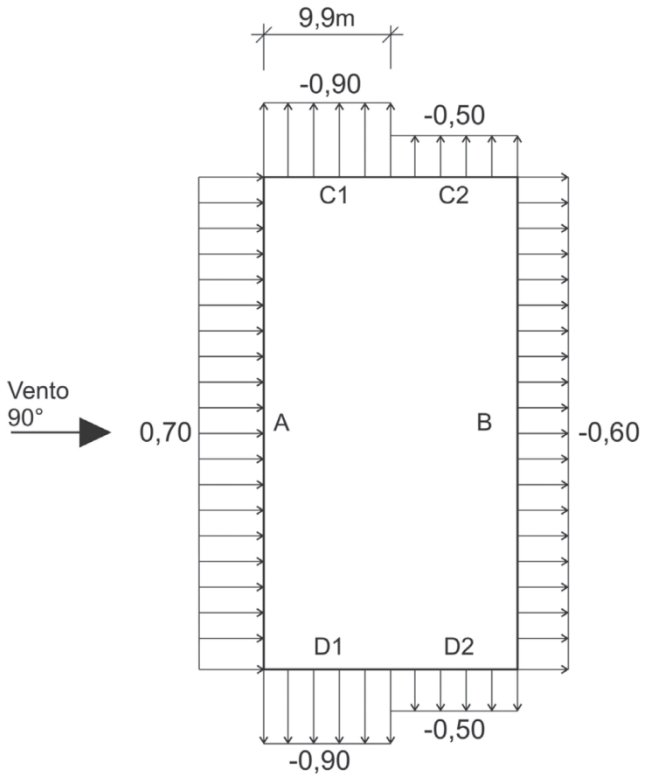

Figure 36: c_{pe} for Walls for Wind at 90°[115]

[114] (DREHMER, MESACASA JÚNIOR, & PRAVIA, 2010) – Figure 30 (Adapted) Page 24
[115] (DREHMER, MESACASA JÚNIOR, & PRAVIA, 2010) – Figure 31 (Adapted) Page 24

0°	length [m]	C_{pe}
A1 = B1 =	12	**-0.9**
A2 = B2 =	12	**-0.4**
A3 = B3 =	24	**-0.2**
C =	19.8	**0.7**
D =	19.8	**-0.3**

90°	length [m]	C_{pe}
A =	48	**0.7**
B =	48	**-0.6**
C1 = D1 =	9.9	**-0.9**
C2 = D2 =	9.9	**-0.5**

Table 31: Values for c_{pe} on the Walls and Lengths for each Section

3.2.4.5.2 c_{pe} for Roof

As in Section 3.2.4.5.1, the c_{pe} for the roof will also be determined by the relation:

$$\frac{h}{b} = \frac{11.9}{19.8} = 0.601$$

a) $0.5 < \frac{h}{b} \leq 1.5$

Since θ = 8.6°, c_{pe} coefficients for the roof for each section, according to Table 30, were determined as follows:

For α = 0°:

- E and G = -0.8
- F and H = -0.6
- I and J = -0.2

For α = 90°:

- E and F = -1.0
- G and H = -0.6
- I = -1.0
- J = -0.6

And the length for each section (exactly as Section 3.2.4.5.1):

The length for E and G should be:

$$L = \max\left\{\frac{b}{3}, \frac{a}{4}\right\} \leq 2h$$

Meaning the largest between b/3 and a/4 but not surpassing 2h.

Since

$$\frac{b}{3} = 6.6 < \frac{a}{4} = 12$$

And

$$\frac{a}{4} = 12 < 2h = 23.8$$

- E and G = 12m
- F and H = 12m
- I and J = 24m

The values of the coefficients for external pressure on the roof and their distribution along the walls of the hall can be seen in Table 32, Figure 37 and Figure 38 .

C_{pe}			
α			
0°		90°	
EG	**-0.8**	EF	**-1**
FH	**-0.6**	GH	**-0.6**
I	**-0.2**	I	**-1**
J	**-0.2**	J	**-0.6**

Table 32: Values for c_{pe} on the Roof for each Section

Altura relativa	θ	Valores de C_e para				c_{pe} médio			
		α = 90° (A)		α = 0°					
		EF	GH	EG	FH				
$\frac{h}{b} \leq \frac{1}{2}$ 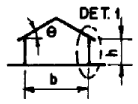	0°	-0,8	-0,4	-0,8	-0,4	-2,0	-2,0	-2,0	--
	5°	-0,9	-0,4	-0,8	-0,4	-1,4	-1,2	-1,2	-1,0
	10°	-1,2	-0,4	-0,8	-0,6	-1,4	-1,4		-1,2
	15°	-1,0	-0,4	-0,8	-0,6	-1,4	-1,2		-1,2
	20°	-0,4	-0,4	-0,7	-0,6	-1,0			-1,2
	30°	0	-0,4	-0,7	-0,6	-0,8			-1,1
	45°	+0,3	-0,5	-0,7	-0,6				-1,1
	60°	+0,7	-0,6	-0,7	-0,6				-1,1
$\frac{1}{2} < \frac{h}{b} \leq \frac{3}{2}$ 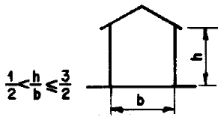	0°	-0,8	-0,6	-1,0	-0,6	-2,0	-2,0	-2,0	--
	5°	-0,9	-0,6	-0,9	-0,6	-2,0	-2,0	-1,5	-1,0
	10°	-1,1	-0,6	-0,8	-0,6	-2,0	-2,0	-1,5	-1,2
	15°	-1,0	-0,6	-0,8	-0,6	-1,8	-1,5	-1,5	-1,2
	20°	-0,7	-0,5	-0,8	-0,6	-1,5	-1,5	-1,5	-1,0
	30°	-0,2	-0,5	-0,8	-0,8	-1,0			-1,0
	45°	+0,2	-0,5	-0,8	-0,8				
	60°	+0,6	-0,5	-0,8	-0,8				
$\frac{3}{2} < \frac{h}{b} \leq 6$ 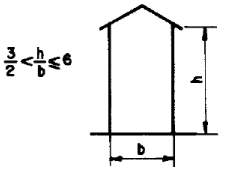	0°	-0,8	-0,6	-0,9	-0,7	-2,0	-2,0	-2,0	--
	5°	-0,8	-0,6	-0,8	-0,8	-2,0	-2,0	-1,5	-1,0
	10°	-0,8	-0,6	-0,8	-0,8	-2,0	-2,0	-1,5	-1,2
	15°	-0,8	-0,6	-0,8	-0,8	-1,8	-1,8	-1,5	-1,2
	20°	-0,8	-0,6	-0,8	-0,8	-1,5	-1,5	-1,5	-1,2
	30°	-1,0	-0,5	-0,8	-0,7	-1,5			
	40°	-0,2	-0,5	-0,8	-0,7	-1,0			
	50°	+0,2	-0,5	-0,8	-0,7				
	60°	+0,5	-0,5	-0,8	-0,7				

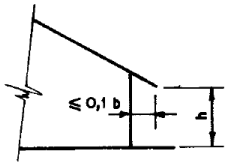

DETALHE 1

Notas: a) O coeficiente de forma C_e na face inferior do beiral é igual ao da parede correspondente.

b) Nas zonas em torno de partes de edificações salientes ao telhado (chaminés, reservatórios, torres, etc.), deve ser considerado um coeficiente de forma C_e = 1,2, até uma distância igual à metade da dimensão da diagonal da saliência vista em planta.

c) Na cobertura de lanternins, c_{pe} médio = - 2,0.

d) Para vento a 0°, nas partes I e J o coeficiente de forma C_e tem os seguintes valores:

a/b = 1: mesmo valor das partes F e H; a/b ≥ 2: C_e = - 0,2.

Interpolar linearmente para valores intermediários de a/b.

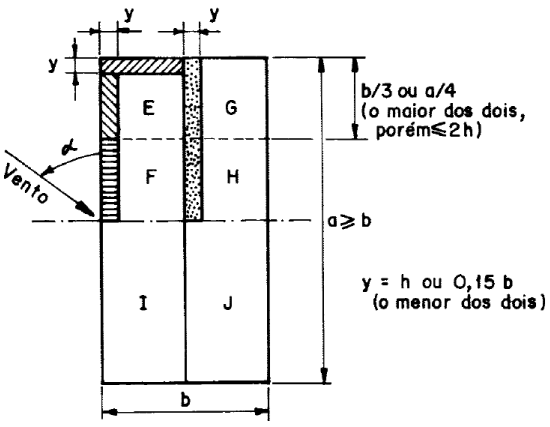

Table 33: External Pressure Coefficient for Roof c_{pe} [116]

[116] (ABNT NBR 6123, 1988) – Table 5 Page 15

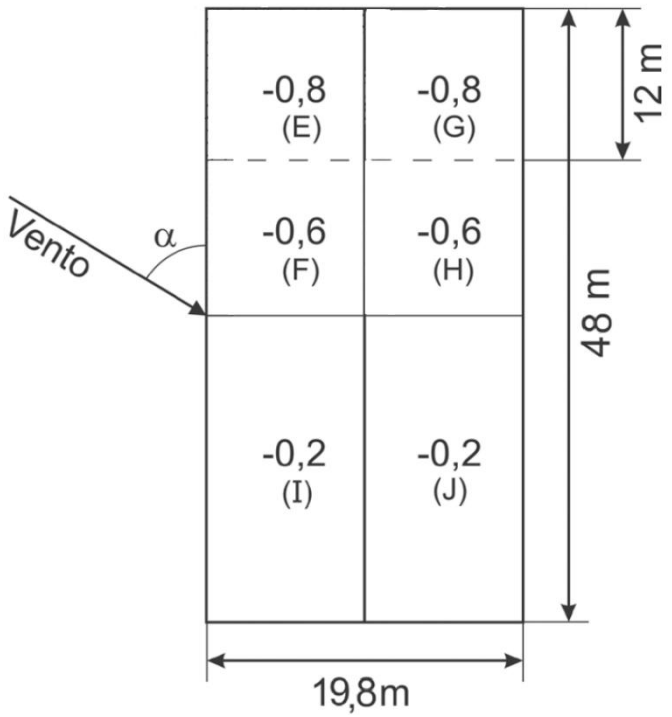

Figure 37: c_{pe} for Roof for Wind at 0°[117]

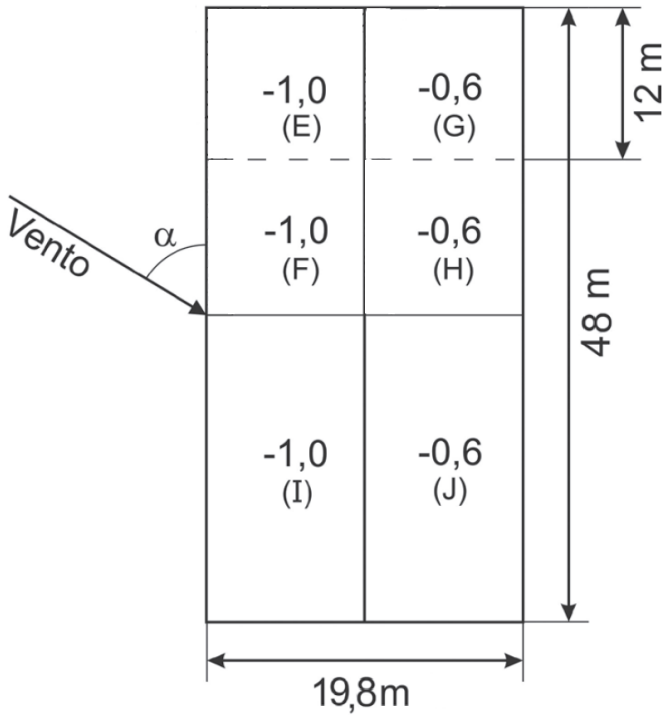

Figure 38: c_{pe} for Roof for Wind at 90°[118]

[117] (DREHMER, MESACASA JÚNIOR, & PRAVIA, 2010) – Figure 33 (Adapted) Page 25
[118] (DREHMER, MESACASA JÚNIOR, & PRAVIA, 2010) – Figure 34 (Adapted) Page 25

3.2.4.6 Combinations of c_{pi} and c_{pe} for the Frames

The c_{pi} coefficients are distributed on the frames as follows:

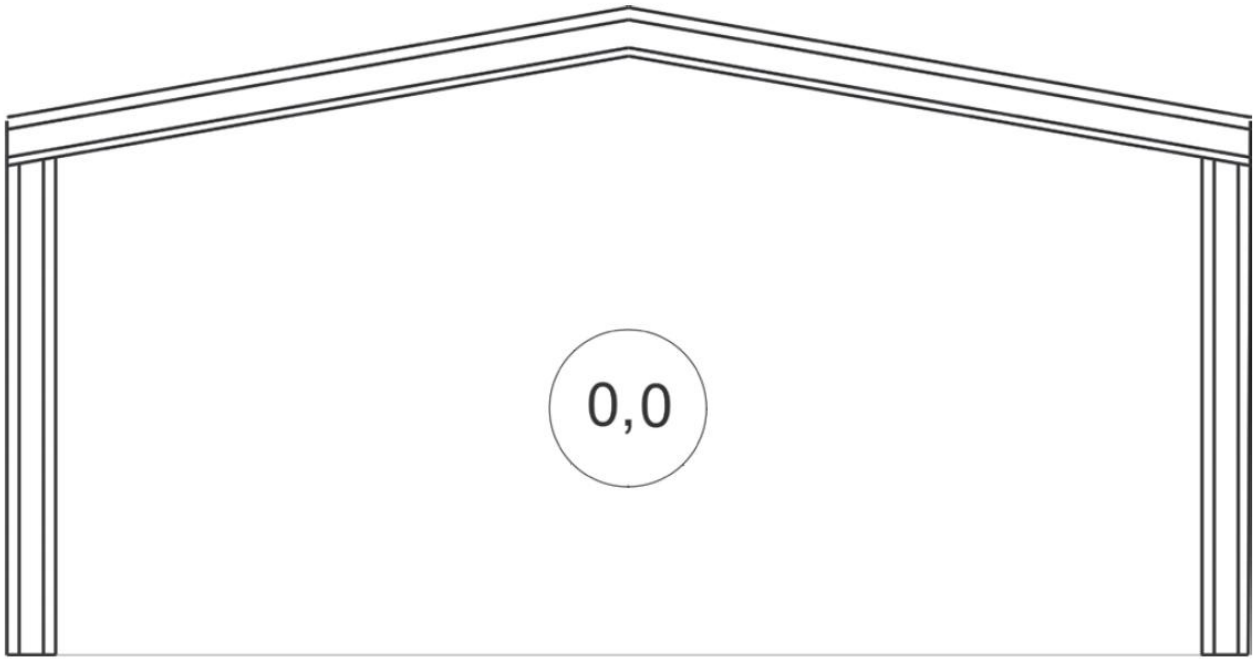

Figure 39: Sketch of c_{pi} = 0[119]

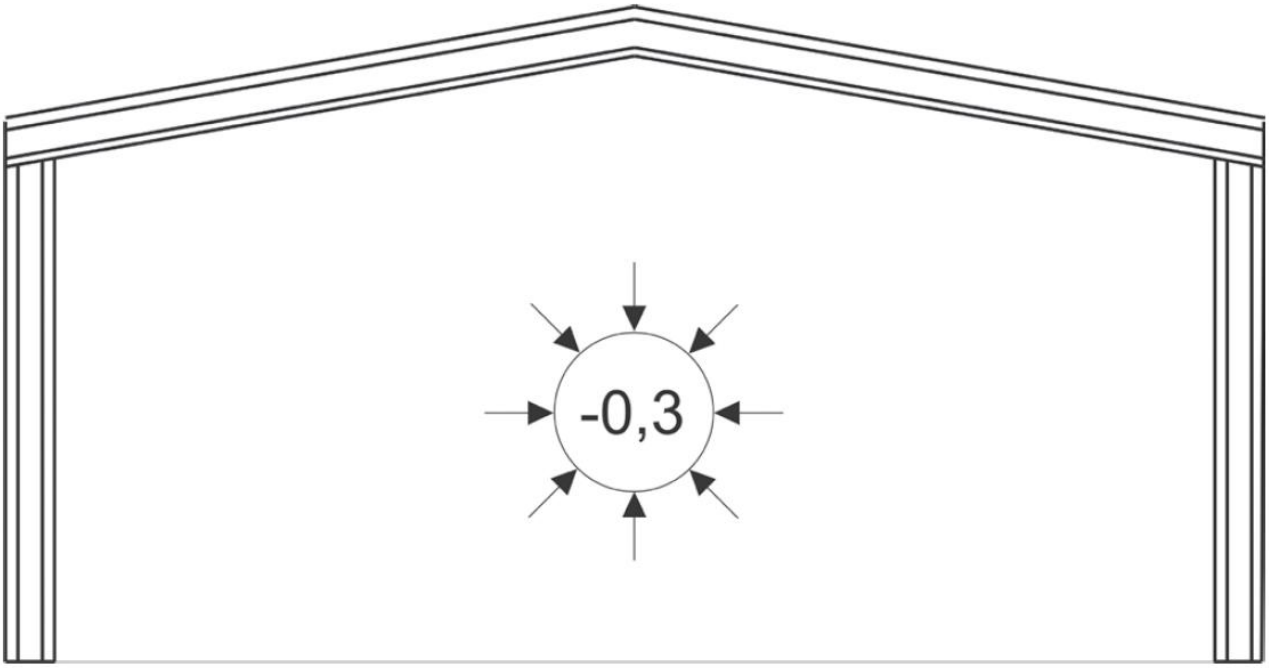

Figure 40: Sketch of c_{pi} = -0.3[120]

[119] (DREHMER, MESACASA JÚNIOR, & PRAVIA, 2010) – Figure 35 (Adapted) Page 25

There were 4 different combinations (or cases) possible, to achieve the most harmful wind pressure:

3.2.4.6.1 Case 1: c_{pi} (0) + c_{pe} (0°)

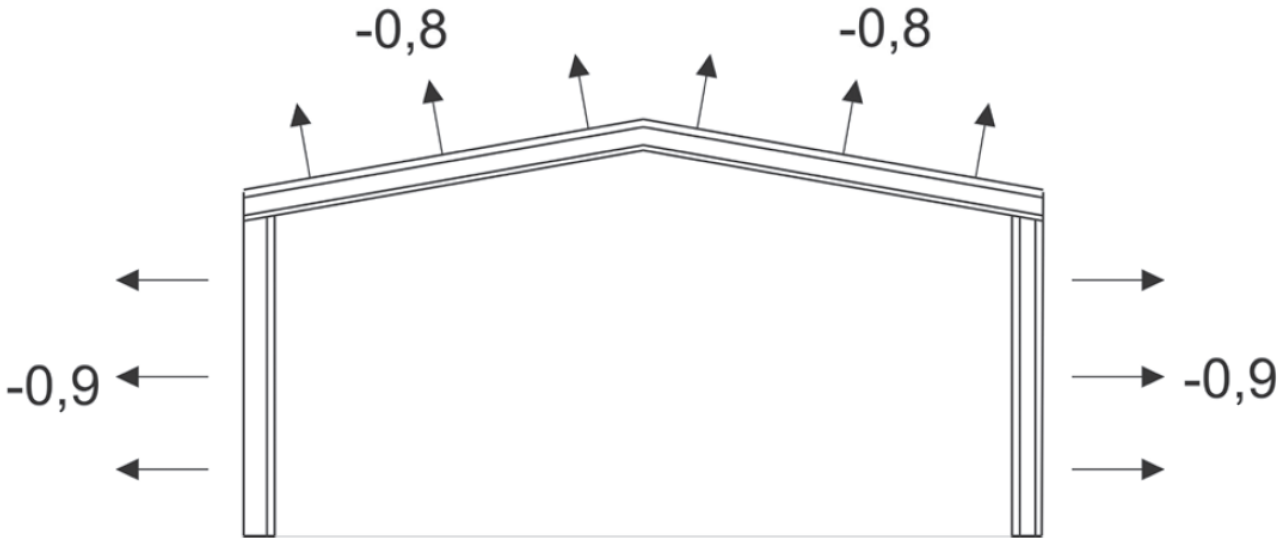

Figure 41: Distribution of Wind Pressure for Case 1: c_{pi} (0) + c_{pe} (0°)[121]

3.2.4.6.2 Case 2: c_{pi} (0) + c_{pe} (90°)

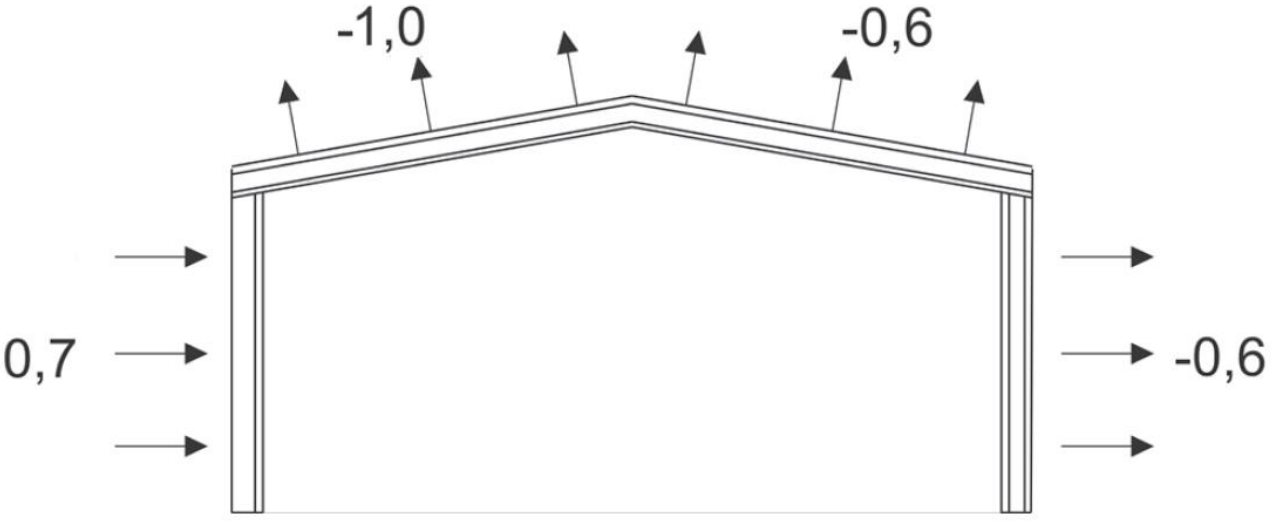

Figure 42: Distribution of Wind Pressure for Case 2: c_{pi} (0) + c_{pe} (90°)[122]

[120] (DREHMER, MESACASA JÚNIOR, & PRAVIA, 2010) – Figure 36 Page 25
[121] (DREHMER, MESACASA JÚNIOR, & PRAVIA, 2010) – Figure 40 (Adapted) Page 26
[122] (DREHMER, MESACASA JÚNIOR, & PRAVIA, 2010) – Figure 42 (Adapted) Page 26

3.2.4.6.3 Case 3: c_{pi} (-0.3) + c_{pe} (0°)

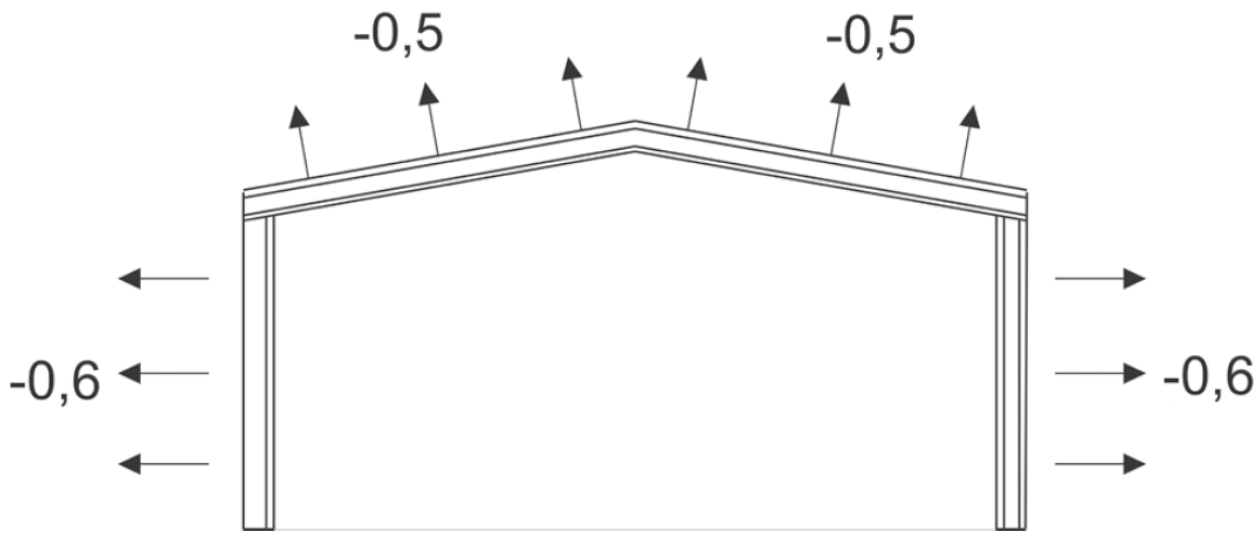

Figure 43: Distribution of Wind Pressure for Case 3: c_{pi} (-0.3) + c_{pe} (0°)[123]

3.2.4.6.4 Case 4: c_{pi} (-0.3) + c_{pe} (90°)

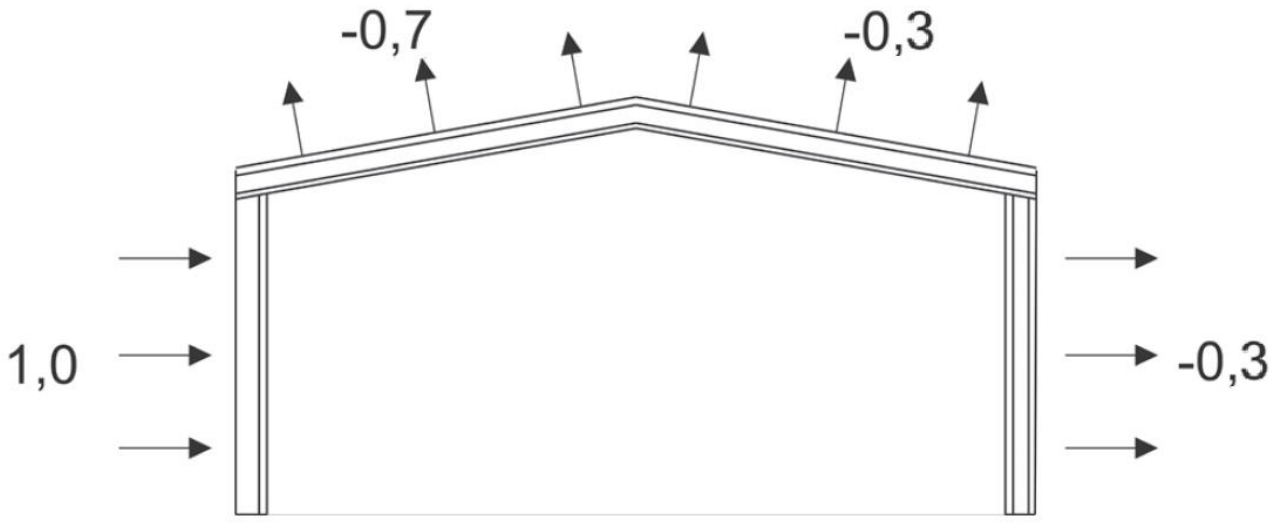

Figure 44: Distribution of Wind Pressure for Case 4: c_{pi} (-0.3) + c_{pe} (90°)[124]

The cases with a most harmful (higher values) wind pressure for the frame were the cases 1 and 2.

[123] (DREHMER, MESACASA JÚNIOR, & PRAVIA, 2010) – Figure 40 (Adapted) Page 26
[124] (DREHMER, MESACASA JÚNIOR, & PRAVIA, 2010) – Figure 42 (Adapted) Page 26

3.2.4.7 Basic Linear Force on the Frames

The forces on the frames were determined in two steps. First, since the distance between each frame is 6m, the dynamic pressure (q) must be multiplied by this distance in order to obtain the linear force acting upon the frame:

$$F = q * 6m = 0.4856 \left[\frac{kN}{m^2}\right] * 6m = 2.91358 \left[\frac{kN}{m}\right]$$

3.2.4.8 Linear Forces on the Frames

After finding the value of the force that will act upon the frame, the second step was to multiply it by the combination of the coefficients (cases 1 and 2). Although only cases 1 and 2 were exemplified, all load cases were applied to the model.

3.2.4.8.1 Linear Forces in Case 1

In Case 1, the combinations of the coefficients were -0.8 and -0.9:

$$F * -0.8 = -2.33 \left[\frac{kN}{m}\right]$$

And

$$F * -0.9 = -2.62 \left[\frac{kN}{m}\right]$$

And the distribution of the final linear loads can be seen in Figure 45 below:

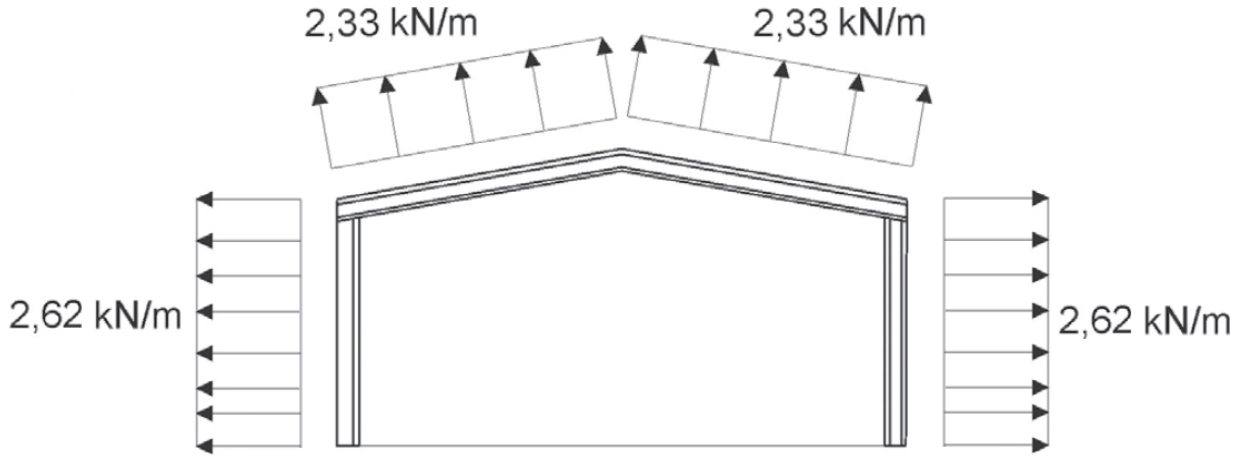

Figure 45: Distribution of Final Linear Loads for Case 1[125]

[125] (DREHMER, MESACASA JÚNIOR, & PRAVIA, 2010) – Figure 43 (Adapted) Page 27

3.2.4.8.2 Linear Forces in Case 2

In Case 2, the combinations of the coefficients were 1.0, 0.7 and -0.6:

$$F * 0.7 = 2.04 \left[\frac{kN}{m}\right]$$

And

$$F * -0.6 = -1.75 \left[\frac{kN}{m}\right]$$

And the distribution of the final linear loads can be seen in

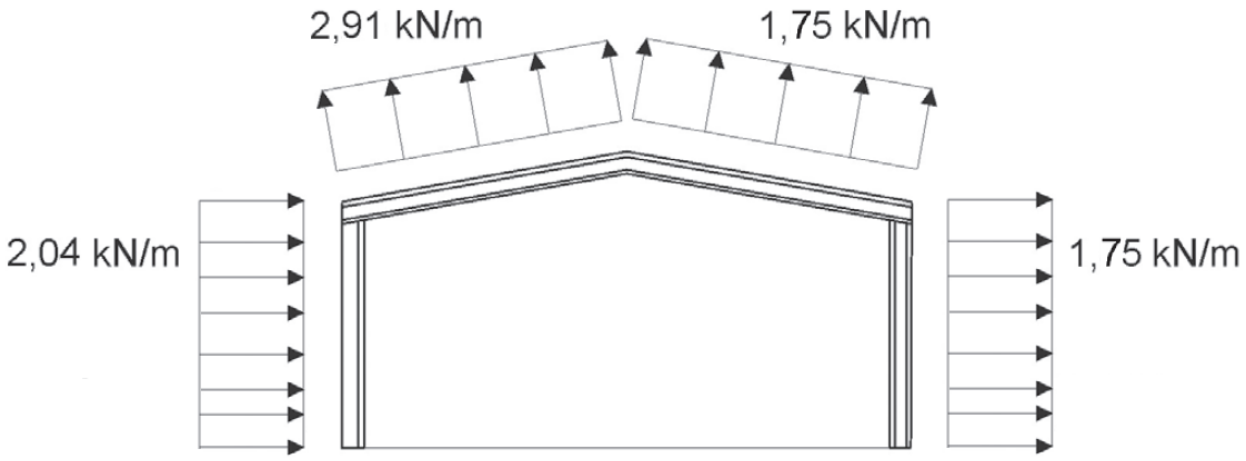

Figure 46: Distribution of Final Linear Loads for Case 2[126]

3.2.5 Snow Loads

As mentioned in Chapter 3 and Section 3.1.5, European norms, such as the German DIN EN, must take snow loads into consideration, while the Brazilian norm NBR by the ABNT has no reference to it. However, the original building is located in Brazil and was built according to the NBR, which does not consider snow loads for the dimensioning of buildings. Thus, in order to achieve a better comparison between the Brazilian modeled structure and the German modeled structure, the snow load calculations were not taken into account. In its place, the Live Load ("*Ação Acidental*") would substitute it accordingly – see explanation in Section 3.1.3.

[126] (DREHMER, MESACASA JÚNIOR, & PRAVIA, 2010) – Figure 43 (Adapted) Page 27

3.2.6 Crane Loads

3.2.6.1 Vertical Loads

The crane load was determined by the combined weight of the maximum lifting load (15 tons), self-weight of the trolley and the self-weight of the crane. The method used in this project was to determine the wheel loads that would act upon the runway girder.

These loads were calculated as if there were 4 wheels (2 on each side). The distance between the runway girders is 19m.

The vertical load was determined by the combined weight of the maximum lifting load, self-weight of the crane and the self-weight of the trolley:

- Maximum Lifting Load: 15 tons
- Self-Weight of Crane: 25%[127] of Max Lifting Load = 25% * 15 tons = 3.75 tons
- Self-Weight of Trolley: 10% of Max Lifting Load = 10% * 15 tons = 1.5 tons

To achieve the maximum load of the crane on the column, the distance of the trolley lifting 15 tons should be closest possible to the column. The closest the lifting load of the crane in the project can get to the column is 1.1m. Figure 47 indicates the distances. In Figure 48, it is possible to see where the crane would be located.

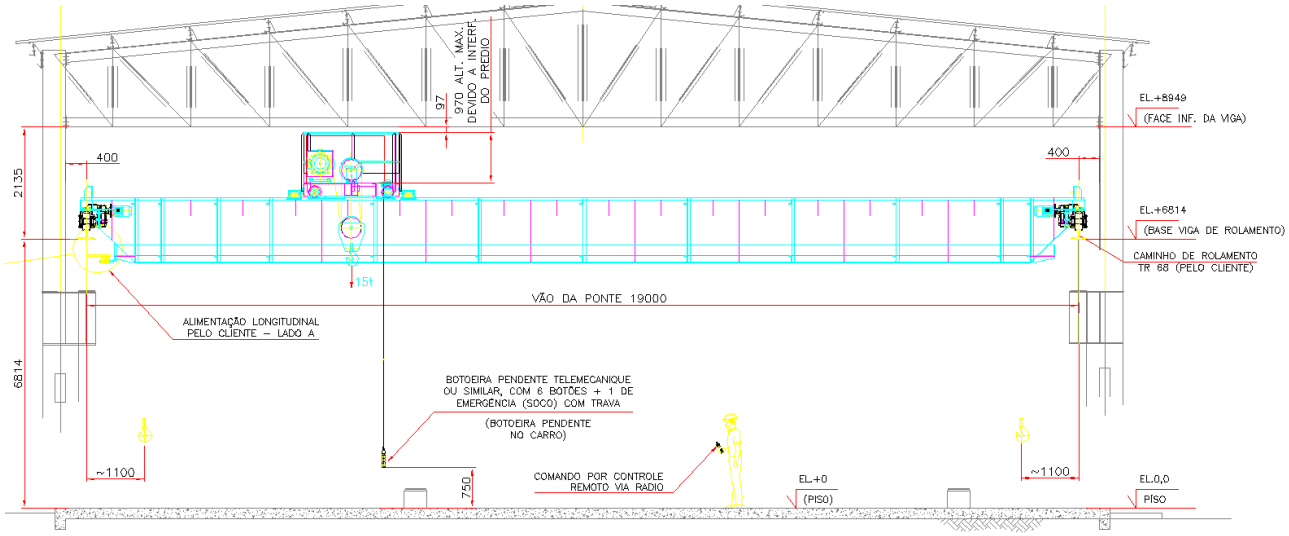

Figure 47: Crane Detail

[127] Obs: an update on the NBR 6120 (Load Analysis) is currently under revision and the new percentage will probably be considered around 20% for crane and trolley combined.

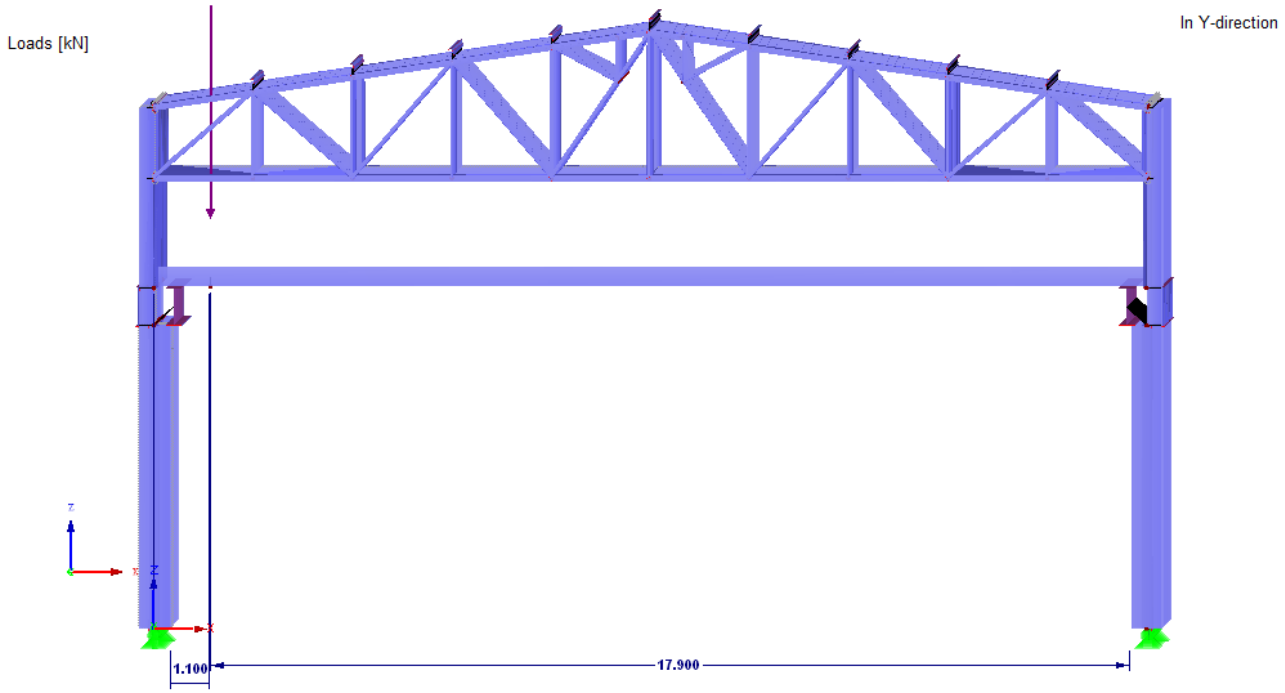

Figure 48: Sketch of the Location of the Trolley for Maximum Load

To calculate the vertical load transferred from the wheels of the crane to the runway girder, 3 calculations were made:

- Self-Weight of the Crane (divided to each wheel):

$$\frac{3.75}{4} = 0.9375\ tons = 9.375\ kN$$

- Self-Weight of the Trolley
  - First determine the vertical load on the column due to the cart:

$$\text{MAX: } 1.5 * \frac{17.9}{19} = 1.41316\ tons = 14.1316\ kN$$

$$\text{MIN: } 1.5 * \frac{1.1}{19} = 0.08684\ tons = 0.8684\ kN$$

  - Then divide it between the 2 wheels of a side:

$$\text{MAX: } \frac{1.41316}{2} = 0.70658\ tons = 7.0658\ kN$$

$$\text{MIN: } \frac{0.08684}{2} = 0.04342\ tons = 0.4342\ kN$$

- Maximum Lifting Load

  - First determine the vertical loads on the column due to the Lifting Load:

$$\text{MAX: } 15 * \frac{17.9}{19} = 14.13158\ tons = 141.3158\ kN$$

$$\text{MIN: } 15 * \frac{1.1}{19} = 0.86842\ tons = 8.6842\ kN$$

  - Then divide it between the 2 wheels of a side:

$$\text{MAX: } \frac{14.13158}{2} = 7.06579\ tons = 70.6579\ kN$$

$$\text{MIN: } \frac{0.86842}{2} = 0.43421\ tons = 4.3421\ kN$$

The combination of the vertical forces (for each wheel) is given by:

$$\text{MAX: } 0.9375 + 0.70658 + 7.06579 = 8.70987\ tons = 87.0987\ kN$$
$$\text{MIN: } 0.9375 + 0.04342 + 0.43421 = 1.41513\ tons = 14.1513\ kN$$

In the NBR[128], cranes controlled by a remote should be increased by 10% due to the impact factor:

$$\text{MAX: } 8.70987 * 1.1 = 9.58089\ tons = 95.8089\ kN = 95.8\ kN$$
$$\text{MIN: } 1.41513 * 1.1 = 1.60441\ tons = 16.0441\ kN = 16\ kN$$

3.2.6.2 Horizontal Loads (Transversal)

In NBR[129], cranes controlled by remote have the horizontal loads (RH) equal to 10% of the sum of the vertical loads:

$$\text{MAX: } (14.13158 + 3.75 + 1.41316) * 0.1 = 1.92947\ tons = 19.2947\ kN$$
$$\text{MIN: } (0.86842 + 3.75 + 0.08684) * 0.1 = 0.47052\ tons = 4.7052\ kN$$

Multiplied by the impact factor:

$$\text{MAX: } 1.92947 * 1.1 = 2.12242\ tons = 21.2242\ kN = 21.2\ kN$$
$$\text{MIN: } 0.47052 * 1.1 = 0.51758\ tons = 5.1758\ kN = 5.2\ kN$$

3.2.6.3 Longitudinal Loads

In NBR[130], cranes have the longitudinal loads (RL) equal to 10% of the sum of the vertical loads on the wheel (not increased by the impact factor of 1.1).

$$\text{MAX: } 8.70987 * 0.1 = 0.87099\ tons = 8.7099\ kN = 8.7\ kN$$
$$\text{MIN: } 1.41513 * 0.1 = 0.14151\ tons = 1.4151\ kN = 1.4\ kN$$

[128] (ABNT NBR 8800, 2008) – Annex B Page 112 (B.4.4b)
[129] (ABNT NBR 8800, 2008) – Annex B Page 113 (B.7.2a)
[130] (ABNT NBR 8800, 2008) – Annex B Page 113 (B.7.2b)

3.2.6.4 Moment Forces (due to Eccentricities)

See Section 3.1.6.4.

3.2.6.5 Modeling of the Runway Girder

As seen in Table 34, the profile of the runway girder is PS 750x128.7. To the program, the modeled cross-section used was the VS 750x125 which was very similar to the original. According to NBR[131], the combination of actions for a single-naved hall with only one crane should consider:

- Vertical loads majored by impact
- 100% from horizontal, transversal and longitudinal forces

The loads imposed on the beam were:

- RV = 95.8 kN
- RH = 21.2 kN
- RL= 8.7 kN (even though it is not necessary for this type of verification)

Similar to the Section 3.1.6.5, there were 2 load cases to be considered. First, the crane was imagined to be in the middle, where the maximum shear forces would occur (for a one-spanned beam). This middle meant that the wheels would have a distance of 1.2m from the edges of the beam and have a distance of 3.6m between them. Figure 49 depicts the modeling of the loads.

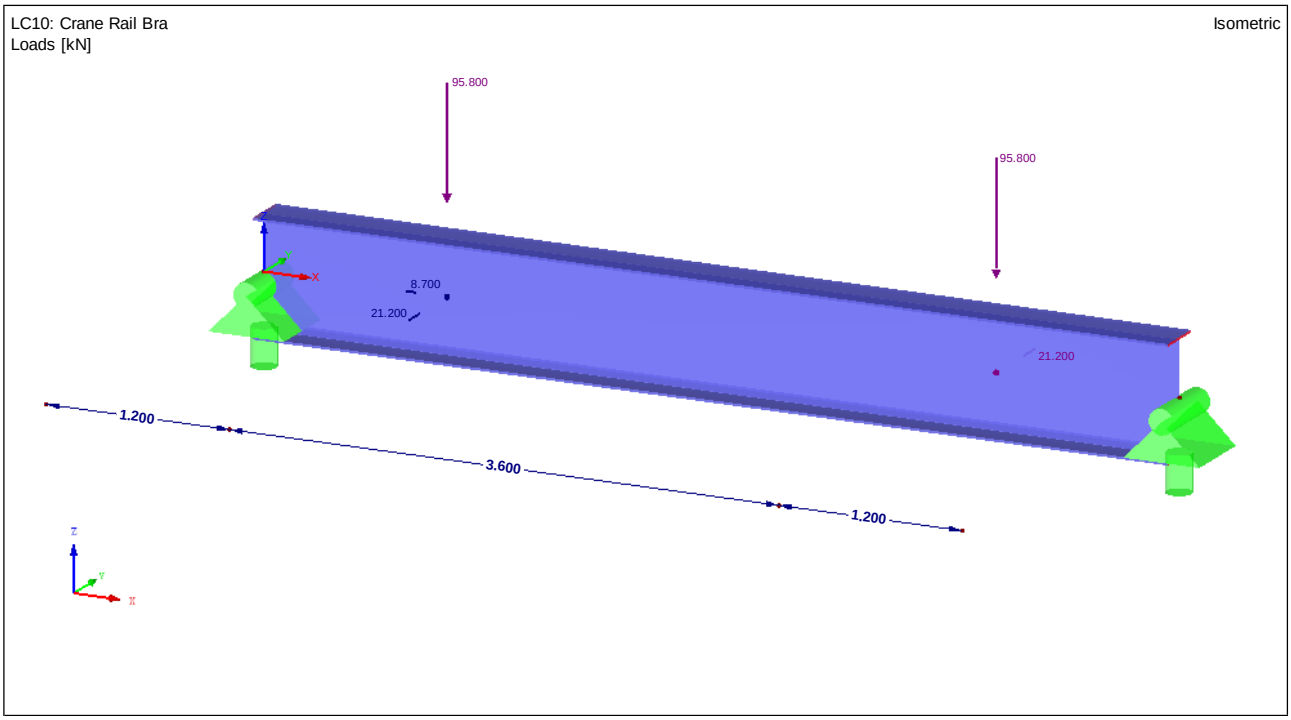

Figure 49: Runway Girder (Crane Middle) Modeling (Brazilian)

[131] (ABNT NBR 8800, 2008) – Section B.7.3.1.1 Page 113

For the other load case, one of the crane wheels was imagined to be in the middle, where the maximum moment forces would occur (for a one-spanned beam). This middle meant that the wheel would have a distance of 3m from the edges of the beam and the other wheel being located on another beam (since the wheels have a distance of 3.6m between them). Figure 50 illustrates the modeling of the load case.

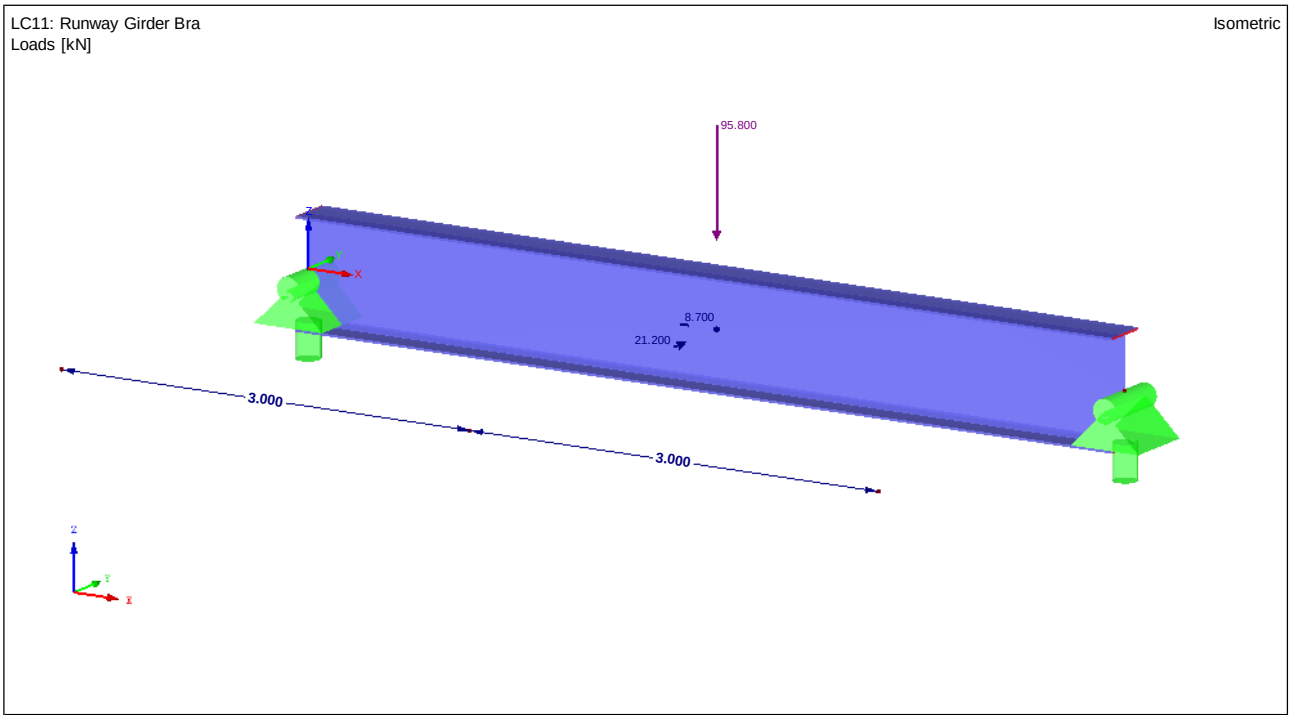

Figure 50: Runway Girder (Wheel Middle) Modeling (Brazilian)

For the results of the verification of the software, see Appendix 39, Appendix 40, Appendix 47 and Appendix 48. The crane runway girder cross-section was verified (see also Chapter 6 LOAD COMBINATIONS ULS (ELU OR GZT) AND SLS (ELS OR GZG) and Chapter 7 RESULTS).

4. MODELING OF THE HALL

The modeling of the industrial steel hall would be in accordance with Figure 7 to Figure 11 in Section 2.1 Dimensions of the Hall. The RSTAB program has a generator for models, and a 3D-Hall model was generated, with the known specifications:

- Length of 48 meters with 9 spans (6 meters each)
- Width of 19.80 meters
  Truss system with 10 spans (1.98 meters each) and the middle having a special configuration with extra trusses connecting the members at one third of their length (zoomed in picture in Figure 51) – at one third of the long diagonal truss member (the member which has the 1.194 m length and the other two-thirds indicated in red with the arrow) and at one third of the roof member (the member which has the 0.681 m length) Roof with the same 10 spans (1.98 meters each) divided by purlins. The purlins intersect with the bay frames at the same point
- Height of the eaves of 10.40 meters
- Roof pitch of approximately 8.6°
- Height of ridge of 11.90 meters

To this generated model, all the appropriate modifications and additions were executed. The structure was represented in five different views:

- Isometric overview of the hall (see Figure 52)
- Frontal view of the hall with measures (see Figure 53)
- 1st Frontal view in perspective of the hall (see Figure 54)
- 2nd Frontal view in perspective of the hall (see Figure 55)
- Lateral view of the hall with measures (see Figure 56)
- Lateral view in perspective of the hall (see Figure 57)
- Top view of the hall with measures (see Figure 58)
- Top view in perspective of the hall (see Figure 59)

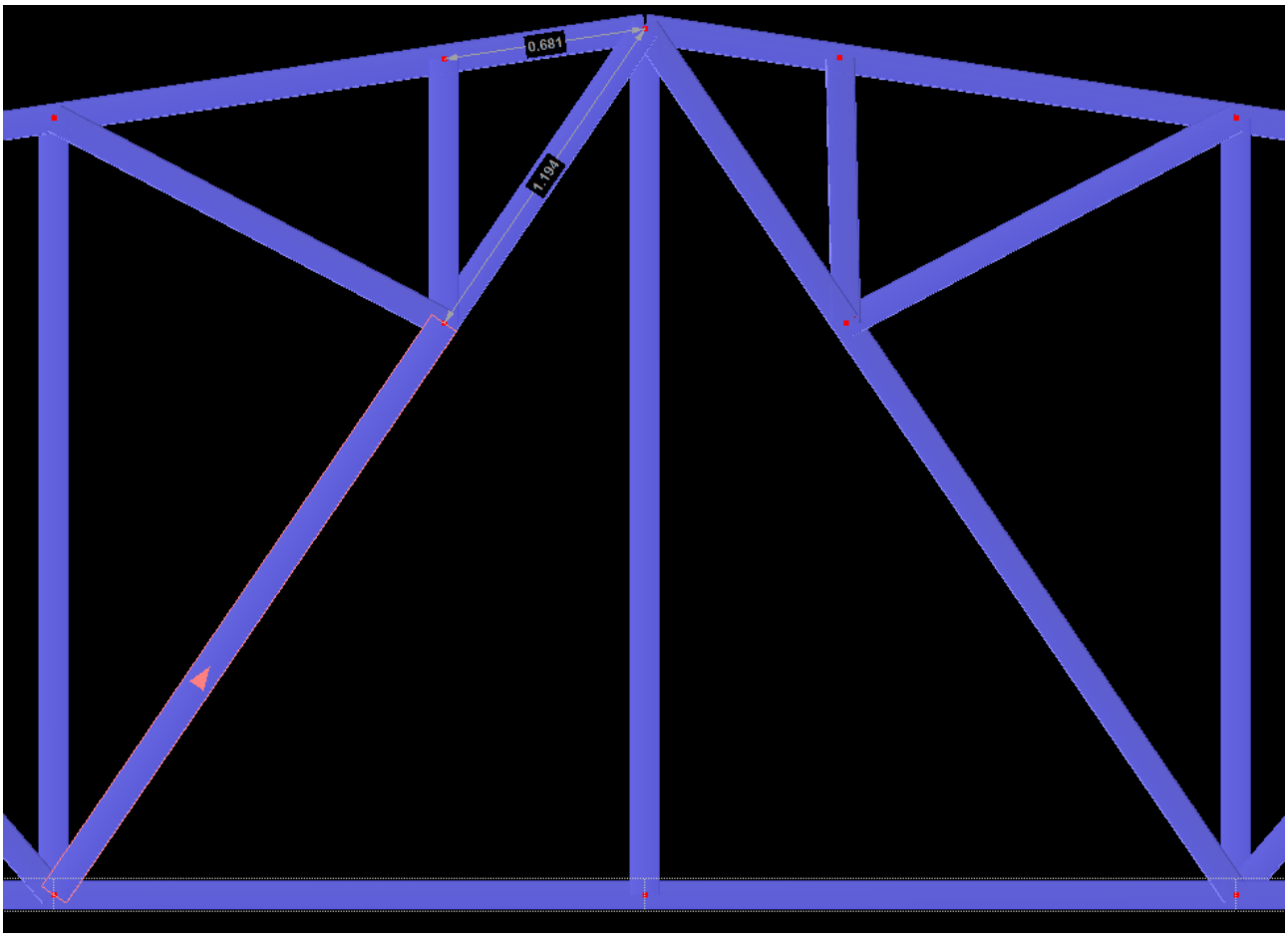

Figure 51: Zoom of the Center of the Truss System

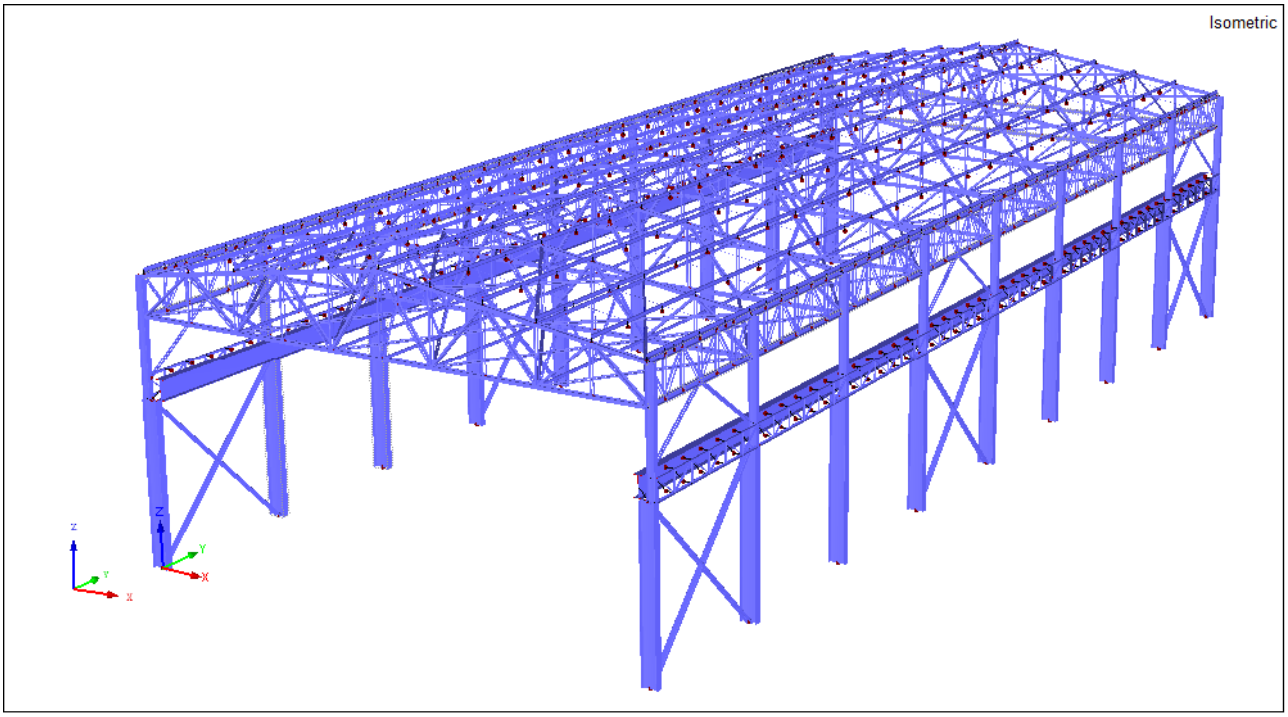

Figure 52: Isometric Overview of the Hall

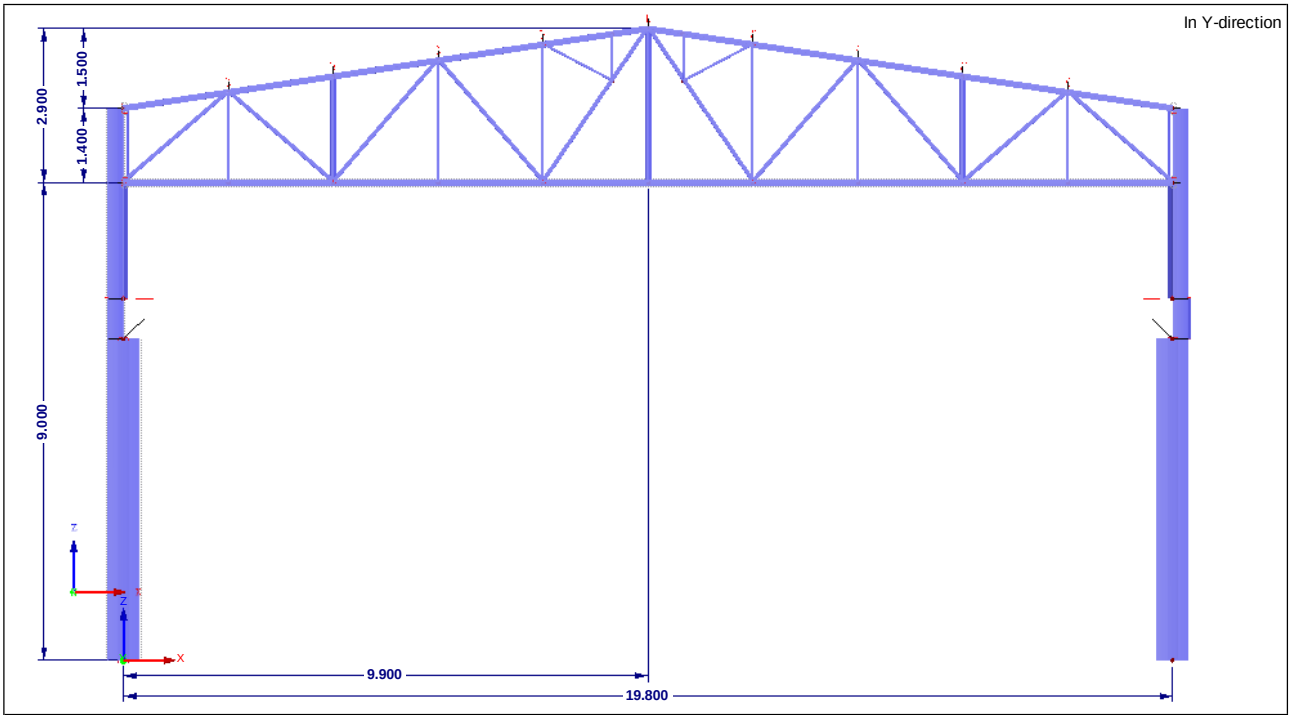

Figure 53: Frontal View of the Hall with Measures

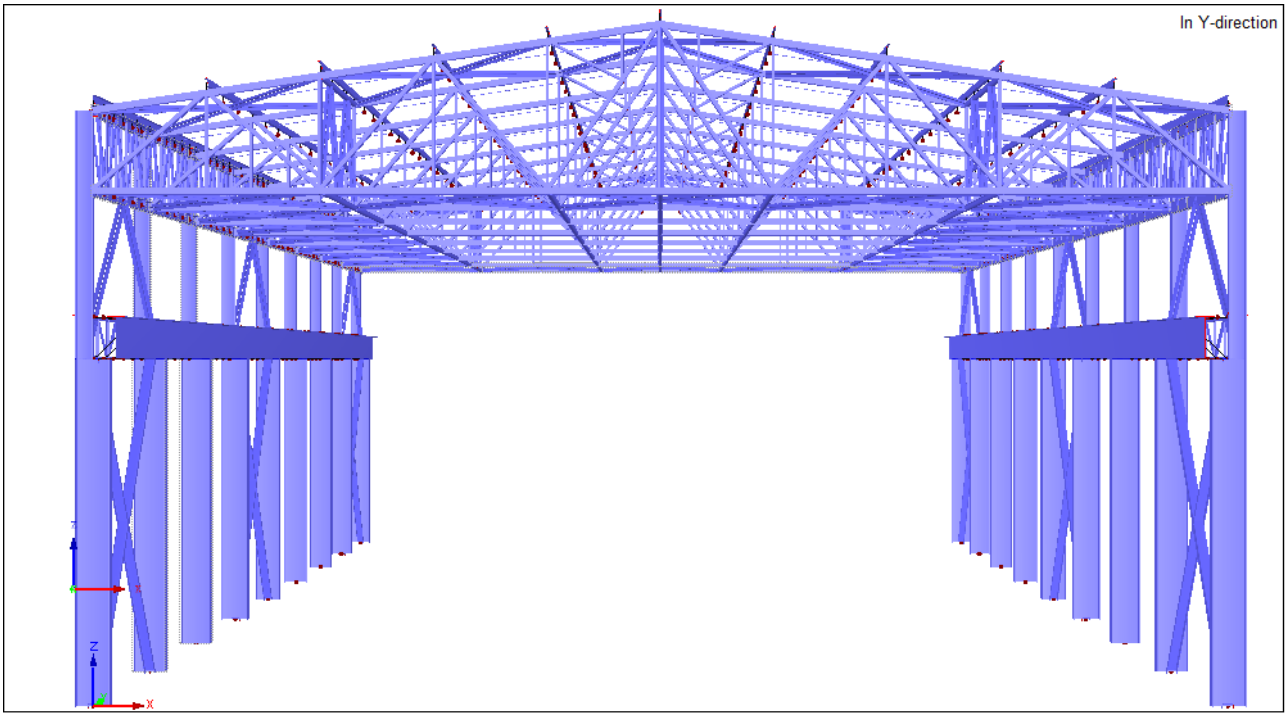

Figure 54: 1st Frontal View in Perspective of the Hall

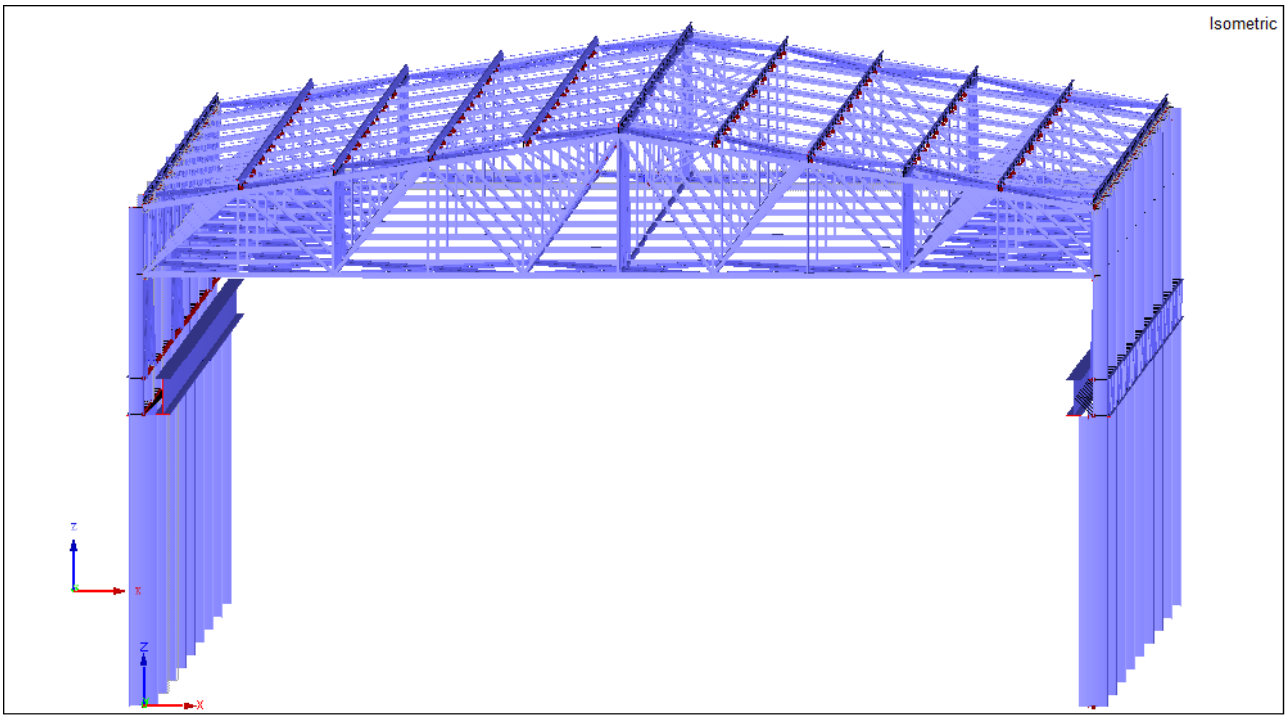

Figure 55: 2nd Frontal View in Perspective of the Hall

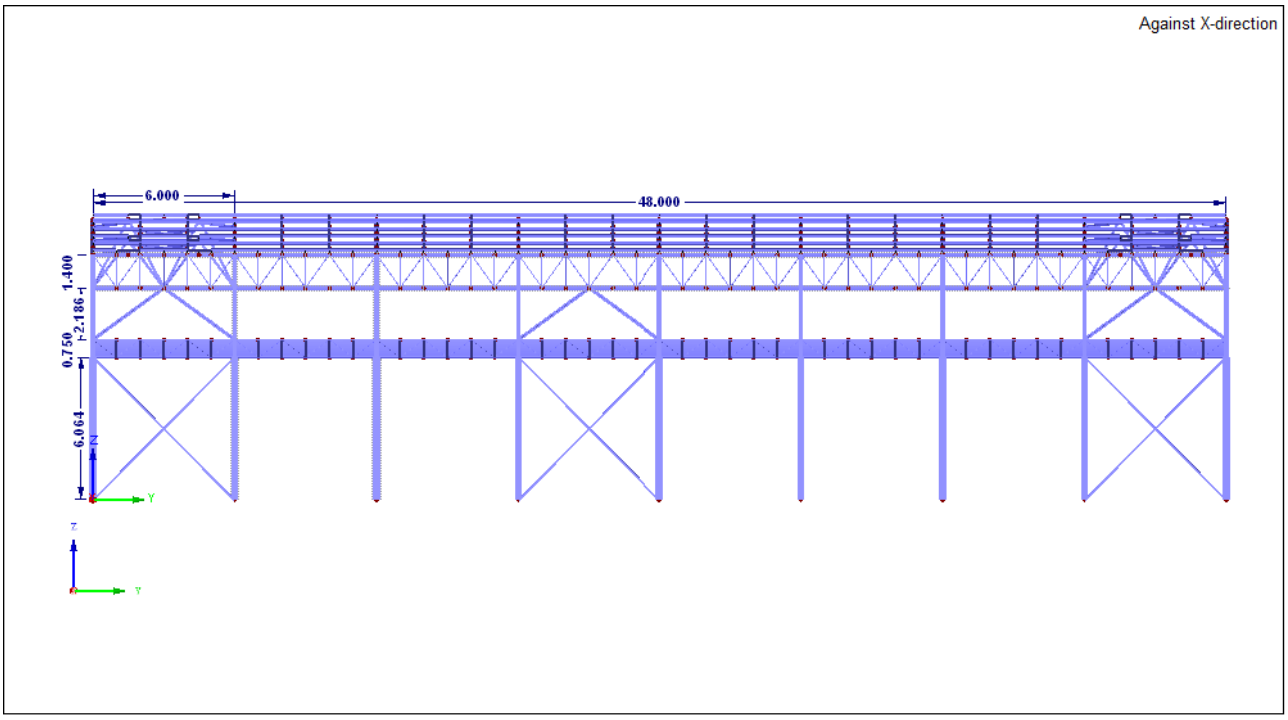

Figure 56: Lateral View of the Hall with Measures

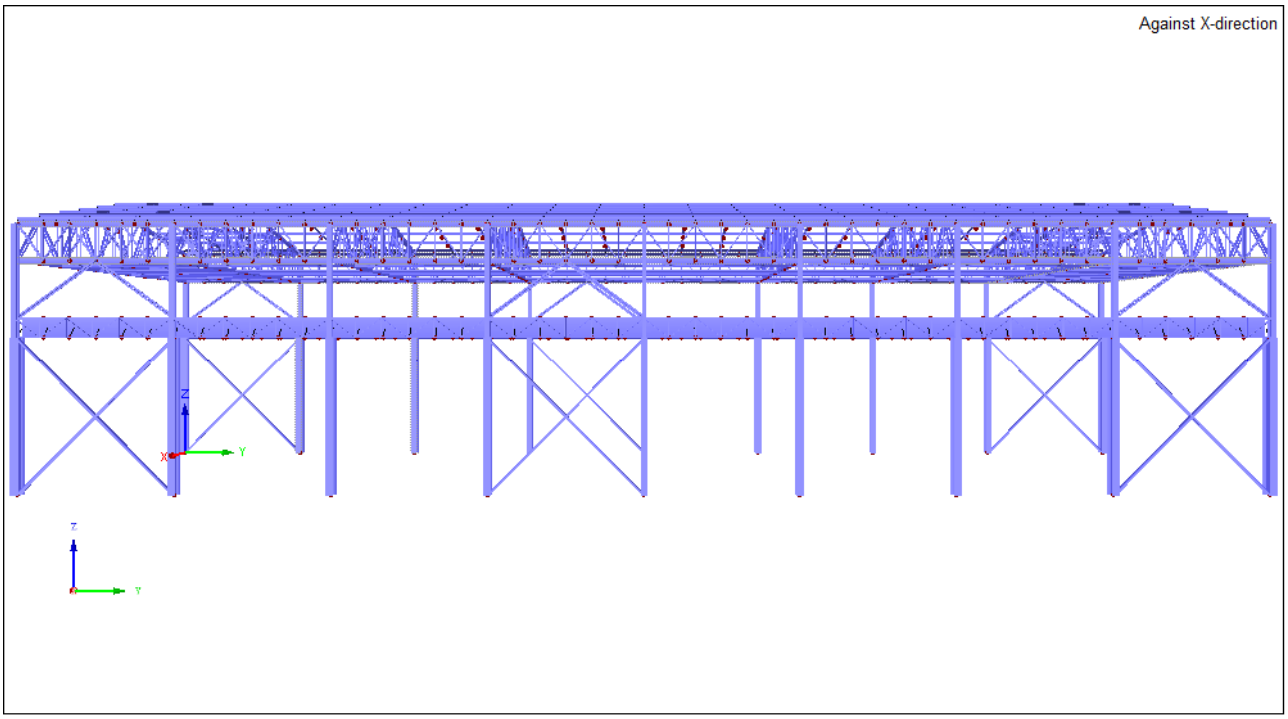

Figure 57: Lateral View in Perspective of the Hall

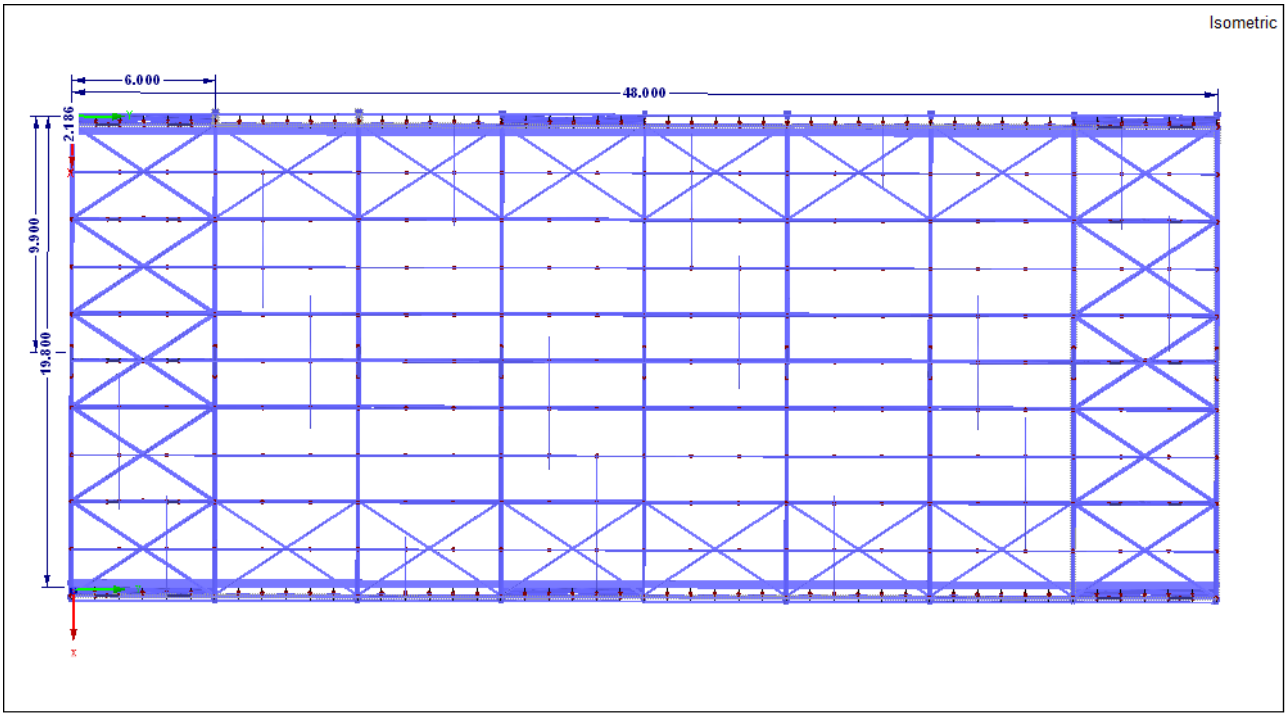

Figure 58: Top View of the Hall with Measures

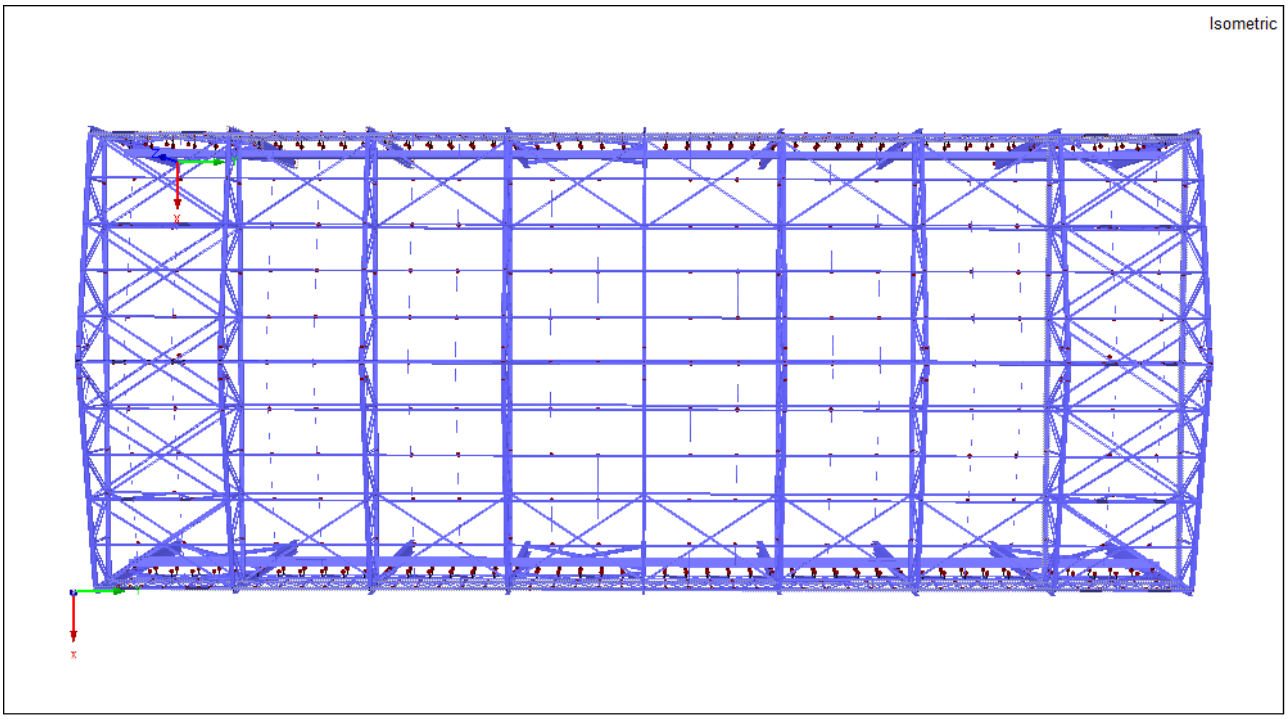

Figure 59: Top View in Perspective of the Hall

It is important to notice that the runway girders and the purlins are one-spanned, having articulations at the appropriate location (end of each beam). In addition, all supports were hidden from Figure 52 to Figure 57 for visualization purposes (for the calculations they are still considered).

An interesting fact was that the vertical and horizontal bracings were designed to “fail” if compression occurred, meaning the program would not consider them in the calculations in case they were compressed. In these occasions, this would lead to an even more secure structure analysis since the combination of the actions would act in favor of security by not decreasing the results of the forces. Moreover, all actions scenarios were calculated one by one, to verify if all of the members would sustain the actions and be secured according to each norm.

One of the main differences between the modeling of both halls was the profile of each cross-section. Table 34 indicates the 18 different cross-sections utilized for the construction of the original hall. By this information, the cross-sections for each Norm were chosen, attempting to minimize the difference between them. The more similar they were to each other, the better would be the comparison provided.

Cross-Sections	ORIGINAL	BRA	GER
Lower Column	PS 600x95.9	VS 600x95	HEA 600
Upper Column	PS 300x57.1	CVS 300x57	IPE 300
Upper and Lower Chords	W 200x19.3	VS 200x19	IPE 200
Vertical Bracings Sup (V)	+ 76x76x8	2LC L 80x8-0	2LC L 75x75x8-0
Vertical Bracings Inf (X)	U* 102x8	2LB L 100x8-200/8	2LB L 100x100x8-200/8
Chords Lateral Sup Truss	U 203x17.1	U 200x100x8	U 200
Lateral Sup Truss	U* 51x6.3	2LB L50x6.3-150/6.3	2LB L 50x50x6-150/6.3
Purlins	U 152 x 12.2	C 6x8.2 (AISC 14)	C 6x8.2 (AISC 14)
Runway Girder	PS 750x128.7	VS 750x125	HEA 700
Chords Lateral Mid Truss	L 76x76x8	L 80x8	L 75x75x8
Lateral Mid Truss	L 51x6.3	L 50x6.3	L50x50x6
Hor Bracings	+ 64x64x6.3	2LC L 60x6.3-0	2LC L 65x65x7-0
Longitudinal Tube	114.3x6	DN 4 (114.3x6)	RO 114.3x6.0
Vertical Bracings Roof (V)	L 64x64x4.8	2LC L 60x4.75-0	2LC L 60x60x5-0
Pole M1	U* 51x4.76	2LB L 50x4.75-200/6.3	2LB L 50x50x5-200/6.3
Diagonal D1	U* 76x6.3	2LB L 80x6-200/6.3	2LB L 75x75x6-200/6.3
Diagonal D2-D4	U* 76x4.76	2LB L 80x4.75-200/6.3	2LB L 75x75x6-200/6.3
Diagonal D5	U* 38x4.76	2LB L 50x4.75-200/6.3	2LB L 40x40x5-200/6.3
Purlin Bracings	Ø 12.7	RB 1/2 (AISC)	RB 1/2 (AISC)

Table 34: Cross-Sections for the Members of the Halls

The only two cross-sections that were not from the NBR or the DIN were the purlin and the sag rods, which were taken from the American Norm (AISC) since both other norms did not have similar cross-sections (that were offered in the software) to the original ones.

5. MODELING OF LOADS

In Chapter 3, all the loads that would be applied on the structure were calculated. In this section, these values were analyzed and modeled to correctly affect the structure.

5.1 Self-Weight

As detailed in Sections 3.1.1 and 3.2.1, the RSTAB program is able to consider the weight of the profiles on its own. However it does not consider the weight of extra pieces, such as screws and other pieces used to connect the steel members. Therefore, with the program, it was input that the factor for the self-weight would be increased from the standard value 1.0 to 1.1 (in the Z-direction).

5.2 Additional Dead Loads

The value for the additional dead loads determined in Sections 3.1.2 and 3.2.2 was 0.40 kN/m² (German) and 0.10 kN/m² (Brazilian). Because this entire load comes from the roof covering and the roof is directly on top of (and only connected to) the purlins, they were the only members to be affected directly. Since all purlins are single-spanned, the simplification of area loads into linear loads can be simplified by area of influence.

The distance between each purlin is of approximately 2m:

$$0.1\ \frac{kN}{m^2}\ *\ 2m = 0.2\frac{kN}{m}$$

Or

$$0.4\ \frac{kN}{m^2}\ *\ 2m = 0.8\frac{kN}{m}$$

On the inner purlins and

$$0.1\frac{kN}{m} * \frac{2m}{2} = 0.1\ kN$$

Or

$$0.4\frac{kN}{m} * \frac{2m}{2} = 0.4\ kN$$

On the outer purlins. Figure 60 illustrates and example of how the Brazilian Norm Additional Dead Loads were imposed.

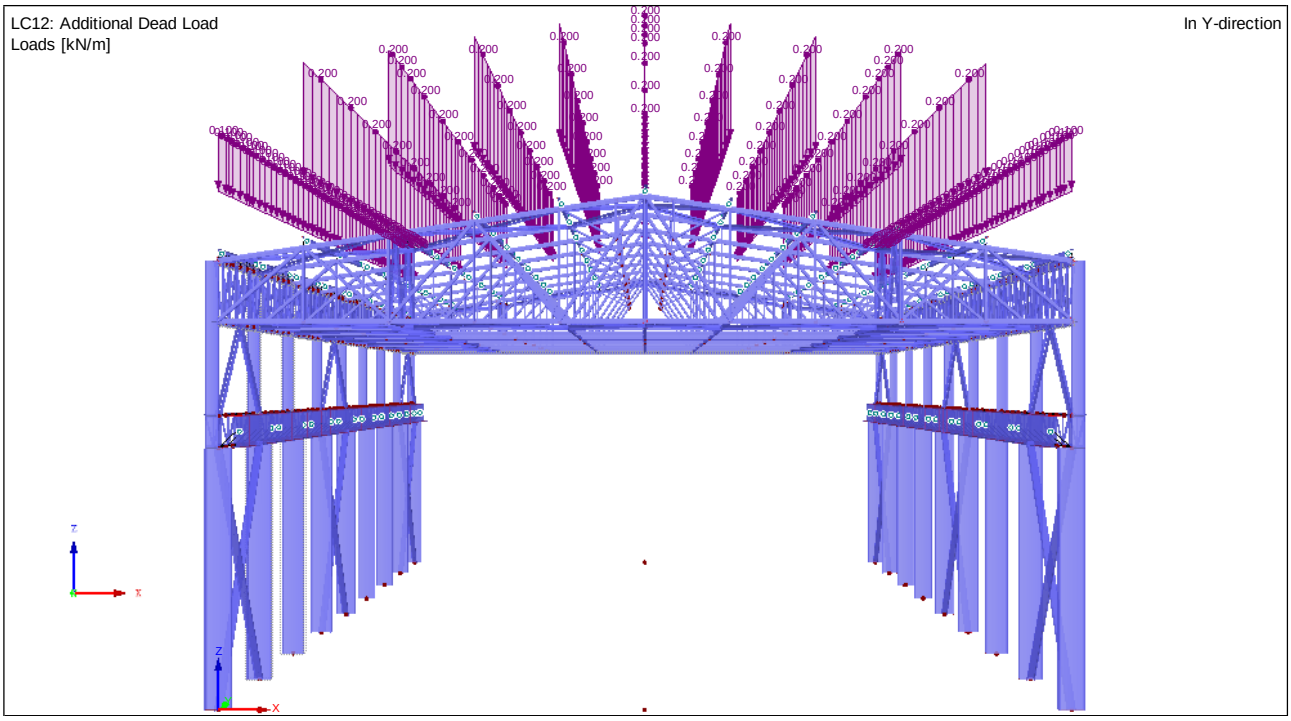

Figure 60: Additional Dead Loads on 3D Model (Brazilian Norm)

5.3Wind Loads

An important observation has to be pointed out: the hall is double-symmetric, meaning that, if the hall were divided into two parts right in the middle, it would be as a mirrored image and if it were divided in two, but this time on the other axis, there would also be two equal parts. In view of this, even if the strongest possible gust of wind would affect the +X direction (side of the building), there would be no need to verify how a wind in the –X direction would affect the building, since the verification would already have been performed. This applies, similarly, to the winds affecting the Y direction. For this reason was the wind only divided into two categories (θ = 0° and θ = 90°) in Section 3.1.4.

5.3.1 Brazilian

The wind loads were modeled as area loads (for walls and roof) that would be applied on specific elements of the structure (for example, columns or purlins). The area load coefficients are specified in Sections 3.2.4.5.1 and 3.2.4.5.2 (Figure 35, Figure 36, Figure 37 and Figure 38). These coefficients were multiplied to the dynamic pressure q to determine the value of each area load.

q [kN/m²] =	0.485596675

C_{pe} / C_{pi}	P [kN/m²]
0.1	0.048559668
0.2	0.097119335
0.3	0.145679003
0.4	0.19423867
0.5	0.242798338
0.6	0.291358005
0.7	0.339917673
0.8	0.38847734
0.9	0.437037008
1.0	0.485596675

Table 35: Area Load Values

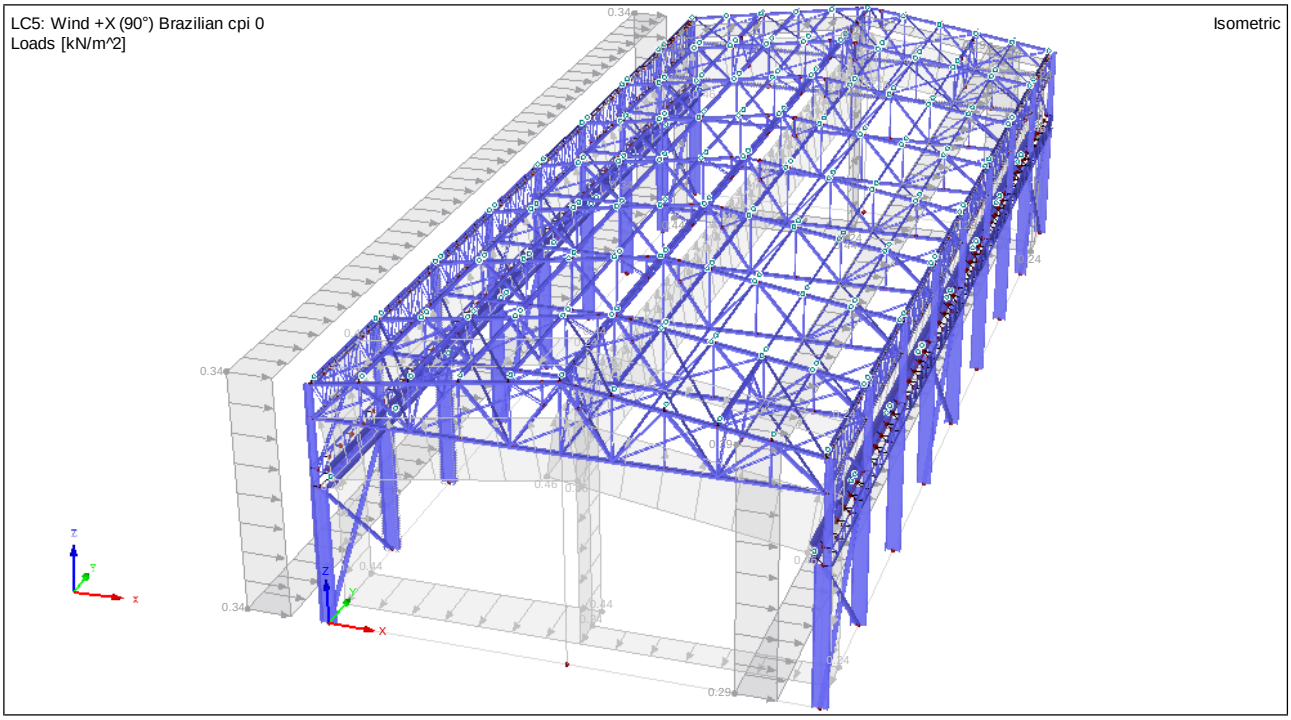

Figure 61: Demonstration of Wind Area Load Directions (Example: Wind +X (90°) Brazilian Norm (c_{pi} 0))

The area loads in the X-Direction were always imposed on the columns (Figure 62) and the area loads in the Y-Direction were always imposed on the columns and upper and lower chords of the truss system (Figure 63). The area loads on the roof (Z-Direction) were always imposed on the purlins (Figure 64).

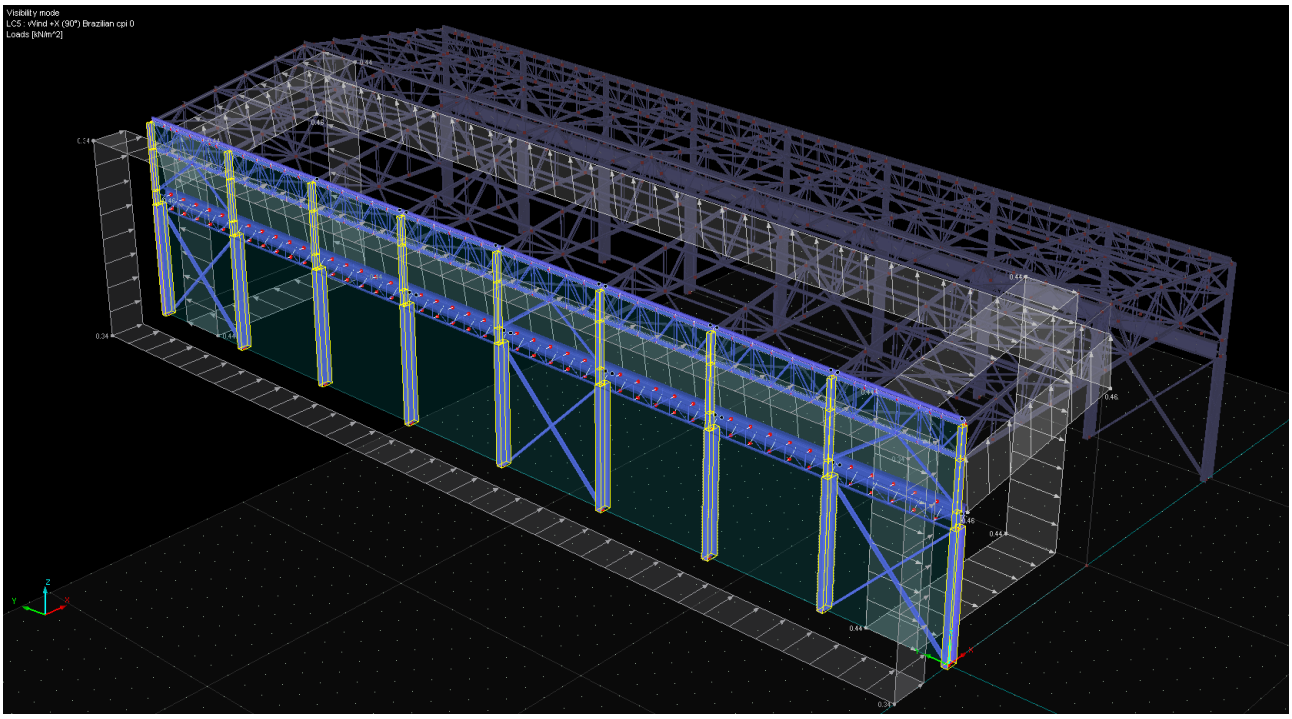

Figure 62: Demonstration of Elements Influenced by the Wind Area Loads (X-Direction)

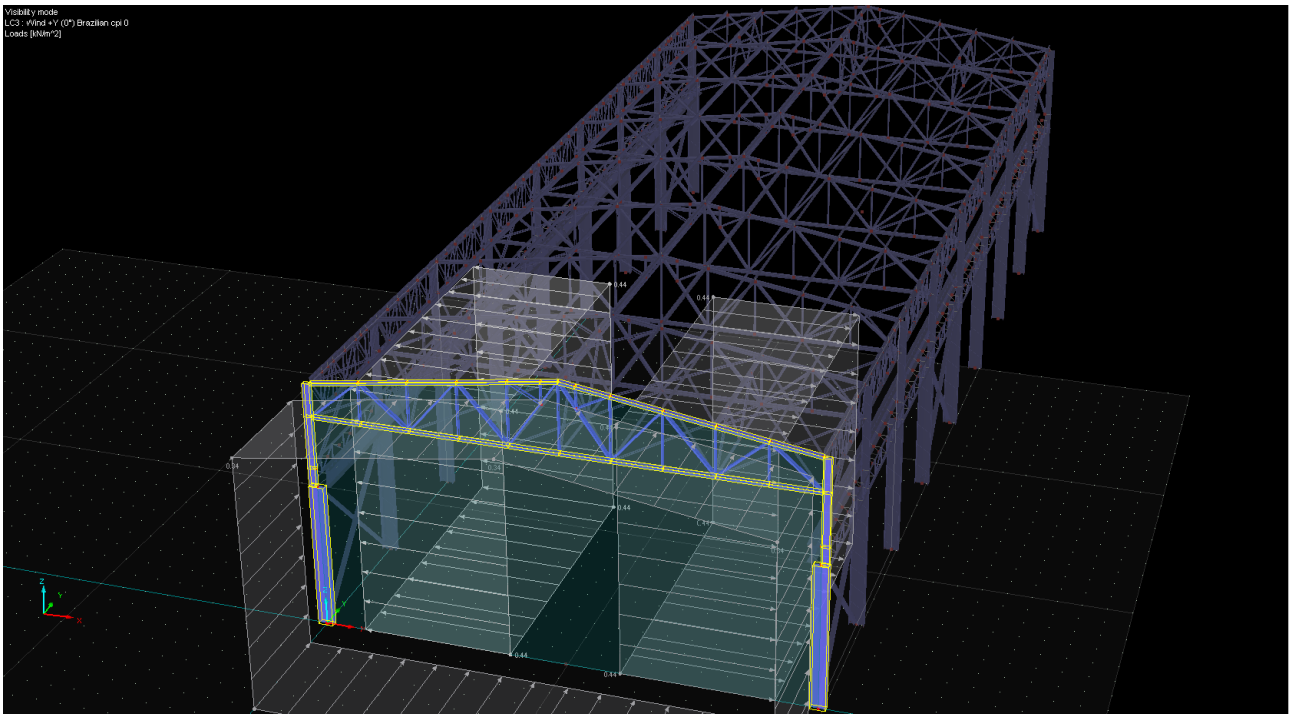

Figure 63: Demonstration of Elements Influenced by the Wind Area Loads (Y-Direction)

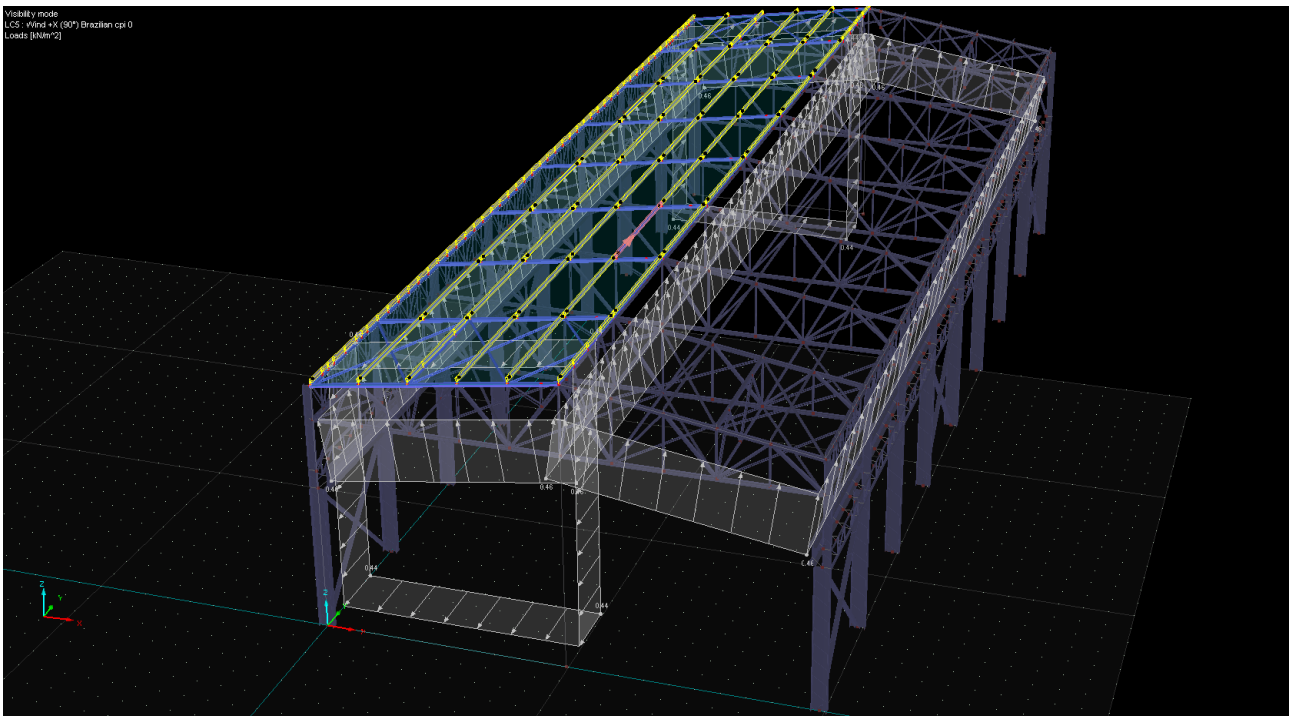

Figure 64: Demonstration of Elements Influenced by the Wind Area Loads (Z-Direction)

An example of how the area loads (on the roof) were transformed into linear loads on the purlins can be seen by the demonstration in Section 5.4 (calculations) and Figure 78 (visual).

5.3.2 German

Since the software is able to create the wind load according to the German norm, this method was applied. By entering the information on the hall and the terrain (Wind Zone 1 and Category III), the wind loads were generated. Figure 65 (θ = 90°) and Figure 66 (θ = 0°) illustrate the dimensions of the wind load areas of the hall (Walls and Saddle Roof):

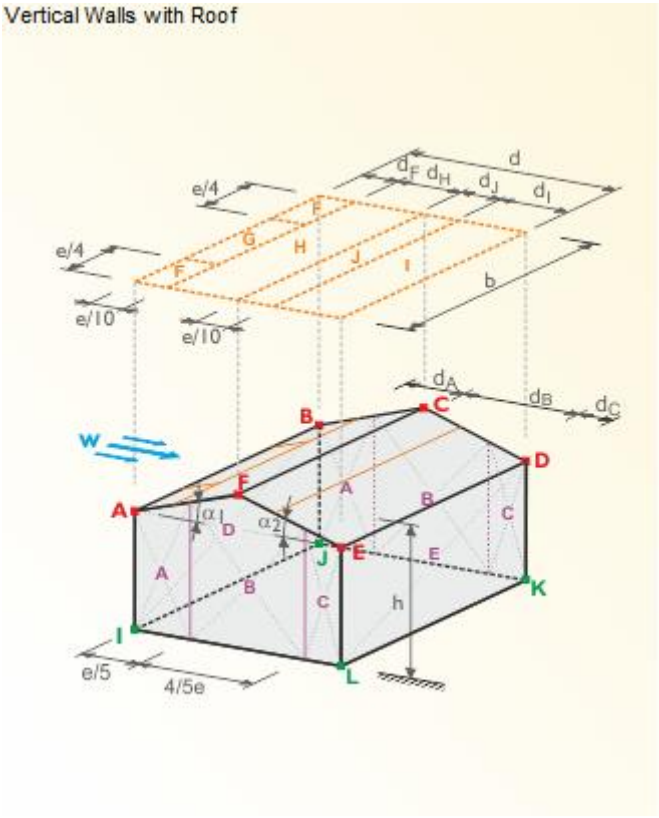

Figure 65: Illustration of the Dimensions of the Wind Load Areas for the Hall when θ = 90°

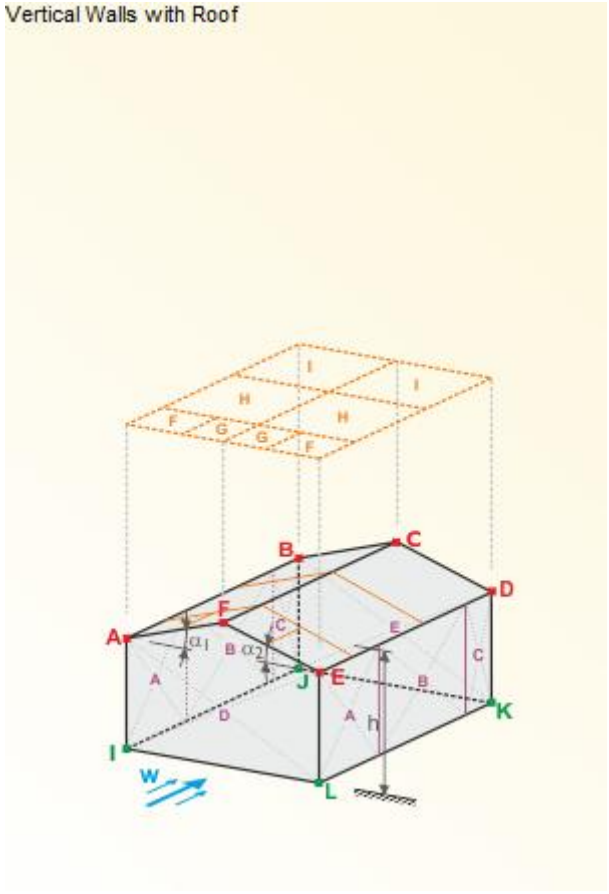

Figure 66: Illustration of the Dimensions of the Wind Load Areas for the Hall when θ = 0°

After its creation, the dimensions of each section were given:

- For θ = 90°[132]:

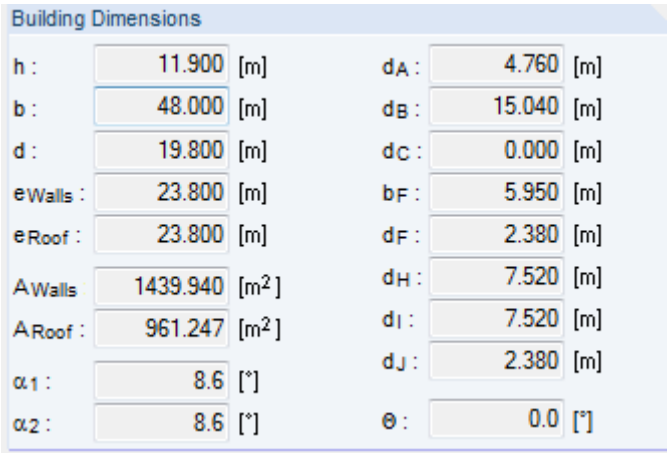

Figure 67: Values of the Dimensions of the Wind Load Areas for the Hall when θ = 90°

These results match exactly with the results calculated in Section a)3.1.4.3.2a). Also the coefficients of external pressure c_{pe} and the wind pressure were given:

		External Pressure Coefficient $c_{pe,10}$		External Pressure w_e [kN/m²]
Zone	A	-1.200	A	-0.64
	B	-0.800	B	-0.43
	C	-0.500	C	-0.27
	D	0.747	D	0.40
	E	-0.394	E	-0.21
	F	0.072	F	0.04
	G	0.072	G	0.04
	H	0.072	H	0.04
	I	0.000	I	0.00
	J	0.128	J	0.07

Figure 68: Values for the External Pressure Coefficient c_{pe} and Wind Pressure for the Saddle Roof for each Division for θ = 90° when α = 8.6° and Combination ++

[132] REMINDER: for standardization purposes, θ = 0° for the German Norm was defined as θ = 90° in this Project (see note in Section 3.1.4.3.2)

Zone		External Pressure Coefficient $c_{pe,10}$		External Pressure w_e [kN/m²]
	A	-1.200	A	-0.64
	B :	-0.800	B :	-0.43
	C :	-0.500	C :	-0.27
	D :	0.747	D :	0.40
	E :	-0.394	E :	-0.21
	F :	-1.411	F :	-0.75
	G :	-1.055	G :	-0.56
	H :	-0.492	H :	-0.26
	I :	-0.528	I :	-0.28
	J :	-0.745	J :	-0.40

Figure 69: Values for the External Pressure Coefficient c_{pe} and Wind Pressure for the Saddle Roof for each Division for θ = 90° when α = 8.6° and Combination --

Zone		External Pressure Coefficient $c_{pe,10}$		External Pressure w_e [kN/m²]
	A	-1.200	A	-0.64
	B :	-0.800	B :	-0.43
	C :	-0.500	C :	-0.27
	D :	0.747	D :	0.40
	E :	-0.394	E :	-0.21
	F :	-1.411	F :	-0.75
	G :	-1.055	G :	-0.56
	H :	-0.492	H :	-0.26
	I :	0.000	I :	0.00
	J :	0.128	J :	0.07

Figure 70: Values for the External Pressure Coefficient c_{pe} and Wind Pressure for the Saddle Roof for each Division for θ = 90° when α = 8.6° and Combination -+

Zone		External Pressure Coefficient $c_{pe,10}$		External Pressure w_e [kN/m²]
	A	-1.200	A	-0.64
	B :	-0.800	B :	-0.43
	C :	-0.500	C :	-0.27
	D :	0.747	D :	0.40
	E :	-0.394	E :	-0.21
	F :	0.072	F :	0.04
	G :	0.072	G :	0.04
	H :	0.072	H :	0.04
	I :	-0.528	I :	-0.28
	J :	-0.745	J :	-0.40

Figure 71: Values for the External Pressure Coefficient c_{pe} and Wind Pressure for the Saddle Roof for each Division for θ = 90° when α = 8.6° and Combination +-

These results also match exactly with the results calculated in Section 3.1.4.3.2b).

- For θ = 0°:

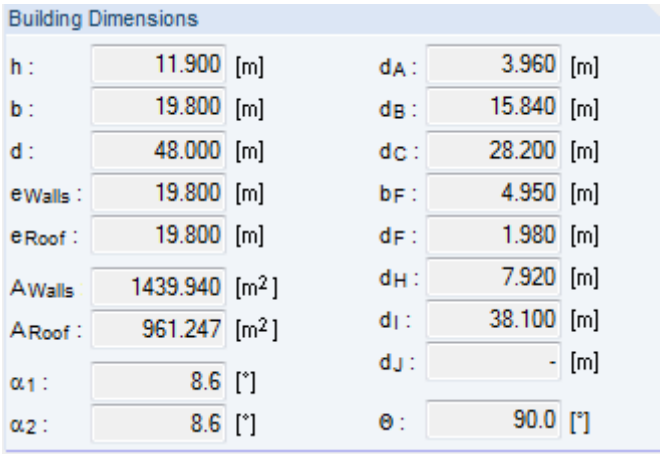

Building Dimensions

h :	11.900	[m]	d_A :	3.960	[m]
b :	19.800	[m]	d_B :	15.840	[m]
d :	48.000	[m]	d_C :	28.200	[m]
e_{Walls} :	19.800	[m]	b_F :	4.950	[m]
e_{Roof} :	19.800	[m]	d_F :	1.980	[m]
A_{Walls}	1439.940	[m²]	d_H :	7.920	[m]
A_{Roof} :	961.247	[m²]	d_I :	38.100	[m]
			d_J :	-	[m]
α_1 :	8.6	[°]			
α_2 :	8.6	[°]	Θ :	90.0	[°]

Figure 72: Values of the Dimensions of the Wind Load Areas for the Hall when θ = 0°

These results match exactly with the results calculated in Section a)3.1.4.3.2a). Also the coefficients of external pressure c_{pe} and the wind pressure were given:

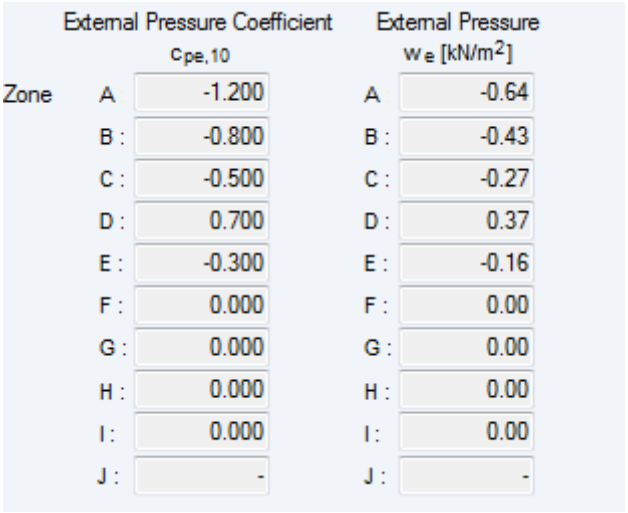

Zone		External Pressure Coefficient $c_{pe,10}$		External Pressure w_e [kN/m²]
	A	-1.200	A	-0.64
	B :	-0.800	B :	-0.43
	C :	-0.500	C :	-0.27
	D :	0.700	D :	0.37
	E :	-0.300	E :	-0.16
	F :	0.000	F :	0.00
	G :	0.000	G :	0.00
	H :	0.000	H :	0.00
	I :	0.000	I :	0.00
	J :	-	J :	-

Figure 73: Values for the External Pressure Coefficient c_{pe} and Wind Pressure for the Saddle Roof for each Division for θ = 0° when α = 8.6° and Combination +

		External Pressure Coefficient $c_{pe,10}$		External Pressure w_e [kN/m²]
Zone	A	-1.200	A	-0.64
	B :	-0.800	B :	-0.43
	C :	-0.500	C :	-0.27
	D :	0.700	D :	0.37
	E :	-0.300	E :	-0.16
	F :	-1.492	F :	-0.80
	G :	-1.300	G :	-0.69
	H :	-0.664	H :	-0.35
	I :	-0.564	I :	-0.30
	J :	-	J :	-

Figure 74: Values for the External Pressure Coefficient c_{pe} and Wind Pressure for the Saddle Roof for each Division for θ = 0° when α = 8.6° and Combination -

An example of the External Wind Pressure can be seen in Figure 75 (Wall Area Loads) and Figure 76 (Roof Area Loads). Although difficult to visualize, the letters correspondent to each Area are also given in the figures that follow:

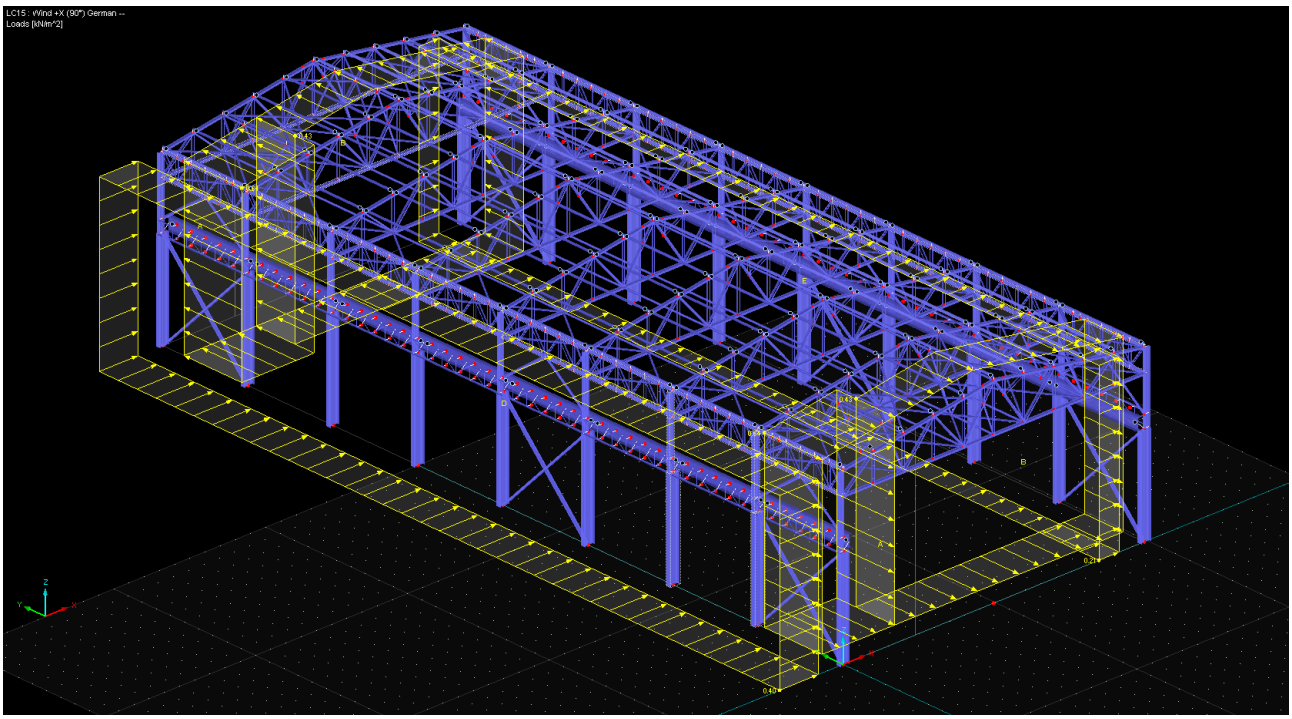

Figure 75: Representation of the External Wind Pressure on the Walls

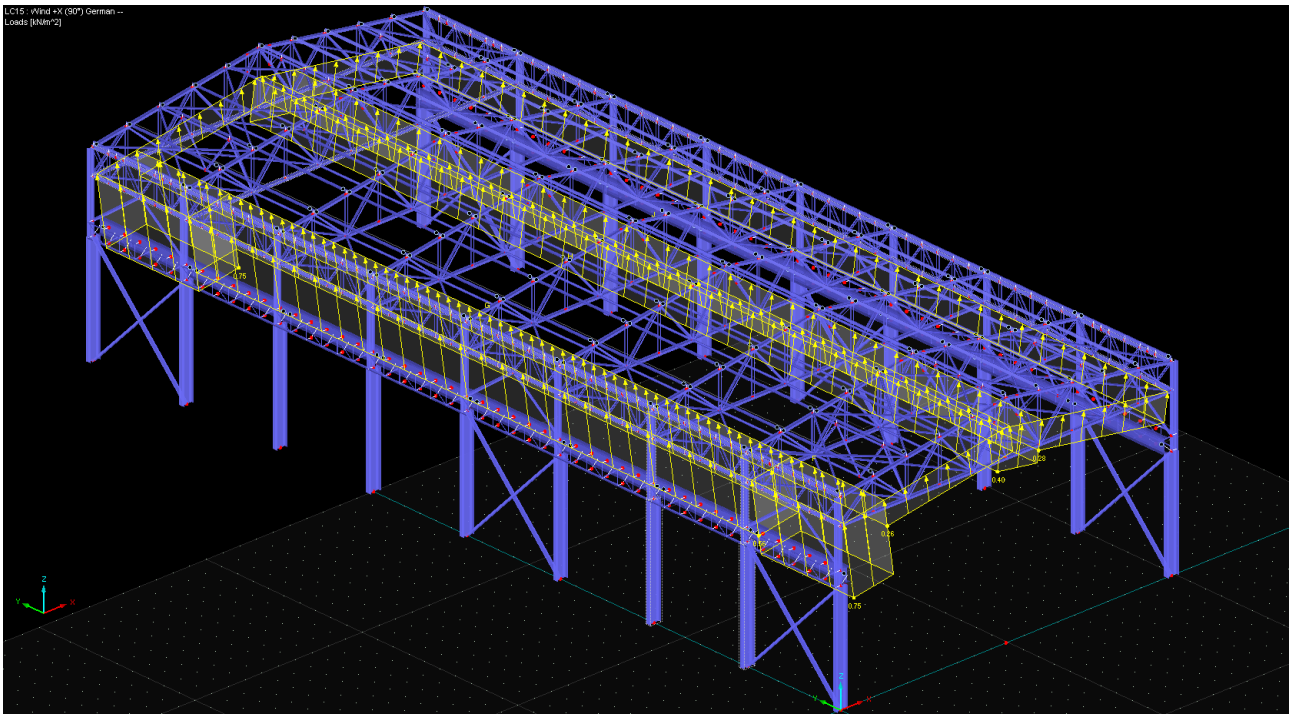

Figure 76: Representation of the External Wind Pressure on the Roof

After all the 6 load cases were appropriately modeled, the c_{pi} Area Loads were also imposed. For the 4 cases of +X (θ = 90°), the W_i was 0.07 kN/m² for all areas (see Figure 77). For the 2 cases of +Y (θ = 0°), the W_i was –0.16 kN/m² (see Section 3.1.4.4). These were simply applied to the model as area loads similar to the area loads imposed for the Brazilian Load model (see Section 5.3.1).

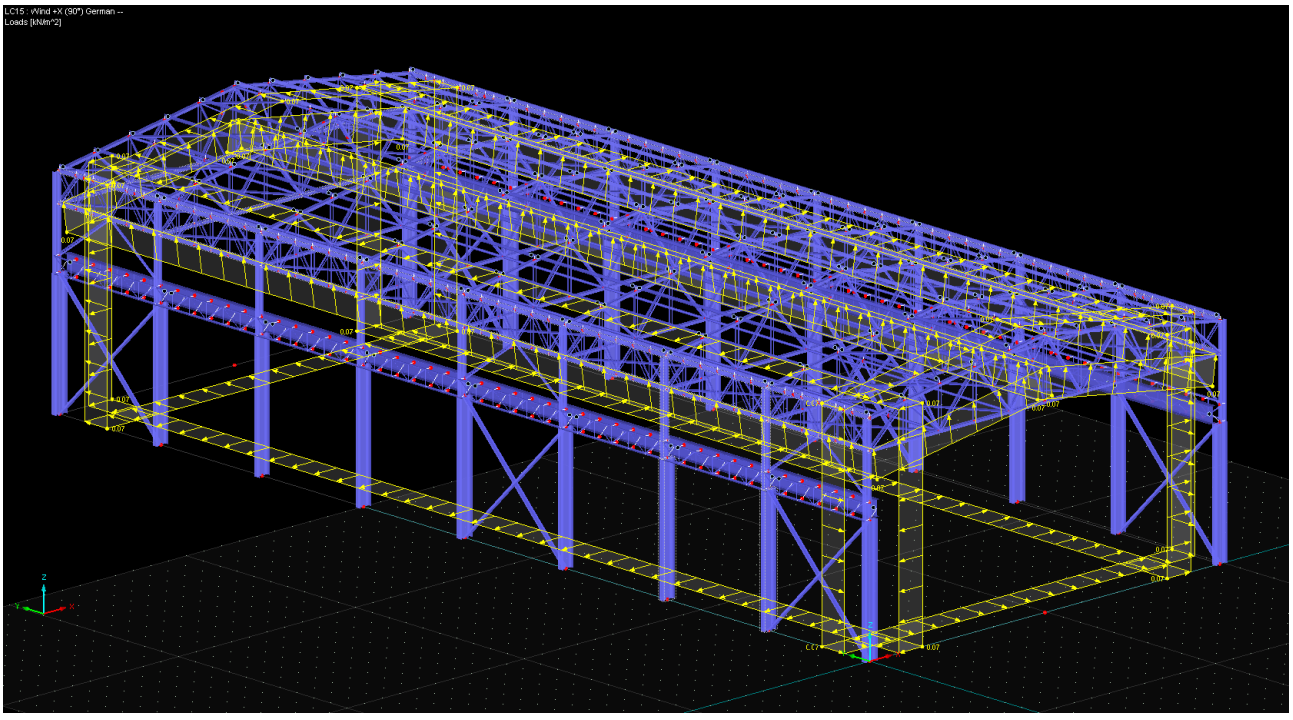

Figure 77: Representation of the Internal Wind Pressure on the Roof (W_i = 0.07 kN/m²)

5.4 Live Loads

The Live Loads can be understood by the "*Ações Acidentais*" (see Sections 3.1.3 and 3.2.3). Since the value was 0.5 kN/m² and the distance between each purlin is of approximately 2m. Therefore, the linear loads on the purlins were:

$$0.5\frac{kN}{m^2} * 2m = 1\frac{kN}{m}$$

On the inner purlins and

$$0.5\frac{kN}{m^2} * \frac{2m}{2} = 0.5\frac{kN}{m}$$

On the outer purlins. Figure 78 shows how the loads were imposed:

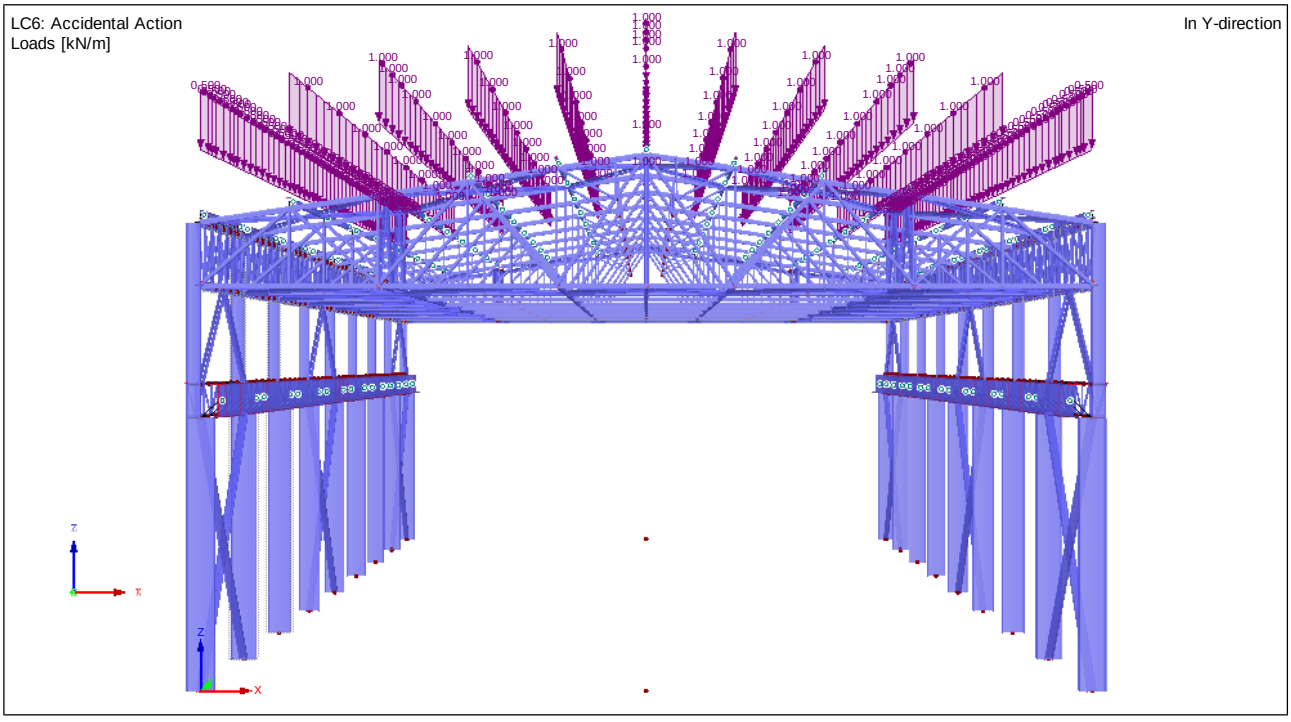

Figure 78: Live Loads on 3D Model

The equivalent forces ("Forças Nocionais" see Section 3.2.3) derived from the imperfections of the elements were also calculated (see Section 5.6.5).

The Equivalent Force ("Força Nocional") would be 0.3% of the combined gravitational load found:

$$F_n = 0.003 * 530.0875\ kN = 1.59\ kN$$

5.5 Crane Loads

5.5.1 Runway Girder

5.5.1.1 Brazilian Design Code

The runway girder was modeled separately in order to verify if the cross-section profiles were sufficient to withstand the loads from both Norms (see Sections 3.1.6.5 and 3.2.6.5.)

Since the beam is articulated at every frame, it is perceived as a one-span beam. In this case, the maximum moment would occur when the bridge crane is located in the middle of the beam (see Figure 84 or Figure 85) and the maximum compression force on the column would occur when the column was in between the wheel loads (see Figure 83).

To verify which frame would have the most aggressive force all wind types (Brazilian Norm) were calculated and run on the software. The choice for analyzing the Wind Loads is due to the fact that the other loads (except Crane Loads) do not have more than one case, meaning they would not change and consequently not differ in the manner that affect one column or another column. Thus, all Wind Loads (for maximum compression on the columns) were analyzed and it was verified that the 5th column from the front was the column that received the most compression force (the frame adjacent to the vertical bracing). Moreover, the right side (from the front, opposite from where the +X Wind Load would be imposed) would have a smaller traction (or bigger compression) than the left side.

Figure 79 through Figure 82 exemplify the wind results for the 4 wind load types from the Brazilian Norm:

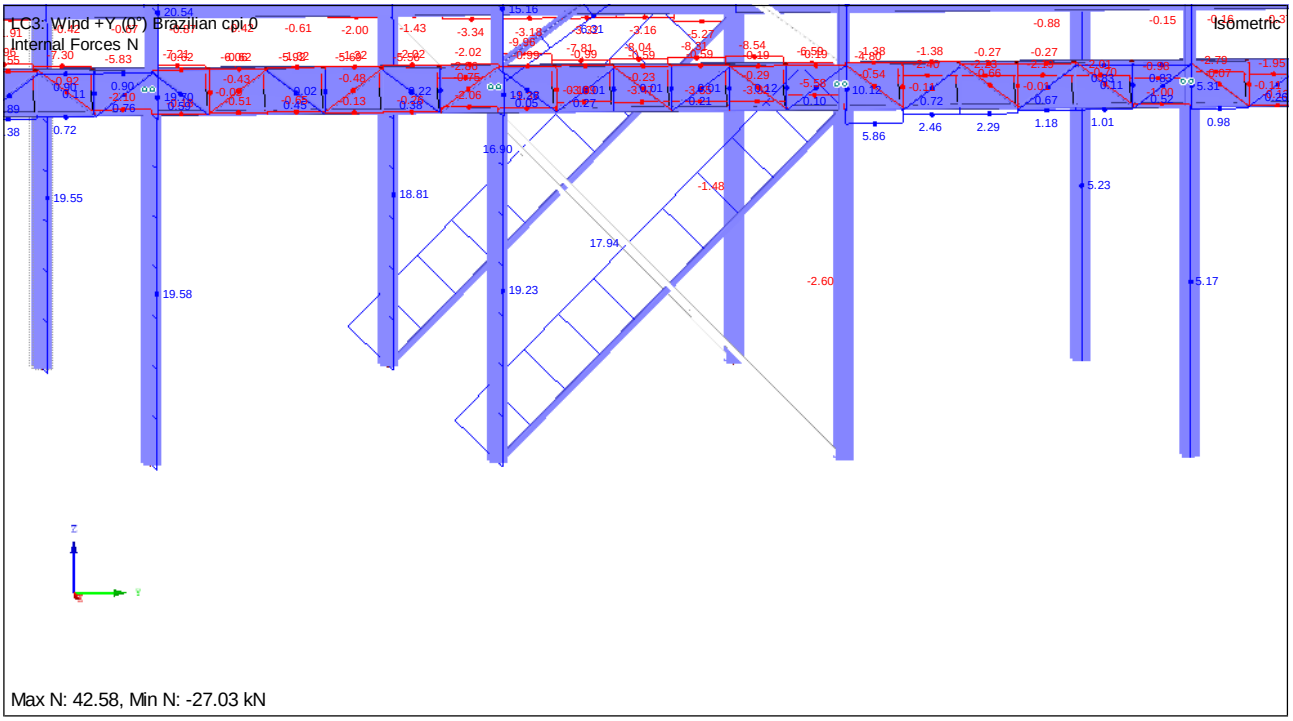

Figure 79: Results for Wind +Y (0°) Brazilian c_{pi} 0[133]

[133] c_{pi} 0 identifies the Wind Load with the value of c_{pi} = 0. Same applies to c_{pi} 0.3

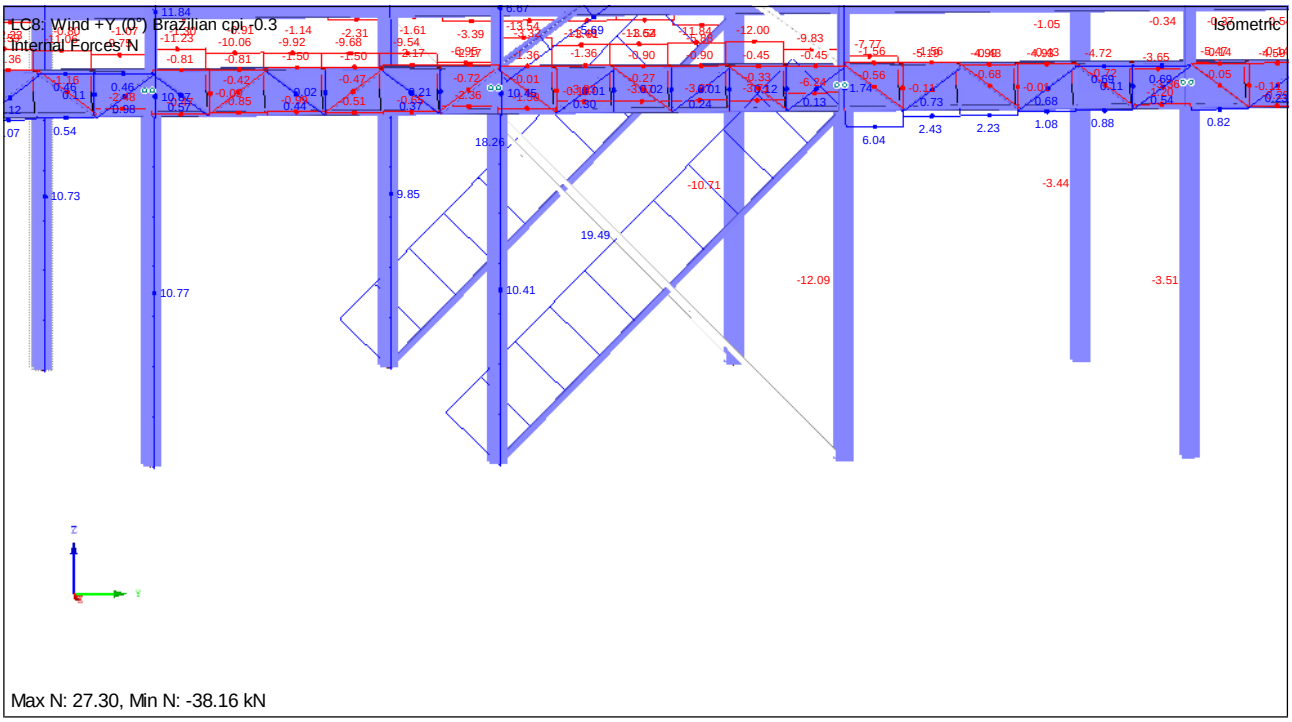

Figure 80: Results for Wind +Y (0°) Brazilian c_{pi} 0.3

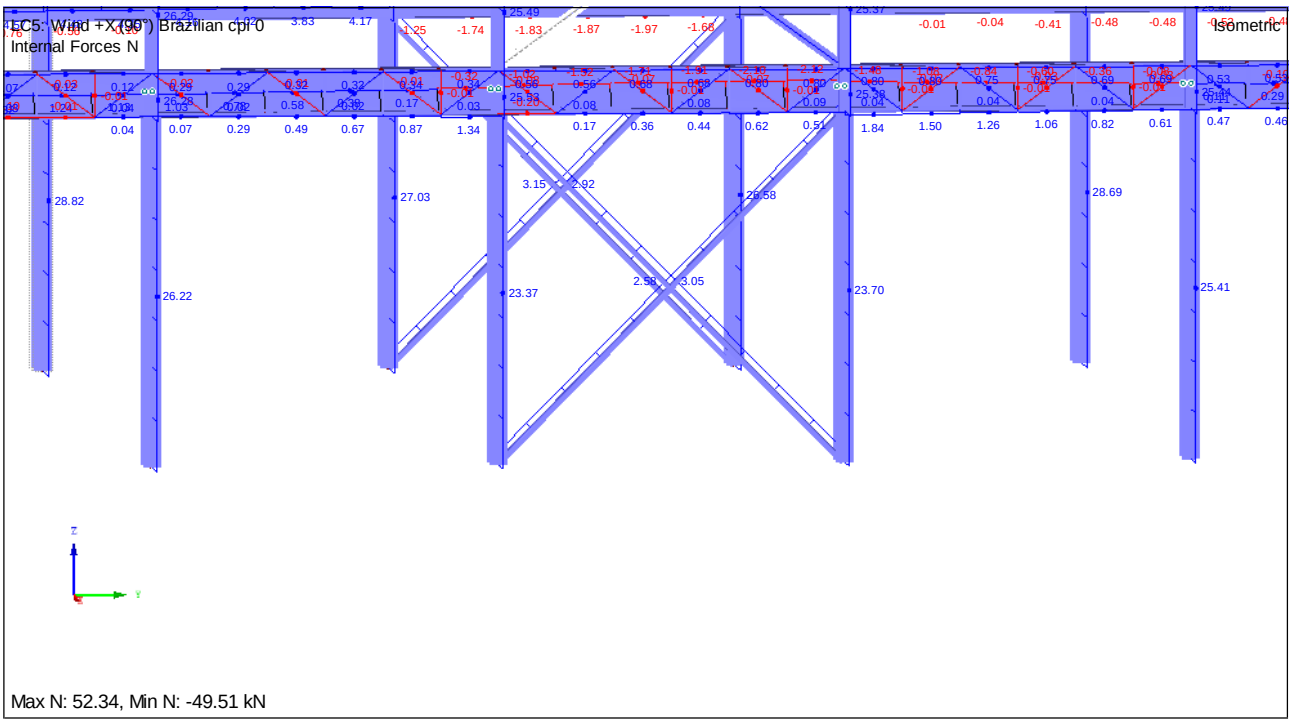

Figure 81: Results for Wind +X (90°) Brazilian c_{pi} 0

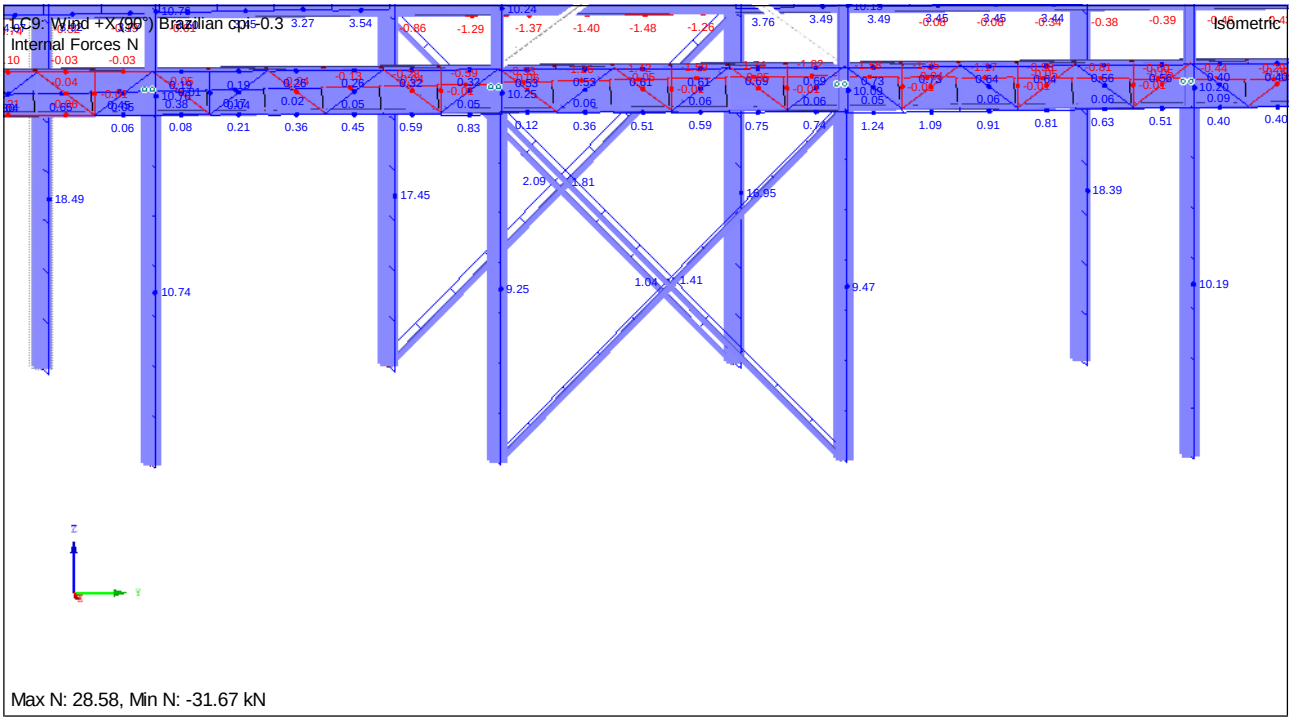

Figure 82: Results for Wind +X (90°) Brazilian c_{pi} -0.3

To discover which position the crane would be most aggressive to the column, 3^{134} positions were chosen (the arrows symbolize the location of the wheels): when the wheel loads have the 5th column between them (Figure 83), in the middle of the 4th span (between frames 4 and 5 – Figure 84) and in the middle of the 5th span (between frames 5 and 6 – Figure 85). Clearly, the largest load would occur when the column is between the loads (Figure 83).

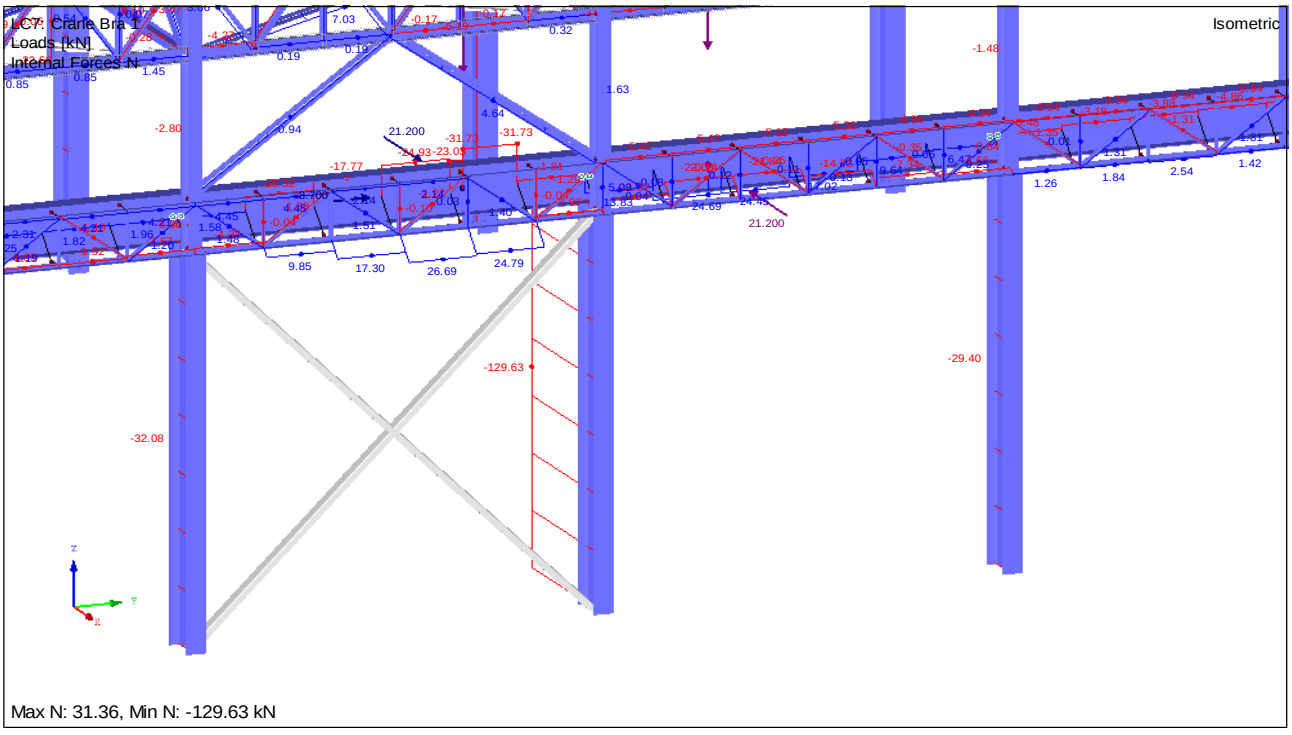

Figure 83: Results for Wheel Loads with Column Between

[134] A 4th position was later analyzed (Appendix 49) and also had a smaller compression as the column between loads.

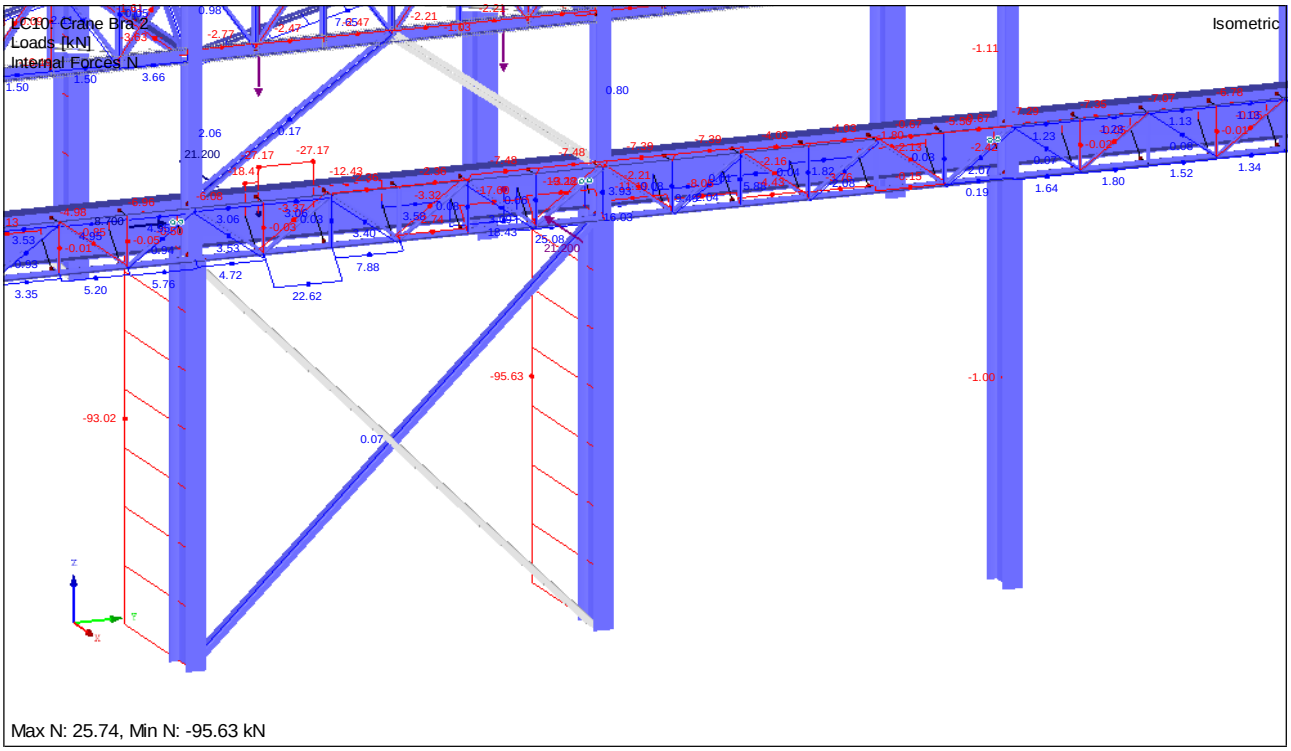

Figure 84: Results for Wheel Loads in the Middle of 4th Span

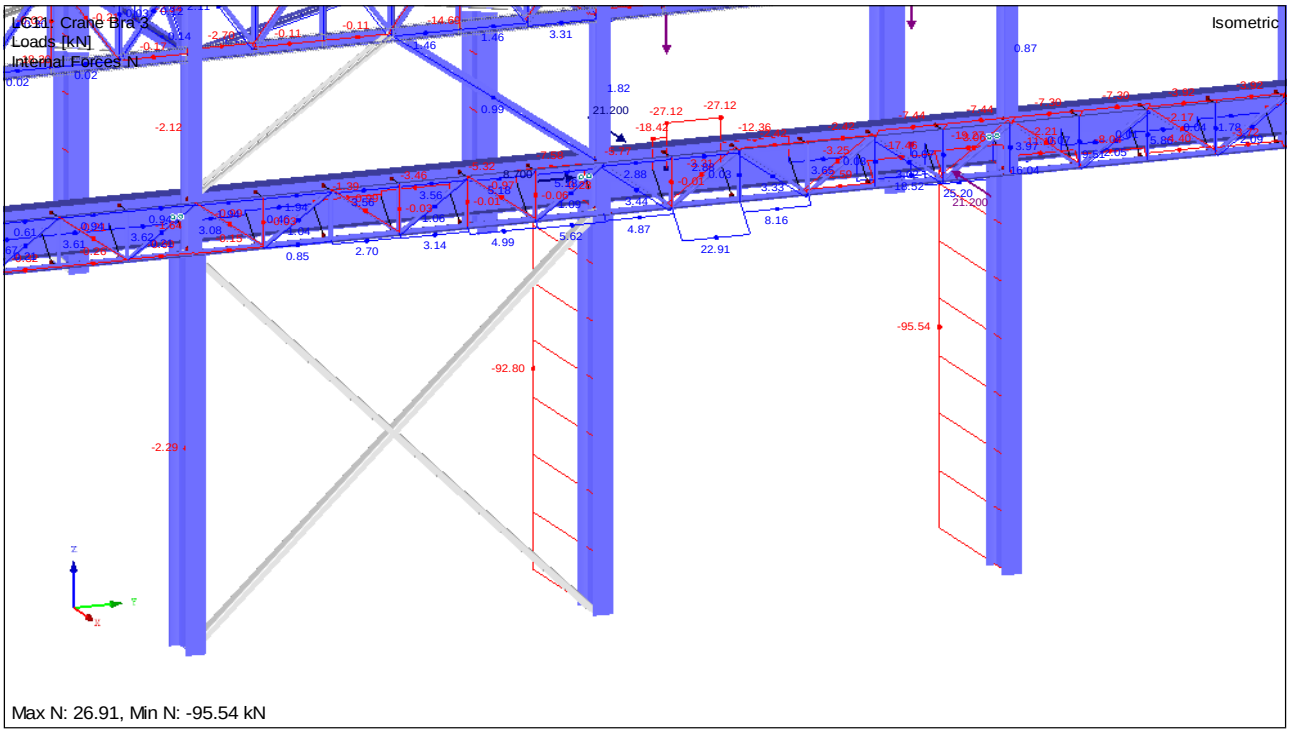

Figure 85: Results for Wheel Loads in the Middle of 5th Span

This meant that by adding the crane load (wheel loads) beside the column (exactly in the middle between the wheel loads) the compression forces on the column would be the most aggressive.

The values for the forces are the same as Section 3.2.6.5:

- Vertical $RV_1 = RV_2 = 95.8$ kN; $RV_3 = RV_4 = 16$ kN
- Transversal RH = 21.2 kN
- Longitudinal RL = 8.7 kN

5.5.1.2 German Design Code

For the German Norm, the result of the combination of the Self-Weight, Additional Dead Load, Live Load and the most aggressive Wind Load was found. The concept was the same as the one made to find the location of the Crane for the Brazilian Norm, but done in a different method in order to demonstrate the Normal Forces with the combination of loads (except the Crane Loads).

Unlike the Brazilian Norm, the German Loads had the most aggressive normal load on the 2nd column from the front, but still on the right side. Figure 86 shows the Normal Forces from the 1st to the 5th column on the right side. Therefore, the same method was applied for the modeling of the Crane Loads for the German Norm, but instead of the 5th column, the loads were applied to the 2nd column (or spans beside the 2nd column). The location was found to be plausible, since the bumper (stopper) was 1m from the first column and there would be enough space for the crane to be there[135].

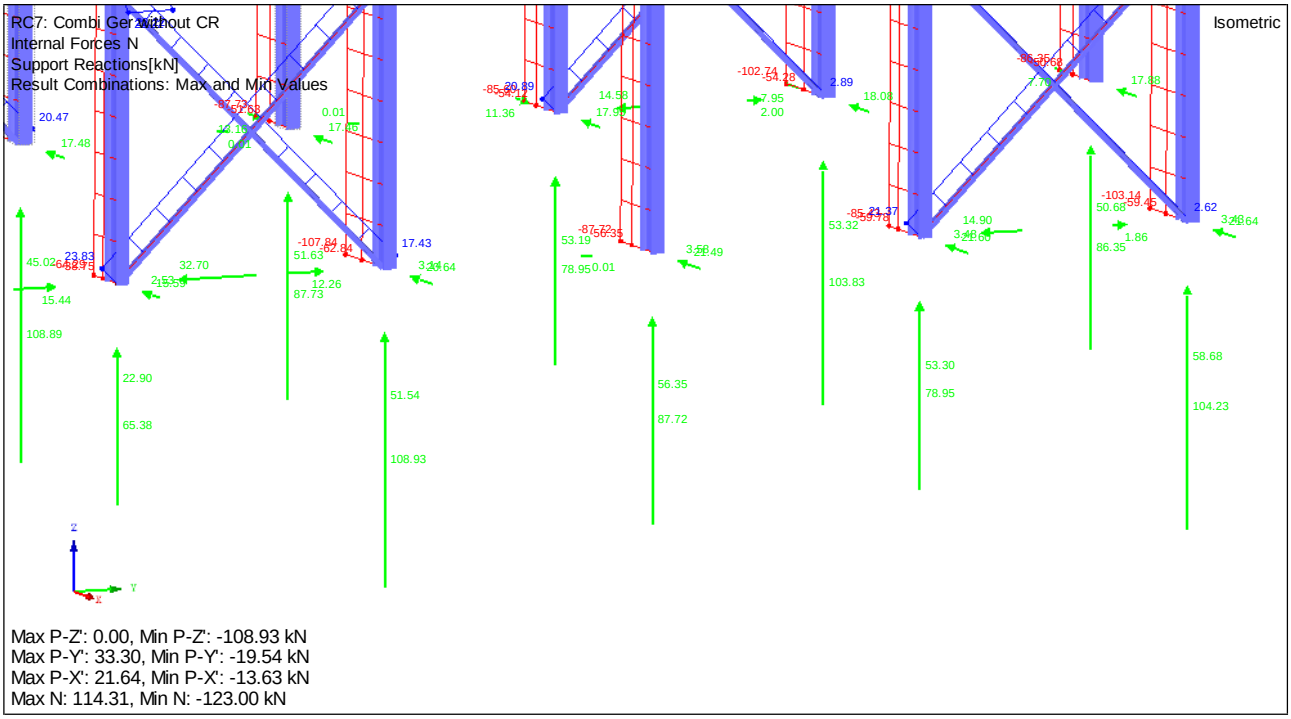

Figure 86: Normal Forces and Reactions on the Right Columns of the Hall for the German Norm

[135] At one end, the bumper was located at 2m from the 1st column, but the most aggressive action was taken into consideration and thus, the locations of the wheels were kept.

The values for the forces are the same as Section 3.1.6.5:

- LG1:
  - Vertical $F_1 = F_2 = 97.2$ kN; $F_3 = F_4 = 15.2$ kN
  - Transversal $H_{T,1} = 8.4$ kN = – $H_{T,2}$
  - Longitudinal $H_L = 5.1$ kN

- LG5:
  - Vertical $F_1 = F_2 = 97.2$ kN; $F_3 = F_4 = 15.2$ kN (the largest values were used for both LGs in favor of security)
  - Transversal $H_{S,1} = 26.1$ kN (Right Side, where the largest vertical force is located, always closest to the column); $H_{S,2} = 0$ kN

Since there are 2 Load Groups for the German Norm and 3 different locations for the wheels, there were a total of 6 Load Cases for the Crane.

It is possible to conclude that the Norms apply the forces at different locations, but the locations of the wheels in relation to the specific column (2^{nd} or 5^{th}) were the same. Moreover, they differ in values, material and in their cross-section profiles.

5.6 2D Model - Frame

To simplify the visualization of the frames of the structure and the combination to reach its most aggressive loads, a 2D model was created (the 5^{th} frame from the front would have most aggressive loads). The area loads were transformed into linear loads (some linear loads were already calculated, for example the Wind Loads in Section 3.2.4.8) and were set on the frame for each type of action. For each type of action, other important nodal loads (concentrated loads) were input:

5.6.1 Self-Weight

Since the Frame is a 2D model, the weights of the elements on the 3D model have to be added. Since the profiles of the cross-sections are very similar (and consequently their weight), these loads were simplified to be the same for German and Brazilian structures. The Loads for each cross-section (Brazilian) were calculated and can be verified in Table 36:

Cross-Sections	ORIGINAL	BRA	Weight [kg/m]	kg	kN
Purlins	U 152 x 12.2	C 6x8.2 (AISC 14)	17	102	1.02
Hor Bracings	+ 64x64x6.3	2LC L 60x6.3-0	10.8	155.52	1.5552
Vert Bracings	+ 76x76x8	2LC L 80x8-0	18.2	67.34	0.6734
Runway Girder	PS 750x128.7	VS 750x125	125.4	752.4	7.524
Chords Lateral Mid Truss	L 76x76x8	L 80x8	9.1	109.2	1.092
Diag Lateral Mid Truss	L 51x6.3	L 50x6.3	4.4	49.5	0.495
Truss System Lateral Mid					1.587
Chords Lateral Sup Truss	U 203x17.1	U 200x100x8	23.3	279.6	2.796
Diag Lateral Sup Truss	U* 51x6.3	2LB L50x6.3-150/6.3	8.9	154.148	1.5415
Truss System Lateral Sup					4.3375

Table 36: Nodal Loads (Self-Weight) on 2D Model from 3D Cross-Sections

These loads were applied to the 2D Model (each load on its specific node – the truss system was simplified to act upon the inferior node of each truss point) as seen in Figure 87:

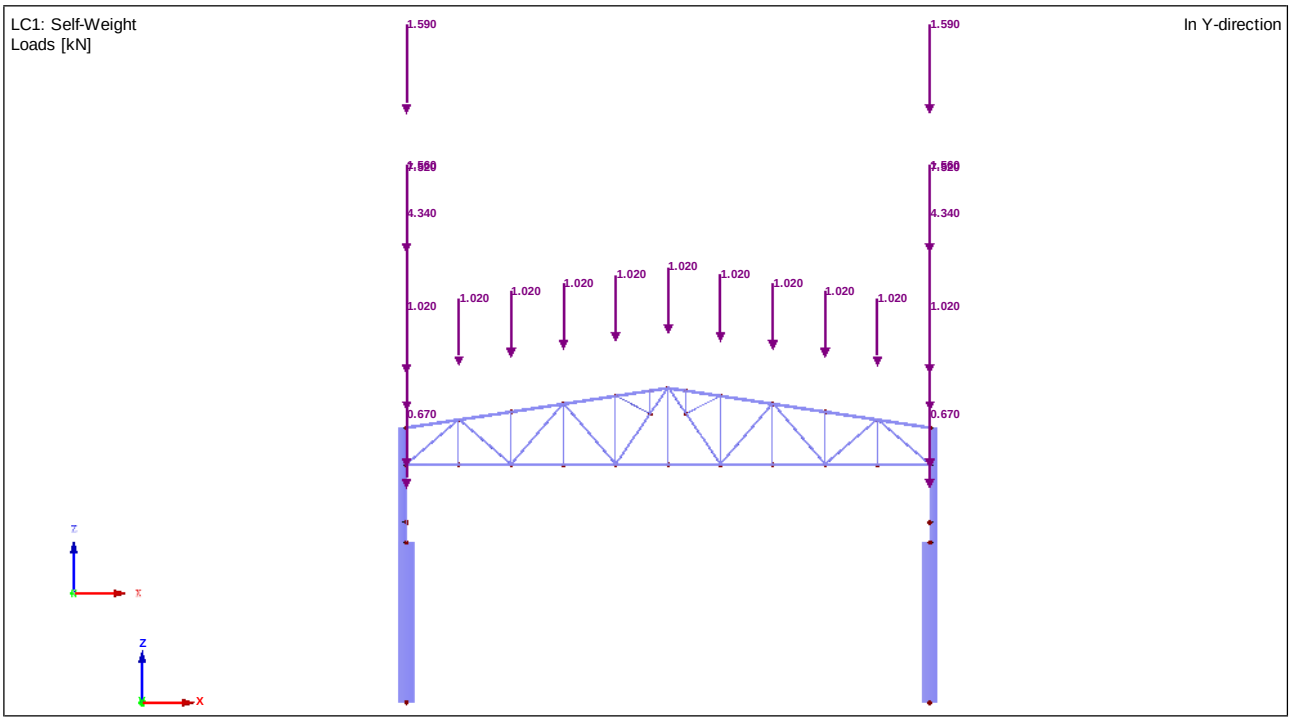

Figure 87: Representation of Self-Weight Loads on the 2D Model

5.6.2 Additional Dead Loads

Since the roof is symmetric, it can be considered as a flat roof, in this case. The flat roof can then be seen, in a 2D view, as a linear load with 10 spans of 2m each (with a total of 10 * 2 = 20m). This load will be transformed into concentrated loads due to the supporting reactions of the purlins on the truss system (in the Z-direction). Since all purlins are single-spanned, the simplification of area loads into linear and concentrated loads can be simplified by area of influence.

For the 2D model, the distance between the frames is 6m (longitude) and therefore, according to Section 5.2:

$$0.2\frac{kN}{m} * 6m = 1.2\ kN$$

Or

$$0.8\frac{kN}{m} * 6m = 4.8\ kN$$

On the inner purlins and

$$0.1\frac{kN}{m} * \frac{6m}{2} = 0.6\ kN$$

Or

$$0.4\frac{kN}{m} * \frac{6m}{2} = 2.4\ kN$$

On the outer purlins. Figure 88 represents the Additional Dead Loads on the 2D Model for the Brazilian Norm:

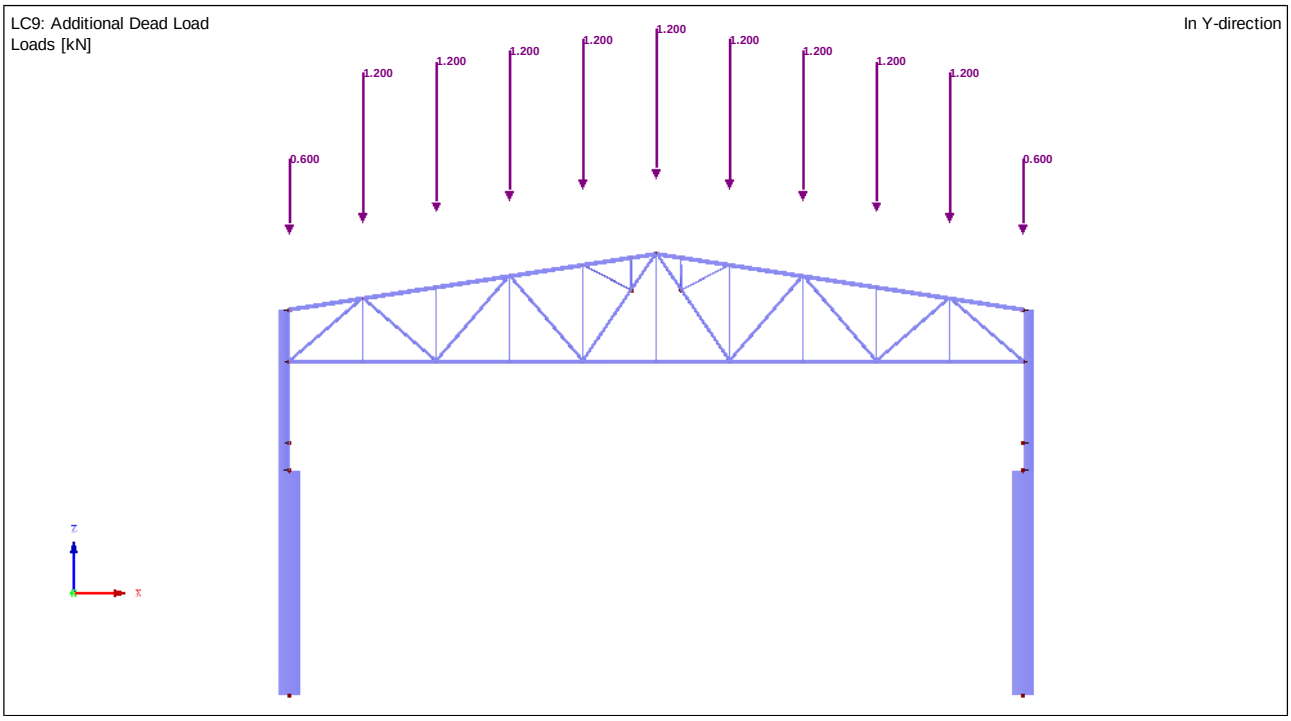

Figure 88: Transformed Additional Dead Loads on 2D Model (Brazilian)

5.6.3 Wind Loads

For the 2D model, the calculations used are given in Section 3.2.4.8. For these cases, the linear load on the roof should be also multiplied by the distance between the purlins, of 2m (inner purlins) or 1m (middle and outer purlins) to achieve concentrated loads on the purlins. However, in this case, to simplify the calculations, due to the angle of the roof, the loads on the roof remained as linear loads. The linear loads applied on the columns coming from the walls remained the same.

This modeling is visible in Figure 89. This figure is the same as Figure 46 but when it was modeled in the software.

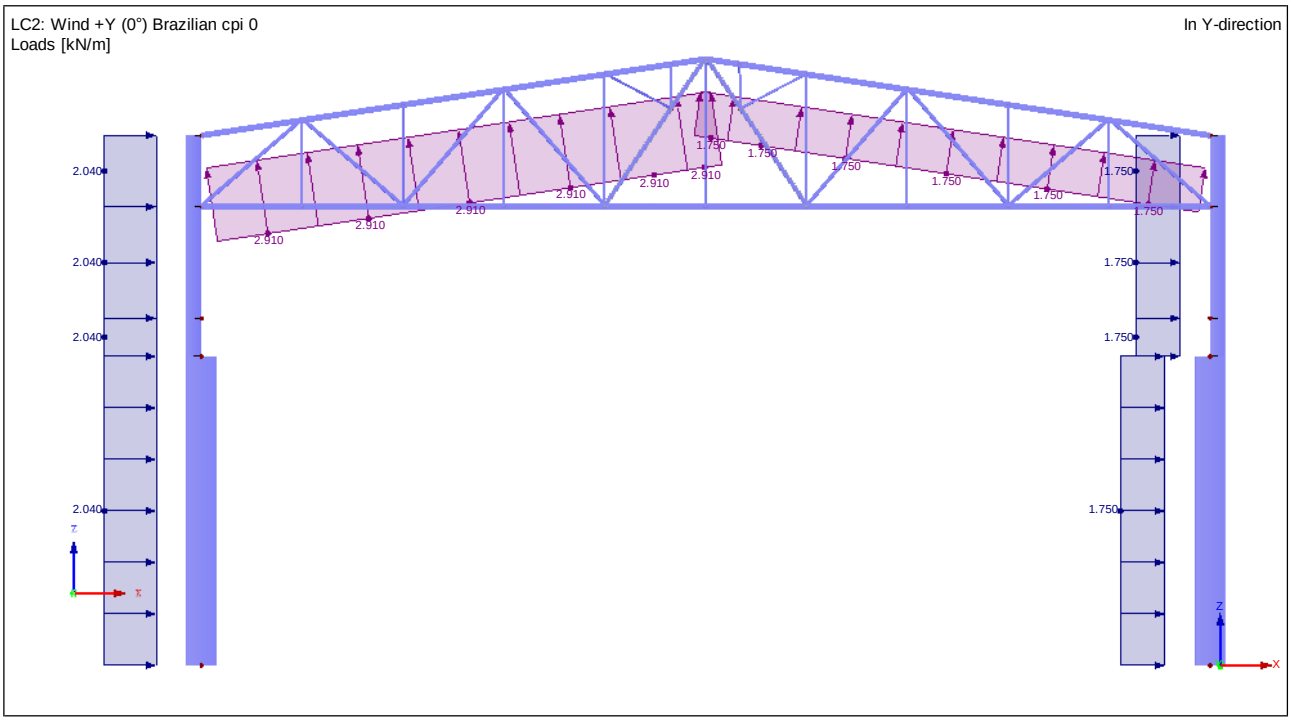

Figure 89: Demonstration of Linear Wind Loads on the Frame

For the German Norm, when the Wind blew in the +X-Direction (90°), the values for D and E were accounted for on the columns (see Table 37). When the Wind blew in the +Y-Direction (0°), the value for A was used since it was the largest between the ones that were applied on the columns (see Table 38).

θ = 90°	$c_{pe} + c_{pi}$			
h/d	**A**	**B**	**D**	**E**
0.6010	-1.0634	-0.6634	0.8834	-0.2570
	A	**B**	**D**	**E**
W [kN/m²]	-0.56	-0.35	0.47	-0.14

Table 37: Combination of c_{pe} and c_{pi} and Wind Loads on Walls when θ = 90°

θ = 0°	$c_{pe} + c_{pi}$				
h/d	**A**	**B**	**C**	**D**	**E**
0.247916667	-1.5	-1.1	-0.8	0.4	-0.3
	A	**B**	**C**	**D**	**E**
W [kN/m²]	-0.80	-0.58	-0.42	0.21	-0.16

Table 38: Combination of c_{pe} and c_{pi} and Wind Loads on Walls when θ = 90°

For the Saddle Roof, the simplified linear loads along the upper chord were chosen among the greatest value. When the Wind blew in the +X-Direction (90°), the values for F, H, I and J were imposed on the chord, with the correct measure for each area. When the Wind blew in the +Y-Direction (0°), the values for F and G were used, or none used in the case of the unloaded roof.

5.6.4 Live Loads

According to the calculations in Section 5.4, for the 2D model, the distance between the frames is 6m (longitude):

$$1.0\ \frac{kN}{m} * 6m = 6\ kN$$

On the inner purlins and

$$0.5\ \frac{kN}{m} * 6m = 3\ kN$$

On the outer purlins. Figure 90 depicts the transformed Live Loads on the 2D Model:

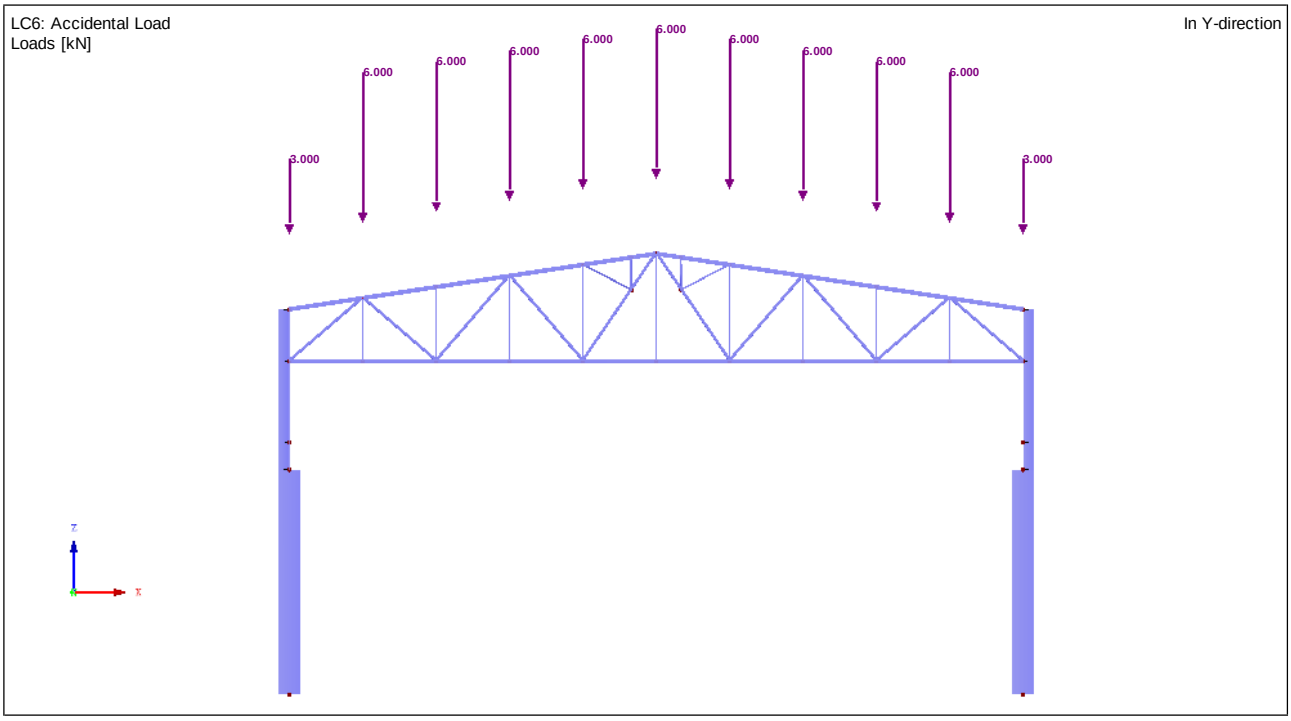

Figure 90: Transformed Live Loads on 2D Model

5.6.5 Notional Loads

The Notional Loads or Equivalent Force ("Forças Nocionais" or "Forças Horizontais Fictícias" see Section 3.2.3) derived from the imperfections of the elements were also calculated. It was calculated by the combination of the Permanent (Self-Weight and Additional Dead Load), Live Load and the Crane Load. The Permanent Load was given by:

Self-Weight of Frame (see Figure 91):

$$2917.17 * 10 /1000 = 29.17\ kN$$

Self-Weight of other members (see Figure 87):

$$11 * 1.02 + 2 * 7.52 + 2 * 0.67 + 2 * 4.34 + 2 * 1.56 + 2 * 1.59 = 42.58\ kN$$

Additional Dead Load (see Figure 88):

$$9 * 1.2 + 2 * 0.6 = 12\ kN$$

And the total Permanent Load was:

$$29.17 + 42.58 + 12 = 83.75\ kN$$

The Live Load (see Figure 90):

$$9 * 6 + 2 * 3 = 60\ kN$$

Crane Load (see Figure 97):

$$191.6 + 32 = 223.6\ kN$$

Thus, the combination was calculated by:

$$\gamma_{g1} * 83.75 + \gamma_{g2} * 60 + \gamma_{g2} * 223.6 = 1.25 * 83.75 + 1.5 * 60 + 1.5 * 223.6 = 530.0875\ kN$$

The Notional Load would be 0.3% of the combined gravitational load found:

$$F_n = 0.003 * 530.0875\ kN = 1.59\ kN$$

Later, it was proven that the Equivalent Force was not necessary[136] (but still kept, for conservative reasons), since the structure is considered of small displacement and some requirements were met[137] – see Section 6.1.2.1.

[136] (ABNT NBR 8800, 2008) – Section 4.9.7.1.1 Page 28
[137] (ABNT NBR 8800, 2008) – Section 4.9.7.1.4 Page 28

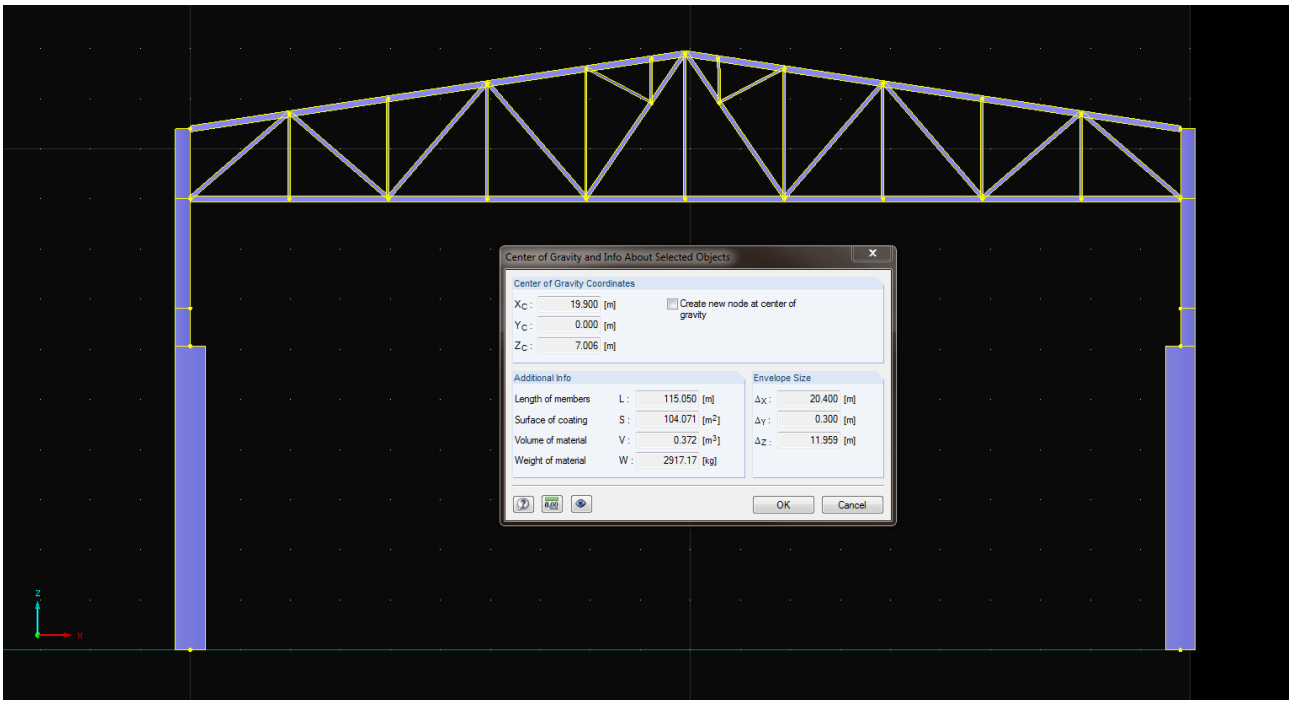

Figure 91: Self-Weight of the 2D Model

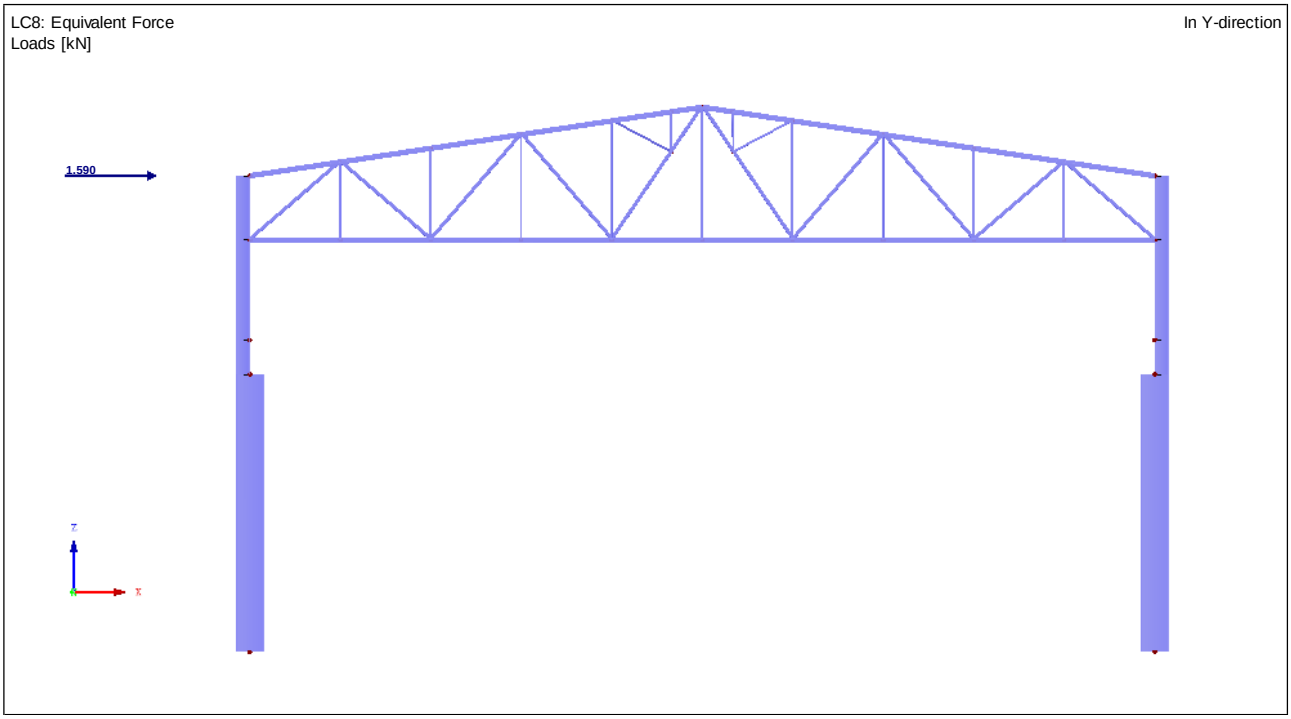

Figure 92: Representation of the Equivalent Force on the 2D Model

According to the DIN Norm[138], the Equivalent Force or the Substitute Force (Figure 94) for Imperfection on the Columns was calculated (not necessary, since the Theory of 2nd Order was disregarded – see Section 6.2.2 – but used to enable a better comparison between the Norms). The angle (Figure 93) of the imperfection was:

$$\phi = \phi_0 * \alpha_h * \alpha_m = \frac{1}{200} * \frac{2}{3} * 1 = 0.0033$$

Where:

- ϕ_0 = 1/200
- Reduction Factor for the Height h: $\alpha_h = \frac{2}{\sqrt{h}} = \frac{2}{3}$, $with \ \frac{2}{3} \leq \alpha_h \leq 1.0$
- Height h = 10.4m
- Reduction Factor for the number of Columns in a Row $\alpha_m = \sqrt{0.5 * \left(1 + \frac{1}{m}\right)} = 1$
- Number of Columns in a Row which have more than 50% the average Vertical Load m = 1

The Substitute Force was:

$$F = \phi * N_{Ed} = 0.0033 * 367.21 = 1.224 \, kN$$

Since the sum of the Horizontal Forces do not surpass 15% of the Vertical Forces (including the Horizontal Equivalent Force) – see Figure 96 – the Substitute Force was applied on the structure in every top and bottom part of the columns:

- ΣH_{Ed} = 39.82 kN
- ΣV_{Ed} = 486.71 kN

$$\frac{\Sigma H_{Ed}}{\Sigma N_{Ed}} = \frac{39.82}{486.71} = 0.082 \leq 0.15$$

[138] (DIN EN 1993-1-1, 2010) – Section 5.3.2 Page 35

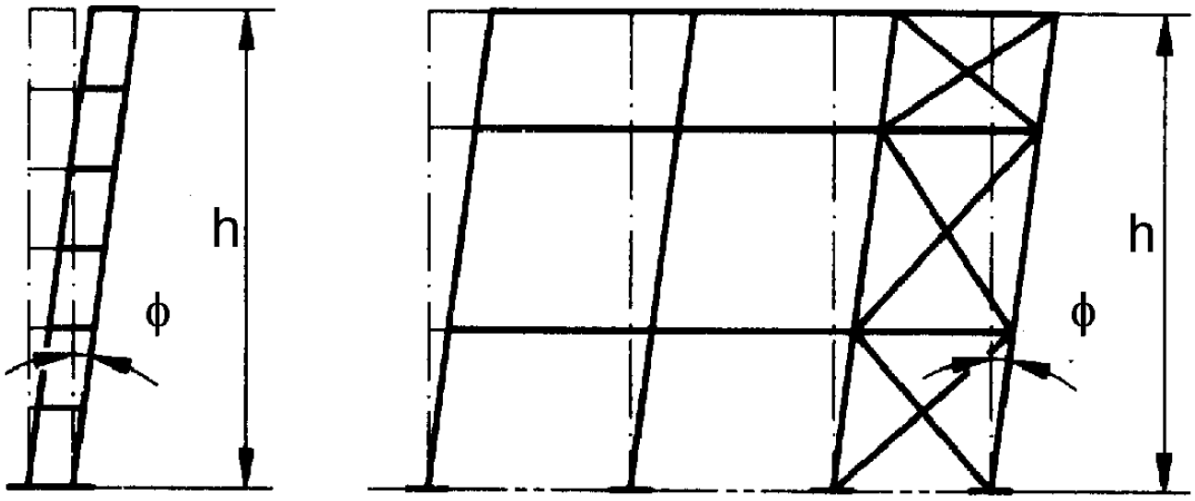

Figure 93: Equivalent Tilting of the Column[139]

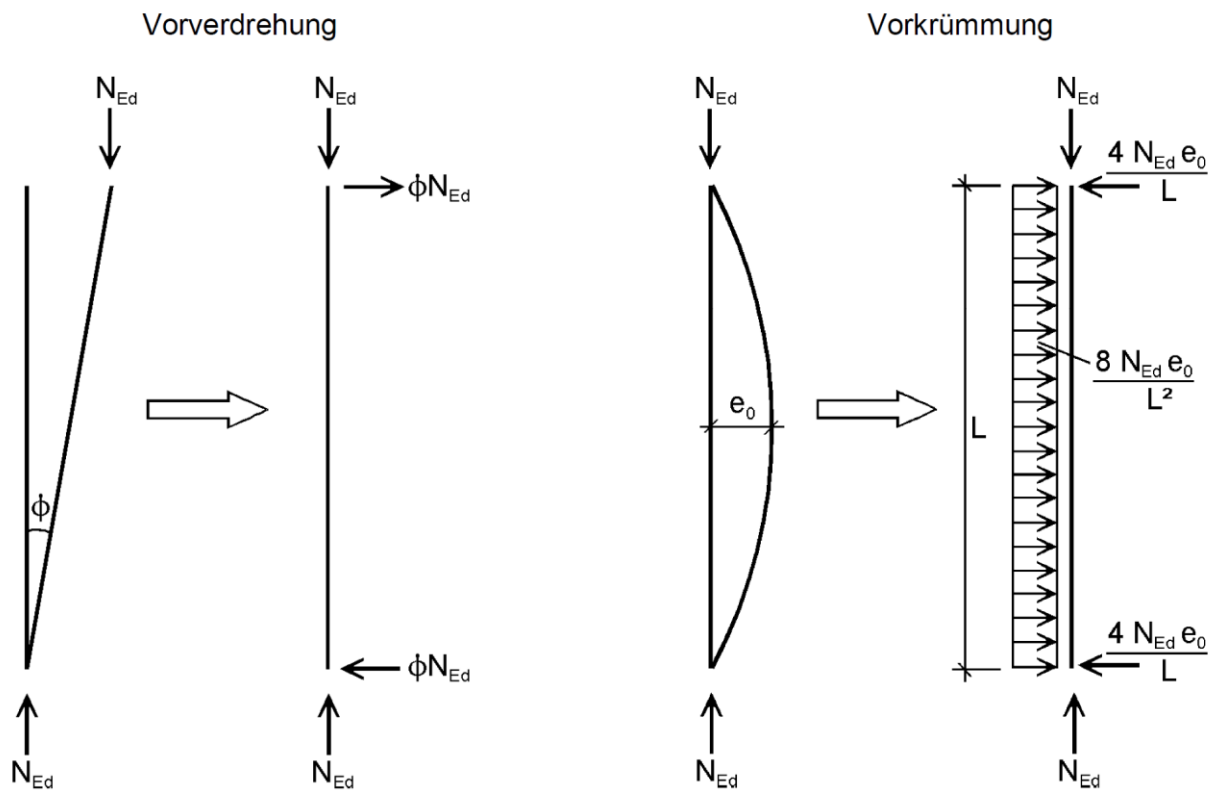

Figure 94: Substitute Forces for Imperfections[140]

[139] (DIN EN 1993-1-1, 2010) – Figure 5.2 Page 36
[140] (DIN EN 1993-1-1, 2010) – Figure 5.4 Page 38

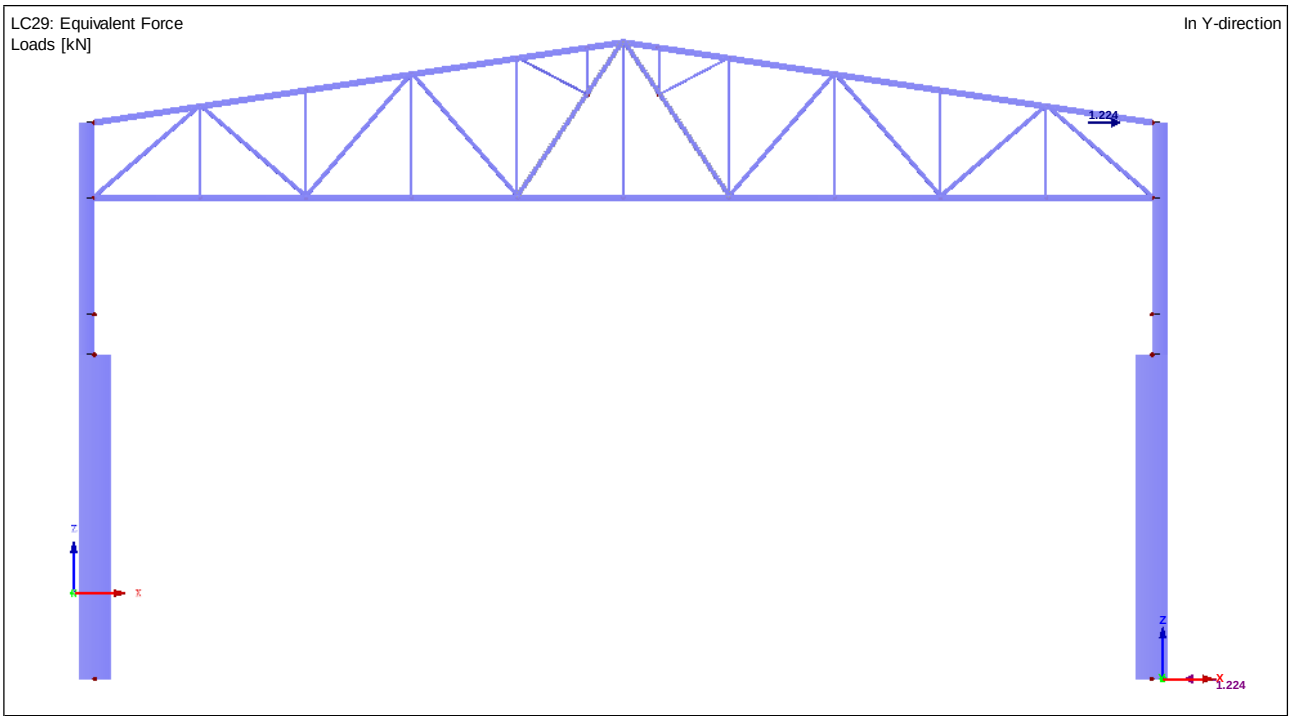

Figure 95: Equivalent (or Substitute) Force on the Top of the Column for the German Norm

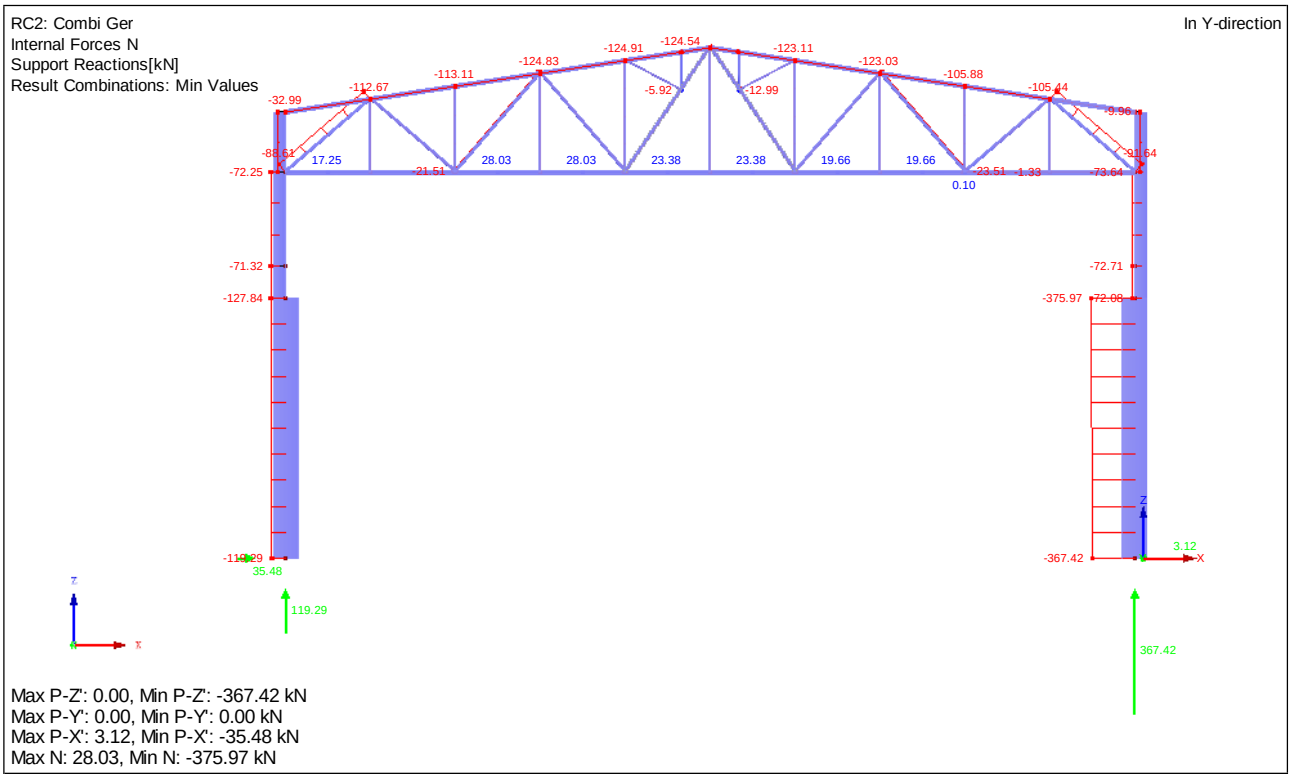

Figure 96: Normal Loads and Reaction Loads for the German Combination

In addition, another Substitute Force (Figure 94 – “Vorkrümmung”) for the Imperfection of the Column (due to Local Geometric Imperfeciton) must be also calculated. However, the structure was not reacting

sensitively to deformations (meaning it did not shift or have a large displacement), having its $\alpha_{cr} > 10$ (see Section 6.2.2), and therefore this force did not need to be applied[141].

These Equivalent Forces were also included on the 3D-Model.

5.6.6 Crane Loads

To apply the crane loads on the 2D Model, the wheel loads on each side (the sum of the wheel loads for the vertical loads) were imposed on the column (simplified method and also in favor of security). Eccentricities derived from these loads were not taken into consideration as explained in Section 3.1.6.4.

5.6.6.1 German Design Code

The values for the forces are the same as Section 3.1.6.5:

- LG1:
  - Vertical $F_{Right} = 2*F_1 = 2 * 97.2$ kN = 194.4 kN; $F_{Left} = 2 * F_3 = 2 * 15.2$ kN = 30.4 kN
  - Transversal $H_{T,1} = 8.4$ kN (on both sides)
- LG5:
  - Vertical $F_{Right} = 2*F_1 = 2 * 97.2$ kN = 194.4 kN; $F_{Left} = 2 * F_3 = 2 * 15.2$ kN = 30.4 kN (the largest values were used for both LGs in favor of security)
  - Transversal $H_{S,1} = 26.1$ kN (Right Side, where the largest vertical force is located); $H_{S,2} = 0$ kN

5.6.6.2 Brazilian Design Code

The values for the forces are the same as Section 3.2.6.5:

- Vertical $RV_{Right} = 2 * RV_1 = 2 * 95.8$ kN = 191.6 kN; $RV_{Left} = 2 * RV_3 = 2 * 16$ kN = 32 kN
- Transversal RH = 21.2 kN

An example of the 2D Model with the crane loads can be seen in Figure 97:

[141] (SCHNEIDER, 2012) – Section 1.6b Page 8.6

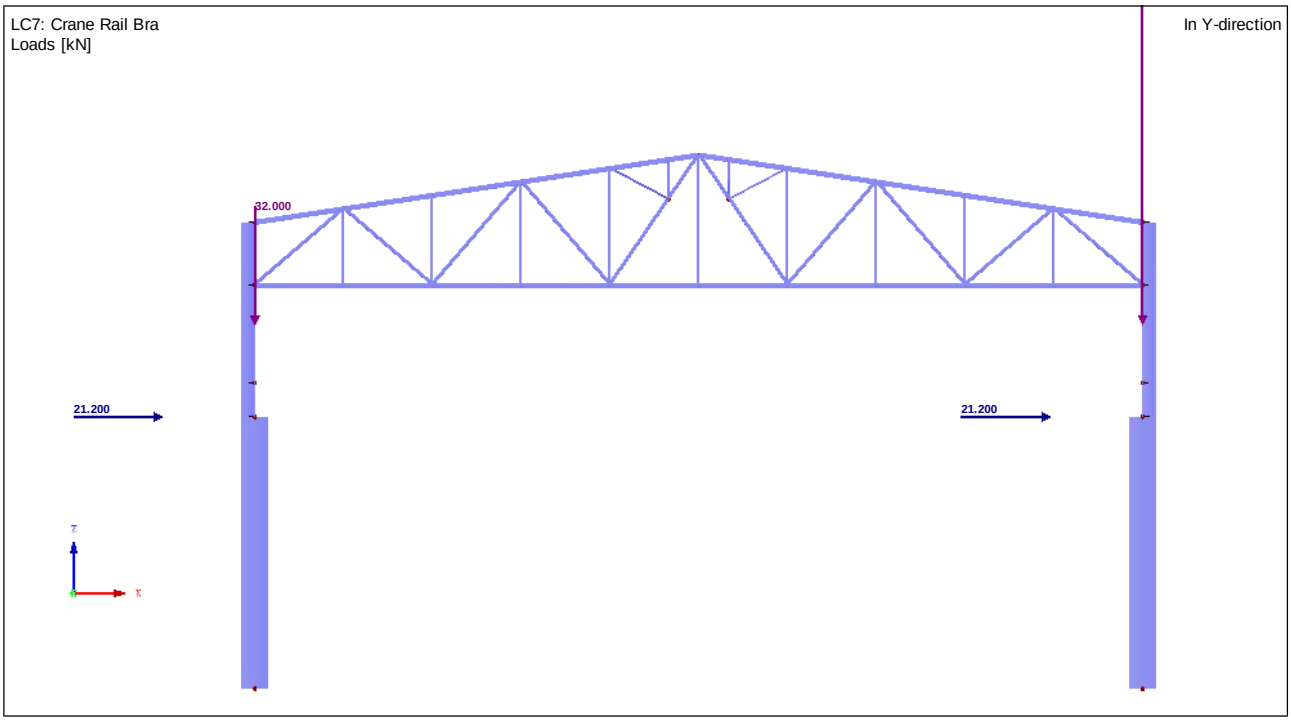

Figure 97: Representation of the 2D Model of the Crane Loads (Brazilian)

6. LOAD COMBINATIONS ULS (ELU OR GZT) AND SLS (ELS OR GZG)

In this project, only the Combination of Ultimate Limit State (ULS – Normal) – for the safety and stability of the structure – and the Combination of Service Limit State (SLS – Quasi-Permanent) – for displacement verifications – were considered. The other Action Combinations were not considered since there were no special actions (ex: construction phase) and fatigue is not considered.

6.1 Brazilian Design Codes

6.1.1 Coefficient of Actions

6.1.1.1 ULS (ELU – Estado-Limite Último)

In accordance to the NBR[142], for the ULS (ELU – Estado-Limite Último), there must be a combination of loads, each having its own multiplying factors. The NBR[143] states that all actions must be multiplied by a coefficient γ_f. The coefficient γ_f is given by the equation:

$$\gamma_f = \gamma_{f1} * \gamma_{f2} * \gamma_{f3}$$

Where:

- γ_{f1} is the coefficient that considers the variability of the actions
- γ_{f2} (or Ψ_i) is the coefficient that considers the simultaneity of the actions
- γ_{f3} is the coefficient that considers the possible errors of the evaluation of the effects of the actions (ex: from construction problems, deficiency of the method of calculation used), with a value of 1.10 or more.

Table 39[144] and Table 40 indicate the γ_f necessary for each action. The coefficients used were:

- Self-Weight: $\gamma_g = 1.25$
- Additional Dead Load: $\gamma_g = 1.25$
- Live Loads: $\gamma_g = 1.50$ and $\Psi_0 = 0.8$
- Crane Loads: $\gamma_q = 1.50$ and $\Psi_0 = 1.0$
- Wind Loads: $\gamma_q = 1.40$ and $\Psi_0 = 0.6$
- Equivalent Force (Imperfection): $\gamma = 1.0$

[142] (ABNT NBR 8800, 2008) – Section 4.7.7.2.1 Page 19
[143] (ABNT NBR 8800, 2008) – Section 4.7.6 Page 17
[144] Important: the γ values in this Table are already combined factor from coefficients γ_{f1} and γ_{f3}

Combinações	Ações permanentes (γ_g) [a c]					
	Diretas					Indiretas
	Peso próprio de estruturas metálicas	Peso próprio de estruturas pré-moldadas	Peso próprio de estruturas moldadas no local e de elementos construtivos industrializados e empuxos permanentes	Peso próprio de elementos construtivos industrializados com adições *in loco*	Peso próprio de elementos construtivos em geral e equipamentos	
Normais	1,25 (1,00)	1,30 (1,00)	1,35 (1,00)	1,40 (1,00)	1,50 (1,00)	1,20 (0)
Especiais ou de construção	1,15 (1,00)	1,20 (1,00)	1,25 (1,00)	1,30 (1,00)	1,40 (1,00)	1,20 (0)
Excepcionais	1,10 (1,00)	1,15 (1,00)	1,15 (1,00)	1,20 (1,00)	1,30 (1,00)	0 (0)
	Ações variáveis (γ_q) [a d]					
	Efeito da temperatura [b]		Ação do vento	Ações truncadas [e]	Demais ações variáveis, incluindo as decorrentes do uso e ocupação	
Normais	1,20		1,40	1,20	1,50	
Especiais ou de construção	1,00		1,20	1,10	1,30	
Excepcionais	1,00		1,00	1,00	1,00	

[a] Os valores entre parênteses correspondem aos coeficientes para as ações permanentes favoráveis à segurança; ações variáveis e excepcionais favoráveis à segurança não devem ser incluídas nas combinações.

[b] O efeito de temperatura citado não inclui o gerado por equipamentos, o qual deve ser considerado ação decorrente do uso e ocupação da edificação.

[c] Nas combinações normais, as ações permanentes diretas que não são favoráveis à segurança podem, opcionalmente, ser consideradas todas agrupadas, com coeficiente de ponderação igual a 1,35 quando as ações variáveis decorrentes do uso e ocupação forem superiores a 5 kN/m^2, ou 1,40 quando isso não ocorrer. Nas combinações especiais ou de construção, os coeficientes de ponderação são respectivamente 1,25 e 1,30, e nas combinações excepcionais, 1,15 e 1,20.

[d] Nas combinações normais, se as ações permanentes diretas que não são favoráveis à segurança forem agrupadas, as ações variáveis que não são favoráveis à segurança podem, opcionalmente, ser consideradas também todas agrupadas, com coeficiente de ponderação igual a 1,50 quando as ações variáveis decorrentes do uso e ocupação forem superiores a 5 kN/m^2, ou 1,40 quando isso não ocorrer (mesmo nesse caso, o efeito da temperatura pode ser considerado isoladamente, com o seu próprio coeficiente de ponderação). Nas combinações especiais ou de construção, os coeficientes de ponderação são respectivamente 1,30 e 1,20, e nas combinações excepcionais, sempre 1,00.

[e] Ações truncadas são consideradas ações variáveis cuja distribuição de máximos é truncada por um dispositivo físico, de modo que o valor dessa ação não possa superar o limite correspondente. O coeficiente de ponderação mostrado nesta Tabela se aplica a este valor-limite.

Table 39: Coefficient of Actions γ_g[145] and γ_q[146] for Brazilian Norm[147]

[145] γ_g is the coefficient for permanent actions
[146] γ_q is the coefficient for varying actions
[147] (ABNT NBR 8800, 2008) – Table 1 Page 18

Ações		γ_{f2} [a]		
		ψ_0	ψ_1 [d]	ψ_2 [e]
Ações variáveis causadas pelo uso e ocupação	Locais em que não há predominância de pesos e de equipamentos que permanecem fixos por longos períodos de tempo, nem de elevadas concentrações de pessoas [b)]	0,5	0,4	0,3
	Locais em que há predominância de pesos e de equipamentos que permanecem fixos por longos períodos de tempo, ou de elevadas concentrações de pessoas [c]	0,7	0,6	0,4
	Bibliotecas, arquivos, depósitos, oficinas e garagens e sobrecargas em coberturas (ver B.5.1)	0,8	0,7	0,6
Vento	Pressão dinâmica do vento nas estruturas em geral	0,6	0,3	0
Temperatura	Variações uniformes de temperatura em relação à média anual local	0,6	0,5	0,3
Cargas móveis e seus efeitos dinâmicos	Passarelas de pedestres	0,6	0,4	0,3
	Vigas de rolamento de pontes rolantes	1,0	0,8	0,5
	Pilares e outros elementos ou subestruturas que suportam vigas de rolamento de pontes rolantes	0,7	0,6	0,4

[a] Ver alínea c) de 4.7.5.3.
[b] Edificações residenciais de acesso restrito.
[c] Edificações comerciais, de escritórios e de acesso público.
[d] Para estado-limite de fadiga (ver Anexo K), usar ψ_1 igual a 1,0.
[e] Para combinações excepcionais onde a ação principal for sismo, admite-se adotar para ψ_2 o valor zero.

Table 40: Coefficient of Actions γ_{f2} (Ψ_i) for Brazilian Norm[148]

6.1.1.2 SLS (ELS – Estado-Limite de Serviço)

Similarly to the ULS (ELU), the SLS (ELS – Estado-Limite de Serviço) for the NBR[149] must also have a combination of coefficients, but the coefficients are different. First, there are no coefficients of actions that consider the variability of the actions (γ_f), only the one that considers the simultaneity (γ_2 or Ψ_2). Second, even though the simultaneity coefficient is considered, there is no main load considered in the combination. Table 40 indicates the Ψ_2 necessary for each action. The coefficients used were:

- Self-Weight: not necessary
- Additional Dead Load: not necessary
- Live Loads: $\Psi_2 = 0.6$
- Crane Loads: $\Psi_2 = 0.5$
- Wind Loads: $\Psi_2 = 0.0$
- Equivalent Force (Imperfection): Ψ_2 = not necessary

[148] (ABNT NBR 8800, 2008) – Table 2 Page 19
[149] (ABNT NBR 8800, 2008) – Section 4.7.7.3.2 Page 21

6.1.2 Load Combinations

6.1.2.1 ULS (ELU – Estado-Limite Último)

From the NBR[150], the equation for the normal ultimate combinations is given by:

$$F_d = \sum_{i=1}^{m}(\gamma_{gi} * F_{Gi,k}) + \gamma_{q1} * F_{Q1,k} + \sum_{j=2}^{n}(\gamma_{qj} * \Psi_{0j} * F_{Qj,k})$$

- $F_{Gi,k}$ represents the characteristic values of the permanent actions
- $F_{Q1,k}$ represents the characteristic value of the main varying action for the combination
- $F_{Qj,k}$ represents the characteristic values of the varying actions that may act simultaneously with the main varying action

This results in 4 different combinations:

1. When the Live Load is the main action:

$$F_d = 1.25 * F_{SW} + 1.5 * F_L + 1.4 * 0.6 * F_W + 1.5 * 1 * F_{CR}$$
$$F_d = 1.25 * F_{SW} + 1.5 * F_L + 0.84 * F_W + 1.5 * F_{CR}$$

2. When the Wind Load is the main action:

$$F_d = 1.25 * F_{SW} + 1.4 * F_W + 1.5 * 0.8 * F_L + 1.5 * 1 * F_{CR}$$
$$F_d = 1.25 * F_{SW} + 1.4 * F_W + 1.2 * F_L + 1.5 * F_{CR}$$

3. When the Crane Load is the main action:

$$F_d = 1.25 * F_{SW} + 1.5 * F_{CR} + 1.5 * 0.8 * F_L + 1.4 * 0.6 * F_W$$
$$F_d = 1.25 * F_{SW} + 1.5 * F_{CR} + 1.2 * F_L + 0.84 * F_W$$

4. When the Wind Load is the main action (without the Live Load):

$$F_d = 1.0 * F_{SW} + 1.4 * F_W + 1.5 * 1 * F_{CR}$$
$$F_d = 1.0 * F_{SW} + 1.4 * F_W + 1.5 * F_{CR}$$

For each of these combinations, the Equivalent Force should be added with a factor of 1.0.

The 4th combination represents the Wind's upward force on the ceiling, in an attempt to rip the ceiling (roof) upwards.

In RSTAB, each type of load was multiplied with its coefficient for each combination accordingly. Figure 98 to Figure 100 show the combination of loads for the Brazilian Norm:

[150] (ABNT NBR 8800, 2008) – Section 4.7.7.2.1 Page 20

Loading in Result Combination RC

Factor	No.	Description	Criterion	Group
1.25	G Me LC1	Self-Weight	Permanent	-
0.84	Qw LC3	Wind +Y (0°) Brazilian cpi 0	Variable	1
0.84	Qw LC5	Wind +X (90°) Brazilian cpi 0	Variable	1
0.84	Qw LC8	Wind +Y (0°) Brazilian cpi -0.3	Variable	1
0.84	Qw LC9	Wind +X (90°) Brazilian cpi -0.3	Variable	1
1.50	G In LC6	Live Load	Permanent	-
1.50	Q Ge LC7	Crane Bra 1	Variable	2
1.50	Q Ge LC10	Crane Bra 2	Variable	2
1.50	Q Ge LC11	Crane Bra 3	Variable	2
1.25	G Me LC12	Additional Dead Load	Permanent	-
1.00	Imp LC13	Equivalent Force	Variable	-

Figure 98: Combination of Loads (Brazilian) with the Respective Coefficients for Live Load as Main Load for ULS (ELU)

Loading in Result Combination RC

Factor	No.	Description	Criterion	Group
1.25	G Me LC1	Self-Weight	Permanent	-
1.40	Qw LC3	Wind +Y (0°) Brazilian cpi 0	Variable	1
1.40	Qw LC5	Wind +X (90°) Brazilian cpi 0	Variable	1
1.40	Qw LC8	Wind +Y (0°) Brazilian cpi -0.3	Variable	1
1.40	Qw LC9	Wind +X (90°) Brazilian cpi -0.3	Variable	1
1.20	G In LC6	Live Load	Permanent	-
1.50	Q Ge LC7	Crane Bra 1	Variable	2
1.50	Q Ge LC10	Crane Bra 2	Variable	2
1.50	Q Ge LC11	Crane Bra 3	Variable	2
1.25	G Me LC12	Additional Dead Load	Permanent	-
1.00	Imp LC13	Equivalent Force	Variable	-

Figure 99: Combination of Loads (Brazilian) with the Respective Coefficients for Wind Load as Main Load for ULS (ELU)

Loading in Result Combination RC

Factor	No.	Description	Criterion	Group
1.25	G Me LC1	Self-Weight	Permanent	-
0.84	Qw LC3	Wind +Y (0°) Brazilian cpi 0	Variable	1
0.84	Qw LC5	Wind +X (90°) Brazilian cpi 0	Variable	1
0.84	Qw LC8	Wind +Y (0°) Brazilian cpi -0.3	Variable	1
0.84	Qw LC9	Wind +X (90°) Brazilian cpi -0.3	Variable	1
1.20	G In LC6	Live Load	Permanent	-
1.50	Q Ge LC7	Crane Bra 1	Variable	2
1.50	Q Ge LC10	Crane Bra 2	Variable	2
1.50	Q Ge LC11	Crane Bra 3	Variable	2
1.25	G Me LC12	Additional Dead Load	Permanent	-
1.00	Imp LC13	Equivalent Force	Variable	-

Figure 100: Combination of Loads (Brazilian) with the Respective Coefficients for Crane Load as Main Load for ULS (ELU)

Loading in Result Combination RC

Factor	No.	Description	Criterion	Group
1.25	G Me LC1	Self-Weight	Permanent	-
1.40	Qw LC3	Wind +Y (0°) Brazilian cpi 0	Variable	1
1.40	Qw LC5	Wind +X (90°) Brazilian cpi 0	Variable	1
1.40	Qw LC8	Wind +Y (0°) Brazilian cpi -0.3	Variable	1
1.40	Qw LC9	Wind +X (90°) Brazilian cpi -0.3	Variable	1
1.50	Q Ge LC7	Crane Bra 1	Variable	2
1.50	Q Ge LC10	Crane Bra 2	Variable	2
1.50	Q Ge LC11	Crane Bra 3	Variable	2
1.25	G Me LC12	Additional Dead Load	Permanent	-
1.00	Imp LC13	Equivalent Force	Variable	-

Figure 101: Combination of Loads (Brazilian) with the Respective Coefficients for Wind Load as Main Load for ULS (ELU) without Live Load

According to NBR[151], a structure is classified as a small displacement if the relation between the horizontal shift of the top of the column for the 2nd Order Theory Analysis (global) and its horizontal shift for the 1st Order Theory is 1.1. In addition, in the NBR[152], it is possible to estimate this relation between the 1st and 2nd Order (global) Theories by calculating the coefficient B_2:

$$B_2 = \frac{1}{1 - \frac{1}{R_S} * \frac{\Delta_h}{h} * \frac{\Sigma N_{Sd}}{\Sigma H_{Sd}}}$$

- R_S : Adjustment coefficient[153]
- Δ_h : Horizontal shift between the top of the column and the bottom (for the 1st Order Analysis)
- ΣN_{Sd} : Sum of the Vertical Loads (also calculated by the sum of the vertical reaction on the supports)
- ΣH_{Sd} : Sum of the Horizontal Loads (also calculated by the sum of the horizontal reaction on the supports)
- h : Height of the column

$$B_2 = \frac{1}{1 - \frac{1}{R_S} * \frac{\Delta_h}{h} * \frac{\Sigma N_{Sd}}{\Sigma H_{Sd}}} = \frac{1}{1 - \frac{1}{0.85} * \frac{1.44}{1040} * \frac{460.66}{71.62}} = 1.01$$

[151] (ABNT NBR 8800, 2008) – Section 4.9.4.2 Page 26
[152] (ABNT NBR 8800, 2008) – Annex D.2 Page 118
[153] 0.85 for structures consisted of frames; 1.0 for all other structures

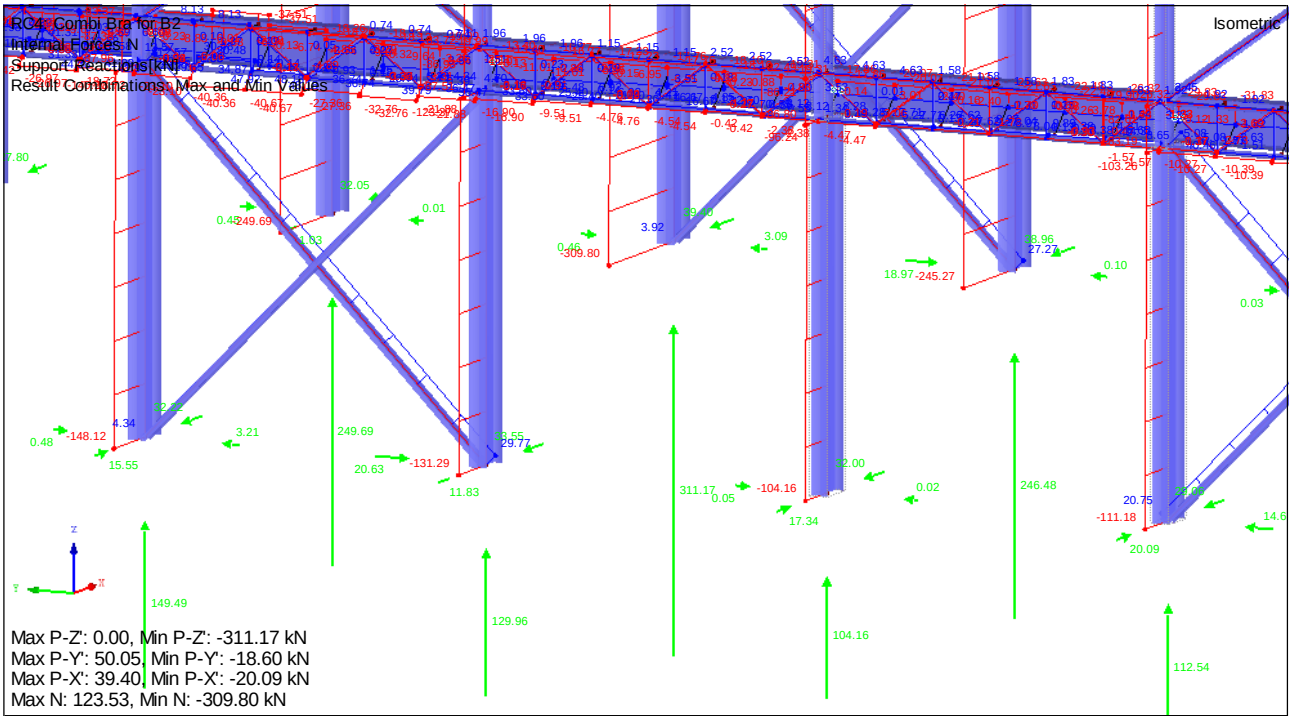

Figure 102: Normal Forces and Support Reactions on 5th Column

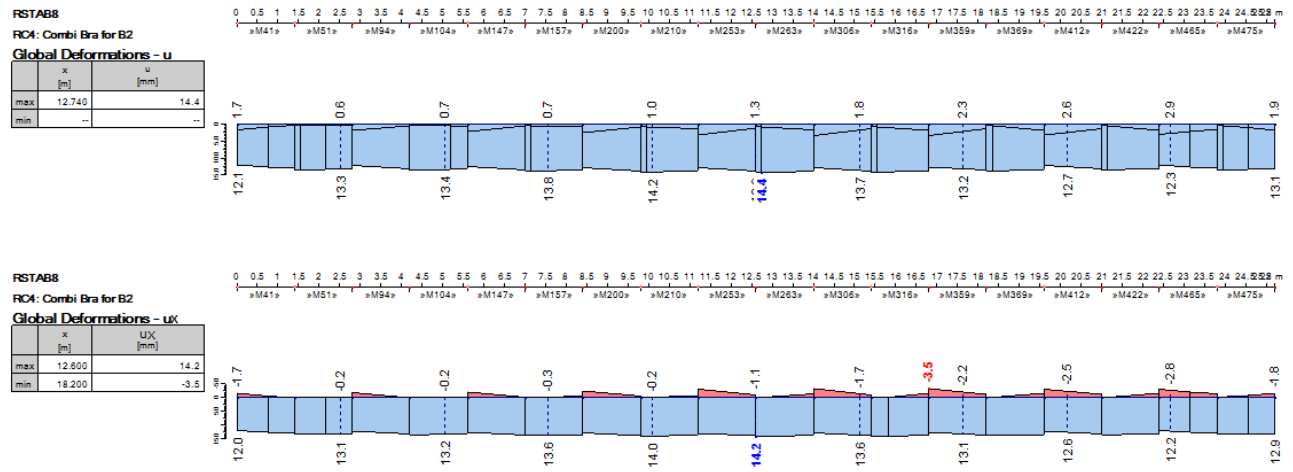

Figure 103: Maximum Horizontal Deformation on the Top of the Column (Member M263 – 5th Column Right)

Since $B_2 < 1.1$, the structure is considered of small displacement.

In the NBR[154], in small displacements structures, the effects of the global 2nd Order Analysis may be disregarded when the normal forces (after the combination of actions) on the columns do not exceed 50% of the plastic normal force (yield strength multiplied by its Area) of the cross-section. For the column, the largest normal force and its plastic normal force are:

[154] (ABNT NBR 8800, 2008) – Section 4.9.7.1.4 Page 28

Max Normal Force: 311.17 kN

Plastic Normal Force: A * f_y = 121 cm² * 25 kN/cm² = 3025 kN

$$N_{Sd} = 311.17\ kN < \frac{A * f_y}{2} = \frac{121 * 25}{2} = \frac{3025}{2} = 1512.5\ kN$$

In this case, the global 2nd Order Analysis can be disregarded (B_2 coefficient). However, the coefficient B_1 (local 2nd Order) must be calculated[155]:

$$B_1 = \frac{C_m}{1 - \frac{N_{Sd1}}{N_e}} \geq 1.0$$

- N_{Sd1} : Normal compression force (1st Order Theory)
- N_e : Normal force that causes buckling calculated with the real length of the beam (on the XZ-Plane)
- C_m : When transversal forces between the extremities of the beam exist, coefficient can be conservatively considered as 1.0

$$B_1 = \frac{C_m}{1 - \frac{N_{Sd1}}{N_e}} = \frac{1}{1 - \frac{311.17}{6145}} = 1.053 \geq 1.0$$

With N_e being calculated with the software SAP 2000 (due to its different cross-sections along its axis) having L_c = 9m.

According to the NBR[156], the new Moment and Normal Forces after a 2nd Order Analysis was given by:

$$M_{Sd} = B_1 * M_{nt} + B_2 * M_{lt} = B_1 * M_{nt}$$

$$N_{Sd} = N_{nt} + B_2 * N_{lt} = N_{nt}$$

Thus, it was not required that the Normal Forces should be multiplied by a factor, but the Moment Forces should. RSTAB offers this by applying a factor to increase the bending moment (see Figure 104) and it was applied as the B_1 factor (1.053).

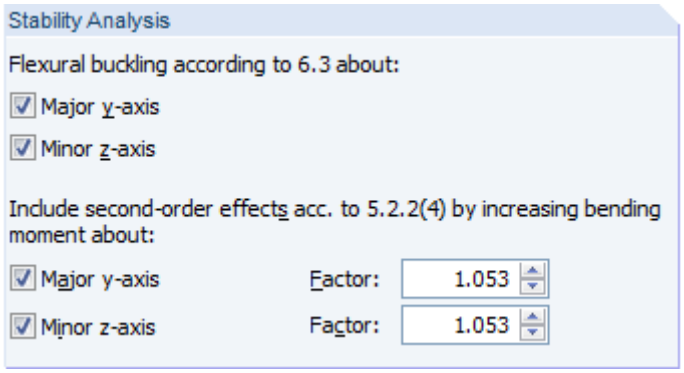

Figure 104: Multiplying Factor (B1) to Increase the Bending Moment

[155] (ABNT NBR 8800, 2008) – Annex D.2 Page 118
[156] (ABNT NBR 8800, 2008) – Annex D.2 Page 118

Furthermore, the Equivalent Force calculated in Section 5.6.5 could be neglected[157], but was still kept for a more conservative view.

6.1.2.2 SLS (ELS – Estado-Limite de Serviço)

From the NBR[158], the equation for the quasi-permanent service combinations is given by:

$$F_{ser} = \sum_{i=1}^{m}(F_{Gi,k}) + \sum_{j=2}^{n}(\Psi_{2j} * F_{Qj,k})$$

- $F_{Gi,k}$ represents the characteristic values of the permanent actions
- $F_{Qj,k}$ represents the characteristic values of the varying actions that may act simultaneously

This results in 1 combination:

$$F_{ser} = F_{SW} + 0.6 * F_L + 0.0 * F_W + 0.5 * F_{CR}$$
$$F_{ser} = F_{SW} + 0.6 * F_L + 0.5 * F_{CR}$$

For this combination, the Equivalent Force should be added with a factor of 1.0.

In RSTAB, each type of load was multiplied with its coefficient for each combination accordingly. Figure 105 shows the combination of loads for the Brazilian Norm:

Loading in Result Combination RC

Factor	No.	Description	Criterion	Group
1.00	G Me LC1	Self-Weight	Permanent	-
0.60	G In LC6	Live Load	Permanent	-
0.50	Q Ge LC7	Crane Bra 1	Variable	1
0.50	Q Ge LC10	Crane Bra 2	Variable	1
0.50	Q Ge LC11	Crane Bra 3	Variable	1
1.00	G Me LC12	Additional Dead Load	Permanent	-
1.00	Imp LC13	Equivalent Force	Variable	-

Figure 105: Combination of Loads (Brazilian) with the Respective Coefficients for SLS (ELS)

[157] (ABNT NBR 8800, 2008) – Section 4.9.7.1.1 Page 28
[158] (ABNT NBR 8800, 2008) – Section 4.7.7.3.2 Page 21

6.2 German Design Codes

6.2.1 Coefficient of Actions

6.2.1.1 ULS (GZT – Grenzzustand der Tragfähigkeit)

Similar to the Brazilian Norm, for the ULS (GZT – Grenzzustand der Tragfähigkeit), the DIN Norm[159] states that there must be a combination of loads, each having its own multiplying factors. The DIN[160] states that all actions must be multiplied by a coefficient γ_F. The coefficient γ_F is given by Table 41:

Nachweis	Einwirkung		Symbol	Bemessungssituation P/T[1)]	Bemessungssituation A[1)]
Lagesicherheit des Tragwerks (EQU)	Ständige Einwirkungen:				
	Eigenlast des Tragwerks und von Ausbauten; ständige Einwirkungen, vom Baugrund herrührend; Grundwasser und frei anstehendes Wasser	destab. stabil.	$\gamma_{G,dst}$ $\gamma_{G,stb}$	1,10 0,90	1,00 0,95
	Bei kleinen Schwankungen der ständigen Einwirkung (z. B. Nachweis der Auftriebssicherheit)	destab. stabil.	$\gamma_{G,dst}$ $\gamma_{G,stb}$	1,05 0,95	1,00 0,95
	Ständige Einwirkungen für kombinierte Nachweise der Lagesicherheit unter Einschluss des Widerstands der Bauteile (z. B. Zugverankerung)	destab. stabil.	$\gamma_{G,dst}$* $\gamma_{G,stb}$*	1,35 1,15	1,00 0,95
	Veränderliche Einwirkungen	destab.	γ_Q	1,50	1,00
	Außergewöhnliche Einwirkungen	destab.	γ_A	–	1,00
Versagen des Tragwerks od. der Gründung, durch Bruch, überm. Verformung (STR/GEO)	Unabhängige ständige Einwirkungen (siehe oben)	ungünstig günstig	$\gamma_{G,sup}$ $\gamma_{G,inf}$	1,35 1,00	1,00 1,00
	Unabhängige veränderliche Einwirkungen	ungünstig günstig	γ_Q γ_Q	1,50 –	1,00 –
	Außergewöhnliche Einwirkungen	ungünstig	γ_A	–	1,00
Baugrundversagen durch Böschungs- od. Geländebruch (GEO)	Unabhängige ständige Einwirkungen (s. o.)		γ_G	1,00	1,00
	Unabhängige veränderliche Einwirkungen	ungünstig günstig	γ_Q γ_Q	1,30 –	1,00 –
	Außergewöhnliche Einwirkungen	ungünstig	γ_A	–	1,00

1) P: Ständige Situation; T: Vorübergehende Situation; A: Außergewöhnliche Situation

Table 41: Coefficient of Actions γ_G[161] and γ_Q[162] for German Norm[163]

The coefficient γ_F represents the safety multiplying factor for permanent and varying actions while Ψ_i is the coefficient that considers the simultaneity of the actions (similar to the Brazilian Norm). Ψ_i is given by Table 42 below:

[159] (DIN EN 1990 NA), (DIN 1055), (DIN 18800)
[160] (DIN EN 1990, 2010) – Section 6.4.3.2 Page 41
[161] γ_G is the coefficient for permanent actions
[162] γ_Q is the coefficient for varying actions
[163] (SCHNEIDER, 2012) – Table 3.5a

Einwirkung			Kombinationsbeiwerte ψ_0	ψ_1	ψ_2
Nutzlast,	Kategorie A, B:	Wohn-, Aufenthalts-, Büroräume	0,7	0,5	0,3
	Kategorie C, D:	Versammlungsräume; Verkaufsräume	0,7	0,7	0,6
	Kategorie E:	Lagerräume	1,0	0,9	0,8
Verkehrslast,	Kategorie F:	Fahrzeuggewicht $F \leq 30$ kN	0,7	0,7	0,6
	Kategorie G:	Fahrzeuggewicht 30 kN $\leq F \leq$ 160 kN	0,7	0,5	0,3
	Kategorie H:	Dächer	0	0	0
Windlasten			0,6	0,2	0
Schneelasten		Orte bis zu NN +1000	0,5	0,2	0
		Orte über NN +1000	0,7	0,5	0,2
Temperatureinwirkungen		(nicht für Brand!)	0,6	0,5	0
Baugrundsetzungen			1,0	1,0	1,0
Sonstige veränderliche Einwirkungen			0,8	0,7	0,5

Table 42: Coefficient of Actions Ψ_i for German Norm[164]

Usually, $\gamma_G = 1.35$ and $\gamma_Q = 1.50$ and in accordance to Table 41, these values were used.

The coefficients used were:

- Self-Weight: $\gamma_g = 1.35$
- Additional Dead Load: $\gamma_g = 1.35$
- Live Loads: $\gamma_g = 1.50$ and $\Psi_0 = 0.8$ (other varying actions – "Sonstige veränderliche Einwirkungen")
- Crane Loads: $\gamma_q = 1.50$ and $\Psi_0 = 0.7$ (Crane of 15 tons = 150 kN → "Kategorie G")
- Wind Loads: $\gamma_q = 1.50$ and $\Psi_0 = 0.6$ ("Windlasten")
- Equivalent Force (Imperfection): $\gamma = 1.0$

6.2.1.2 SLS (GZG – Grenzzustand der Gebrauchstauglichkeit)

Similarly to the ULS (GZT), the SLS (GZG – Grenzzustand der Gebrauchstauglichkeit) for the DIN[165] must also have a combination of coefficients, but the coefficients are different. First, there are no coefficients of actions that consider the variability of the actions (γ_f), only the one that considers the simultaneity (Ψ_2). Second, even though the simultaneity coefficient is considered, there is no main load considered in the combination. Table 42 indicates the Ψ_2 necessary for each action. The coefficients used were:

- Self-Weight: not necessary
- Additional Dead Load: not necessary
- Live Loads: $\Psi_2 = 0.5$
- Crane Loads: $\Psi_2 = 0.3$
- Wind Loads: $\Psi_2 = 0.0$
- Equivalent Force (Imperfection): Ψ_2 = not necessary

[164] (SCHNEIDER, 2012) – Table 3.5b
[165] (DIN EN 1990, 2010) – Section 6.5.3 Page 43

6.2.2 Load Combinations

6.2.2.1 ULS (GZT – Grenzzustand der Tragfähigkeit)

The Load Combination for the German Norm is very similar to the Brazilian Norm, with their difference being the different values for the coefficients. The equation for the Basic Combination of Actions for the German Norm[166] was:

$$\sum_{j\geq 1} \gamma_{G,j} * G_{k,j} + \gamma_P * P + \gamma_{Q,1} * Q_{k,1} + \sum_{i>1} \gamma_{Q,i} * \psi_{0,i} * Q_{k,i}$$

- $G_{k,j}$ represents the characteristic values of the permanent actions
- $Q_{k,1}$ represents the characteristic value of the main varying action for the combination
- $Q_{k,i}$ represents the characteristic values of the varying actions that may act simultaneously with the main varying action
- P represents pre-tension actions

This results again in 4 different combinations, with different factors:

1. When the Live Load is the main action:

$$F_d = 1.35 * F_{SW} + 1.5 * F_L + 1.5 * 0.6 * F_W + 1.5 * 0.7 * F_{CR}$$
$$F_d = 1.35 * F_{SW} + 1.5 * F_L + 0.9 * F_W + 1.05 * F_{CR}$$

2. When the Wind Load is the main action:

$$F_d = 1.35 * F_{SW} + 1.5 * F_W + 1.5 * 0.8 * F_L + 1.5 * 0.7 * F_{CR}$$
$$F_d = 1.35 * F_{SW} + 1.5 * F_W + 1.2 * F_L + 1.05 * F_{CR}$$

3. When the Crane Load is the main action:

$$F_d = 1.35 * F_{SW} + 1.5 * F_{CR} + 1.5 * 0.8 * F_L + 1.5 * 0.6 * F_W$$
$$F_d = 1.35 * F_{SW} + 1.5 * F_{CR} + 1.2 * F_L + 0.9 * F_W$$

For each of these combinations, the Equivalent Force should be added with a factor of 1.0 (P Action).

[166] (DIN EN 1990, 2010) – Section 6.4.3.2 Equation (6.10) Page 41

The combinations in the software for the German Norm can be seen in Figure 106 to Figure 108:

Loading in Result Combination RC

Factor	No.	Description	Criterion	Group
1.35	G Me LC1	Self-Weight	Permanent	-
1.50	G In LC6	Live Load	Permanent	-
1.35	G Me LC12	Additional Dead Load	Permanent	-
0.90	Qw LC14	Wind +X (90°) German ++	Variable	1
0.90	Qw LC15	Wind +X (90°) German --	Variable	1
0.90	Qw LC16	Wind +X (90°) German -+	Variable	1
0.90	Qw LC17	Wind +X (90°) German+-	Variable	1
0.90	Qw LC18	Wind +Y (0°) German +	Variable	1
0.90	Qw LC19	Wind +Y (0°) German -	Variable	1
1.05	Q Ge LC21	Crane Ger 1 LG1	Variable	2
1.05	Q Ge LC22	Crane Ger 2 LG1	Variable	2
1.05	Q Ge LC23	Crane Ger 3 LG1	Variable	2
1.05	Q Ge LC24	Crane Ger 1 LG5	Variable	2
1.05	Q Ge LC25	Crane Ger 2 LG5	Variable	2
1.05	Q Ge LC26	Crane Ger 3 LG5	Variable	2
1.00	Imp LC31	Equivalent Force Ger	Variable	-

Figure 106: Combination of Loads (German) with the Respective Coefficients for Live Load as Main Load for ULS (GZT)

Loading in Result Combination RC

Factor	No.	Description	Criterion	Group
1.35	G Me LC1	Self-Weight	Permanent	-
1.20	G In LC6	Live Load	Permanent	-
1.35	G Me LC12	Additional Dead Load	Permanent	-
1.50	Qw LC14	Wind +X (90°) German ++	Variable	1
1.50	Qw LC15	Wind +X (90°) German --	Variable	1
1.50	Qw LC16	Wind +X (90°) German -+	Variable	1
1.50	Qw LC17	Wind +X (90°) German+-	Variable	1
1.50	Qw LC18	Wind +Y (0°) German +	Variable	1
1.50	Qw LC19	Wind +Y (0°) German -	Variable	1
1.05	Q Ge LC21	Crane Ger 1 LG1	Variable	2
1.05	Q Ge LC22	Crane Ger 2 LG1	Variable	2
1.05	Q Ge LC23	Crane Ger 3 LG1	Variable	2
1.05	Q Ge LC24	Crane Ger 1 LG5	Variable	2
1.05	Q Ge LC25	Crane Ger 2 LG5	Variable	2
1.05	Q Ge LC26	Crane Ger 3 LG5	Variable	2
1.00	Imp LC31	Equivalent Force Ger	Variable	-

Figure 107: Combination of Loads (German) with the Respective Coefficients for Wind Load as Main Load for ULS (GZT)

Loading in Result Combination RC

Factor	No.	Description	Criterion	Group
1.35	G Me LC1	Self-Weight	Permanent	-
1.20	G In LC6	Live Load	Permanent	-
1.35	G Me LC12	Additional Dead Load	Permanent	-
0.90	Qw LC14	Wind +X (90°) German ++	Variable	1
0.90	Qw LC15	Wind +X (90°) German --	Variable	1
0.90	Qw LC16	Wind +X (90°) German -+	Variable	1
0.90	Qw LC17	Wind +X (90°) German+-	Variable	1
0.90	Qw LC18	Wind +Y (0°) German +	Variable	1
0.90	Qw LC19	Wind +Y (0°) German -	Variable	1
1.50	Q Ge LC21	Crane Ger 1 LG1	Variable	2
1.50	Q Ge LC22	Crane Ger 2 LG1	Variable	2
1.50	Q Ge LC23	Crane Ger 3 LG1	Variable	2
1.50	Q Ge LC24	Crane Ger 1 LG5	Variable	2
1.50	Q Ge LC25	Crane Ger 2 LG5	Variable	2
1.50	Q Ge LC26	Crane Ger 3 LG5	Variable	2
1.00	Imp LC31	Equivalent Force Ger	Variable	-

Figure 108: Combination of Loads (German) with the Respective Coefficients for Crane Load as Main Load for ULS (GZT)

According to DIN[167], a hall with small angle of the roof (less than 26°[168]) can be calculated by the Theory of 1st Order when:

$$\alpha_{cr} = \left(\frac{H_{Ed}}{V_{Ed}}\right) * \left(\frac{h}{\delta_{H,Ed}}\right) \geq 10$$

With:

- H_{Ed} : Sum of the Horizontal Loads (also calculated by the sum of the horizontal reaction on the supports)
- V_{Ed} : Sum of the Vertical Loads (also calculated by the sum of the vertical reaction on the supports)
- $\delta_{H,Ed}$: Horizontal shift between the top of the column and the bottom (for the 1st Order Analysis)
- h : Height of the column

$$\alpha_{cr} = \left(\frac{H_{Ed}}{V_{Ed}}\right) * \left(\frac{h}{\delta_{H,Ed}}\right) = \frac{73.54}{534.34} * \frac{1040}{1.17} = 122.3358 \geq 10$$

Since $\alpha_{cr} > 10$, the effects of the 2nd Order Analysis were disregarded.

[167] (DIN EN 1993-1-1, 2010) – Section 5.2.1 Page 32
[168] (SCHNEIDER, 2012) – Section 3.1 Page 8.23

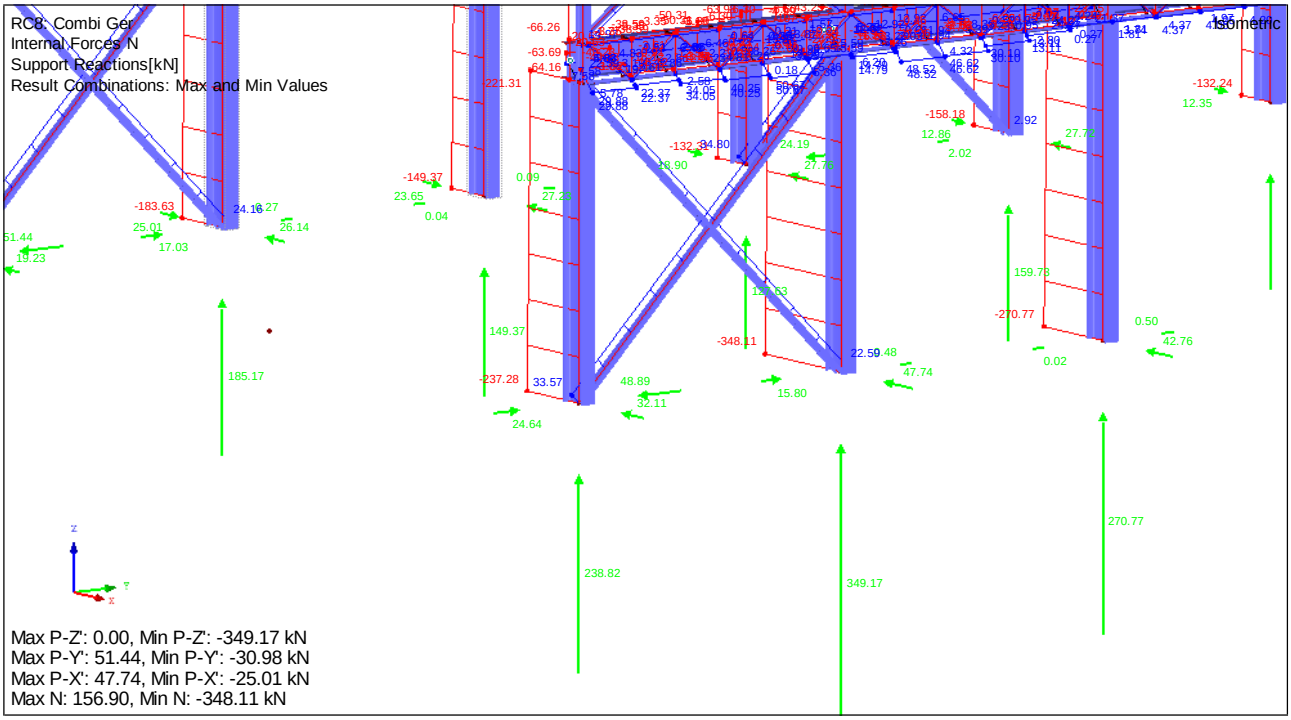

Figure 109: Normal Forces and Support Reactions on 2nd Column

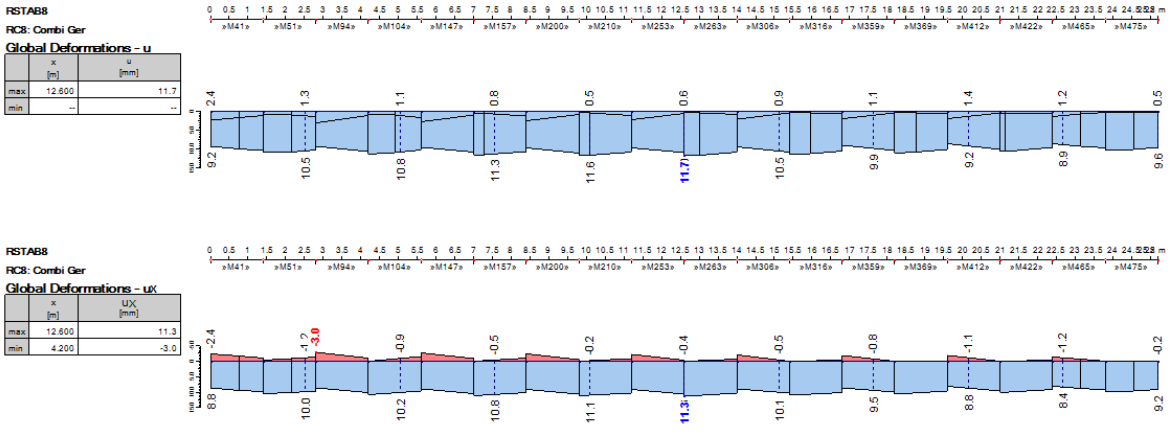

Figure 110: Maximum Horizontal Deformation on the Top of the Column (Member M263 – 5th Column Right)[169]

[169] Obs: the results from RSTAB for Deformations or Forces were in this format. The number of the members is indicated on the top (with the members' borders also being shown) while its respective result is shown exactly below. For example: the first member shown is M41 and in the graphic, the subsequent one is M51 and so on. For each member, their results are shown underneath the space provided by the top line.

6.2.2.2 SLS (GZG – Grenzzustand der Gebrauchstauglichkeit)

From the DIN[170], the equation for the quasi-permanent service combinations is given by:

$$\sum_{j\geq 1} G_{k,j} + P + \sum_{i>1} \psi_{2,i} * Q_{k,i}$$

- $G_{k,j}$ represents the characteristic values of the permanent actions
- $Q_{k,i}$ represents the characteristic values of the varying actions that may act simultaneously
- P represents pre-tension actions

This results in 1 combination:

$$F_{ser} = F_{SW} + 0.5 * F_L + 0.0 * F_W + 0.3 * F_{CR}$$
$$F_{ser} = F_{SW} + 0.5 * F_L + 0.3 * F_{CR}$$

For this combination, the Equivalent Force should be added with a factor of 1.0 (P Action).

In RSTAB, each type of load was multiplied with its coefficient for each combination accordingly. Figure 105 shows the combination of loads for the Brazilian Norm:

Loading in Result Combination RC

Factor	No.	Description	Criterion	Group
1.00	G Me LC1	Self-Weight	Permanent	-
0.50	G In LC6	Live Load	Permanent	-
1.00	G Me LC12	Additional Dead Load	Permanent	-
0.30	Q Ge LC21	Crane Ger 1 LG1	Variable	1
0.30	Q Ge LC22	Crane Ger 2 LG1	Variable	1
0.30	Q Ge LC23	Crane Ger 3 LG1	Variable	1
0.30	Q Ge LC24	Crane Ger 1 LG5	Variable	1
0.30	Q Ge LC25	Crane Ger 2 LG5	Variable	1
0.30	Q Ge LC26	Crane Ger 3 LG5	Variable	1
1.00	Imp LC31	Equivalent Force Ger	Variable	-

Figure 111: Combination of Loads (German) with the Respective Coefficients for SLS (GZG)

[170] (DIN EN 1990, 2010) – Section 6.5.3 Equation (6.16b) Page 43

7. RESULTS

7.1 ULS (ELU and GZT)

The ULS is calculated to verify if the structure would not suffer from instability and/or rupture due to a combination of actions that could act simultaneously on it.

After modeling the complete industrial steel hall and the loads that would affect it, the software would bring the results from verifications from both, the EC-3 and the NBR, and additionally, a third verification was made: the ASD verification. The ASD (Allowable Strength Design) verification certified that the stress levels of each member did not exceed their stress ratios of 1.0, meaning that the maximum stress due to service load should not exceed a specified allowable stress[171]. These verifications were also done for the runway girders in Appendix 7, Appendix 8, Appendix 16, Appendix 17, Appendix 23, Appendix 24, Appendix 31, Appendix 32, Appendix 47 and Appendix 48. The results of each type of Force can also be seen (visually on the hall) in Appendix 52 to Appendix 69.

The software ran the verifications from the EC-3, NBR and ASD (STEEL) and the results showed that the only type of member that did not comply with the norms was the purlin.

Table 43 indicates the Design and Stress Ratios of each verification. The values in green represent design ratios between 0.0 and 0.70. If the values were in yellow, the design ratios were between 0.70 and 1.0. If the design ratios were in red, the design ratios exceeded the limit, meaning they were greater than 1.0.

[171] (SALMON, JOHNSON, & MALHAS, 2009) – Section 1.8 Page 24

	BRA		GER	
	NBR	ASD	EC-3	ASD
Lower Column PS 600x95.9	0.39	0.35	0.31	0.28
Upper Column PS 300x57,1	0.43	0.57	0.76	0.78
Lower Chords W 200x19.3	0.18	0.19	0.17	0.17
Bracing Longitudinal Vertical Superior (V) + 76x76x8	0.03	0.03	0.03	0.03
Bracing Longitudinal Vertical Inferior (X) U* 102x8 pl. 6.3x100	0.06	0.06	0.05	0.05
Upper and Lower Chords Lateral U 203x17,1	0.14	0.12	0.07	0.07
Trusss Lateral U* 51x6.3 pl 6.3x50	0.10	0.04	0.10	0.04
Purlins Central U 152x12.2	0.83	0.70	**1.13**	0.84
Purlins Left U 152x12.2	**1.12**	**1.22**	**1.14**	**1.37**
Purlins Right U 152x12.2	**1.11**	**1.21**	**1.14**	**1.37**
Purlins Lateral Left U 152x12.2	0.09	0.12	0.06	0.09
Purlins Lateral Right U 152x12.2	0.09	0.14	0.06	0.09
Runway Girder Left PS 750x128.7	0.12	0.15	0.15	0.14
Runway Girder Right PS 750x128.7	0.25	0.30	0.25	0.25
Upper and Lower Chords Lateral of Runway Girder Left Superior L 76x76x8	0.26	0.18	0.11	0.27
Upper and Lower Chords Lateral of Runway Girder Left Inferior L 76x76x8	0.26	0.19	0.24	0.19
Upper and Lower Chords Lateral of Runway Girder Right Superior L 76x76x8	0.26	0.18	0.25	0.29
Upper and Lower Chords Lateral of Runway Girder Right Inferior L 76x76x8	0.22	0.15	0.24	0.19
Truss Lateral of Runway Girder Left L 51x6.3	0.15	0.05	0.08	0.03
Truss Lateral of Runway Girder Right L 51x6.3	0.13	0.05	0.10	0.05
Bracing Longitudinal Horizontal Superior L 64x64x6,3	0.02	0.02	0.02	0.02
Bars Longitudinal Horizontal Roof Superior Tube 114.3x6	0.11	0.10	0.12	0.12
Bars Longitudinal Horizontal Roof Inferior Tube 114.3x6	0.18	0.06	0.21	0.07
Bracing Longitudinal Horizontal Inferior L 64x64x6,3	0.07	0.07	0.06	0.06
Bracing Longitudinal Vertical B-B (x = 3.96) L 64x64x4.8	0.02	0.02	0.02	0.02
Bracing Longitudinal Vertical A-A (x = 9.9 Middle) L 64x64x4.8	0.03	0.02	0.02	0.02
Truss M1 U* 51x4.76	0.27	0.07	0.30	0.08
Truss D1 U* 76x6.3	0.47	0.24	0.74	0.32
Truss D2 U* 76x4.76	0.19	0.17	0.17	0.17
Truss D3 U* 76x4.76	0.19	0.08	0.23	0.08
Truss D4 U* 76x4.76	0.05	0.04	0.05	0.05
Truss D5 U* 38x4.76	0.01	0.01	0.01	0.01
Upper Chords Left W 200x19.3	0.34	0.31	0.39	0.29
Upper Chords Right W 200x19.3	0.34	0.31	0.39	0.29
RB 1/2 | AISC Purlin Bracings Ø 12.7	0.10	0.09	0.10	0.10

Table 43: Table of Design and Stress Ratios for the Verifications

For the EC-3, the left and right roof purlins had the highest design ratio of 1.14 (not including the outermost purlins on the left and right) and the central purlins had 1.13. For the ASD (German), only the purlins in between had a design ratio larger than 1.0 (1.37). The central and outer purlins did not. The fact that the outermost purlins, left and right, did not exceed their design ratios, may be explained because the wind loads on them were much less than on the other purlins.

When the software ran the verifications for the NBR and the ASD (Brazilian), the results were similar: only the purlins had exceeded the design ratio of 1.0. For the ASD, the locations maintained the same: the left and right (excluding the outer) but had the design ratios a little lower, of 1.22 and 1.21. For the NBR, in comparison to the EC-3, the central purlins were not surpassing the design ratio, only the left and right (excluding the outer). However, their design ratio was lower than in EC-3, being only 1.12 and 1.11 and not 1.14, although very similar.

Figure 112 to Figure 115 show examples of how the software would calculate the verifications for the purlins for the EC-3, ASD and NBR. Table 44 and Table 46 indicate the results for the EC-3 and NBR, showing the design ratios for each verification made. The final design ratio would be the largest. Table 45 and Table 47 exhibit the results for the ASD verification and the stress ratios.

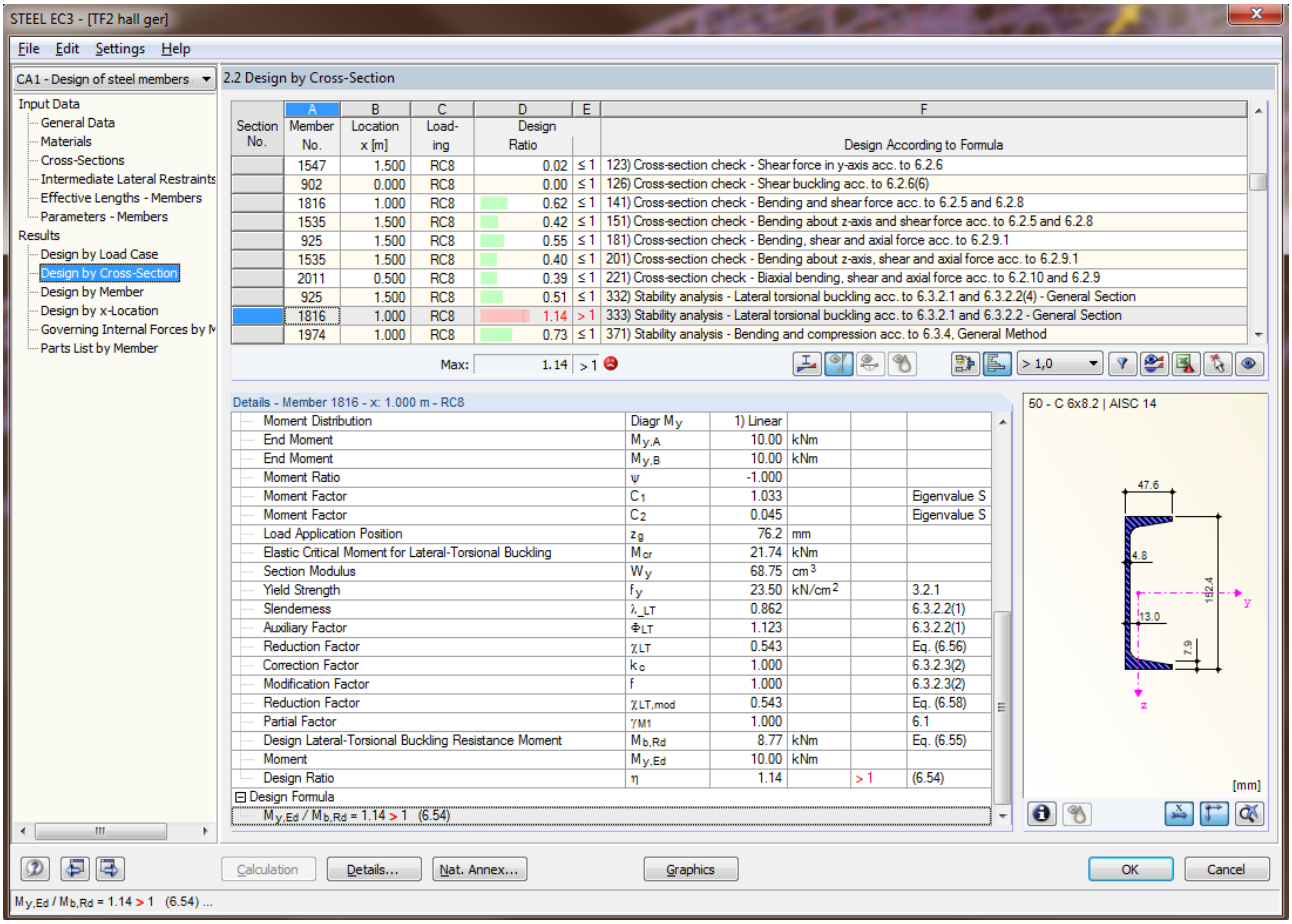

Figure 112: Example of EC-3 Verification for the Purlin

48	C 6x8.2 | AISC 14 Purlins Central U 152x12.2					
	1594	0.000	RC8	0.06	≤ 1	101) Cross-section check - Tension acc. to 6.2.3
	847	0.000	RC8	0.17	≤ 1	102) Cross-section check - Compression acc. to 6.2.4
	893	0.000	RC8	0.08	≤ 1	121) Cross-section check - Shear force in z-axis acc. to 6.2.6
	846	0.000	RC8	0.00	≤ 1	126) Cross-section check - Shear buckling acc. to 6.2.6(6)
	893	1.500	RC8	0.87	≤ 1	181) Cross-section check - Bending, shear and axial force acc. to 6.2.9.1
	846	0.900	RC8	0.13	≤ 1	201) Cross-section check - Bending about z-axis, shear and axial force acc. to 6.2.9.1
	2036	1.000	RC8	0.34	≤ 1	221) Cross-section check - Biaxial bending, shear and axial force acc. to 6.2.10 and 6.2.9
	1791	0.000	RC8	1.13	> 1	333) Stability analysis - Lateral torsional buckling acc. to 6.3.2.1 and 6.3.2.2 - General Section
	1774	1.000	RC8	0.54	≤ 1	371) Stability analysis - Bending and compression acc. to 6.3.4, General Method
49	C 6x8.2 | AISC 14 Purlins Left U 152x12.2					
	855	0.000	RC8	0.01	≤ 1	101) Cross-section check - Tension acc. to 6.2.3
	2030	0.000	RC8	0.13	≤ 1	102) Cross-section check - Compression acc. to 6.2.4
	1758	1.000	RC8	0.62	≤ 1	111) Cross-section check - Bending about y-axis acc. to 6.2.5 - Class 1 or 2
	1583	1.500	RC8	0.42	≤ 1	116) Cross-section check - Bending about z-axis acc. to 6.2.5 - Class 1 or 2
	854	0.000	RC8	0.06	≤ 1	121) Cross-section check - Shear force in z-axis acc. to 6.2.6
	1585	1.500	RC8	0.02	≤ 1	123) Cross-section check - Shear force in y-axis acc. to 6.2.6
	854	0.000	RC8	0.00	≤ 1	126) Cross-section check - Shear buckling acc. to 6.2.6(6)
	1758	1.000	RC8	0.62	≤ 1	141) Cross-section check - Bending and shear force acc. to 6.2.5 and 6.2.8
	1583	1.500	RC8	0.42	≤ 1	151) Cross-section check - Bending about z-axis and shear force acc. to 6.2.5 and 6.2.8
	854	1.500	RC8	0.57	≤ 1	181) Cross-section check - Bending, shear and axial force acc. to 6.2.9.1
	1585	1.500	RC8	0.41	≤ 1	201) Cross-section check - Bending about z-axis, shear and axial force acc. to 6.2.9.1
	1582	0.000	RC8	0.39	≤ 1	221) Cross-section check - Biaxial bending, shear and axial force acc. to 6.2.10 and 6.2.9
	861	1.500	RC8	0.51	≤ 1	332) Stability analysis - Lateral torsional buckling acc. to 6.3.2.1 and 6.3.2.2(4) - General Section
	1758	1.000	RC8	1.14	> 1	333) Stability analysis - Lateral torsional buckling acc. to 6.3.2.1 and 6.3.2.2 - General Section
	2030	1.000	RC8	0.73	≤ 1	371) Stability analysis - Bending and compression acc. to 6.3.4, General Method
50	C 6x8.2 | AISC 14 Purlins Right U 152x12.2					
	919	0.000	RC8	0.01	≤ 1	101) Cross-section check - Tension acc. to 6.2.3
	1974	0.000	RC8	0.13	≤ 1	102) Cross-section check - Compression acc. to 6.2.4
	1816	1.000	RC8	0.62	≤ 1	111) Cross-section check - Bending about y-axis acc. to 6.2.5 - Class 1 or 2
	1535	1.500	RC8	0.42	≤ 1	116) Cross-section check - Bending about z-axis acc. to 6.2.5 - Class 1 or 2
	918	0.000	RC8	0.06	≤ 1	121) Cross-section check - Shear force in z-axis acc. to 6.2.6
	1547	1.500	RC8	0.02	≤ 1	123) Cross-section check - Shear force in y-axis acc. to 6.2.6
	902	0.000	RC8	0.00	≤ 1	126) Cross-section check - Shear buckling acc. to 6.2.6(6)
	1816	1.000	RC8	0.62	≤ 1	141) Cross-section check - Bending and shear force acc. to 6.2.5 and 6.2.8
	1535	1.500	RC8	0.42	≤ 1	151) Cross-section check - Bending about z-axis and shear force acc. to 6.2.5 and 6.2.8
	925	1.500	RC8	0.55	≤ 1	181) Cross-section check - Bending, shear and axial force acc. to 6.2.9.1
	1535	1.500	RC8	0.40	≤ 1	201) Cross-section check - Bending about z-axis, shear and axial force acc. to 6.2.9.1
	2011	0.500	RC8	0.39	≤ 1	221) Cross-section check - Biaxial bending, shear and axial force acc. to 6.2.10 and 6.2.9
	925	1.500	RC8	0.51	≤ 1	332) Stability analysis - Lateral torsional buckling acc. to 6.3.2.1 and 6.3.2.2(4) - General Section
	1816	1.000	RC8	1.14	> 1	333) Stability analysis - Lateral torsional buckling acc. to 6.3.2.1 and 6.3.2.2 - General Section
	1974	1.000	RC8	0.73	≤ 1	371) Stability analysis - Bending and compression acc. to 6.3.4, General Method

Table 44: Results for the Purlins (Excluding Outer) for the EC-3

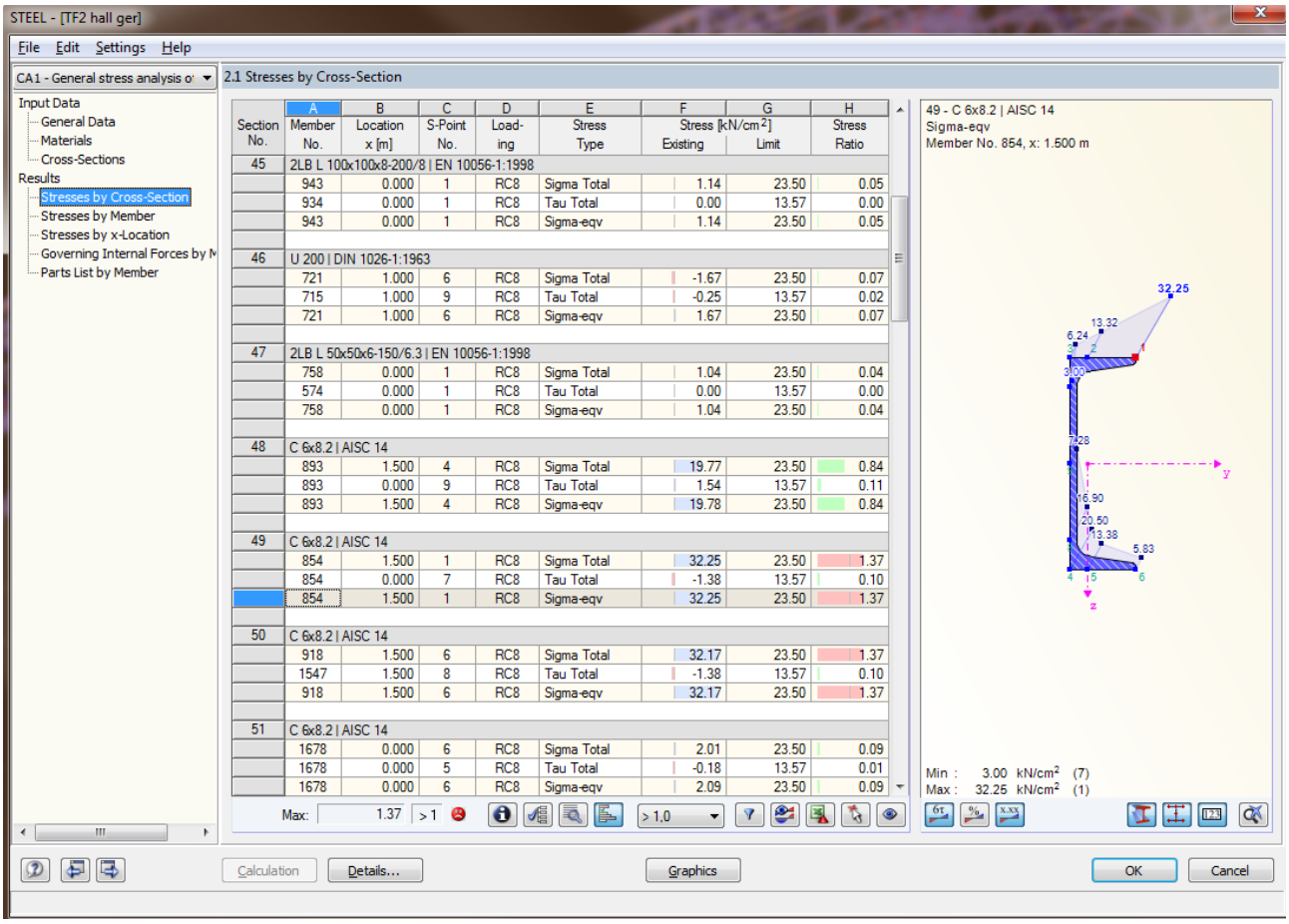

Figure 113: Example of ASD (German) Verification for the Purlin

48	C 6x8.2 | AISC 14 Purlins Central U 152x12.2							
	893	1.500	4	RC8	Sigma Total	19.77	23.50	0.84
	893	0.000	9	RC8	Tau Total	1.54	13.57	0.11
	893	1.500	4	RC8	Sigma-eqv	19.78	23.50	0.84
49	C 6x8.2 | AISC 14 Purlins Left U 152x12.2							
	854	1.500	1	RC8	Sigma Total	32.25	23.50	1.37
	854	0.000	7	RC8	Tau Total	-1.38	13.57	0.10
	854	1.500	1	RC8	Sigma-eqv	32.25	23.50	1.37
50	C 6x8.2 | AISC 14 Purlins Right U 152x12.2							
	918	1.500	6	RC8	Sigma Total	32.17	23.50	1.37
	1547	1.500	8	RC8	Tau Total	-1.38	13.57	0.10
	918	1.500	6	RC8	Sigma-eqv	32.17	23.50	1.37

Table 45: Results for the Purlins (Excluding Outer) for the ASD (German)

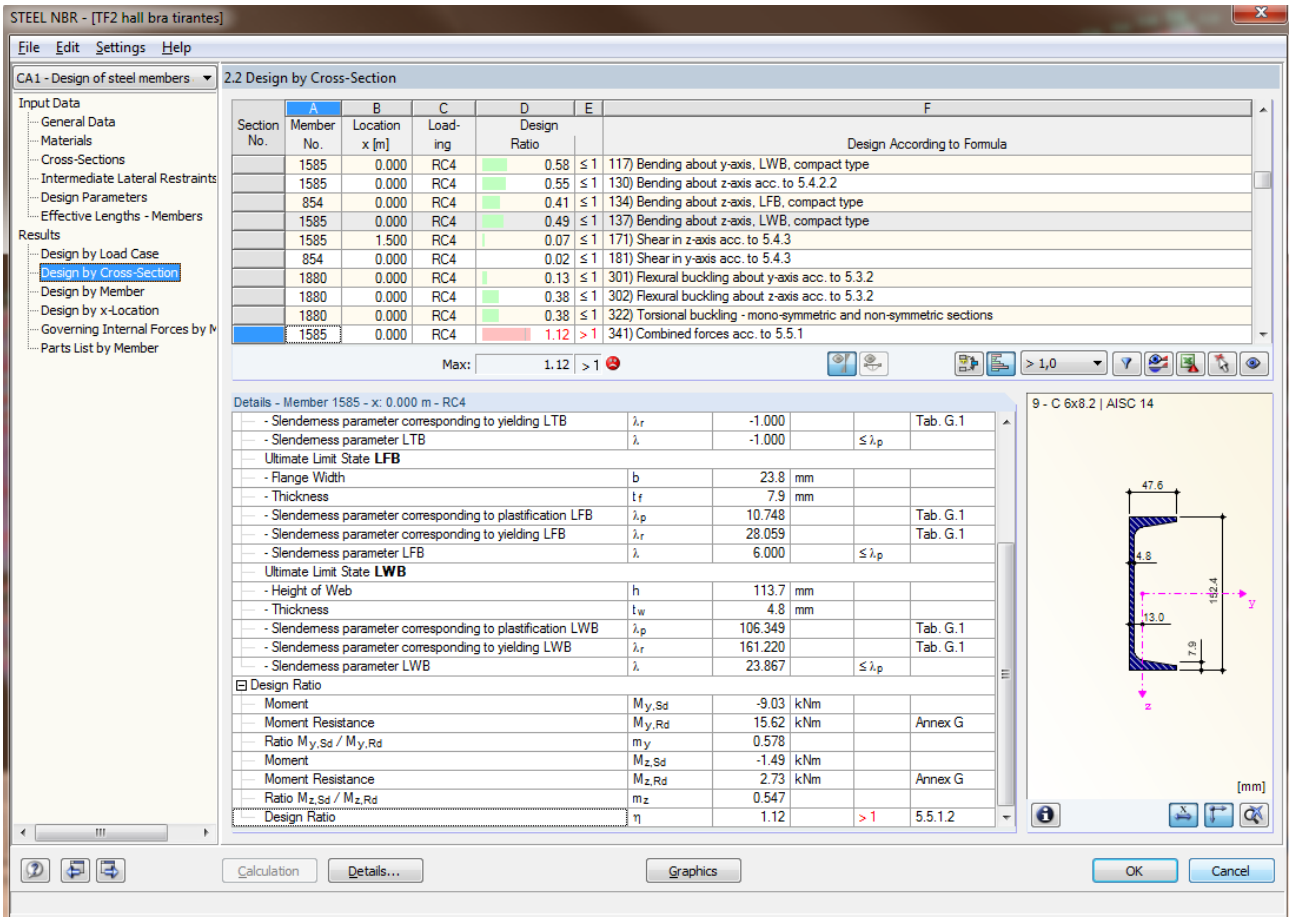

Figure 114: Example of NBR Verification for the Purlin

8	C 6x8.2 | AISC 14 Purlins Central U 152x12.2					
	890	1.800	RC4	0.01	≤ 1	100) Negligible internal forces
	893	0.000	RC4	0.06	≤ 1	101) Tension acc. to 5.2.2
	847	0.000	RC4	0.14	≤ 1	102) Compression without buckling acc. to 5.3.2
	1600	0.000	RC4	0.79	≤ 1	110) Bending about y-axis acc. to 5.4.2.2
	1719	0.000	RC4	0.15	≤ 1	111) Bending about y-axis, LTB, compact type
	2008	0.000	RC4	0.81	≤ 1	112) Bending about y-axis, LTB, semi compact type
	1600	0.000	RC4	0.79	≤ 1	114) Bending about y-axis, LFB, compact type
	1600	0.000	RC4	0.79	≤ 1	117) Bending about y-axis, LWB, compact type
	893	0.000	RC4	0.09	≤ 1	171) Shear in z-axis acc. to 5.4.3
	847	0.000	RC4	0.16	≤ 1	301) Flexural buckling about y-axis acc. to 5.3.2
	1813	0.000	RC4	0.33	≤ 1	302) Flexural buckling about z-axis acc. to 5.3.2
	1813	0.000	RC4	0.33	≤ 1	322) Torsional buckling - mono-symmetric and non-symmetric sections
	2008	0.000	RC4	0.83	≤ 1	341) Combined forces acc. to 5.5.1
9	C 6x8.2 | AISC 14 Purlins Left U 152x12.2					
	1771	1.000	RC4	0.01	≤ 1	100) Negligible internal forces
	1880	0.000	RC4	0.11	≤ 1	102) Compression without buckling acc. to 5.3.2
	1585	0.000	RC4	0.58	≤ 1	110) Bending about y-axis acc. to 5.4.2.2
	2037	0.000	RC4	0.18	≤ 1	111) Bending about y-axis, LTB, compact type
	1871	1.000	RC4	0.67	≤ 1	112) Bending about y-axis, LTB, semi compact type
	1585	0.000	RC4	0.58	≤ 1	114) Bending about y-axis, LFB, compact type
	1585	0.000	RC4	0.58	≤ 1	117) Bending about y-axis, LWB, compact type
	1585	0.000	RC4	0.55	≤ 1	130) Bending about z-axis acc. to 5.4.2.2
	854	0.000	RC4	0.41	≤ 1	134) Bending about z-axis, LFB, compact type
	1585	0.000	RC4	0.49	≤ 1	137) Bending about z-axis, LWB, compact type
	1585	1.500	RC4	0.07	≤ 1	171) Shear in z-axis acc. to 5.4.3
	854	0.000	RC4	0.02	≤ 1	181) Shear in y-axis acc. to 5.4.3
	1880	0.000	RC4	0.13	≤ 1	301) Flexural buckling about y-axis acc. to 5.3.2
	1880	0.000	RC4	0.38	≤ 1	302) Flexural buckling about z-axis acc. to 5.3.2
	1880	0.000	RC4	0.38	≤ 1	322) Torsional buckling - mono-symmetric and non-symmetric sections
	1585	0.000	RC4	1.12	> 1	341) Combined forces acc. to 5.5.1
10	C 6x8.2 | AISC 14 Purlins Right U 152x12.2					
	1776	1.000	RC4	0.01	≤ 1	100) Negligible internal forces
	1877	0.000	RC4	0.11	≤ 1	102) Compression without buckling acc. to 5.3.2
	1872	1.000	RC4	0.57	≤ 1	110) Bending about y-axis acc. to 5.4.2.2
	2034	0.000	RC4	0.18	≤ 1	111) Bending about y-axis, LTB, compact type
	1872	1.000	RC4	0.67	≤ 1	112) Bending about y-axis, LTB, semi compact type
	1872	1.000	RC4	0.57	≤ 1	114) Bending about y-axis, LFB, compact type
	1872	1.000	RC4	0.57	≤ 1	117) Bending about y-axis, LWB, compact type
	918	1.500	RC4	0.54	≤ 1	130) Bending about z-axis acc. to 5.4.2.2
	918	0.000	RC4	0.41	≤ 1	134) Bending about z-axis, LFB, compact type
	918	1.500	RC4	0.48	≤ 1	137) Bending about z-axis, LWB, compact type
	1547	1.500	RC4	0.07	≤ 1	171) Shear in z-axis acc. to 5.4.3
	1547	1.500	RC4	0.02	≤ 1	181) Shear in y-axis acc. to 5.4.3
	1877	0.000	RC4	0.13	≤ 1	301) Flexural buckling about y-axis acc. to 5.3.2
	1877	0.000	RC4	0.38	≤ 1	302) Flexural buckling about z-axis acc. to 5.3.2
	1877	0.000	RC4	0.38	≤ 1	322) Torsional buckling - mono-symmetric and non-symmetric sections
	918	1.500	RC4	1.11	> 1	341) Combined forces acc. to 5.5.1

Table 46: Results for the Purlins (Excluding Outer) for the NBR

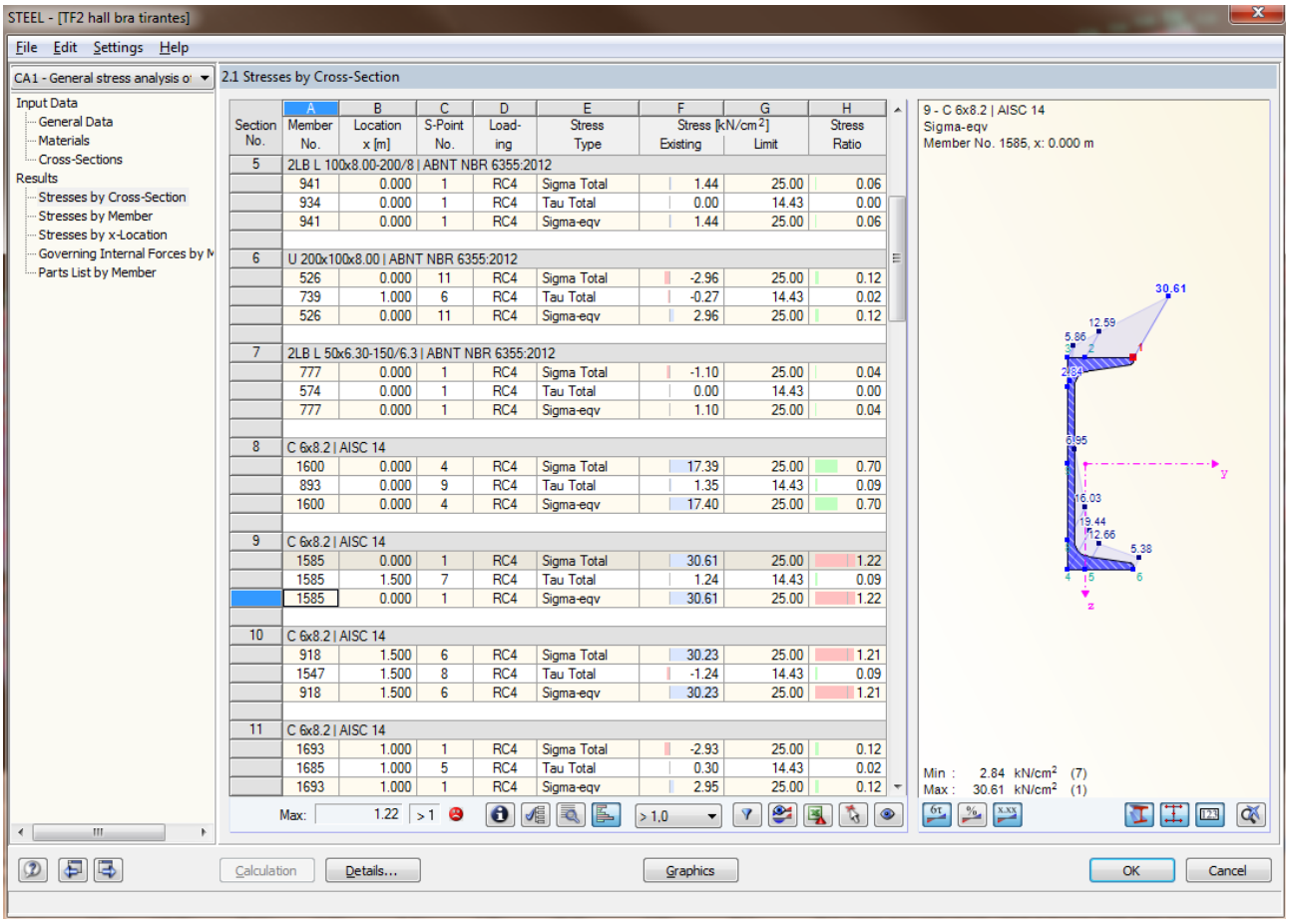

Figure 115: Example of ASD (Brazilian) Verification for the Purlin

8	C 6x8.2 | AISC 14 Purlins Central U 152x12.2							
	1600	0.000	4	RC4	Sigma Total	17.39	25.00	0.70
	893	0.000	9	RC4	Tau Total	1.35	14.43	0.09
	1600	0.000	4	RC4	Sigma-eqv	17.40	25.00	0.70
9	C 6x8.2 | AISC 14 Purlins Left U 152x12.2							
	1585	0.000	1	RC4	Sigma Total	30.61	25.00	1.22
	1585	1.500	7	RC4	Tau Total	1.24	14.43	0.09
	1585	0.000	1	RC4	Sigma-eqv	30.61	25.00	1.22
10	C 6x8.2 | AISC 14 Purlins Right U 152x12.2							
	918	1.500	6	RC4	Sigma Total	30.23	25.00	1.21
	1547	1.500	8	RC4	Tau Total	-1.24	14.43	0.09
	918	1.500	6	RC4	Sigma-eqv	30.23	25.00	1.21

Table 47: Results for the Purlins (Excluding Outer) for the ASD (Brazilian)

7.2 SLS (ELS and GZG)

The SLS is calculated to verify if the displacements of the structure along the years would exceed the limit imposed by each Norm.

The limits for the maximum deformations were:

- Vertical Deformation of the Truss:

$$\frac{L}{250} = \frac{19.8m}{250} = 0.0792m = 79.2\ mm$$

- Horizontal Deformation of the Column:

$$\frac{H}{300} = \frac{9m}{300} = 0.03m = 30\ mm$$

Figure 116 (Brazilian) and Figure 119 (German) depict the deformations the halls would suffer according to the SLS combinations for each Norm. Figure 117 (Brazilian) and Figure 120 (German) indicate the maximum vertical deformation on the truss system. The frame with the maximum vertical deformation was the 8th frame from the front (Member 391). Figure 118 (Brazilian) and Figure 121 (German) indicate the maximum horizontal deformation on the columns. The column that had the maximum horizontal deformation was the column with the crane load, the 2nd column on the right (Member 104). The maximum horizontal deformation occurred on the height of 9m, where the truss was located.

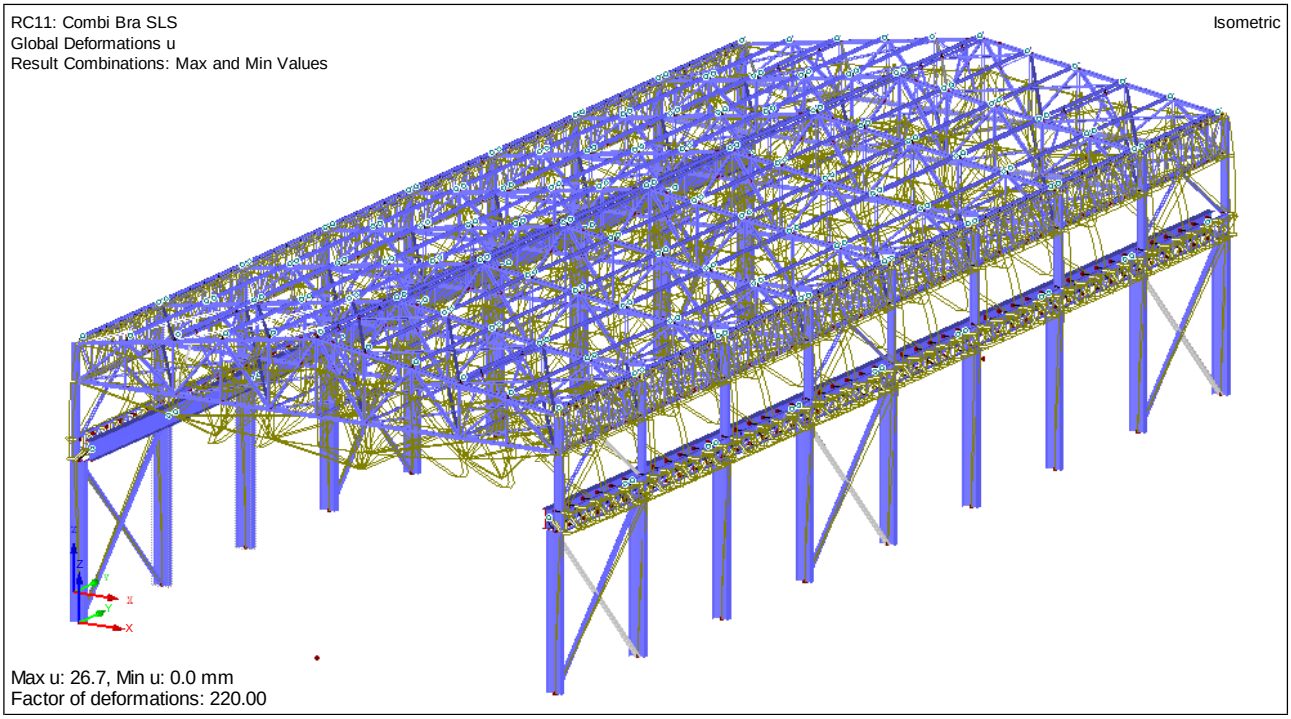

Figure 116: Deformation of the Brazilian Hall for SLS (ELS)

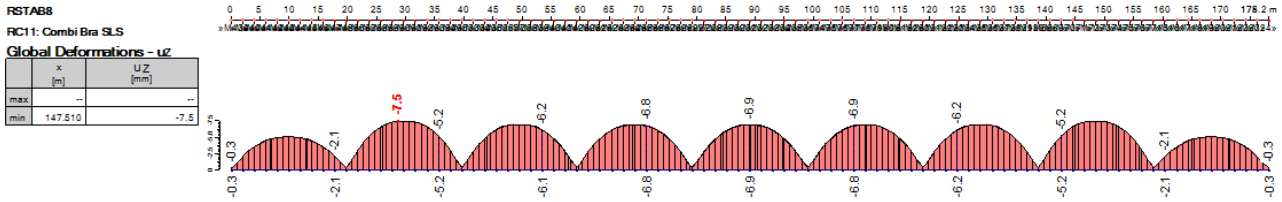

Figure 117: Maximum Vertical Deformation on Lower Chord of the Brazilian Hall for SLS (ELS) (Member M391 – 8th Frame)

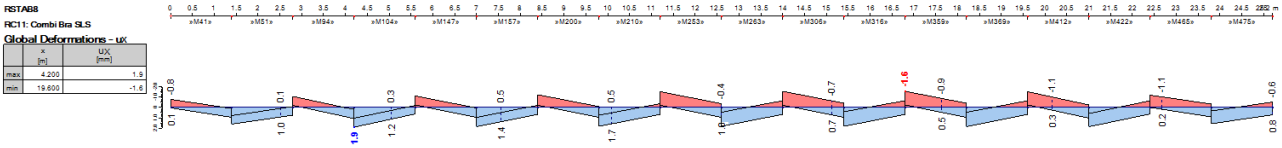

Figure 118: Maximum Horizontal Deformation on Column of the Brazilian Hall for SLS (ELS) (Member M104 – 2nd Column Right)

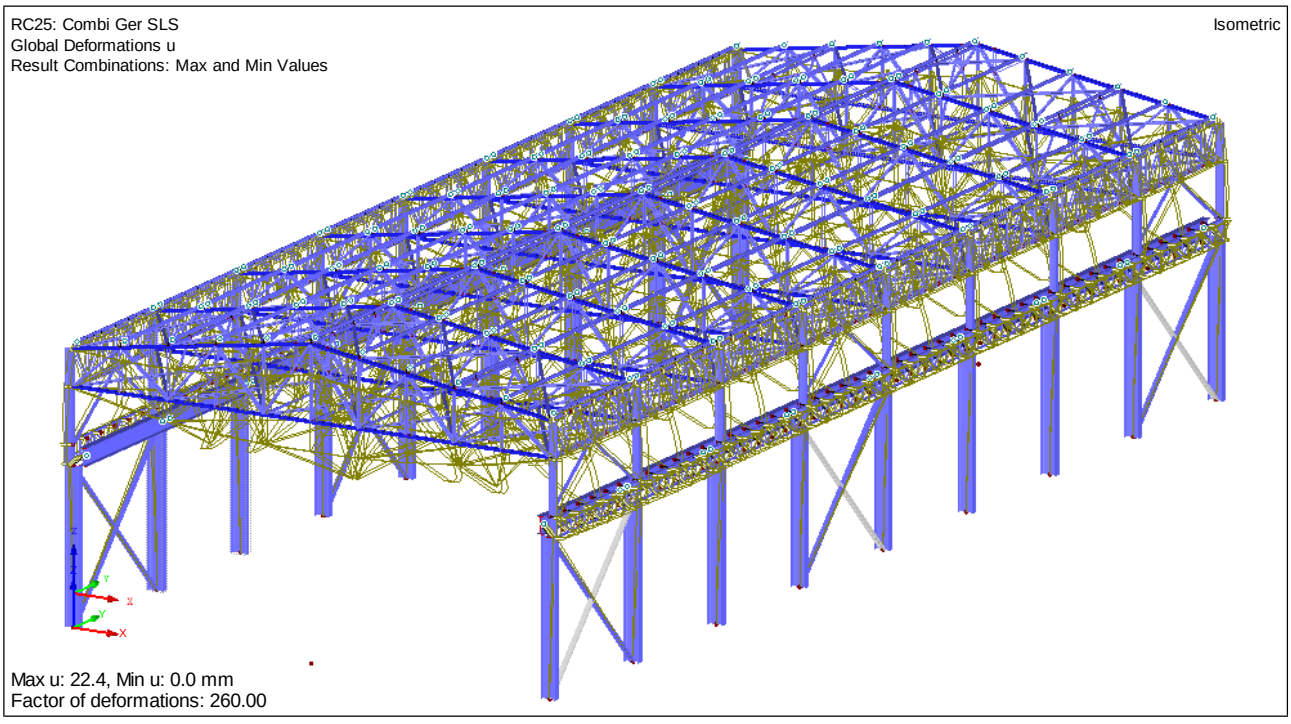

Figure 119: Deformation of the German Hall for SLS (GZG)

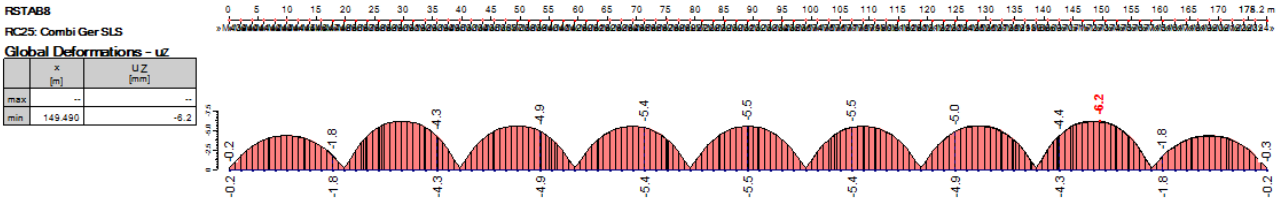

Figure 120: Maximum Vertical Deformation on Lower Chord of the German Hall for SLS (GZG) (Member M391 – 8th Frame)

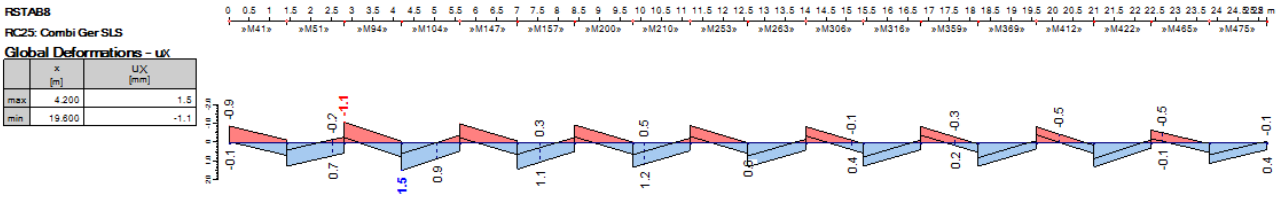

Figure 121: Maximum Horizontal Deformation on Column of the German Hall for SLS (GZG) (Member M104 – 2nd Column Right)

From these results, it is possible to realize that the members with the maximum deformations are the same for both structures:

- Vertical Deformation of the Truss: Member 391 on the 8th Frame (from Front)
- Horizontal Deformation of the Columns: Member 104 on the top right corner of the 2nd Column (from Front)

The difference between them is the value that they present:

- Vertical Deformation of the Truss:
  - Brazilian: 7.5mm
  - German: 6.2mm
- Horizontal Deformation of the Columns:
  - Brazilian: 1.9mm
  - German: 1.5mm

For both deformations, the Brazilian hall had higher values. Nevertheless, for both structures, the 4 different deformations did not exceed the limit and were therefore verified.

8. VERIFICATIONS – FTB AND COMBINATIONS

Although the verifications for the model have been done, the verification for instability due to compression and Flexural Torsional Buckling had to be done specifically for the columns and the chords of the truss system. The software does not calculate this verification correctly, since it does not recognize the critical buckling length (L_{cr}) correctly and thus sometimes considers this length shorter than it should actually be, subsequently defining the critical buckling load higher than it also should be. The verification for traction (tension) would not be affected and would be correctly performed since it does not require the real length of the element, but its cross-section parameters.

In view of this matter, the FTB Flexural Torsional Buckling (FLT – Flexão Lateral com Torsão – or BDK – Biegedrillknicken) verifications were re-done for the column, both upper chords (left and right) and the lower chord. Further, the verifications for the combination of forces were also verified (which would also be affected by the software's inability to recognize the true critical buckling length).

The results of the Internal Forces for each of the 4 beams are given in Table 48 and Table 49:

BRA	[kN]		[kN]		[kN]		[kNm]		[kNm]		[kNm]	
	N Min	N Max	V_y Min	V_y Max	V_z Min	V_z Max	M_T Min	M_T Max	M_y Min	M_y Max	M_z Min	M_z Max
Column	-309.66	0.00	-28.19	24.23	-19.96	39.64	-0.16	0.18	-149.06	62.22	-23.13	25.54
Upper Chords L	-148.83	12.81	-2.74	0.61	-4.01	2.22	-0.01	0.01	-4.48	2.80	-0.57	1.24
Upper Chords R	-148.82	26.28	-0.60	2.81	-2.04	4.05	-0.01	0.01	-4.48	2.80	-0.56	1.24
Lower Chords	-15.48	125.62	-0.85	0.79	-13.85	13.84	0.00	0.00	-7.40	7.40	-0.25	0.98

Table 48: Internal Forces for the Members of the Brazilian Hall

GER	[kN]		[kN]		[kN]		[kNm]		[kNm]		[kNm]	
	N Min	N Max	V_y Min	V_y Max	V_z Min	V_z Max	M_T Min	M_T Max	M_y Min	M_y Max	M_z Min	M_z Max
Column	-348.31	0.00	-30.89	31.07	-25.01	48.36	-0.15	0.14	-207.05	94.32	-36.80	36.07
Upper Chords L	-174.27	7.05	-2.33	0.62	-4.79	3.12	-0.02	0.02	-5.47	4.29	-0.44	1.00
Upper Chords R	-174.28	19.98	-0.62	2.28	-3.08	4.88	-0.02	0.02	-5.47	4.29	-0.44	1.00
Lower Chords	0.00	157.12	-0.85	0.80	-9.82	10.09	0.00	0.00	-5.25	5.21	-0.24	0.87

Table 49: Internal Forces for the Members of the German Hall

These tables were created in order to facilitate the comprehension of the results for these members, also seen in Appendix 70 to Appendix 77.

8.1 Brazilian Design Codes

8.1.1 Local Buckling Reduction Factor

For the Brazilian Norm, the first step was to inspect the cross-sections' parameters to understand their effect on the resistance to the compression. Depending on the parameters, a reduction factor Q must be multiplied to the resistant compression force $N_{c,Rd}$. According to the NBR Annex[172], for double-symmetric profiles, the Flange (Group AL) and the Web (Group AA) must be analyzed (see Figure 124):

- Column

Cross-Section Type					
Uniform Compression in Flange					
Parameters of Table F.1					
- Half of Full Flange Width	b	150.0	mm		
- Thickness	t_f	12.5	mm		
- Limit b/t	$(b/t)_{lim}$	15.839			Tab. F1
- b/t ratio	(b/t)	12.000		$\leq (b/t)_{lim}$	
Uniform Compression in Web					
- Height of Web	h	575.0	mm		
- Thickness	t_w	8.0	mm		
- Limit b/t	$(b/t)_{lim}$	42.144			Tab. F1
- b/t ratio	(b/t)	71.875		$> (b/t)_{lim}$	

Figure 122: Cross-Section Parameters for Column (Brazilian)

- Web: $(b/t)_{lim}$ exceeded → $Q_a < 1$
  - $c_a = 0.34$
  - $b_{ef} = 37.63$ cm (see below)
  - $Q_a = A_{ef} / A_g = 0.868641$
- Flange: $(b/t)_{lim}$ not exceeded → $Q_s = 1$ (see Figure 122)

$Q = Q_a * Q_s = 0.868641$

With b_{ef}[173]:

$$b_{ef} = 1.92 * t * \sqrt{\frac{E}{\sigma}} * \left[1 - \frac{c_a}{\frac{b}{t}} * \sqrt{\frac{E}{\sigma}}\right] \leq b$$

[172] (ABNT NBR 8800, 2008) – Annex F Page 128
[173] (ABNT NBR 8800, 2008) – Annex F.3 Page 129

- Chords

Cross-Section Type					
Uniform Compression in Flange					
Parameters of Table F.1					
- Half of Full Flange Width	b	60.0	mm		
- Thickness	t_f	6.3	mm		
- Limit b/t	$(b/t)_{lim}$	13.483			Tab. F1
- b/t ratio	(b/t)	9.524		$\leq (b/t)_{lin}$	
Uniform Compression in Web					
- Height of Web	h	187.4	mm		
- Thickness	t_w	4.8	mm		
- Limit b/t	$(b/t)_{lim}$	35.875			Tab. F1
- b/t ratio	(b/t)	39.453		$> (b/t)_{lin}$	

Figure 123: Cross-Section Parameters for Chords (Brazilian)

- Web: $(b/t)_{lim}$ exceeded → $Q_a = 1$
  - $c_a = 0.34$
  - $b_{ef} = 18.74$ cm (see above)
  - $Q_a = A_{ef} / A_g = 1$
- Flange: $(b/t)_{lim}$ not exceeded → $Q_s = 1$ (see Figure 123)

$Q = Q_a * Q_s = 1$

Elementos	Grupo	Descrição dos elementos	Alguns exemplos com indicação de b e t	$(b/t)_{lim}$
AA	1	— Mesas ou almas de seções tubulares retangulares — Lamelas e chapas de diafragmas entre linhas de parafusos ou soldas	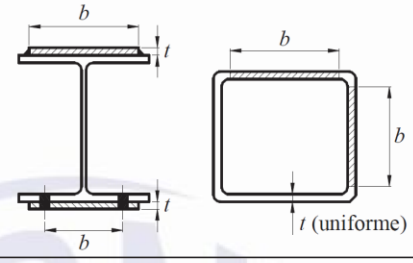	$1{,}40\sqrt{\frac{E}{f_y}}$
	2	— Almas de seções I, H ou U — Mesas ou almas de seção-caixão — Todos os demais elementos que não integram o Grupo 1	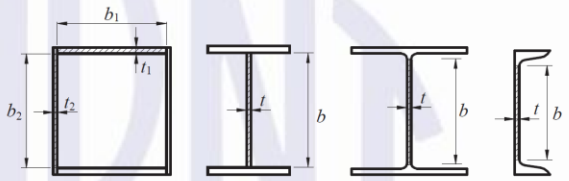	$1{,}49\sqrt{\frac{E}{f_y}}$
AL	3	— Abas de cantoneiras simples ou múltiplas providas de chapas de travejamento	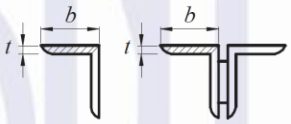	$0{,}45\sqrt{\frac{E}{f_y}}$
	4	— Mesas de seções I, H, T ou U laminadas — Abas de cantoneiras ligadas continuamente ou projetadas de seções I, H, T ou U laminadas ou soldadas — Chapas projetadas de seções I, H, T ou U laminadas ou soldadas	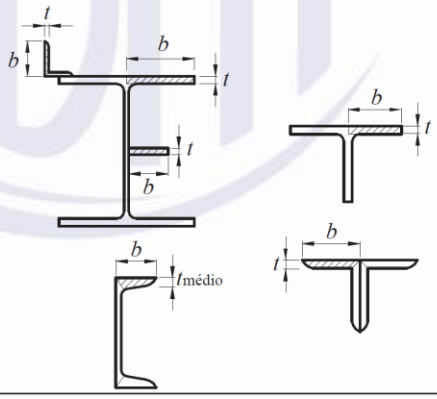	$0{,}56\sqrt{\frac{E}{f_y}}$
	5	— Mesas de seções I, H, T ou U soldadas [a]	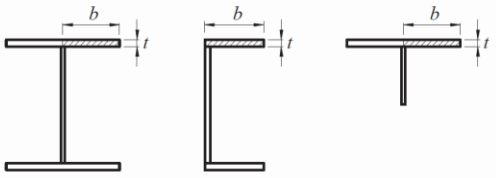	$0{,}64\sqrt{\frac{E}{(f_y/k_c)}}$
	6	— Almas de seções T	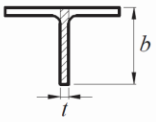	$0{,}75\sqrt{\frac{E}{f_y}}$

[a] O coeficiente k_c é dado em F.2.

Figure 124: Table for the Values of $(b/t)_{lim}$ for Verification of Local Buckling[174]

[174] (ABNT NBR 8800, 2008) – Table F.1 Page 128

8.1.2 Critical Buckling Load

$$N_{ey} = \frac{\pi^2 * E * I_y}{\left(K_y * L_y\right)^2}$$

$$N_{ez} = \frac{\pi^2 * E * I_z}{(K_z * L_z)^2}$$

There are 3 possible Critical Buckling Loads (N_e) for the beams, but only the first 2 (Y and Z axis) – see Equations[175] above – were studied in this Chapter (X axis not). The Buckling Load is the load that would cause buckling by bending in relation to its central axis of Inertia (Y or Z) of the cross-section. Important to notice that the X and Y for the Brazilian Norm indicate the stronger and weaker axis and were classified in this project as Y and Z, respectively. Furthermore, the longitudinal axis was classified as the X-axis. Given that:

- Column
  - L_y = 9m
  - L_z = 6.064m = 6m
  - N_{ey} = 6145 kN (calculated with SAP)
  - N_{ez} = 755 kN (calculated with SAP)

- Upper Chords
  - L_y = 4.003m = 4m
  - L_z = 2.003m = 2m
  - K_y = 1.0
  - K_z = 1.0
  - N_{ey} = 2071 kN
  - N_{ez} = 898 kN

- Lower Chords
  - L_y = 3.96m = 4m
  - L_z = 1.98m = 2m
  - K_y = 1.0
  - K_z = 1.0
  - N_{ey} = 2071 kN
  - N_{ez} = 898 kN

[175] (ABNT NBR 8800, 2008) – Annex E Page 121

A linha tracejada indica a linha elástica de flambagem	(a)	(b)	(c)	(d)	(e)	(f)
						
Valores teóricos de K_x ou K_y	0,5	0,7	1,0	1,0	2,0	2,0
Valores recomendados	0,65	0,80	1,2	1,0	2,1	2,0
Código para condição de apoio		Rotação e translação impedidas Rotação livre, translação impedida Rotação impedida, translação livre Rotação e translação livres				

Table 50: Buckling Coefficient[176]

8.1.3 Resistant Axial Force

To determine the Resistant Compression Force, the reduction factor χ must be found. The equations to determine the Reduced Slenderness λ_0[177] and the reduction factor for the Resistance Compression Force χ[178] are shown below. Table 51 and Table 52 show the parameters and the Resistant Compression Force for the columns and the chords. Since the Lower Chords have a larger tension force than the compression force, the Resistant Tension Force was also calculated. Its Resistant Compression Force was verified, since the parameters are the same for the Upper Chords. The equations for the Resistant Compression Force $N_{c,Rd}$[179] and the equations for the Resistant Tension Force $N_{t,Rd}$[180] are also shown below:

- Reduced Slenderness λ_0:

$$\lambda_0 = \sqrt{\frac{Q * A_g * f_y}{N_e}}$$

[176] (ABNT NBR 8800, 2008) – Table E.1 Page 125
[177] (ABNT NBR 8800, 2008) – Section 5.3.3 Page 44
[178] (ABNT NBR 8800, 2008) – Section 5.3.3 Page 44
[179] (ABNT NBR 8800, 2008) – Section 5.3.2 Page 44
[180] (ABNT NBR 8800, 2008) – Section 5..2.2 Page 37

- Resistance Compression Force Coefficient χ:

$$if\ \lambda_0 \leq 1.5 :\ \chi = 0.658^{\lambda_0^2}$$

$$if\ \lambda_0 > 1.5 :\ \chi = \frac{0.877}{\lambda_0}$$

- Resistant Compression Force $N_{c,Rd}$:

$$N_{c,Rd} = \frac{\chi * Q * A_g * f_y}{\gamma_{a1}}$$

- Resistant Tension Force $N_{t,Rd}$:

$$N_{t,Rd} = \frac{A_g * f_y}{\gamma_{a1}}$$

$$N_{t,Rd} = \frac{A_e * f_u}{\gamma_{a2}}$$

N_{ey}:	6145.0	N_{ez}:	755.0	[kN]
λ_{0y}:	0.608	λ_{0z}:	1.736	[-]
χ_{0y}:	0.601	χ_{0z}:	0.291	[-]
$N_{c,Rdy}$:	1242.391	$N_{c,Rdz}$:	601.941	[kN]

Table 51: Parameters for the Resistant Compression Force in the Columns

N_{ey}:	2071.4	N_{ez}:	898.1	[kN]
λ_{0y}:	0.625	λ_{0z}:	0.949	[-]
χ_{0y}:	0.593	χ_{0z}:	0.452	[-]
$N_{c,Rdy}$:	435.502	$N_{c,Rdz}$:	332.062	[kN]

Table 52: Parameters for the Resistant Compression Force in the Chords

N_{Rdbrut}:	752.7	$N_{t,Rd}$:	720.0	[kN]
N_{Rdnet}:	720.0			

Table 53: Resistant Tension Force in the Chords

Columns:

$$N_{c,Edy} = |-309.66\ kN| \leq 1242\ kN = N_{c,Rdy}$$

$$N_{c,Edz} = |-309.66\ kN| \leq 602\ kN = N_{c,Rdz}$$

N_{Sd}:	-309.7	[kN]
N_{Rd}:	601.9	
$\mathbf{N}_{Sd}/N_{Rd}$:	0.514	ok

Table 54: Verification of Compression Force on Columns

Upper Chords:

$$N_{c,Edy} = |-148.83\ kN| \leq 436\ kN = N_{c,Rdy}$$

$$N_{c,Edz} = |-148.83\ kN| \leq 332\ kN = N_{c,Rdz}$$

N_{Sd}:	-148.8	[kN]
N_{Rd}:	332.1	
$\mathbf{N}_{Sd}/N_{Rd}$:	0.448	ok

Table 55: Verification of Compression Force on Upper Chords

Lower Chords:

$$N_{t,Ed} = |125.6\ kN| \leq 720\ kN = N_{t,Rd}$$

N_{Sd}:	125.6	[kN]
N_{Rd}:	720.0	
$\mathbf{N}_{Sd}/N_{Rd}$:	0.174	ok

Table 56: Verification of Tension Force on Lower Chords

According to Table 48 and Table 49, and to Table 54 and Table 55, the compression loads on each member do not exceed the Resistant Compression Force and therefore, the members are verified against instability due to compression. The tension loads on the chords are also secured (shown in Table 56).

8.1.4 Resistant Moment Force

The NBR Annex[181] allows us to calculate the Resistant Moment Force (M_{Rdy} or M_{Rdz}). Table 57 shows the parameters for the calculation of the M_{Rd}. The M_{Rd} searched were for the cross-sections for I or H profiles with bending on the strong and weak axis. The M_{Rd} for each axis was the smallest between the ones found for the FLT (Flambagem Lateral com Torsão – Lateral Buckling with Torsion), FLM (Flambagem Local da Mesa – Local Buckling of the Flange) or FLA (Flambagem Local da Alma – Local Buckling of the Web). The cross-sections for the columns and chords were all classified as having a non-slender Web[182] (the cross-sections in study all had slenderness of the web $\lambda = h/t_w$ below $5.70*\sqrt{(E/fy)}$)and thus could the calculations for Table 57 be proceeded.

[181] (ABNT NBR 8800, 2008) – Annex G Page 130
[182] (ABNT NBR 8800, 2008) – Section H.1.2 Page 138

Tipo de seção e eixo de flexão	Estados-limites aplicáveis	M_r	M_{cr}	λ	λ_p	λ_r
Seções I e H com dois eixos de simetria e seções U não sujeitas a momento de torção, fletidas em relação ao eixo de maior momento de inércia	FLT	$(f_y - \sigma_r)W$ Ver Nota 5	Ver Nota 1	$\frac{L_b}{r_y}$	$1{,}76\sqrt{\frac{E}{f_y}}$	Ver Nota 1
	FLM	$(f_y - \sigma_r)W$ Ver Nota 5	Ver Nota 6	$\frac{b/t}{\text{Ver Nota 8}}$	$0{,}38\sqrt{\frac{E}{f_y}}$	Ver Nota 6
	FLA	$f_y W$	Viga de alma esbelta (Anexo H)	$\frac{h}{t_w}$	$3{,}76\sqrt{\frac{E}{f_y}}$	$5{,}70\sqrt{\frac{E}{f_y}}$
Seções I e H com apenas um eixo de simetria situado no plano médio da alma, fletidas em relação ao eixo de maior momento de inércia (ver Nota 9)	FLT	$(f_y - \sigma_r)W_c \leq f_y W_t$ Ver Nota 5	Ver Nota 2	$\frac{L_b}{r_{yc}}$	$1{,}76\sqrt{\frac{E}{f_y}}$	Ver Nota 2
	FLM	$(f_y - \sigma_r)W_c$ Ver Nota 5	Ver Nota 6	$\frac{b/t}{\text{Ver Nota 8}}$	$0{,}38\sqrt{\frac{E}{f_y}}$	Ver Nota 6
	FLA	$f_y W$	Viga de alma esbelta (Anexo H)	$\frac{h_c}{t_w}$	$\frac{\frac{h_c}{h_p}\sqrt{\frac{E}{f_y}}}{\left(0{,}54\frac{M_{p\ell}}{M_r} - 0{,}09\right)^2} \leq \lambda_r$	$5{,}70\sqrt{\frac{E}{f_y}}$
Seções I e H com dois eixos de simetria e seções U fletidas em relação ao eixo de menor momento de inércia	FLM Ver Nota 3	$(f_y - \sigma_r)W$	Ver Nota 6	$\frac{b/t}{\text{Ver Nota 8}}$	$0{,}38\sqrt{\frac{E}{f_y}}$	Ver Nota 6
	FLA Ver Nota 3	$f_y W_{ef}$ Ver Nota 4	$\frac{W_{ef}^2}{W} f_y$ Ver Nota 4	$\frac{h}{t_w}$	$1{,}12\sqrt{\frac{E}{f_y}}$	$1{,}40\sqrt{\frac{E}{f_y}}$
Seções sólidas retangulares fletidas em relação ao eixo de maior momento de inércia	FLT	$f_y W$	$\frac{2{,}00\,C_b\,E}{\lambda}\sqrt{JA}$	$\frac{L_b}{r_y}$	$\frac{0{,}13\,E}{M_{p\ell}}\sqrt{JA}$	$\frac{2{,}00\,E}{M_r}\sqrt{JA}$
Seções-caixão e tubulares retangulares, duplamente simétricas, fletidas em relação a um dos eixos de simetria que seja paralelo a dois lados	FLT Ver Nota 7	$(f_y - \sigma_r)W$ Ver Nota 5	$\frac{2{,}00\,C_b\,E}{\lambda}\sqrt{JA}$	$\frac{L_b}{r_y}$	$\frac{0{,}13\,E}{M_{p\ell}}\sqrt{JA}$	$\frac{2{,}00\,E}{M_r}\sqrt{JA}$
	FLM	$f_y W_{ef}$ Ver Nota 4	$\frac{W_{ef}^2}{W} f_y$ Ver Nota 4	$\frac{b/t}{\text{Ver Nota 8}}$	$1{,}12\sqrt{\frac{E}{f_y}}$	$1{,}40\sqrt{\frac{E}{f_y}}$
	FLA	$f_y W$	-	$\frac{h}{t_w}$	Ver Nota 10	$5{,}70\sqrt{\frac{E}{f_y}}$

Table 57: Parameters for Resistant Moment Force[183]

[183] (ABNT NBR 8800, 2008) – Table G.1 Page 14

For the FLT[184]:

$$if\ \lambda \leq \lambda_p:\ \ M_{Rd} = \frac{M_{pl}}{\gamma_{a1}}$$

$$if\ \lambda_p < \lambda \leq \lambda_r:\ \ M_{Rd} = \frac{C_b}{\gamma_{a1}} * \left[M_{pl} - \left(M_{pl} - M_r\right) * \frac{\lambda - \lambda_p}{\lambda_r - \lambda_p}\right] \leq \frac{M_{pl}}{\gamma_{a1}}$$

$$if\ \lambda > \lambda_r:\ \ M_{Rd} = \frac{M_{cr}}{\gamma_{a1}} \leq \frac{M_{pl}}{\gamma_{a1}}$$

For the FLM and FLA[185]:

$$if\ \lambda \leq \lambda_p:\ \ M_{Rd} = \frac{M_{pl}}{\gamma_{a1}}$$

$$if\ \lambda_p < \lambda \leq \lambda_r:\ \ M_{Rd} = \frac{1}{\gamma_{a1}} * \left[M_{pl} - \left(M_{pl} - M_r\right) * \frac{\lambda - \lambda_p}{\lambda_r - \lambda_p}\right]$$

$$if\ \lambda > \lambda_r:\ \ M_{Rd} = \frac{M_{cr}}{\gamma_{a1}},\qquad not\ applicable\ to\ FLA$$

Given the equations, Table 58 to Table 61 show the determined M_{Rdy} and M_{Rdz} for the column and the chords:

Double-sym I and H and U with no torsion, on largest I (I_y)									[kNcm]
	M_r	M_{cr}	λ	λ_p	λ_r	β_1	C_w		**M_{Rdy}**
FLT	29417.5	141253.3	55.67594	49.78032	134.0909	0.036947	12066277		41338.77
FLM	29417.5	302580	10	10.74802	23.79167				42436.14
FLA	29417.5		53.125	106.3489	161.2203				42436.14
								M_{Rdy} =	**41338.77**

Table 58: Determination of the M_{Rdy} for the Column

Double-sym I and H (Us have no moment in structure) with no torsion, on smallest I (I_z)										[kNcm]
	M_r	M_{cr}	λ	λ_p	λ_r	c_a or β_1	b_{ef} or C_w	W_{ef}:		**M_{Rdz}**
FLT	4742.5	43606.09	105.8922	49.78032	535.9512	0.005956	1482512			8801.633
FLM	4742.5	238.7397	10	10.74802	23.79167					9387.5
FLA	4219.864	2628.377	53.125	31.67838	39.59798	0.34	35.58032	168.7946		NA
									M_{Rdz} =	**8801.633**

Table 59: Determination of the M_{Rdz} for the Column

[184] (ABNT NBR 8800, 2008) – Section G.2.1 Page 130
[185] (ABNT NBR 8800, 2008) – Section G.2.2 Page 130

Double-sym I and H and U with no torsion, on largest I (I_y)									[kNcm]
	M_r	M_{cr}	λ	λ_p	λ_r	β_1	C_w		M_{Rdy}
FLT	4057.2	21095.82	47.84689	42.37582	121.2424	0.075978	157488.9		5747.278
FLM	4057.2	33339.6	9.52381	9.149325	21.87399				5835.644
FLA	4057.2		39.04167	90.53016	137.2399				5900.755
								M_{Rdy} =	**5747.278**

Table 60: Determination of the M_{Rdy} for the Chords

Double-sym I and H (Us have no moment in structure) with no torsion, on smallest I (I_z)									[kNcm]
	M_r	M_{cr}	λ	λ_p	λ_r	c_a or β_1	b_{ef} or C_w	W_{ef}:	M_{Rdz}
FLT	724.5	9701.716	72.72727	42.37582	454.0566	0.013567	17071.46		1397.121
FLM	724.5	65.35743	9.52381	9.149325	21.87399				1432.437
FLA	848.8118	696.1173	39.04167	26.96643	33.70804	0.34	17.53683	24.60324	NA
								M_{Rdz} =	**1397.121**

Table 61: Determination of the M_{Rdz} for the Chords

M_{Sdy}:	-14906	M_{Sdz}:	2554	[kNcm]
M_{Rdy}:	41338.8	M_{Rdz}:	8801.633	
M_{Sdy}/M_{Rdy} :	0.361	M_{Sdz}/M_{Rdz} :	0.290	
	ok		ok	

Table 62: Verification of the Moments on the Columns

M_{Sdy}:	-448	M_{Sdz}:	124	[kNcm]
M_{Rdy}:	5747.3	M_{Rdz}:	1397.121	
M_{Sdy}/M_{Rdy} :	0.078	M_{Sdz}/M_{Rdz} :	0.089	
	ok		ok	

Table 63: Verification of the Moments on the Upper Chords

M_{Sdy}:	-740	M_{Sdz}:	98	[kNcm]
M_{Rdy}:	5747.3	M_{Rdz}:	1397.121	
M_{Sdy}/M_{Rdy} :	0.129	M_{Sdz}/M_{Rdz} :	0.070	
	ok		ok	

Table 64: Verification of the Moments on the Lower Chords

Table 62, Table 63 and Table 64 demonstrate that the Verification of the Moment is satisfied for the columns and the chords.

8.1.5 Verification of the Combination of Forces

The Lower Chords have a tension force greater than the compression force, so the verification for the combination of forces will use the tension force for the Lower Chords. The Columns and the Upper Chords will use the compression force. The equations below show the Verification of the Combination of Forces when the Axial Force Ratio is greater than 0.2[186] and when it is lower than 0.2[187]:

$$if\ \frac{N_{Sd}}{N_{Rd}} \geq 0.2: \quad \frac{N_{Sd}}{N_{Rd}} + \frac{8}{9}\left(\frac{M_{y,Sd}}{M_{y,Rd}} + \frac{M_{z,Sd}}{M_{z,Rd}}\right) \leq 1.0$$

$$if\ \frac{N_{Sd}}{N_{Rd}} < 0.2: \quad \frac{N_{Sd}}{2 * N_{Rd}} + \left(\frac{M_{y,Sd}}{M_{y,Rd}} + \frac{M_{z,Sd}}{M_{z,Rd}}\right) \leq 1.0$$

[kN]		[kNcm]		[kNcm]	
N_{Sd}:	-309.7	M_{Sdy}:	-14906.0	M_{Sdz}:	2554.0
N_{Rd}:	601.9	M_{Rdy}:	41338.8	M_{Rdz}:	8801.6
N_{Sd} / N_{Rd} >= 0.2?	Yes	**1.093**	<= 1.0	!	

Table 65: Verification of the Combination of Forces on the Columns

[kN]		[kNcm]		[kNcm]	
N_{Sd}:	-148.8	M_{Sdy}:	-448.0	M_{Sdz}:	124.0
N_{Rd}:	332.1	M_{Rdy}:	5747.3	M_{Rdz}:	1397.1
N_{Sd} / N_{Rd} >= 0.2?	No	**0.596**	<= 1.0	ok	

Table 66: Verification of the Combination of Forces on the Upper Chords

[kN]		[kNcm]		[kNcm]	
N_{Sd}:	125.6	M_{Sdy}:	-740.0	M_{Sdz}:	98.0
N_{Rd}:	720.0	M_{Rdy}:	5747.3	M_{Rdz}:	1397.1
N_{Sd} / N_{Rd} >= 0.2?	No	**0.286**	<= 1.0	ok	

Table 67: Verification of the Combination of Forces on the Lower Chords

[186] (ABNT NBR 8800, 2008) – Section 5.5.1.2 Page 54
[187] (ABNT NBR 8800, 2008) – Section 5.5.1.2 Page 55

For the Upper and Lower Chords the verification was satisfied. For the Column, the ratio was 9.3% above the limit. Since this analysis used the maximum values of each force, it is possible that these forces do not act upon the same location (for example: the maximum moment in Y acts upon the 9th column while the maximum compression is located on the 5th column). Therefore, it is possible that all the columns are secure for this verification. Nonetheless, a deeper analysis was undertaken.

The maximum values for the most compressed column (5th Column on the Right) at its most aggressive location (bottom) were secured:

[kN]		[kNcm]		[kNcm]	
N_{Sd}:	-309.7	M_{Sdy}:	-14906.0	M_{Sdz}:	0.0
N_{Rd}:	601.9	M_{Rdy}:	41338.8	M_{Rdz}:	8801.6
N_{Sd} / N_{Rd} >= 0.2?		Yes	**0.835**	<= 1.0	ok

Table 68: Verification of the Combination of Forces on the Column (Bottom of the 5th on the Right) – Max M_{Edy}

In fact, M_{Edz} (= M_{Sdz}) was always equal to 0 at its most aggressive location for all the columns (bottom). When the M_{Edz} was maximum (x = 2.421m from the bottom at the 1st Left Column), the M_{Edy} was -4826 kNcm and the Normal Force N was -67.34 kN (see Figure 125). Table 69 shows that the verification of this combination is also secured.

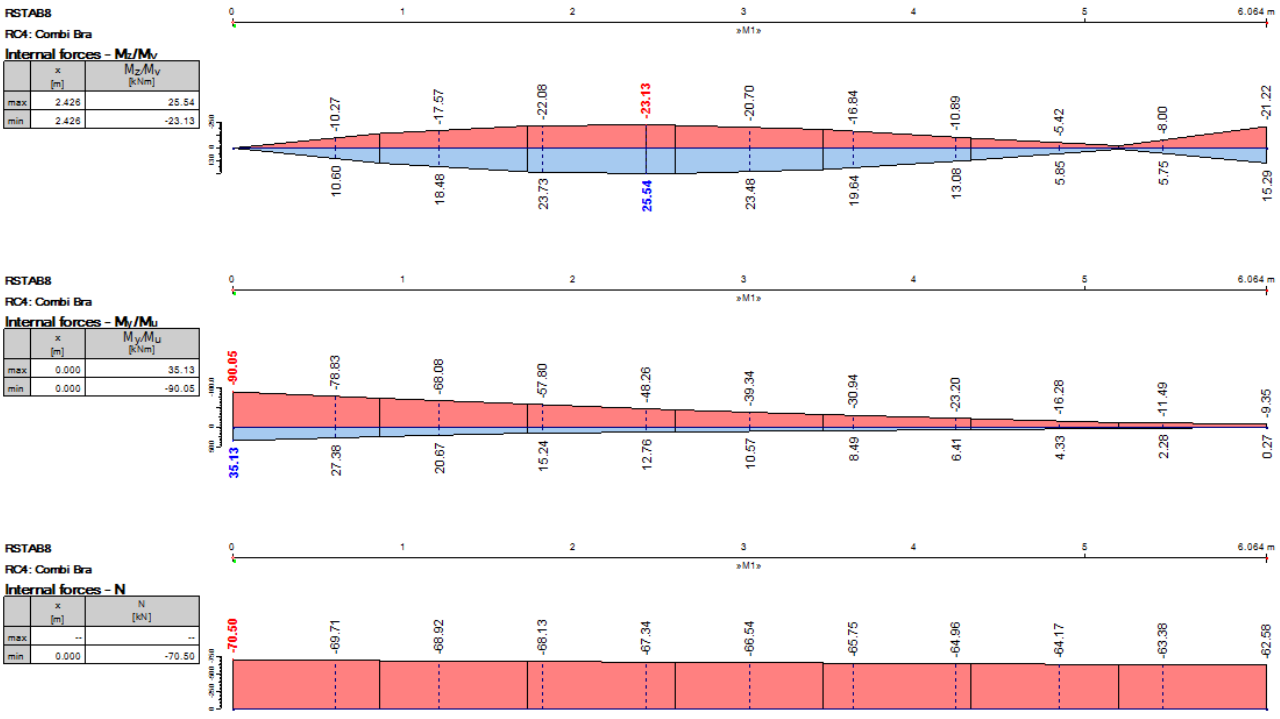

Figure 125: Results of the Internal Forces of Member M1 (1st Column on the Left) – Max M_{Edz} Location

[kN]		[kNcm]		[kNcm]	
N_{Sd}:	-67.3	M_{Sdy}:	-4826.0	M_{Sdz}:	2554.0
N_{Rd}:	601.9	M_{Rdy}:	41338.8	M_{Rdz}:	8801.6
N_{Sd} / N_{Rd} >= 0.2?		No	**0.463**	<= 1.0	ok

Table 69: Verification of the Combination of Forces on the Column (at x = 2.4m from the Ground of the 1st on the Left) - Max M_{Edz}

Thus, the columns and the chords were all secured.

8.2 German Design Codes

8.2.1 Classification of the Cross-Section (Querschnittsklasse)

Different from the Brazilian Norm, the German Norm inspects and evaluates the cross-sections and then groups these cross-sections in 4 categories: QK1 to QK4 (Querschnittsklasse). The inspections are also for both, the Web and the Flange (Table 70 and Table 71). The cross-sections chosen for the German structure are rolled (HEA and IPE) and their QK are given in Schneider[188]. Since the column is made up of the steel S235 and from 2 rolled sections (HEA 600 and IPE 300), the QK for N was assumed to be 2 (on the safe side, like HEA 600) and QK for M_y and M_z was 1. The chords were made up of the steel 355 and cross-section of IPE 200, the QK for the N was 2 and for the M_y and M_z, also 1 (see Table 72).

[188] (SCHNEIDER, 2012) – Section 8F Page 8.159

Beidseitig gestützte druckbeanspruchte Querschnittsteile

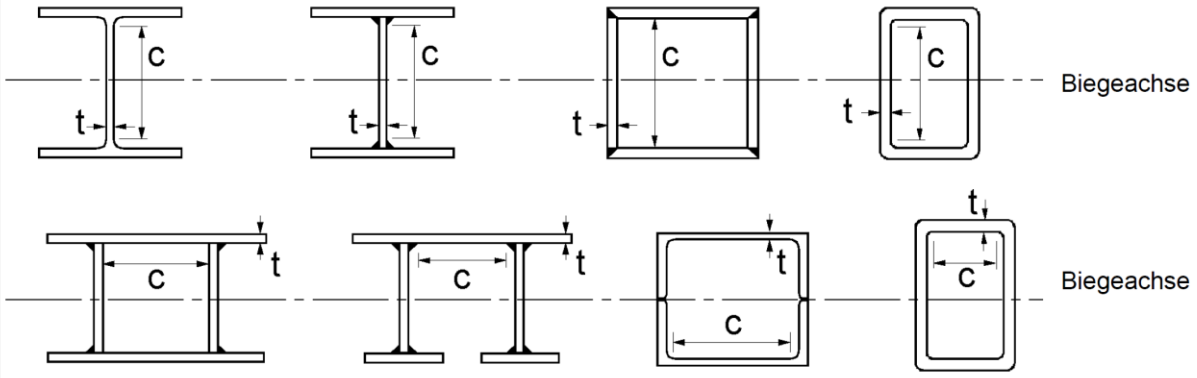

Klasse	auf Biegung beanspruchte Querschnittsteile	auf Druck beanspruchte Querschnittsteile	auf Druck und Biegung beanspruchte Querschnittsteile
Spannungs-verteilung über Querschnittsteile (Druck positiv)	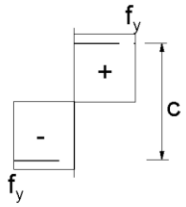	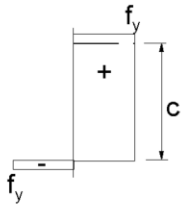	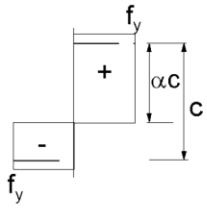
1	$c/t \le 72\varepsilon$	$c/t \le 33\varepsilon$	für $\alpha > 0{,}5$: $c/t \le \frac{396\varepsilon}{13\alpha - 1}$ für $\alpha \le 0{,}5$: $c/t \le \frac{36\varepsilon}{\alpha}$
2	$c/t \le 83\varepsilon$	$c/t \le 38\varepsilon$	für $\alpha > 0{,}5$: $c/t \le \frac{456\varepsilon}{13\alpha - 1}$ für $\alpha \le 0{,}5$: $c/t \le \frac{41{,}5\varepsilon}{\alpha}$
Spannungs-verteilung über Querschnittsteile (Druck positiv)	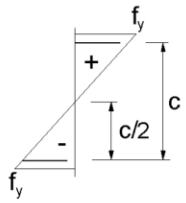	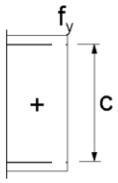	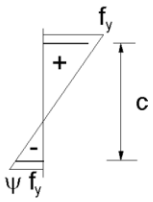
3	$c/t \le 124\varepsilon$	$c/t \le 42\varepsilon$	für $\psi > -1$: $c/t \le \frac{42\varepsilon}{0{,}67 + 0{,}33\psi}$ für $\psi \le -1$[a]: $c/t \le 62\varepsilon\,(1 - \psi)\sqrt{(-\psi)}$

$\varepsilon = \sqrt{235 / f_y}$	f_y	235	275	355	420	460
	ε	1,00	0,92	0,81	0,75	0,71

[a] Es gilt $\psi \le -1$ falls entweder die Druckspannungen $\sigma \le f_y$ oder die Dehnungen infolge Zug $\varepsilon_y > \frac{f_y}{E}$ sind.

Table 70: Cross-Section Category (QK) for the Web for max c/t[189]

[189] (DIN EN 1993-1-1, 2010) – Table 5.2 Page 46

Einseitig gestützte Flansche

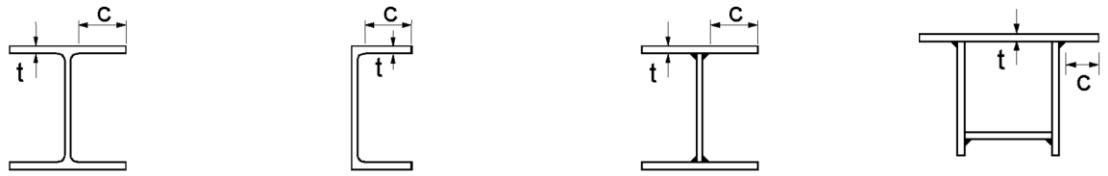

Gewalzte Querschnitte | Geschweißte Querschnitte

Klasse	auf Druck beanspruchte Querschnittsteile	auf Druck und Biegung beanspruchte Querschnittsteile	
		freier Rand im Druckbereich	freier Rand im Zugbereich
Spannungs-verteilung über Querschnittsteile (Druck positiv)	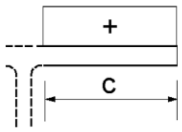	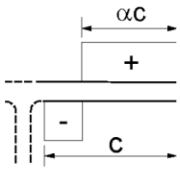	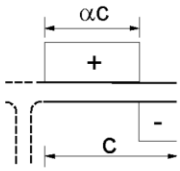
1	$c/t \le 9\varepsilon$	$c/t \le \frac{9\varepsilon}{\alpha}$	$c/t \le \frac{9\varepsilon}{\alpha\sqrt{\alpha}}$
2	$c/t \le 10\varepsilon$	$c/t \le \frac{10\varepsilon}{\alpha}$	$c/t \le \frac{10\varepsilon}{\alpha\sqrt{\alpha}}$
Spannungs-verteilung über Querschnittsteile (Druck positiv)	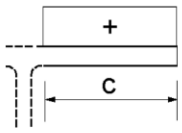	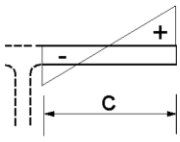	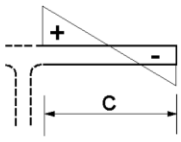
3	$c/t \le 14\varepsilon$	$c/t \le 21\varepsilon\sqrt{k_\sigma}$ Für k_σ siehe EN 1993-1-5	

$\varepsilon = \sqrt{235/f_y}$	f_y	235	275	355	420	460
	ε	1,00	0,92	0,81	0,75	0,71

Table 71: Cross-Section Category for the Flange for max c/t[190]

[190] (DIN EN 1993-1-1, 2010) – Table 5.2 (continued) Page 47

Profilreihen IPE, HEA, HEB, HEM

Profilreihe		IPE								
Nennhöhe		**80**	**100**	**120**	**140**	**160**	**180**	**200**	**220**	**240**
h	mm	80	100	120	140	160	180	200	220	240
b	mm	46	55	64	73	82	91	100	110	120
t_w	mm	3,8	4,1	4,4	4,7	5	5,3	5,6	5,9	6,2
t_f	mm	5,2	5,7	6,3	6,9	7,4	8	8,5	9,2	9,8
r	mm	5	7	7	7	9	9	12	12	15
d	mm	59,6	74,6	93,4	112	127	146	159	178	190
A	cm^2	7,64	10,3	13,2	16,4	20,1	23,9	28,5	33,4	39,1
A_{Vy}	cm^2	4,78	6,27	8,06	10,1	12,1	14,6	17,0	20,2	23,5
A_{Vz}	cm^2	3,6	5,1	6,3	7,6	9,7	11,2	14	15,9	19,1
A_w	cm^2	26,45	36,33	47,26	59,31	72,60	86,92	102,5	118,9	136,6
g_k	kN/m	0,06	0,081	0,104	0,129	0,158	0,188	0,224	0,262	0,307
U	m^2/m	0,3278	0,3998	0,4752	0,5502	0,6221	0,6979	0,7682	0,8484	0,9210
a	-	0,374	0,391	0,389	0,386	0,396	0,391	0,404	0,394	0,398
d/t_w	-	15,7	18,2	21,2	23,9	25,4	27,5	28,4	30,1	30,7
c/t_f	-	3,1	3,2	3,6	3,9	4	4,2	4,1	4,4	4,3
I_y	cm^4	80,1	171	318	541	869	1320	1940	2770	3890
$W_{el,y}$	cm^3	20	34,2	53	77,3	109	146	194	252	324
$W_{pl,y}$	cm^3	23,22	39,41	60,73	88,34	123,9	166,4	220,6	285,4	366,6
k_{My}	-	0,3409	0,37	0,351	0,336	0,355	0,342	0,369	0,352	0,371
a_{Vy}	-	0,6538	0,647	0,642	0,638	0,639	0,636	0,64	0,644	0,651
i_y	cm	3,24	4,07	4,9	5,74	6,58	7,42	8,26	9,11	9,97
KL ⊥ yy *)	-	a	a	a	a	a	a	a	a	a
I_z	cm^4	8,49	15,9	27,7	44,9	68,3	101	142	205	284
$W_{el,z}$	cm^3	3,69	5,79	8,65	12,3	16,7	22,2	28,5	37,3	47,3
$W_{pl,z}$	cm^3	5,818	9,146	13,58	19,25	26,1	34,6	44,61	58,11	73,92
a_{Vz}	-	0,468	0,493	0,477	0,465	0,481	0,47	0,492	0,476	0,489
i_z	cm	1,05	1,24	1,45	1,65	1,84	2,05	2,24	2,48	2,69
$i_{f,z}$	cm	1,2	1,42	1,66	1,9	2,11	2,36	2,56	2,84	3,08
KL ⊥ zz *)	-	b	b	b	b	b	b	b	b	b
S_y	cm^3	11,6	19,7	30,4	44,2	61,9	83,2	110	143	183
I_T	cm^4	0,698	1,2	1,74	2,45	3,6	4,79	6,98	9,07	12,9
I_w / 1000	cm^6	0,118	0,351	0,89	1,981	3,959	7,431	12,99	22,67	37,39
w_M	cm^2	8,6	13	18,2	24,3	31,3	39,1	47,9	58	69,1
$\lambda \cdot 1000$	cm^{-1}	47,77	36,31	27,46	21,84	18,73	15,77	14,40	12,42	11,54
$N_{pl,Rd}$ **)	kN	179,5	242,1	310,2	385,4	472,4	561,7	669,8	784,9	918,9
$M_{pl,y,Rd}$ **)	kNm	5,5	9,3	14,3	20,8	29,1	39,1	51,8	67,1	86,2
$M_{el,y,Rd}$ **)	kNm	4,7	8	12,5	18,2	25,6	34,3	45,6	59,2	76,1
$V_{pl,y,Rd}$ **)	kN	64,9	85,1	109	137	165	198	231	275	319
$M_{pl,z,Rd}$ **)	kNm	1,4	2,1	3,2	4,5	6,1	8,1	10,5	13,7	17,4
$M_{el,z,Rd}$ **)	kNm	0,9	1,4	2	2,9	3,9	5,2	6,7	8,8	11,1
$V_{pl,z,Rd}$ **)	kN	48,5	68,7	85,4	103,3	131,1	152	190,2	215,9	259,5
$M_{pl,w,Rd}$ **)	kNm^2	0,048	0,096	0,172	0,288	0,446	0,669	0,956	1,38	1,91
QK N	***)	1/1/1/1	1/1/1/1	1/1/1/1	1/1/1/2	1/1/1/2	1/1/2/3	1/1/2/3	1/1/2/4	1/2/2/4
QK M_y; M_z	***)	1/1/1/1	1/1/1/1	1/1/1/1	1/1/1/1	1/1/1/1	1/1/1/1	1/1/1/1	1/1/1/1	1/1/1/1
Nennhöhe		**80**	**100**	**120**	**140**	**160**	**180**	**200**	**220**	**240**

*) KL nur für Stahlgüten S 235 / S 275 / S 355 / S 420; KL für S 460 siehe Tafel 8.25

**) Grenzschnittgröße = Tafelwert × (f_y / 235) mit f_y in N/mm^2 ; $\gamma_{M0} = 1,0$

***) QK für Stahlgüten S 235 / S 275 / S 355 / S 460

Table 72: IPE Cross-Section Parameters[191]

[191] (SCHNEIDER, 2012) – Section 8F Page 8.161

8.2.2 Critical Buckling Load

The Critical Buckling Load N_{cr} is calculated by the formula[192]:

$$N_{cr} = \frac{\pi^2 * E * I}{s_k^2}$$

And s_k is the buckling length, the same as the one calculated in the Brazilian method (see Section 8.1.2).

8.2.3 Resistant Axial Force

Similar to the Brazilian Norm, the slenderness factor must be determined in order to define the reduction factor χ. It was assumed that the columns and the chords would have the imperfection factors (α) in y-y as "a" and z-z as "b" (exactly as HEA 600, IPE 300 and IPE 200 – see also Table 72). The Slenderness is given by the equation[193]:

$$\lambda = \sqrt{\frac{A * f_y}{N_{cr}}} = \frac{L_{cr}}{i} * \frac{1}{\lambda_1} \qquad for\ QK\ 1, 2\ and\ 3$$

From Table 75, it is possible to determine the reduction factor χ having α and λ. The reduction factor was then defined (Table 73 and Table 74):

	[kN]		[-]		[-]		[-]
N_{cry}:	6145	λ_y:	0.731445	α_y:	a	χ_y:	0.835
N_{crz}:	755	λ_z:	2.086745	α_z:	b	χ_z:	0.2

Table 73: Parameters of the Column

	[kN]		[-]		[-]		[-]
N_{cry}:	2513.048	λ_y:	0.625506	α_y:	a	χ_y:	0.88
N_{crz}:	735.779	λ_z:	1.156001	α_z:	b	χ_z:	0.51

Table 74: Parameters of the Chords

The Equation for the Resistant Buckling Force[194] was almost the same as the Brazilian, except for the missing Reduction Factor Q (from the Flange and Web):

$$N_{b,Rd} = \frac{\chi * A * f_y}{\gamma_{M1}} \qquad for\ QK\ 1, 2\ and\ 3$$

[192] (SCHNEIDER, 2012) – Section 8 Page 4.60
[193] (DIN EN 1993-1-1, 2010) – Section 6.3.1.3 Page 65
[194] (DIN EN 1993-1-1, 2010) – Section 6.3.1.1 Page 62

Bezogener Schlankheitsgrad $\bar{\lambda}$ für Knicklinie:						Bezogener Schlankheitsgrad $\bar{\lambda}$ für Knicklinie:					
a_0	a	b	c	d	χ	a_0	a	b	c	d	χ
0,20	0,20	0,20	0,20	0,20	**1,00**	1,24	1,17	1,08	0,99	0,85	**0,55**
0,28	0,25	0,23	0,22	0,22	**0,99**	1,25	1,19	1,10	1,00	0,87	**0,54**
0,34	0,29	0,26	0,24	0,23	**0,98**	1,27	1,20	1,11	1,02	0,89	**0,53**
0,41	0,34	0,29	0,26	0,24	**0,97**	1,28	1,22	1,13	1,04	0,91	**0,52**
0,46	0,38	0,32	0,28	0,26	**0,96**	1,30	1,24	1,15	1,06	0,92	**0,51**
0,51	0,42	0,34	0,30	0,27	**0,95**	1,31	1,25	1,17	1,08	0,94	**0,50**
0,56	0,45	0,37	0,32	0,28	**0,94**	1,33	1,27	1,18	1,09	0,96	**0,49**
0,60	0,49	0,40	0,34	0,30	**0,93**	1,35	1,29	1,20	1,11	0,98	**0,48**
0,63	0,52	0,42	0,36	0,31	**0,92**	1,36	1,31	1,22	1,13	1,00	**0,47**
0,66	0,55	0,44	0,38	0,32	**0,91**	1,38	1,32	1,24	1,15	1,02	**0,46**
0,69	0,58	0,47	0,40	0,34	**0,90**	1,40	1,34	1,26	1,17	1,04	**0,45**
0,72	0,60	0,49	0,42	0,35	**0,89**	1,42	1,36	1,28	1,19	1,06	**0,44**
0,75	0,63	0,51	0,44	0,36	**0,88**	1,44	1,38	1,30	1,21	1,08	**0,43**
0,77	0,66	0,54	0,46	0,38	**0,87**	1,45	1,40	1,32	1,23	1,10	**0,42**
0,79	0,68	0,56	0,47	0,39	**0,86**	1,47	1,42	1,34	1,26	1,12	**0,41**
0,81	0,70	0,58	0,49	0,41	**0,85**	1,50	1,44	1,36	1,28	1,15	**0,40**
0,83	0,72	0,60	0,51	0,42	**0,84**	1,52	1,46	1,39	1,30	1,17	**0,39**
0,85	0,74	0,62	0,53	0,43	**0,83**	1,54	1,49	1,41	1,33	1,20	**0,38**
0,87	0,76	0,64	0,55	0,45	**0,82**	1,56	1,51	1,43	1,35	1,22	**0,37**
0,88	0,78	0,66	0,56	0,46	**0,81**	1,59	1,54	1,46	1,38	1,25	**0,36**
0,90	0,80	0,68	0,58	0,48	**0,80**	1,61	1,56	1,48	1,40	1,27	**0,35**
0,91	0,81	0,69	0,60	0,49	**0,79**	1,64	1,59	1,51	1,43	1,30	**0,34**
0,93	0,83	0,71	0,61	0,50	**0,78**	1,66	1,61	1,54	1,46	1,33	**0,33**
0,94	0,85	0,73	0,63	0,52	**0,77**	1,69	1,64	1,57	1,49	1,36	**0,32**
0,96	0,86	0,75	0,65	0,53	**0,76**	1,72	1,67	1,60	1,52	1,39	**0,31**
0,97	0,88	0,76	0,66	0,55	**0,75**	1,75	1,70	1,63	1,55	1,42	**0,30**
0,99	0,90	0,78	0,68	0,56	**0,74**	1,78	1,74	1,66	1,58	1,46	**0,29**
1,00	0,91	0,80	0,70	0,58	**0,73**	1,82	1,77	1,70	1,62	1,49	**0,28**
1,01	0,93	0,81	0,71	0,59	**0,72**	1,85	1,81	1,73	1,66	1,53	**0,27**
1,03	0,94	0,83	0,73	0,61	**0,71**	1,89	1,84	1,77	1,70	1,57	**0,26**
1,04	0,96	0,84	0,74	0,62	**0,70**	1,93	1,88	1,81	1,74	1,61	**0,25**
1,05	0,97	0,86	0,76	0,63	**0,69**	1,97	1,93	1,86	1,78	1,65	**0,24**
1,06	0,98	0,88	0,78	0,65	**0,68**	2,02	1,97	1,90	1,83	1,70	**0,23**
1,08	1,00	0,89	0,79	0,66	**0,67**	2,06	2,02	1,95	1,87	1,75	**0,22**
1,09	1,01	0,91	0,81	0,68	**0,66**	2,11	2,07	2,00	1,93	1,80	**0,21**
1,10	1,03	0,92	0,82	0,69	**0,65**	2,17	2,13	2,06	1,98	1,86	**0,20**
1,12	1,04	0,94	0,84	0,71	**0,64**	2,23	2,18	2,12	2,04	1,92	**0,19**
1,13	1,06	0,95	0,86	0,73	**0,63**	2,29	2,25	2,18	2,11	1,98	**0,18**
1,14	1,07	0,97	0,87	0,74	**0,62**	2,36	2,32	2,25	2,18	2,05	**0,17**
1,16	1,08	0,98	0,89	0,76	**0,61**	2,43	2,39	2,33	2,25	2,13	**0,16**
1,17	1,10	1,00	0,90	0,77	**0,60**	2,52	2,48	2,41	2,34	2,21	**0,15**
1,18	1,11	1,02	0,92	0,79	**0,59**	2,61	2,57	2,50	2,43	2,30	**0,14**
1,20	1,13	1,03	0,94	0,80	**0,58**	2,71	2,67	2,60	2,53	2,41	**0,13**
1,21	1,14	1,05	0,95	0,82	**0,57**	2,82	2,78	2,72	2,65	2,52	**0,12**
1,22	1,16	1,06	0,97	0,84	**0,56**	2,95	2,91	2,85	2,78	2,65	**0,11**
						3,10	3,06	3,00	2,92	2,80	**0,10**

Die aufnehmbare Normalkraft von zentrisch gedrückten Stäben aus Walzprofilen kann den Tafeln 8.27 bis 8.30 entnommen werden.

Table 75: Reduction Factor for Buckling (from α and λ)[195]

[195] (SCHNEIDER, 2012) – Table 8.26

The Resistant Buckling Forces were then calculated (Table 76 and Table 77):

$N_{b,Rdy}$:	2495.6	[kN]
$N_{b,Rdz}$:	597.755	

Table 76: Resistant Buckling Force in the Columns

$N_{b,Rdy}$:	786.6	[kN]
$N_{b,Rdz}$:	455.870	

Table 77: Resistant Buckling Force in the Chords

Similarly to the Brazilian method, the Resistant Tension Force on the Lower Chord was calculated by the same formula (although written differently). However, the security factors have different values:

- Brazilian[196]:
  - $\gamma_{a1} = \gamma_{M0} = 1.10$
  - $\gamma_{a2} = \gamma_{M2} = 1.35$
- German[197]:
  - $\gamma_{a1} = \gamma_{M0} = 1.00$
  - $\gamma_{a2} = \gamma_{M2} = 1.25$

The Equation for the Resistant Tension Force[198]:

$$N_{t,Rd} = min \begin{cases} N_{pl,Rd} = \dfrac{A * f_y}{\gamma_{M0}} \\ N_{u,Rd} = \dfrac{0.9 * A_{net} * f_u}{\gamma_{M2}} \end{cases}$$

$N_{t,Rdbrut}$:	983.3	$N_{t,Rd}$:	964.4	[kN]
$N_{t,Rdnet}$:	964.4			

Table 78: Resistant Tension Force in the Chords

Columns:

$$N_{c,Edy} = |-348.3\ kN| \leq 2496\ kN = N_{c,Rdy}$$

$$N_{c,Edz} = |-348.3\ kN| \leq 598\ kN = N_{c,Rdz}$$

N_{Ed}:	-348.3	[kN]
N_{Rd}:	597.8	
N_{Sd}/N_{Rd} :	0.583	ok

Table 79: Verification of Compression Force on Columns

[196] (ABNT NBR 8800, 2008) – Table 3 Page 23
[197] (DIN EN 1993-1-1, 2010) – Section 6.1 Page 49
[198] (SCHNEIDER, 2012) – Section 2.2.2a Page 8.14

Upper Chords:

$$N_{c,Edy} = |-174.3\ kN| \leq 787\ kN = N_{c,Rdy}$$

$$N_{c,Edz} = |-174.3\ kN| \leq 456\ kN = N_{c,Rdz}$$

N_{Ed}:	-174.3	[kN]
N_{Rd}:	455.9	
N_{Sd}/N_{Rd} :	0.382	ok

Table 80: Verification of Compression Force on Upper Chords

Lower Chords:

$$N_{t,Ed} = |157.1\ kN| \leq 964\ kN = N_{t,Rd}$$

N_{Ed}:	157.1	[kN]
N_{Rd}:	964.4	
N_{Sd}/N_{Rd} :	0.163	ok

Table 81: Verification of Tension Force on Lower Chords

According to Table 48 and Table 49, and to Table 79 and Table 80 the compression loads on each member do not exceed the Resistant Compression Force and therefore, the members were verified against instability due to compression. The tension loads on the chords are also secured (shown in Table 81).

8.2.4 Resistant Moment Force

According to the German Norm, the Resistant Moment Force was calculated by[199]:

$$M_{c,Rd} = M_{pl,Rd} = \frac{W_{pl} * f_y}{\gamma_{M0}} \qquad for\ QK\ 1\ or\ 2$$

[199] (DIN EN 1993-1-1, 2010) – Section 6.2.5 Page 54

M_{Sdy}:	-20705	M_{Sdz}:	-3680	[kNcm]
M_{Rdy}:	63962.7	M_{Rdz}:	13682.13	
$\mathbf{M}_{Sdy}/M_{Rdy}$:	0.324 ok	$\mathbf{M}_{Sdz}/M_{Rdz}$:	0.269 ok	

Table 82: Verification of the Moments on the Columns

M_{Sdy}:	-547	M_{Sdz}:	100	[kNcm]
M_{Rdy}:	6900.0	M_{Rdz}:	1399.132	
$\mathbf{M}_{Sdy}/M_{Rdy}$:	0.079 ok	$\mathbf{M}_{Sdz}/M_{Rdz}$:	0.071 ok	

Table 83: Verification of the Moments on the Upper Chords

M_{Sdy}:	-525	M_{Sdz}:	87	[kNcm]
M_{Rdy}:	6900.0	M_{Rdz}:	1399.132	
$\mathbf{M}_{Sdy}/M_{Rdy}$:	0.076 ok	$\mathbf{M}_{Sdz}/M_{Rdz}$:	0.062 ok	

Table 84: Verification of the Moments on the Lower Chords

Table 82, Table 83 and Table 84 demonstrate that the Verification of the Moment is satisfied for the columns and the chords.

8.2.5 Verification of the Flexural Torsional Buckling (Biegedrillknicken)

According to Schneider[200], the verification for FTB would be satisfied if the formula[201] for BDK was satisfied (see also Figure 126):

$$\frac{M_{E,d}}{M_{b,Rd}} \leq 1.0$$

With:

$$M_{b,Rd} = \chi_{LT} * W_y * \frac{f_y}{\gamma_{M1}} \quad with\ \gamma_{M1} = 1.10\ and\ W_y = W_{pl,y}$$

As the calculation for the Resistant Axial Forces, there must be a reduction factor χ_{LT} for the Moment Resistant Force (for BDK Verification) and a Slenderness must be attributed to it:

$$\lambda_{LT} = \sqrt{\frac{W_y * f_y}{M_{cr}}}$$

[200] (SCHNEIDER, 2012) – Section 3.3.2 Page 8.33
[201] (DIN EN 1993-1-1, 2010) – Section 6.3.2.1 Page 66

a) Nachweis gegen Biegedrillknicken [-1-1/6.3.2.1]

Der BDK-Nachweis nach dem Ersatzstabverfahren lautet:

$$\frac{M_{\mathrm{Ed}}}{M_{\mathrm{b,Rd}}} \le 1{,}0 \qquad \text{mit: } M_{\mathrm{b,Rd}} = \chi_{\mathrm{LT}} \cdot W_{\mathrm{y}} \cdot \frac{f_{\mathrm{y}}}{\gamma_{\mathrm{M1}}} \qquad \gamma_{\mathrm{M1}} = 1{,}10$$

Für W_y ist das maßgebende Widerstandsmoment einzusetzen:

$W_{\mathrm{y}} = W_{\mathrm{pl,y}}$ QK 1 und 2

$W_{\mathrm{y}} = W_{\mathrm{el,y}}$ QK 3

$W_{\mathrm{y}} = W_{\mathrm{eff,y}}$ QK 4

χ_{LT} ist der Abminderungsfaktor für Biegedrillknicken. Zu seiner Ermittlung wird die BDK-Schlankheit benötigt:

$\overline{\lambda}_{\mathrm{LT}} = \sqrt{W_{\mathrm{y}} \cdot f_{\mathrm{y}} / M_{\mathrm{cr}}}$ bezogene BDK-Schlankheit, Auswahl von W_y s.o.

Das ideale Biegedrillknickmoment M_{cr} kann der Literatur, z. B [8.6] oder [8.11], entnommen werden. Alternativ kann M_{cr} mit Hilfe der Hilfe von Programmen, z. B. [8.9], bestimmt werden. Für doppeltsymmetrische I-Profile gilt:

$$M_{\mathrm{cr}} = \zeta \cdot N_{\mathrm{cr,z}} \cdot \left[\sqrt{(c^2 + 0{,}25 \cdot z_{\mathrm{p}}^2)} + 0{,}5 \cdot z_{\mathrm{p}} \right] \qquad N_{\mathrm{cr,z}} = \frac{\pi^2 \cdot E \cdot I_z}{l^2}$$

Figure 126: Verification Against FTB (BDK)[202]

ζ: Momentenbeiwert für Gabellagerung an den Stabenden, s. Tafel 8.34a

l: Abstand der Gabellager

z_p: Abstand des Angriffspunktes der Belastung vom Schwerpunkt, bei rückdrehender Wirkung der Belastung positiv (Beispiel Einfeldträger: $z_P < 0$ bei Lastangriff am Druckgurt)

c: Drehradius des Querschnitts $c^2 = \left(I_w + 0{,}039 \cdot l^2 \cdot I_T\right)/I_z$

I_T: Torsionsflächenmoment 2. Grades (siehe Kap. 8F)

I_w: Wölbflächenmoment 2. Grades bezogen auf den Schubmittelpunkt (siehe Kap. 8F)

Tafel 8.34a Momentenbeiwert ζ

Momentenverlauf	ζ
	1,0
	1,12
	1,35
ψM_{max} M_{max} $-1 \le \psi \le 1$	$1{,}77 - 0{,}77 \cdot \psi$
$0{,}56 M_{max}$ M_{max}	2,25
	1,35

Tafel 8.34b Zuordnung der Knicklinien nach [-1-1/Tab.6.5]

Querschnitt	Grenzen	Knicklinien
Gewalztes I-Profil	$h/b \le 2$	b
	$h/b > 2$	c
Geschweißtes I-Profil	$h/b \le 2$	c
	$h/b > 2$	d

Tafel 8.34c Imperfektionsbeiwerte BDK

Knicklinie	a	b	c	d
α_{LT}	0,21	0,34	0,49	0,76

Tafel 8.34d Korrekturbeiwerte k_c

Momentenverlauf	k_c
$\psi = 1{,}0$	1,0
$-1 \le \psi \le 1$	$\frac{1}{1{,}33 - 0{,}33 \cdot \psi}$
	0,94
	0,90
	0,91
	0,86
	0,77
	0,82

Figure 127: Verification Against FTB (BDK) *(cont.)*[203]

[202] (SCHNEIDER, 2012) – Section 3.3.2 Page 8.33

[203] (SCHNEIDER, 2012) – Section 3.3.2 Page 8.34

Bezogener Schlankheitsgrad $\bar{\lambda}_{LT}$ für Knicklinie:					Bezogener Schlankheitsgrad $\bar{\lambda}_{LT}$ für Knicklinie:				
a	b	c	d	χ_{LT}	a	b	c	d	χ_{LT}
0,40	0,40	0,40	0,40	**1,00**	1,35	1,26	1,16	1,02	**0,55**
0,45	0,43	0,42	0,42	**0,99**	1,37	1,27	1,18	1,04	**0,54**
0,49	0,46	0,44	0,43	**0,98**	1,38	1,29	1,20	1,06	**0,53**
0,52	0,48	0,46	0,44	**0,97**	1,39	1,31	1,21	1,08	**0,52**
0,56	0,51	0,48	0,45	**0,96**	1,41	1,33	1,23	1,09	**0,51**
0,59	0,53	0,49	0,46	**0,95**	1,42	1,35	1,25	1,11	**0,50**
0,63	0,55	0,51	0,48	**0,94**	1,43	1,37	1,27	1,13	**0,49**
0,66	0,58	0,53	0,49	**0,93**	1,45	1,39	1,29	1,15	**0,48**
0,69	0,60	0,55	0,50	**0,92**	1,46	1,41	1,31	1,17	**0,47**
0,71	0,62	0,56	0,51	**0,91**	1,48	1,43	1,34	1,19	**0,46**
0,74	0,64	0,58	0,52	**0,90**	1,50	1,45	1,36	1,22	**0,45**
0,77	0,66	0,60	0,54	**0,89**	1,51	1,48	1,38	1,24	**0,44**
0,79	0,68	0,61	0,55	**0,88**	1,53	1,50	1,40	1,26	**0,43**
0,81	0,70	0,63	0,56	**0,87**	1,55	1,52	1,43	1,28	**0,42**
0,84	0,72	0,65	0,57	**0,86**	1,57	1,55	1,45	1,31	**0,41**
0,86	0,74	0,67	0,59	**0,85**	1,59	1,57	1,48	1,33	**0,40**
0,88	0,76	0,68	0,60	**0,84**	1,61	1,60	1,50	1,36	**0,39**
0,90	0,78	0,70	0,61	**0,83**	1,63	1,62	1,53	1,39	**0,38**
0,92	0,80	0,71	0,63	**0,82**	1,65	1,65	1,56	1,41	**0,37**
0,94	0,82	0,73	0,64	**0,81**	1,67	1,67	1,59	1,44	**0,36**
0,95	0,84	0,75	0,65	**0,80**	1,70	1,70	1,62	1,47	**0,35**
0,97	0,85	0,76	0,66	**0,79**	1,72	1,72	1,65	1,50	**0,34**
0,99	0,87	0,78	0,68	**0,78**	1,75	1,75	1,68	1,53	**0,33**
1,01	0,89	0,79	0,69	**0,77**	1,77	1,77	1,71	1,57	**0,32**
1,02	0,90	0,81	0,70	**0,76**	1,80	1,80	1,75	1,60	**0,31**
1,04	0,92	0,83	0,72	**0,75**	1,83	1,83	1,78	1,64	**0,30**
1,05	0,94	0,84	0,73	**0,74**	1,86	1,86	1,82	1,67	**0,29**
1,07	0,96	0,86	0,75	**0,73**	1,89	1,89	1,86	1,71	**0,28**
1,09	0,97	0,87	0,76	**0,72**	1,93	1,93	1,90	1,76	**0,27**
1,10	0,99	0,89	0,77	**0,71**	1,97	1,97	1,95	1,80	**0,26**
1,12	1,00	0,91	0,79	**0,70**	2,01	2,01	1,99	1,85	**0,25**
1,13	1,02	0,92	0,80	**0,69**	2,05	2,05	2,04	1,89	**0,24**
1,15	1,04	0,94	0,82	**0,68**	2,09	2,09	2,09	1,95	**0,23**
1,16	1,05	0,95	0,83	**0,67**	2,14	2,14	2,14	2,00	**0,22**
1,18	1,07	0,97	0,85	**0,66**	2,19	2,19	2,19	2,06	**0,21**
1,20	1,09	0,99	0,86	**0,65**	2,24	2,24	2,24	2,12	**0,20**
1,21	1,10	1,00	0,88	**0,64**	2,30	2,30	2,30	2,19	**0,19**
1,23	1,12	1,02	0,89	**0,63**	2,36	2,36	2,36	2,27	**0,18**
1,24	1,14	1,04	0,91	**0,62**	2,43	2,43	2,43	2,34	**0,17**
1,26	1,15	1,05	0,92	**0,61**	2,51	2,51	2,51	2,43	**0,16**
1,28	1,17	1,07	0,94	**0,60**	2,59	2,59	2,59	2,53	**0,15**
1,29	1,19	1,09	0,95	**0,59**	2,68	2,68	2,68	2,63	**0,14**
1,31	1,20	1,10	0,97	**0,58**	2,78	2,78	2,78	2,75	**0,13**
1,32	1,22	1,12	0,99	**0,57**	2,89	2,89	2,89	2,88	**0,12**
1,34	1,24	1,14	1,00	**0,56**	3,02	3,02	3,02	3,02	**0,11**
					3,17	3,17	3,17	3,17	**0,10**

Table 85: Reduction Factor χ_{LT} for FTB (from α and λ_{LT})[204]

[204] (SCHNEIDER, 2012) – Table 8.35

For double-symmetric cross-sections, M_{cr} is:

$$M_{cr} = \varsigma * N_{cr,z} * \left[\sqrt{(c^2 + 0.25 * z_p^2)} + 0.5 * z_p\right]$$

With the Rotation Radius c:

$$c^2 = \frac{(I_w + 0.039 * l^2 * I_T)}{I_z}$$

The z_p is the distance from the point that the load would act upon the cross-section and its center of gravity and was determined as –h/2 since the loads acted upon the compression flange). ς represented the Moment factor depending on the Moment Line on the member (see Figure 127). As $N_{cr,z}$ is already known, M_{cr} could be calculated and subsequently λ_{LT} was determined. The Reduction Factor χ_{LT} could be then defined the same way for the Axial Force, using a table. Table 85 has the same function as Table 75, but for BDK instead of normal buckling. The next step was to modify the Reduction Factor χ_{LT} by dividing it by a factor f[205]:

$$f = 1 - 0.5 * (1 - k_c) * [1 - 2.0 * (\lambda_{LT} - 0.8)^2]$$

The Correction Factor k_c was also determined by Figure 127. The modified Reduction Factor $\chi_{LT,mod}$ was then calculated[206]:

$$\chi_{LT,mod} = \frac{\chi_{LT}}{f} \quad although \begin{cases} \chi_{LT,mod} \leq 1 \\ \chi_{LT,mod} \leq \frac{1}{\lambda_{LT}^2} \end{cases}$$

The parameters were then determined for the columns and the chords (see Table 86 and Table 87). The verification of FTB can be disregarded for the Chords, as reported by the DIN[207], by reason of the Moment Forces on the Chords not being greater than 16% of the M_{cr} of the Chords. As stated in the DIN Norm[208], on account of λ_{LT} for the column being more than $\lambda_{LT,0}$ = 0.40, and the M_{Ed} not being greater than 16% of the M_{cr}, the column is not readily secured against the FTB and must be verified. The reduction factor $\chi_{LT,mod}$ was calculated for the this verification and would also be used for the verification of the combination of forces (see Section 8.2.6).

[205] (DIN EN 1993-1-1, 2010) – Section 6.3.2.3 Page 69
[206] (DIN EN 1993-1-1, 2010) – Section 6.3.2.3 Page 69
[207] (DIN EN 1993-1-1, 2010) – Section 6.3.2.2 Page 68
[208] (DIN EN 1993-1-1, 2010) – Section 6.3.2.2 Page 68

ς:	1.12	[-]
$N_{cr,z}$:	1783.688	[kN]
c^2:	2419.101	[cm²]
z_p:	-22.25	[cm]
M_{cr}:	78514.47	[kNcm]
λ_{LT}:	0.947	[-]
χ_{LT}:	0.74	[-]
k_c:	0.94	[-]
f:	0.97129	[-]
$\chi_{LT,mod}$:	0.761873	[-]

Table 86: Parameters for M_{cr} for the Columns

ς:	1.77	[-]
$N_{cr,z}$:	735.779	[kN]
c^2:	168.6	[cm²]
z_p:	-10	[cm]
M_{cr}:	11608.99	[kNcm]
λ_{LT}:	0.809	[-]
χ_{LT}:	0.82	[-]
k_c:	0.75188	[-]
f:	0.875958	[-]
$\chi_{LT,mod}$:	0.936118	[-]

Table 87: Parameters for the M_{cr} for the Chords

M_{Edy}:	-20705	[kNcm]
$M_{b,Rd}$:	48731.5	
$M_{Edy}/M_{b,Rd}$:	0.294	ok

Table 88: Verification Against BDK on the Columns

Therefore, the verification for FTB is complete.

8.2.6 Verification of the Combination of Forces

Similar to the Brazilian method, the Lower Chords have a tension force greater than the compression force, so the verification for the combination of forces will use the tension force for the Lower Chords. The Columns and the Upper Chords will use the compression force. The concept of the equations for the verification of the combination of forces was the same, but different factors were used[209]:

$$\frac{N_{Ed}}{\frac{\chi_y * N_{Rk}}{\gamma_{M1}}} + k_{yy} * \frac{M_{y,Ed} + \Delta M_{y,Ed}}{\chi_{LT} * \frac{M_{y,Rk}}{\gamma_{M1}}} + k_{yz} * \frac{M_{z,Ed} + \Delta M_{z,Ed}}{\frac{M_{z,Rk}}{\gamma_{M1}}} \leq 1$$

$$\frac{N_{Ed}}{\frac{\chi_z * N_{Rk}}{\gamma_{M1}}} + k_{zy} * \frac{M_{y,Ed} + \Delta M_{y,Ed}}{\chi_{LT} * \frac{M_{y,Rk}}{\gamma_{M1}}} + k_{zz} * \frac{M_{z,Ed} + \Delta M_{z,Ed}}{\frac{M_{z,Rk}}{\gamma_{M1}}} \leq 1$$

Klasse	1	2	3	4
A_i	A	A	A	A_{eff}
W_y	$W_{pl,y}$	$W_{pl,y}$	$W_{el,y}$	$W_{eff,y}$
W_z	$W_{pl,z}$	$W_{pl,z}$	$W_{el,z}$	$W_{eff,z}$
$\Delta M_{y,Ed}$	0	0	0	$e_{N,y} N_{Ed}$
$\Delta M_{z,Ed}$	0	0	0	$e_{N,z} N_{Ed}$

Table 89: Parameters for the Verification of Combination of Forces[210]

$\Delta M_{y,Ed}$ and $\Delta M_{y,Ed}$ were considered as 0 (see Table 89). All Resistant Forces were already calculated in Section 8.2.3 and Section 8.2.4. The interaction factors k_{yy}, k_{yz}, k_{zy}, k_{zz}, were the last parameters to be determined. Fortunately, as stated in Schneider[211] (see Table 90), for torsionally flexible ("*verdrehweich*") cross-sections (as I-Profiles), these parameters can be easily found by the verification of the Axial Force:

[209] (DIN EN 1993-1-1, 2010) – Section 6.3.3 Page 72
[210] (DIN EN 1993-1-1, 2010) – Table 6.7 Page 72
[211] (SCHNEIDER, 2012) – Table 8.40b

$\frac{N_{Ed}}{\chi_{y/z} \cdot N_{Rk}/\gamma_{M1}}$ [1]	QK 1 und 2			
	k_{yy}	k_{yz}	k_{zy} [2]	k_{zz}
0,0	1,000	0,600	1,000	1,000
0,1	1,080	0,684	0,987	1,140
0,2	1,160	0,768	0,973	1,280
0,3	1,240	0,852	0,960	1,420
0,4	1,320	0,936	0,947	1,560
0,5	1,400	1,020	0,933	1,700
0,6	1,480	1,104	0,920	1,840
0,7	1,560	1,188	0,907	1,980
0,8	1,640	1,272	0,893	2,120
0,9	1,720	1,356	0,880	2,260
1,0	1,800	1,440	0,867	2,400

[1] Für die Ermittlung von k_{yy} ist χ_y einzusetzen, sonst χ_z.

[2] Gilt nur für $\bar{\lambda}_z \geq 1{,}0$, sonst $k_{zy} = 1{,}0$.

Table 90: Simplified Interaction Factor for the Verification of the Combination of Forces[212]

After interpolating the values, the results were given in Table 91:

Column		Upper Chord		Lower Chord	
k_{yy}:	1.09419	k_{yy}:	1.15136	k_{yy}:	1.12776
k_{yz}:	0.94130	k_{yz}:	0.79424	k_{yz}:	0.76396
k_{zy}:	0.94618	k_{zy}:	1.00000	k_{zy}:	1.00000
k_{zz}:	1.56883	k_{zz}:	1.32373	k_{zz}:	1.27326

Table 91: Simplified Interaction Factors after Interpolation

[212] (SCHNEIDER, 2012) – Table 8.40b

And the verifications obtained:

	[kN]		[kNcm]		[kNcm]
N_{Ed}:	-348.3	M_{Edy}:	-20705.0	M_{Edz}:	-3680.0
N_{Rd}:	597.8	M_{Rdy}:	63962.7	M_{Rdz}:	13682.1
	k_{yy} & k_{yz}:	**1.301**	<= 1.0	!	
	k_{zy} & k_{zz}:	**1.407**	<= 1.0	!	

Table 92: Verification of the Combination of Forces on the Columns

	[kN]		[kNcm]		[kNcm]
N_{Ed}:	-174.3	M_{Edy}:	-547.0	M_{Edz}:	100.0
N_{Rd}:	455.9	M_{Rdy}:	6900.0	M_{Rdz}:	1399.1
	k_{yy} & k_{yz}:	**0.537**	<= 1.0	ok	
	k_{zy} & k_{zz}:	**0.562**	<= 1.0	ok	

Table 93: Verification of the Combination of Forces on the Upper Chords

	[kN]		[kNcm]		[kNcm]
N_{Ed}:	157.1	M_{Edy}:	-525.0	M_{Edz}:	87.0
N_{Rd}:	964.4	M_{Rdy}:	6900.0	M_{Rdz}:	1399.1
	k_{yy} & k_{yz}:	**0.302**	<= 1.0	ok	
	k_{zy} & k_{zz}:	**0.323**	<= 1.0	ok	

Table 94: Verification of the Combination of Forces on the Lower Chords

Similar to the Brazilian norm, the verification for the Upper and Lower Chords was satisfied. For the Column, the ratio was 30.1% and 40.7% above the limit. Since this analysis used the maximum values of each force, it is possible that these forces do not act upon the same location (for example: the maximum moment in Y acts upon the 9th column while the maximum compression is located on the 2nd column). Therefore, it is possible that all the columns are secure for this verification. Nonetheless, a deeper analysis was undertaken.

The maximum values for the most compressed column (2nd Column on the Right) at its most aggressive location (bottom) were:

	[kN]		[kNcm]		[kNcm]
N_{Ed}:	-348.3	M_{Edy}:	-20705.0	M_{Edz}:	0.0
N_{Rd}:	597.8	M_{Rdy}:	63962.7	M_{Rdz}:	13682.1
	k_{yy} & k_{yz}:	**1.048**	<= 1.0	!	
	k_{zy} & k_{zz}:	**0.985**	<= 1.0	ok	

Table 95: Verification of the Combination of Forces on the Column (Bottom of the 2nd on the Right) – Max M_{Edy}

In fact, M_{Edz} was always equal to 0 at its most aggressive location for all the columns (bottom). By the results in Table 95, the most compressed column was verified for one equation but not for the other one. This meant that it was still above the stress limit ratio, by 4.8%. In this case, it is necessary to either make adjustments to the column (if already built) or modify the cross-section.

When the M_{Edz} was maximum (x = 2.600m from the bottom at the 1st Left Column), the M_{Edy} was -2804 kNcm and the Normal Force N was -106.3 kN (see Figure 128). Table 96 shows that the verification of this combination is secured.

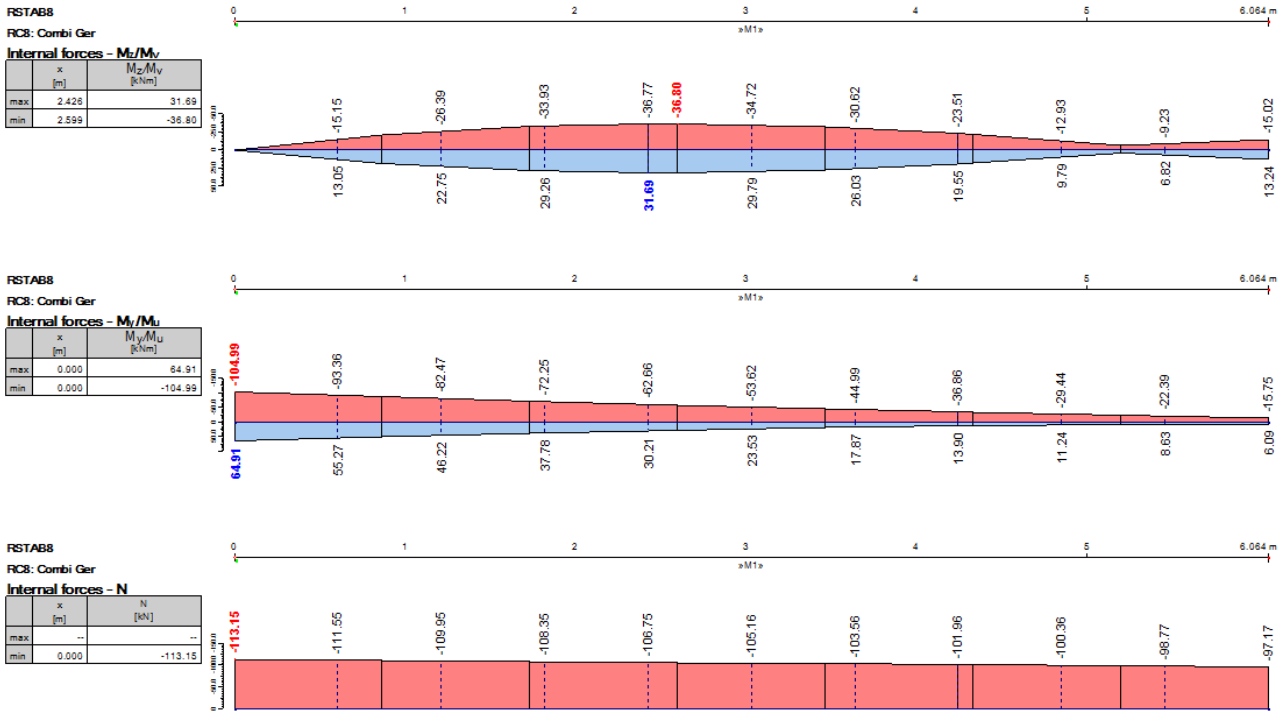

Figure 128: Results of the Internal Forces of Member M1 (1st Column on the Left) – Max M_{Edz} Location

[kN]		[kNcm]		[kNcm]	
N_{Ed}:	-106.3	M_{Edy}:	-2804.0	M_{Edz}:	-3680.0
N_{Rd}:	597.8	M_{Rdy}:	63962.7	M_{Rdz}:	13682.1
	k_{yy} & k_{yz}:	**0.494**	<= 1.0	ok	
	k_{zy} & k_{zz}:	**0.654**	<= 1.0	ok	

Table 96: Verification of the Combination of Forces on the Column (at x = 2.6m from the Ground of the 1st on the Left) - Max M_{Edz}

Thus, the columns and the chords were all secured.

9. COMPARISON AND ANALYSIS OF RESULTS

A comparison between both halls and both norms can be very must be proceeded with caution while analyzing the data beforehand. Many assumptions must be taken and other normally used premises were disregarded (for example: Snow Loads in Brazil). These were improvised as to provide a better comparison.

9.1 Location

The location is the most obvious difference between the halls. The Brazilian hall would be at the location of the original project (São Luís, Maranhão – northeast of Brazil) while the German location would be in Darmstadt, at the mid-southwest of Germany. São Luís is typically hot and humid (average annual temperature of 27°C and annual rainfall of 1896mm)[213], whereas Darmstadt may have mild to warmer temperatures during summer and mild to cold during winter, but not extreme cold (average annual temperature of 9.5°C and annual rainfall of 653mm), but its climate is typically dry (in comparison to São Luís)[214]. This difference is quite remarkable, however, since the location of the original project is São Luís, where average temperatures vary about 1.4°C (although Darmstadt's temperatures may vary 18.6°C), variations of temperatures for the calculations were disregarded. This led to the neglect of temperature variations and consequently of the occurrence of internal forces that could appear from rigid supports and the temperature oscillation. In order to better compare the halls, this was found plausible.

In addition, the terrain categorization was the same, being an industrial region with few obstacles (information used to determine the Wind Loads – comparison in Section 9.4.4) and Darmstadt is a city that may snow, in contrast to São Luís, which never had snow (further explanation in Section 9.4.2).

9.2 Material

The material used for both was the steel. For each norm, 2 different types of steel were used (see Section 2.6):

- Brazilian:
  - ASTM A-36 (MR250 used in RSTAB)
  - ASTM A-572 (G-35 used in RSTAB)

- German:
  - S235
  - S355

[213] (Climate-Data Org 2), (Norwegian Metereological Institute and Norwegian Broadcasting Corporation 2) and (World Weather Online 2) – (01.02.2017)
[214] (Climate-Data Org 1), (Norwegian Metereological Institute and Norwegian Broadcasting Corporation 1) and (World Weather Online 1) – (01.02.2017)

The main differences were the yield and tensile strengths (or resistance). Almost all cross-sections used the MR250 (or S235) and their difference in yield strength was of 1.5kN/cm² (25 and 23.5, respectively). The tensile resistance difference was 4 kN/cm² (40 and 36, respectively). The only cross-sections with the G-35 (or S355) were the chords and their yield resistance was almost the same (34.5 and 35.5 kN/cm²), although their tensile strength had a difference of 2 kN/cm² (45 and 47, respectively).

The Modulus of Elasticity and the Shear Modulus were also different. The Brazilian materials had the Elasticity Modulus of 20,000 kN/cm² and the German had 21,000 kN/cm², having a difference of 1000 kN/cm². The Brazilian Shear Modulus was 7700 kN/cm² while the German was 8100 kN/cm², having a difference of 400 kN/cm².

The density of the materials were the same, ρ = 7850 kg/m³, and this was crucial, given that this could greatly affect one of the most important aspects of a steel construction project: the price. The next Section explains the topics weight and price.

9.3 Self-Weight

In the construction of a steel hall, material expenses can make up to 40% of the total budget. For this reason, the choice of the cross-sections that will be used is of extreme importance, since the viability of any venture usually depends mostly on its budget. In other words, the less material used (less weight), the lower will be the cost of steel needed (in kilograms), offering a better price for the project and thus making it a favorable alternative. In view of this matter, the Self-Weight of both structures were calculated in the software and Figure 129 (Brazilian) and Figure 130 (German) show the basic information of the Frame and Figure 131 (Brazilian) and Figure 132 (German) show the basic information from the whole constructions.

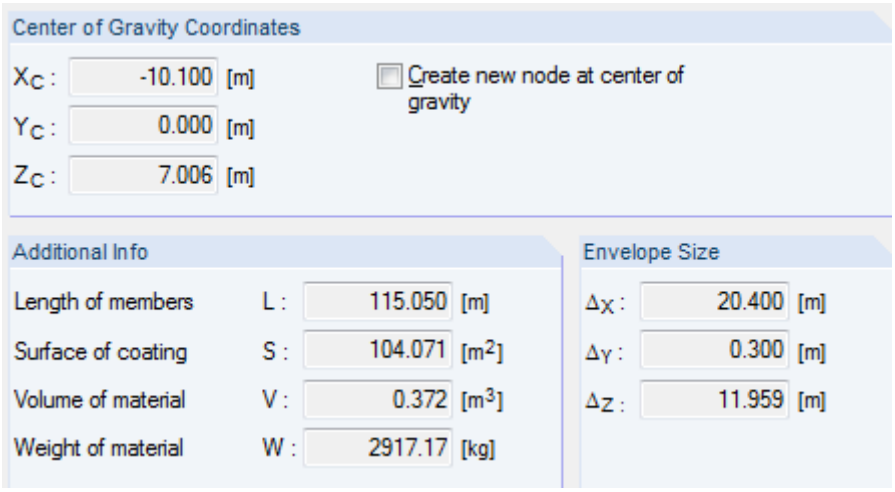

Figure 129: Basic Information of the Frame (Brazilian)

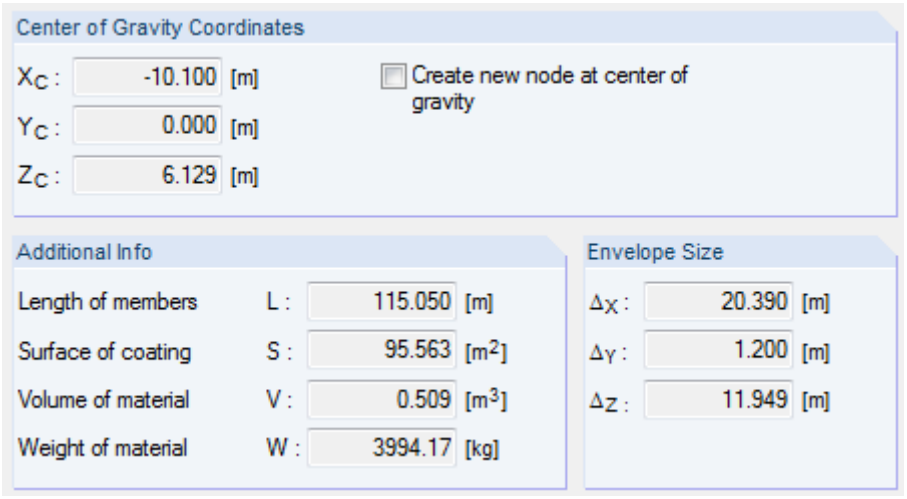

Figure 130: Basic Information of the Frame (German)

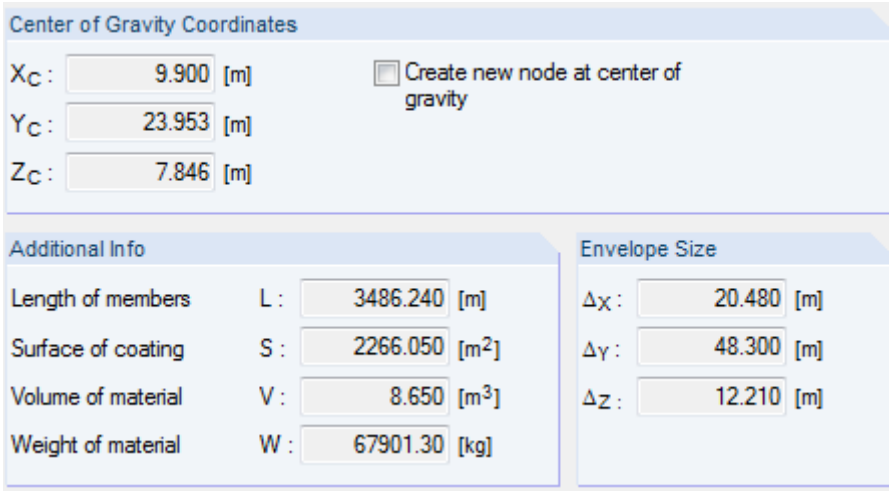

Figure 131: Basic Information of the Hall (Brazilian)

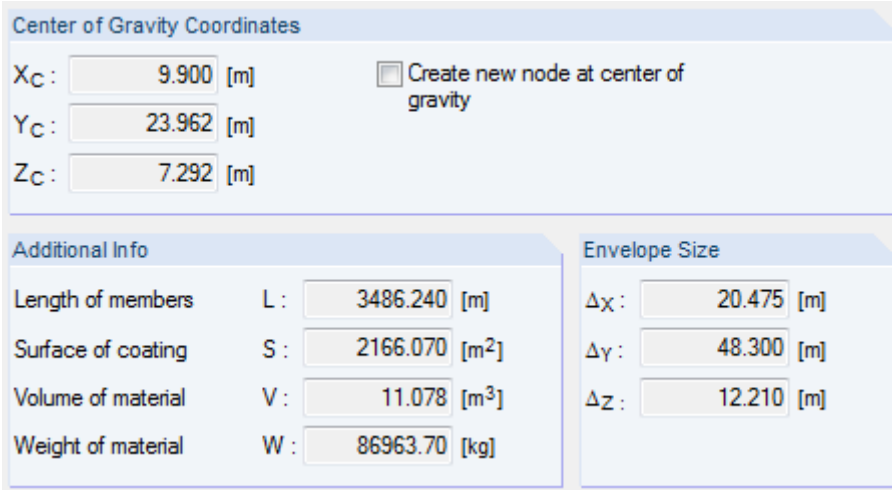

Figure 132: Basic Information of the Hall (German)

	FRAMES		HALL	
	Volume [m³]	Weight [kg]	Volume [m³]	Weight [kg]
BRA	0.372	2917.17	8650	67901.3
GER	0.509	3994.17	11078	86963.7
Difference	0.137	1077	2428	19062.4

Table 97: Volume and Weight (in kgs) for the Frames and the Halls

Comparing the frames (see Table 97), the Brazilian Frame and Hall had less volumes of steel and thus less weight, having a slight advantage over the German structure. This meant that the Brazilian hall had a cheaper solution, taking into account the cross-sections selected. This comparison is solely based on the choice of the cross-sections available in the software and how they were similar to the profiles of the original structure. In most occasions, there was no profile exactly the same as the original, in which this case a very similar cross-section was chosen. The only 2 cross-sections exactly the same for both halls (chosen from the same Norm) were the purlin – C 6x8.2 (AISC 14) – and the purlin bracings – RB 1/2 (AISC) – since both, NBR and DIN, did not have a similar cross-section in RSTAB.

The project did not evaluate if an optimization of the cross-sections would lead to a different outcome. An optimization would mean to modify the profiles and choose smaller ones to the point that they would be closer to or even reach the stress and design ratio limit. Table 43 indicates that not even half of the 35 different types of members reach the 0.20 ratio. This occurred because these profiles originated from a pre-existing project, and the client's demands included the calculations of larger security factors and overloads, being very conservative.

9.4 Loads

9.4.1 Additional Dead Load

The Additional Dead Loads were different, on account of the roof covering having different purposes. In Brazil, it is usual for roof coverings to be very light, only having a metal sheet (bedding), while in Germany, due to the cold weather, it is usual to have other layers of coating like insulation, sealing and barriers (vapor). In view of this, it is noticeable that the German Additional Dead Load would be greater. As calculated in Section 3.1.2, the load was 0.40 kN/m² and the Brazilian Additional Dead Load was 0.10 kN/m² (Section 3.2.2). The difference of 0.30 kN/m² accounted for these other layers.

9.4.2 Live and Snow Loads

As explained in Sections 3.1.3, 3.1.5, 3.2.3 and 3.2.5, the Snow Loads were not considered in order to maintain a coherent comparison, seeing that São Luís does not have snow. In its place, the Live Loads ("*Ações Acidentais*") were applied as a plausible substitute for the Snow Load for the German Hall. The Live Load was defined as 0.50 kN/m² (see Section 3.2.3), double the minimum load of 0.25 kN/m², and insomuch as to design a conservative project.

9.4.3 Equivalent Forces

The Equivalent Forces, calculated in Section 5.6.5, also had their differences. The Brazilian Equivalent Force admitted that the Force would be 0.3% of all the gravitational applied to the columns. The German Force inspected not only the vertical force, but also the angle of possible imperfection and some other factors. In addition, the German Force was applied on top and on the bottom of the column, whereas the Brazilian only on the top. In the end, the Brazilian had an Equivalent Force of 1.59 kN and the German had 1.224 kN. None of these Forces were necessary, since both were classified as being able to be calculated only by the 1st Order Theory Analysis, but were nevertheless calculated and applied to the structures. Since they both had similar load values, this was found acceptable.

9.4.4 Wind Loads

The Wind Loads had similar approaches, calculating the wind pressure by evaluating the terrain and multiplying some factors with the wind speed. The terrain category was the same (Category III), an industrial region with few obstacles. The basic wind speed was given from the norms by different methods (although both were from measurements at 10m high and at a plain field), having the Brazilian measure a burst of wind over 3 seconds which will be overcome in average only once in 50 years, and the German calculate empirically the middle values of the wind in a period of 10 minutes, with a probability of exceeding it in a year of 0.02.

After the Wind Speeds are defined, they were multiplied to find the Wind Pressures. While the German Norm determined a basic wind pressure that was then used in a formula according to the terrain category, the Brazilian Norm used 3 different factors to find the velocity of the wind. The first was the topographic S_1 factor, the second was the terrain roughness S_2 factor (roughness of the terrain and the dimensions of the building) and the third was the statistical S_3 factor. These were multiplied to the Wind Speed to calculate the characteristic velocity and then use this value in a formula to find the Wind Pressure. Despite the methods to calculate the Wind Pressure being distinct, the concept of height of the building, wind speed, and terrain type were all used. Also, there was a difference in their Wind Speeds: German was 22.5m/s while the Brazilian was 30m/s. Albeit lower, the German Wind Speed had a higher Wind Pressure (0.57 kN/m² against 0.49kN/m²). Since the program calculated the Wind Pressure at 0.53kN/m², this value was used since it was even closer to the Brazilian one and would provide a better comparison.

The hall is double-symmetric, meaning that it was valid to consider only 2 directions for the wind. These directions (or angle of the wind θ) were the same, acting on the + X-Direction (90°) or + Y-Direction (0°). Although the Figures from the German Norm indicate the angle of wind θ = 0° to act upon the longer side, it was considered that both should have the same standardization, to avoid possible confusion.

For both norms, an external Wind Pressure and an internal Wind Pressure were calculated. For the external, similar methods were done, calculating areas that would have different coefficients for the walls and for the roof. Despite being very alike, the Brazilian method was marginally more simple. The German method depended on the quotient of the dimensions of the hall to interpolate and calculate the size of the areas and values of the external pressure coefficients – the Brazilian seldom depended on interpolation. Moreover, there were more wind cases of study according to the German Norm – 6 against 4 (Brazilian).

For the internal coefficients, the German was once more somewhat more complicated. The Brazilian appointed an internal pressure coefficient for when there were 4 equal permeable sides while the German Norm demanded a calculation for the coefficient depending on the areas of opening and total areas of the walls.

It is complicated to make a comparison for the value of the coefficients, since there are many combinations possible to compare. In general, the external coefficients for the Walls at Wind 0° and 90° were quite similar. For the roof, at Wind 0°, the F and G areas are much bigger, while the H is almost the same and I is quite bigger (for German). At Wind 90°, the comparisons vary a lot, having in general the first "+" making FGH much bigger (for Brazilian), the second "+" making IJ also bigger (for Brazilian), the first "-" making F bigger, G almost the same and H smaller (for German) and the second "-" making IJ close to the same value.

The German internal coefficients were calculated simply appointing as -0.3 for the 0° and 0.1366 for the 90°. The Brazilian internal coefficients were 0 and -0.3, whichever most aggressive, but to both, 0° and 90°.

9.4.5 Crane Loads

As the Wind Loads, the concept of the Crane Loads was similar, having vertical and horizontal loads (longitudinal and transversal) for both. However, the Brazilian method was less complicated, having these loads being defined by simple calculations. Meanwhile, the German method used oscillation coefficients and different load cases (LG – Load Groups) to verify the runway girders against many possible outcomes and situations. This in turn leads to a deeper inspection and ergo a possible better security.

As there were two different Load Groups for the German method (LG1 and LG5), the modeling of the runway girder had 2 different cases while the Brazilian had only 1. Each case had its own different loads applied on the runway girder. On the 3D model, since there were 3 different locations for the crane wheels, there were 9 possible crane load cases in total (6 for the German and 3 for the Brazilian).

9.5 Load Combinations

9.5.1 ULS

For both Norms, the ULS was calculated according to the Normal category. The Load Combinations were calculated and both had coefficients of variability (γ_i) and coefficients of simultaneity (Ψ_i). The Norms point out that a main action must be taken into consideration and the other secondary actions must be reduced by the Ψ_0 coefficient. They do differ, however, on the values of these coefficients:

ULS		SW	Live	Wind	CR
γ_i	BRA	1.25	1.50	1.40	1.50
	GER	1.35	1.50	1.50	1.50
Ψ_0	BRA	0.00	0.80	0.60	1.00
	GER	0.00	0.80	0.60	0.70

Table 98: ULS Coefficients

The Permanent actions would have a lower coefficient on the Brazilian hall, as well as the Wind when it was not the main action. On the contrary, the Crane Actions would be larger when it was a secondary action. The Live Load Actions would remain with the same coefficient at all times (being the main or secondary action).

For the 4th combination of the Brazilian norm, the coefficients of the Self-Weight changed from 1.25 to 1.0 (the German norm does not account for this combination, thus, it was not considered) and the Live Loads are not considered since it would aid in the stability of the structure. In this case, this combination was found irrelevant, as the other 3 combinations would create more harmful forces on the hall. Nevertheless, it is a combination that must always be considered.

As mentioned in Section 9.4.4 and Section 9.4.5, there were 6 different Wind Load cases for the German and 4 for the Brazilian and 6 different Crane cases for the German and 3 for the Brazilian.

In order to classify if the 2nd Order Theory (Global) is necessary, both have formulas to estimate its effect on the structure. The Brazilian Norm uses the formula to determine B_2 (see Section 6.1.2.1) and the German uses the formula for α_{cr} (see Section 6.2.2.1). All of them use the parameters: height of the building, horizontal forces, vertical forces and the horizontal displacement. The Brazilian Norm also considers an Adjustment Coefficient:

$$B_2 = \frac{1}{1 - \frac{1}{R_S} * \frac{\Delta_h}{h} * \frac{\Sigma N_{Sd}}{\Sigma H_{Sd}}} \leq 1.1$$

$$\alpha_{cr} = \left(\frac{H_{Ed}}{V_{Ed}}\right) * \left(\frac{h}{\delta_{H,Ed}}\right) \geq 10$$

Nevertheless, both formulas are practically the same formula, written in different ways. Rewritten (for better comprehension), they would be:

$$B_2\ Formula\colon \frac{1}{R_S} * \frac{\Delta_h}{h} * \frac{\Sigma N_{Sd}}{\Sigma H_{Sd}} \leq 0.0909$$

$$\alpha_{cr}\ Formula\colon \left(\frac{V_{Ed}}{H_{Ed}}\right) * \left(\frac{\delta_{H,Ed}}{h}\right) \leq 0.10$$

When B_2 is less than 1.1, it is considered to be of small displacement and with the other requirements calculated in Section 6.1.2.1, the Global 2nd Order Theory could be disregarded[215]. Likewise, when α_{cr} is larger than 10, the 2nd Order Theory could be neglected[216]. Yet, the Brazilian method goes further and calculates a B_1 factor that considers a local 2nd Order effect (for each member) – calculated in Section 6.1.2.1 – which increased the Moments of every member in 1.053.

9.5.2 SLS

For both Norms, the SLS was calculated according to the Quasi-Permanent category. The Load Combinations were calculated and, unlike the ULS, both lacked the coefficients of variability (γ_i) but included the coefficients of simultaneity (Ψ_i). Furthermore, the Norms state that the Wind coefficient can be considered as 0. They do differ, once again, on the values of these coefficients (the Permanent coefficient is not necessary, because the permanent load would always be in the formula):

SLS		SW	Acc	Wind	CR
Ψ_2	**BRA**	-	0.60	0.00	0.50
	GER	-	0.50	0.00	0.30

Table 99: SLS Coefficients

[215] (ABNT NBR 8800, 2008) – Section 4.9.7.1.4 Page 28
[216] (SCHNEIDER, 2012) – Section 3.1 Page 8.23

9.6 FTB and Verifications

Both Norms consider the FTB. They do, however, have different approaches towards the determination of the members' security. Both classify the cross-sections as a first step, according to their b/t or h/t ratios (which is an indicator of a local buckling). Later, however, the Brazilian Norm appoints, after the classification, a reduction factor that would later be used for the calculations of the Resistant Forces (Axial and Moment). The German does not designate a reduction factor at first: it rather groups the cross-sections (QK 1 to 4) and later uses different formulas for its calculations depending on the cross-section class. Then, the critical buckling load could be calculated and the formula for the N_{cr} (or N_{ki}) was the same (Section 8.2.2)[217].

Determining the slenderness and the reduction factor of the member were the next steps in order to calculate the Resistant Axial Force. Both have different formulas and while the Brazilian reduction factor was calculated, the German value was taken from a ready-made Table (Table 75) – but could also have been calculated. Finally, the Resistant Compression Force could be determined (Section 8.1.3 and Section 8.2.3). Also, the Resistant Tension Force was calculated and the formulas were the same, but the values for the stability factors were different. As shown in Section 8.2.3, the security coefficient against instability γ_{a1} (or γ_{M0}) was 1.10 for the Brazilian Norm[218] and 1.00 for the German[219]. The security coefficient for rupture γ_{a2} (or γ_{M2}) was 1.35 for the Brazilian Norm and 1.25 for the German. In the end, all 3 types of members were secured against Axial Forces (Compression for Columns and Upper Chords and Tension for Lower Chords).

To calculate the Moment Resistant Forces, the formulas were very different, depending on the slenderness coefficients for the Brazilian Norm (Table 57). A very interesting fact: the Brazilian Norm already calculates the Moment Resistant Force for the FTB (globally and locally – on the Flange or Web) while the German Norm usually calculates the Moment Resistance and verifies the member for single-axis bending and then analyzes if the member is secure against the FTB (exactly what occurred for the columns and chords in this project – see Section 8.2.4 and 8.2.5). Both structures were secured against FTB for the columns and the chords.

All members must satisfy the condition of the stress ratio limit. The verification of combined forces secures the members from exceeding this limit. Both Norms calculate the combined stresses from Normal and Moment Forces (in Y [strong] and Z [weak] axis for the German Norm or X [strong] and Y [weak] axis for the Brazilian Norm). The Brazilian Norm calculates this stress by 2 simple formulas, which depends if the applied Normal Force is greater or less than 20% of the Normal Resistant Force. The German Norm had also 2 different formulas, but depended on the interaction factors k_{yy}, k_{yz}, k_{zy}, and k_{zz}. These had to be calculated by interpolation (by the simplified method with Table 90) and only then could the verification be made.

By these new calculations (which RSTAB could not verify correctly – for explanation see Chapter 8 VERIFICATIONS – FTB AND COMBINATIONS), the column did not satisfy the limit and exceeded in 9.3% for the NBR and 30.1% and 40.7% for the DIN, while the chords were proven satisfactory. In this case, a deeper inspection took place. During the verification, only the maximum values of the forces of all the members of

[217] Obs: since the Elasticity Modulus was not the same, the critical buckling load for the halls were different, except for the column, which was calculated by the software STRAP
[218] (ABNT NBR 8800, 2008) – Table 3 Page 23
[219] (DIN EN 1993-1-1, 2010) – Section 6.1 Page 49

each type (columns, upper chords or lower chords) were used. There was a great probability that the highest values were not occurring at the same location (for example, the maximum Moment in Y and the maximum Moment in Z occurring in the same column at the same spot). And by searching thoroughly, it was discovered that the 1st column on the left had the greatest Moment in Z-axis while the greatest compression and Moment in Y-axis occurred in other columns. After new verifications on the column that had the largest Moment in Y-axis and the column that had the largest Moment in Z-axis, all Brazilian columns were secured against any trespass of the stress ratio limit while the German was still unsatisfactory. For these new verifications, the Brazilian hall had a stress ratio of 83.5% while the German had 104.8% (an excess of 4.8%) and 98.5% for the column with the most aggressive Moment in Y-axis (and also the largest Normal Force) – see Table 68 and Table 69. For the new verification of the column with the most aggressive Moment in Z-axis was the 1st on the left, having 46.3% for the NBR and 49.4% and 65.4% for the DIN (see Table 95 and Table 96). As none of the stress ratios surpassed the limit of 100%, these columns (Moment in Z-axis) were classified as secured.

While all chords were secured against FTB, only the Brazilian columns were secured – the German column exceeded the verification limit by 4.8%.

9.7 Results

According to the results of the software for the EC-3, NBR and the ASD (STEEL), the only type of member that had exceeded the ratios was the purlin. Table 43 displays the Design and Stress Ratios for each verification.

Analyzing the design ratio results, it is possible to notice that for the German hall, the design ratios were normally higher than the Brazilian hall. In 17 cases the German was higher, for 12 times was the Brazilian higher and in 5 cases they were the same.

From all the 34 different types of members, 3 were over the limit (purlin central, left and right – excluding the outer most purlins) 20 were practically the same, 5 exactly the same (vertical bracing superior in V, lateral truss, horizontal superior bracings, vertical bracings B-B Cut and Truss D5) and 6 somewhat different: upper column, upper and lower chords (lateral truss), outermost purlins on the left, upper chords of runway girder truss system on the left, truss system on the left of the runway girder and D1. Among these, only 2 were considered very different and above the ratio of 0.70: the upper column and the D1 truss.

For the upper columns, the NBR had a ratio of 0.43 while the EC-3 had 0.76 (ASD was 0.57 and 0.78 for Brazilian and German, respectively). The D1 truss had a 0.47 for NBR and 0.73 for the EC-3. Although these types of members had differences, none of them surpassed the limit.

The left and right purlins (excluding the outer) were the members that had the worst ratios. The NBR had a 1.09 comparing to a 2.28 of the EC-3. And the ASD (Brazilian) was 1.19 against a 1.30 for the ASD (German). The central purlins also had their difference: NBR had 0.76, being under the limit, while the EC-3

had 2.35 (the largest ratio from the total results). And for the ASD, both were under the limit, with the Brazilian having 0.67 and the German having 0.77.

The fact that the outermost purlins, left and right, did not exceed their design ratios, may be explained because the wind loads on them were much less than on the other purlins. Also, it is possible to affirm that since the wind pressure of the DIN was higher than of the NBR, this could greatly affect the results on the purlins. As seen in Section 9.4.4, it was very complicated to compare the external and internal pressure coefficients between the halls. Nonetheless, in general, it is possible to say that the German Wind Loads had stronger effect on the purlins, not only do to the design and stress ratios, but because the c_{pe} for the most aggressive German Wind Load is greater than the c_{pe} for the Brazilian Wind Load, and the software always takes into account the most aggressive/stressed member. Also, the difference between the values of Additional Dead Loads is of great importance. The German Load is 4 times larger than the Brazilian, by reason of its many other layers.

These results were found to be very similar and this came to no surprise. Even though there were many differences on the methods of reaching the results, some improvisations were made (Snow, Temperature etc) in order to achieve a better comparison.

10. CONCLUSION

This project sought to analyze an existing industrial steel hall with a crane. Since the structure already existed, some premises were to be followed. During this evaluation, the software RSTAB was utilized. In the scope, an investigation to compare and analyze the differences between the dimensioning methods between the Brazilian Norm NBR and the German Norm DIN EN would also occur. Although the German code considers the snow loads to be very important in the calculations, the Brazilian code does not and therefore, the snow loads were not considered, due to the fact that a better comparison between the two norms could be achieved. It was substituted by the Live Load, which could be close to the actual value of snow for the region of Darmstadt, but if applied, could change the results greatly.

The research of how the Wind Loads affected the structure was by far the most important from the ones observed. By most important, it was meant that the other loads were much more similar between the Norms and the most different was the Wind Load. Although the Additional Dead Loads had different values, these loads were affecting exactly the same place with the same area (on top of the purlins). In another definition, the most important load could also be the Crane Load, in view of its much greater force and its effect on the structure.

It was interesting to notice how different norms having different formulas, methods of calculations and different premises converge to the similar results. Despite the similarities in the results, one is able to perceive that the Norms cannot be actually used for the other country, since specific regulations (like snow, temperature variation and earthquake) must be strictly followed for each location. This was only acceptable for the project, in reason of better comparison, albeit it must not be done.

A very interesting observation to be made is how the angle between the columns and the roof has the power to substantially modify the effect that the wind has on the structure, especially for the German Norm.

Another observation to be made is on the German Column. The beam did not pass the verification of stress from combined forces and imagining the hall is already built, a possible solution for this problem would be to first identify the column(s) that do(es) not satisfy the stress limit and then modify them by making them stronger. This modification may be done by welding some plates, making it stiffer. In case the project is still in its conception phase, one may simply just change the cross-section of the column or do the same as the mentioned before.

At first glance, one may perceive a comparison between the structures and the norms as trivial, but a deeper analysis of the results may come as a surprise. By only looking at the self-weight of the German hall (or the cross-sections), and presuming that the loads would be fairly equal, one could come to a false conclusion and presume that the German hall would be stronger. Despite the fact that German cross-sections were frequently slightly bigger in their widths, one must not forget that the materials have different yield strengths (with a difference of 1.5 kN/cm^2). In fact, the German design and stress ratios were generally larger than the Brazilian. Most importantly, a direction to an answer to the central question of the study appears: yes, the Norms are different, but how much different? Results show that the German hall could not withstand the actions upon it whilst the Brazilian did (excluding the purlins). And although the Wind Loads may be the most influential factor for this failure, it is not yet possible to conclude with such certainty. Thus, a question still remains: what was the variable that most influenced the failure of the

German hall and the difference between the structures? Possible answers would be: the Wind Load, the Additional Dead Load (difference of 0.30 kN/m²), the cross-sections or the material (type of steel).

The best comparison would have been to apply different loads according exactly to each Norm (as to compare the method of loads) or to apply the exact same loads on different types of cross-sections (with the same material). Since the research had a goal to compare halls that would suppose that each one would be located in its own country, this process of exact comparison was not achieved.

In addition, a point to be noticed is the fact that there was no optimization done to the members. The analysis and comparison were made but the hall was not optimized. This meant that during the verifications, the member's sizes would be reduced when possible (meaning members with high safety margin would be resized), but the stresses would be limited to avoid fatigue concerns, promoting the so called optimization of the structure. The optimization consists of finding the best steel arrangement of the steel hall by searching for the cheapest solution. In this case, the definition of cheapest means that the profiles should be modified to discover an arrangement that would use the lightest profiles but that would result in a stable construction. Since the material steel is expensive, the less a profile weighs, the lower the cost of the profile. In this sense, the concept of optimization could be simplified to the tonnage of the structure (the expenses from material purchase reach 30%-40% of the total expenses for the construction of a steel hall). Although there are many factors that influence the cost of a steel hall construction, for example manufacturing, assembly, personnel costs, and electricity, the main focus of this optimization would be the total weight of the members. Since the hall was deliberately over-dimensioned, it is clear that an optimization would be necessary. The optimization of a structure is always the slowest process and the one that requires the most effort.

As mentioned before, the Brazilian Norm has, at some points, less complicated calculations to be made. However, this does not reflect on the strictness of the Norm, but it may, indeed, mean that the German Norm can be more specific sometimes, as recalled in Section 9.4.5, and may even be slightly more secure. This statement causes curiosity and brings a very interesting topic for a debate and for another research.

In conclusion, this thesis allows one to have an overview of the basics of the dimensioning and analysis of an industrial steel hall according to Norms of 2 different countries, located in 2 different continents. Starting from the inspection of the original hall, to the analysis of the loads that would fall upon the structures to the verification and comparison of results. A critical analysis regarding the norms and their comparison was developed and also the enhancement of the knowledge on a subject that is very interesting to any structural engineer involved in the area of steel constructions was possible. In a future project, for an even deeper analysis and comparison, a different method of comparison can be pursued (addition of snow loads, standardization of a most influential factor like maintaining the cross-sections the same etc), and/or optimization may be sought.

11. LITERATURE INDEX

ABNT NBR 6123. (1988). *ABNT NBR 6123.*

ABNT NBR 8800. (2008). *ABNT NBR 8800.*

ACKERMANN, K. (1984). *Industriebau* (2. ed.). Stuttgart: Deutsche Verlags-Anstalt GmbH.

Allianz Arena. (s.d.). Tratto da General information about the Allianz Arena: https://allianz-arena.com/en/arena/facts/general-information

Allianz Parque. (s.d.). Tratto da Sobre o Allianz Parque: http://www.allianzparque.com.br/sobre/index

Bautechnik, D. I. (2015, April). *Bauregellisten/Technische Baubestimmungen*. Tratto da DIBt: https://www.dibt.de/de/Geschaeftsfelder/BRL-TB.html#TB

BUCAK, P. Ö., SEILER, P. C., GEBHARD, P. P., HAUSSER, P. C., MAINZ, P. J., & SEEßELBERG, P. C. (2007). *Praxisbeispiele für Einwirkungen nach neuen Normen.* Berlin: Bauwerk Verlag GmbH.

BÜTTNER, O., & STENKER, H. (1986). *Stahlhallen: Entwurf und Konstruktion.* Berlin: VEB Verlag für Bauwesen.

Climate-Data Org 1. (s.d.). *Climate: Darmstadt*. Tratto da Climate-Data Org: https://en.climate-data.org/location/2129/

Climate-Data Org 2. (s.d.). *Climate: São Luís*. Tratto da Climate-Data Org: https://en.climate-data.org/location/1671/

DIN 1055. *DIN 1055.*

DIN 18800. *DIN 18800.*

DIN EN 1990. (2010). *DIN EN 1990.*

DIN EN 1990 NA. *DIN EN 1990 NA.*

DIN EN 1991-1-4 NA. (2010). *DIN EN 1991-1-4 NA.*

DIN EN 1991-3. (2010). *DIN EN 1991-3.*

DIN EN 1993-1-1. (2010). *DIN EN 1993-1-1.*

Dlubal. (s.d.). Tratto da RSTAB - Structural Frame & Truss Analysis Software: https://www.dlubal.com/en/products/rstab-beam-structures/what-is-rstab

DREHMER, G. A., MESACASA JÚNIOR, E., & PRAVIA, Z. M. (2010). *Galpões para Usos Gerais.*

G1 Globo. (2017, 01 03). *Especialistas explicam causas do tremor de magnitude 4.7 no MA*. Tratto da G1 Globo: http://g1.globo.com/ma/maranhao/noticia/2017/01/especialistas-explicam-que-tremor-de-magnitude-47-no-maranhao.html

GRIMM, P. F., & KOCKER, R. (2011 (Aktualisierte Ausgabe 2015)). *Hallen aus Stahl: Planungsleitfaden Nr. B 401.* Düsseldorf: bauforumstahl e.V.

KINDMANN, P. R., & KRAHWINKEL, M. (2012). *Stahl- und Verbundkonstruktionen.* Wiesbaden: Springer Vieweg.

KOCKER, R. (2014). *Musterstatik: 15 x 60 x 5 m³ Stahlhallenkonstruktion aus warm gewalzten Profilen.* Düsseldorf: bauforumstahl e.V.

Mairie de Paris. (s.d.). Tratto da The Eiffel Tower at a glance: http://www.toureiffel.paris/en/everything-about-the-tower/the-eiffel-tower-at-a-glance.html

Norwegian Metereological Institute and Norwegian Broadcasting Corporation 1. (s.d.). *Weather Statistics for Darmstadt*. Tratto da YR: https://www.yr.no/place/Germany/Hesse/Darmstadt/statistics.html

Norwegian Metereological Institute and Norwegian Broadcasting Corporation 2. (s.d.). *Weather Statistics for São Luís*. Tratto da YR: https://www.yr.no/place/Brazil/Maranh%C3%A3o/S%C3%A3o_Lu%C3%ADs/statistics.html

PASTERNAK, H., HOCH, H.-U., & FÜG, D. (2010). *Stahltragwerke im Industriebau* (1. ed.). Berlin: Wilhelm Ernst & Sohn.

Portal Met@lica Construção Civil. (s.d.). Tratto da Galpões em Pórticos de Aço: http://wwwo.metalica.com.br/tipos-de-galpoes-em-porticos-de-aco

Renewable Energy Concepts. (s.d.). *Schneelasten und Windlasten*. Tratto da Renewable Energy Concepts: http://www.renewable-energy-concepts.com/german/sonnenenergie/basiswissen-solarenergie/schneelasten-windlasten.html

RICCABONA, C., & MEZERA, K. (2012). *Baukonstruktionslehre 5: Sanierungen, Ferigteilbau und Fassaden, Industriehallen.* Wien: MANZ Verlag Schulbuch GmbH.

RUGA, J. (2010 (erweiterte Ausgabe 2013)). *Sporthallen aus Stahl: Planungsleitfaden Nr. B 402.* Düsseldorf: bauforumstahl e.V.

SALMON, C. G., JOHNSON, J. E., & MALHAS, F. A. (2009). *Steel Structures Design and Behavior.* Pearson Education, Inc.

SANTIAGO, R. (2015, Abril 02). *Exercício Cargas na Estruturas*. Tratto da http://rosaliasantiago.weebly.com/portifoacutelio/exercicio-cargas-na-estruturas

SCHMIDT, P. P. (2014, März 24). Tratto da Windlasten: https://www.bundesanzeiger-verlag.de/fileadmin/BIV-Portal/Bautechnik_WKD/Schneider-Bautabellen/Ingenieure/LP_BTI_2014_03_024-047.pdf

SCHNEIDER, K. (2012). *Bautabellen für Ingenieure - mit Berechnungshinweisen und Beispielen* (20. ed.). Köln: Werner Verlag.

SEEßELBERG, P. C. (2005). *Kranbahnen: Bemessung und konstruktive Gestaltung.* Berlin: Bauwerk Verlag GmbH.

SEEßELBERG, P. C. (2005). Zum Entwurf von Kranbahnträgern für Laufkrane. *FriLo Magazin* , 20-30.

Steel Business Briefing. (s.d.). Tratto da Steel & Construction: http://www.slideshare.net/SteelBusinessBriefing/steel-construction

Telegraph. (s.d.). Tratto da Moment terrified players flee sports hall as roof collapses above them: http://www.telegraph.co.uk/news/2017/01/16/moment-terrified-players-flee-sports-hall-roof-collapses/

TICHELMANN, P. K., WELLAN, V., & WERKMEISTER, D. (2015). *Dach- und Wandkonstruktionen aus Stahl Nr. B 405.* Düsseldorf: bauforumstahl e.V.

Türkiye Rehberi. (s.d.). Tratto da Almanya: http://www.turkiye-rehberi.net/almanya.asp

USGS - United States Geological Survey 1. (2016, January). Tratto da Iron and Steel: http://minerals.usgs.gov/minerals/pubs/commodity/iron_&_steel/mcs-2016-feste.pdf

USGS - United States Geological Survey 2. (2016, January). Tratto da Iron Ore: http://minerals.usgs.gov/minerals/pubs/commodity/iron_ore/mcs-2016-feore.pdf

VON BERG, D. (1989). *Krane und Kranbahnen: Berechnung, Konstruktion und Ausführung.* Stuttgart: B. G. Teubner.

Weather Forecast. (s.d.). Tratto da São Luís Location Guide: http://www.weather-forecast.com/locations/Sao-Luis

Wiki Spaces 1. (s.d.). Tratto da West Berlin Congress Hall Collapse (1980): https://failures.wikispaces.com/West+Berlin+Congress+Hall

Wiki Spaces 2. (s.d.). Tratto da Magic Mart Roof Collapse: http://failures.wikispaces.com/Magic+Mart+Store%2C+Roof+Collapse%2C

Wikimedia Commons. (s.d.). Tratto da File:Hesse DA(city).svg: https://commons.wikimedia.org/wiki/File:Hesse_DA(city).svg

Wikipedia 1. (s.d.). Tratto da São Luís (Maranhão): https://pt.wikipedia.org/wiki/S%C3%A3o_Lu%C3%ADs_(Maranh%C3%A3o)

Wikipedia 2. (s.d.). Tratto da São Luís, Maranhão: https://en.wikipedia.org/wiki/S%C3%A3o_Lu%C3%ADs,_Maranh%C3%A3o

Wikipedia 3. (s.d.). Tratto da Knick-Ei: https://en.wikipedia.org/wiki/Knick-Ei

Wikipedia 4. (s.d.). Tratto da History of the steel industry (1850–1970): https://en.wikipedia.org/wiki/History_of_the_steel_industry_(1850%E2%80%931970)

Wikipedia 5. (s.d.). Tratto da List of countries by iron ore production: https://en.wikipedia.org/wiki/List_of_countries_by_iron_ore_production

Wikipedia 6. (s.d.). Tratto da Bad Reichenhall Ice Rink roof collapse: https://en.wikipedia.org/wiki/Bad_Reichenhall_Ice_Rink_roof_collapse

Wikipedia 7. (s.d.). Tratto da Bessemer process: https://en.wikipedia.org/wiki/Bessemer_process#Bessemer_converter

Wikipedia 8. (s.d.). Tratto da Carajás Mine: https://en.wikipedia.org/wiki/Caraj%C3%A1s_Mine

World Weather Online 1. (s.d.). *Darmstadt, Hessen Monthly Climate Average, Germany*. Tratto da World Weather Online: https://www.worldweatheronline.com/darmstadt-weather-averages/hessen/de.aspx

World Weather Online 2. (s.d.). *Sao Luis, Maranhao Monthly Climate Average, Brazil*. Tratto da World Weather Online: https://www.worldweatheronline.com/sao-luis-weather-averages/maranhao/br.aspx

YouTube. (s.d.). Tratto da Roof Collapse of Czech Republic Sports Hall: https://www.youtube.com/watch?v=mYOZlzsmdTY

12. APPENDIX

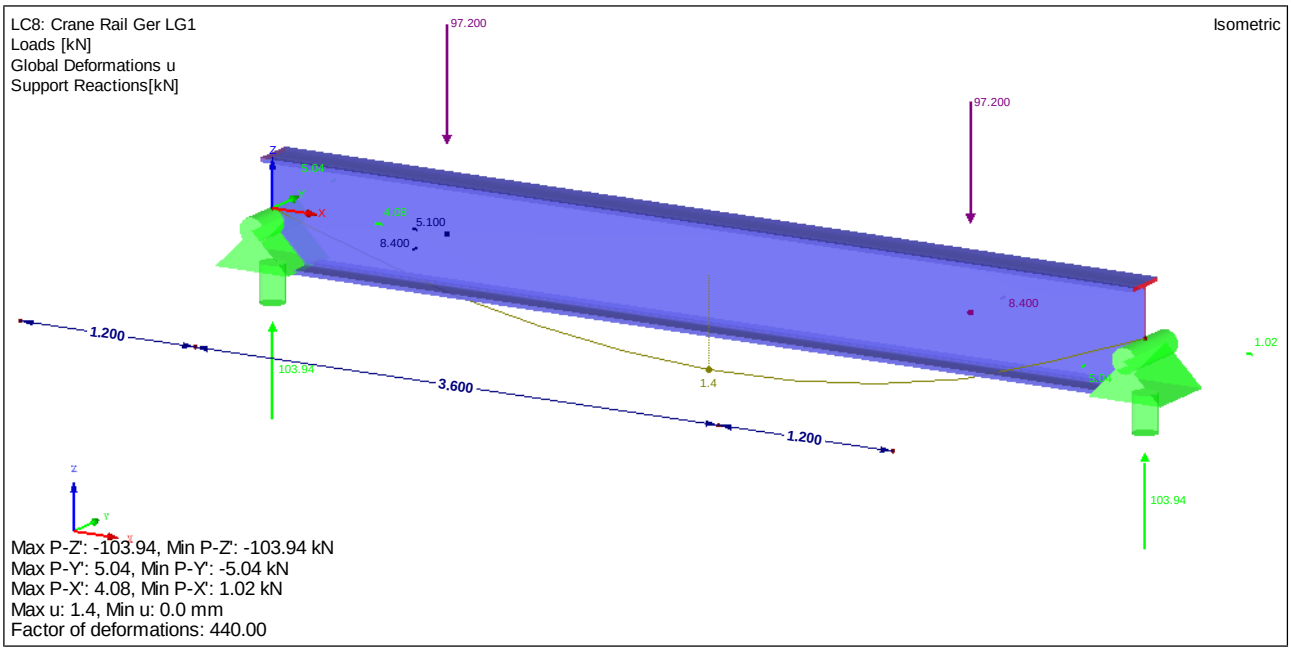

Appendix 1: Deformation for German Runway Girder Verification LG1 (Crane Middle)

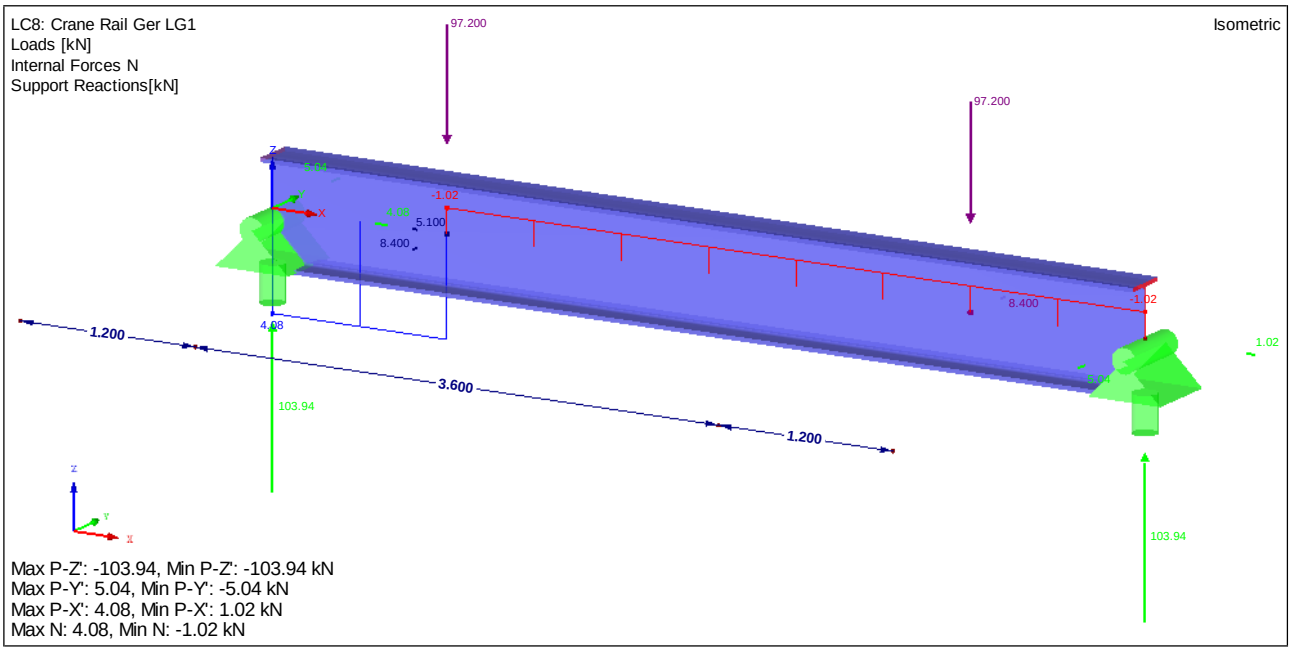

Appendix 2: Normal Force N for German Runway Girder Verification LG1 (Crane Middle)

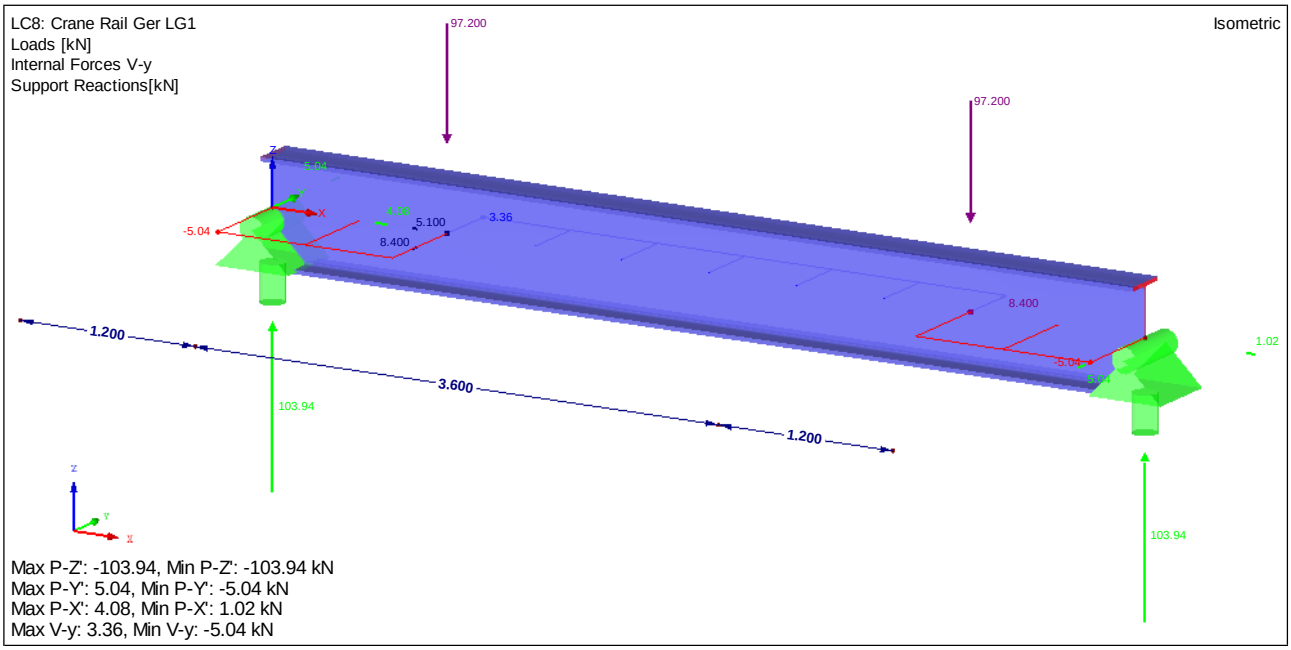

Appendix 3: Shear Force V_y for German Runway Girder Verification LG1 (Crane Middle)

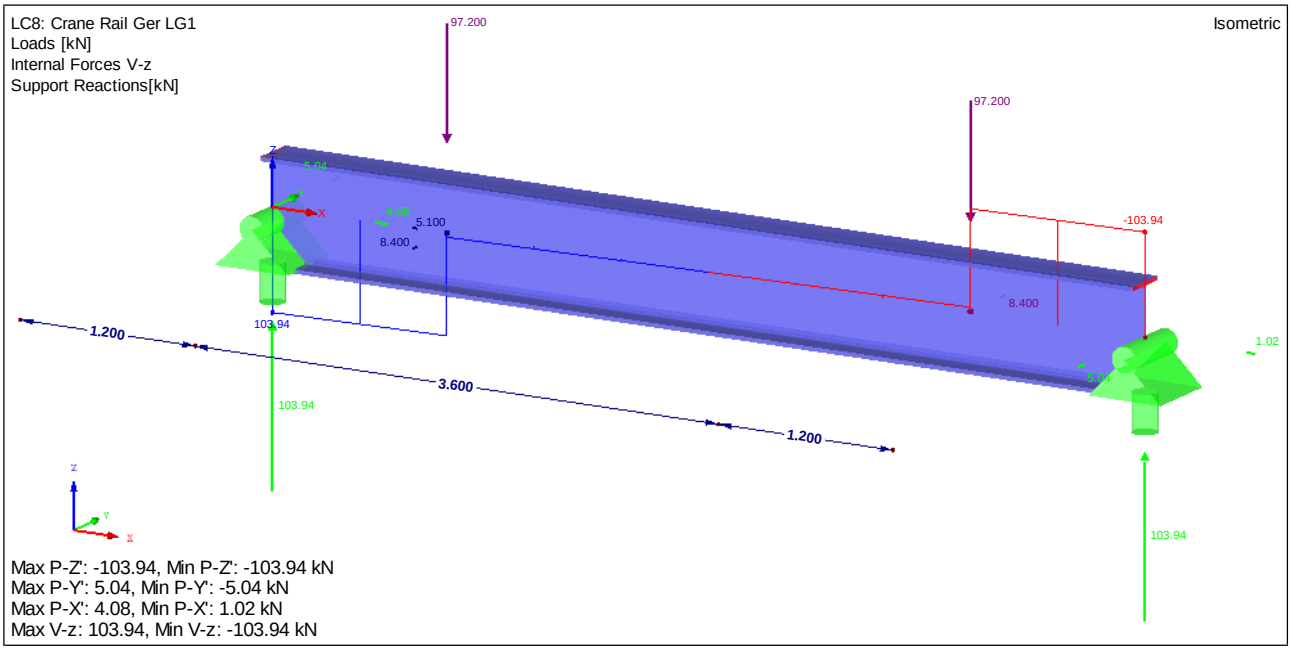

Appendix 4: Shear Force V_z for German Runway Girder Verification LG1 (Crane Middle)

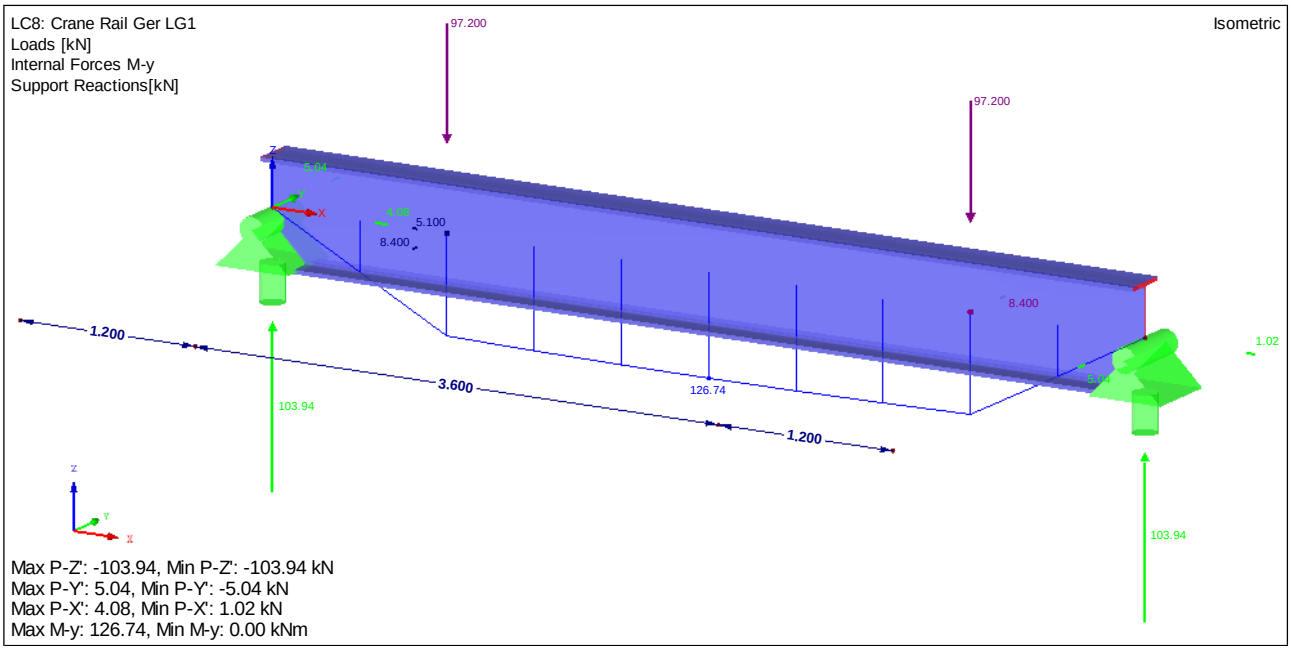

Appendix 5: Moment Force M_y for German Runway Girder Verification LG1 (Crane Middle)

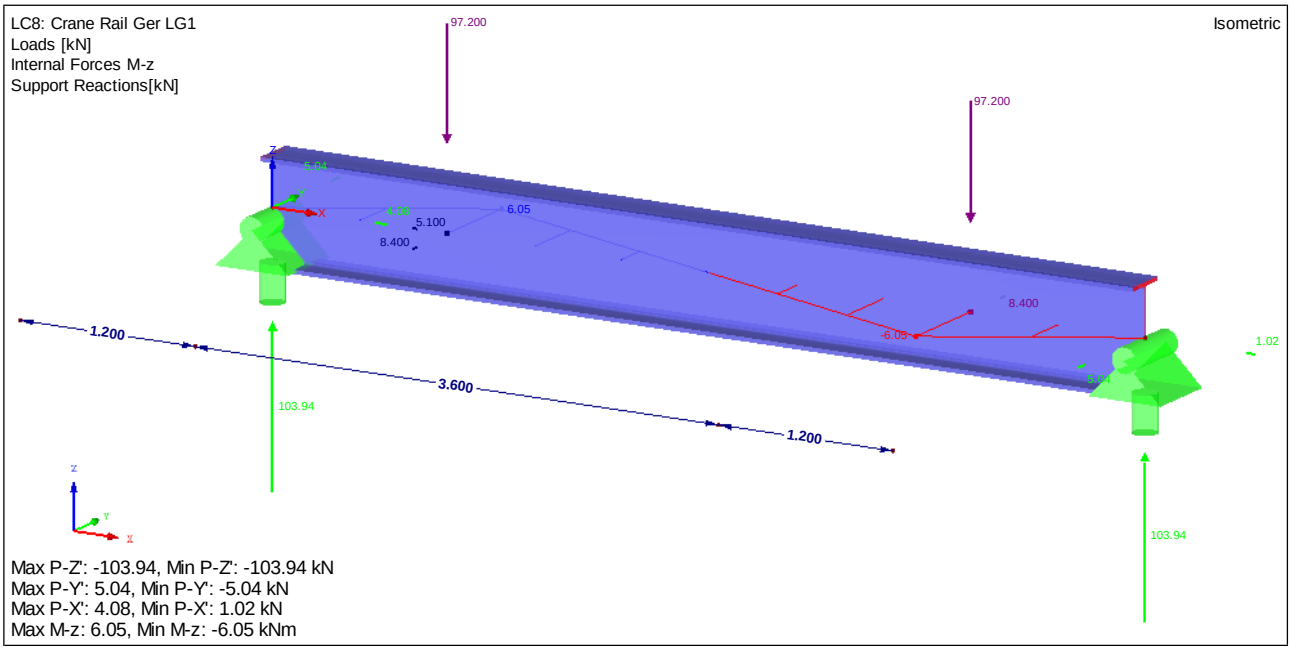

Appendix 6: Moment Force M_z for German Runway Girder Verification LG1 (Crane Middle)

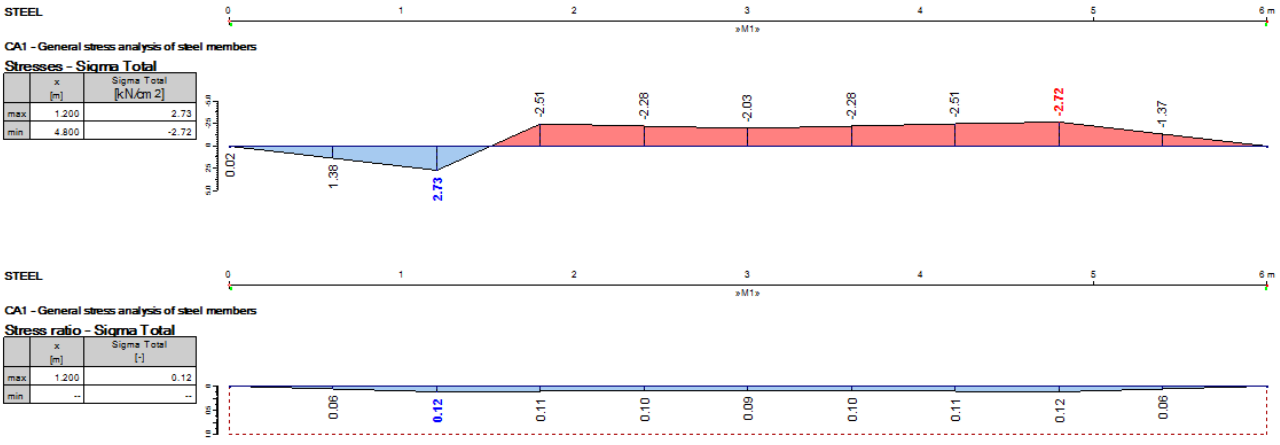

Appendix 7: Stress Ratio of the Runway Girder LG1 (Crane Middle) for the ASD (German)

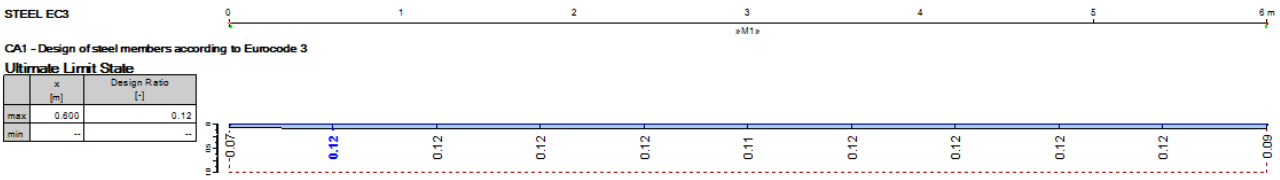

Appendix 8: Design Ratio of the Runway Girder LG1 (Crane Middle) for the EC-3 (ULS)

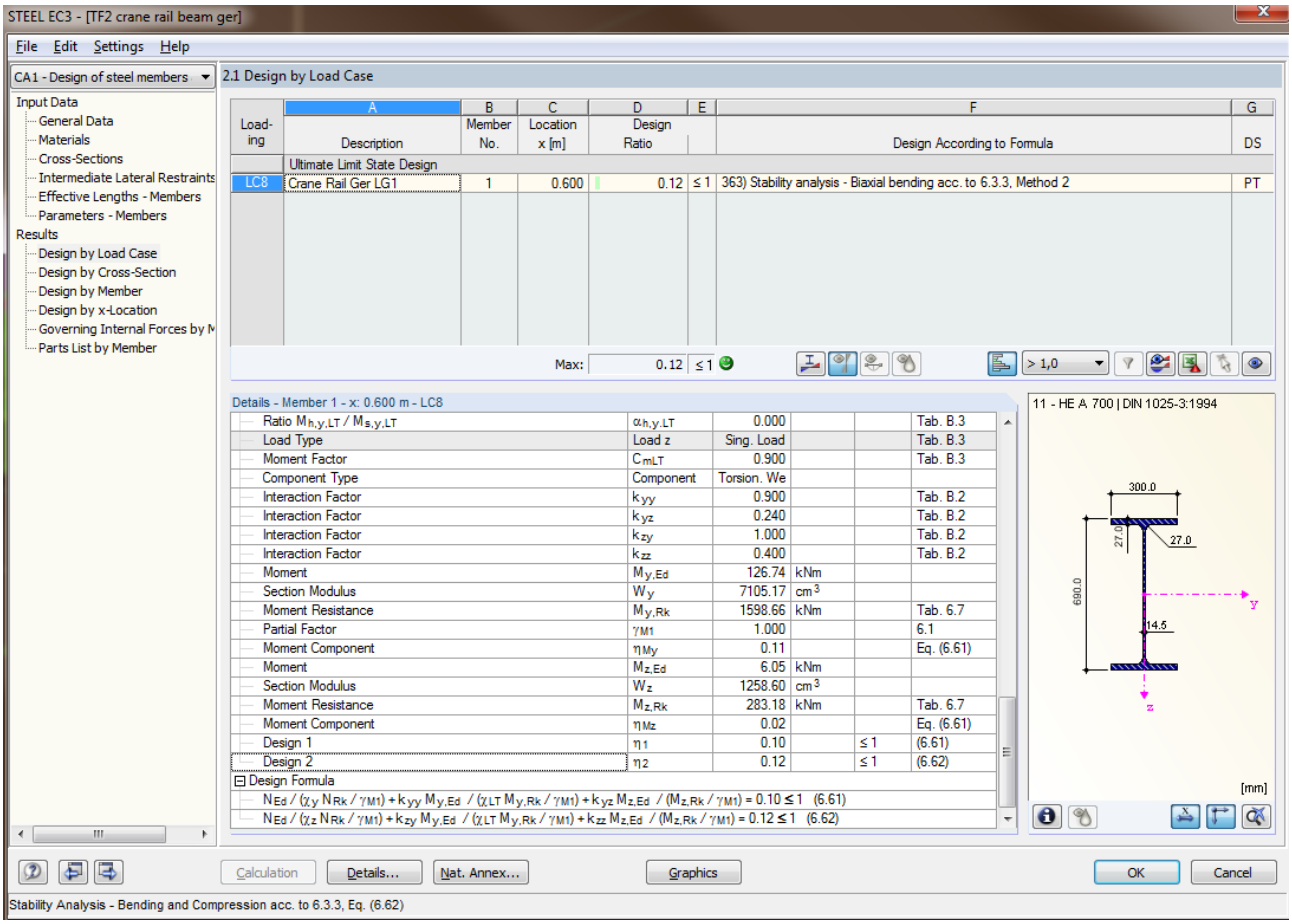

Appendix 9: Demonstration of German Norm Verification (Design Ratio Calculations) for LG1 (Crane Middle)

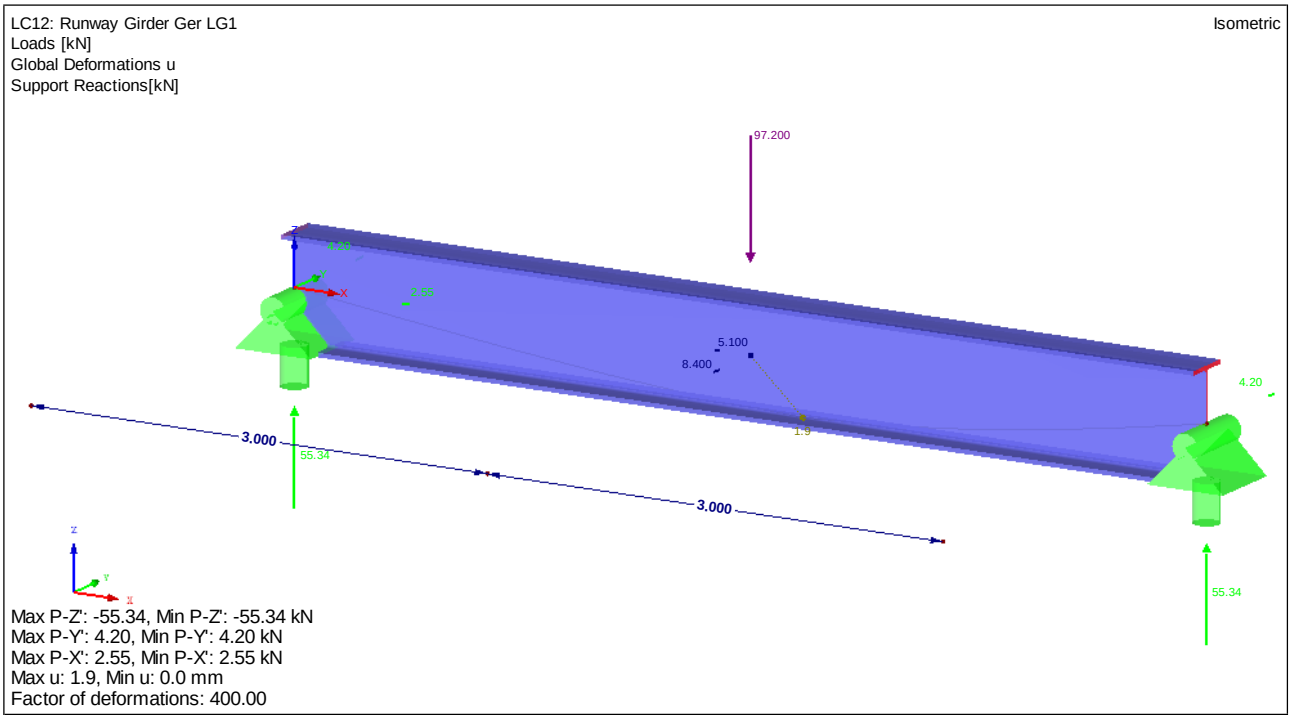

Appendix 10: Deformation for German Runway Girder Verification LG1 (Wheel Middle)

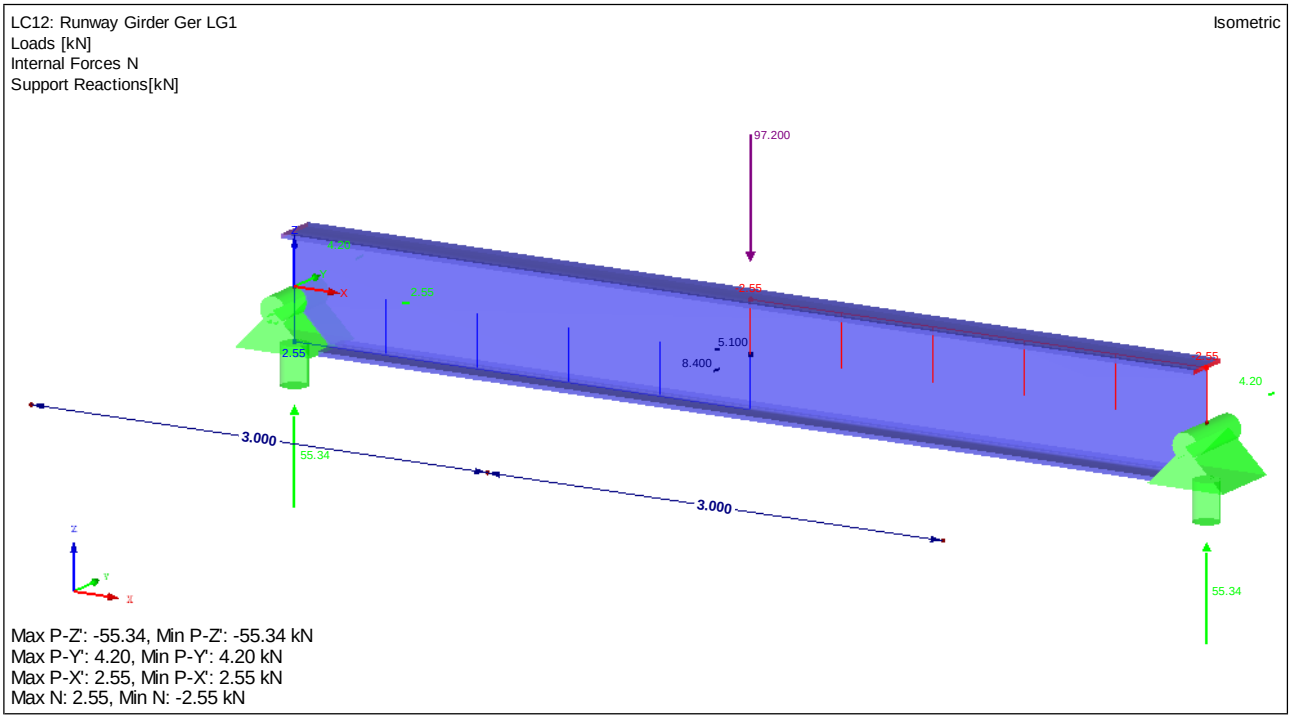

Appendix 11: Normal Force N for German Runway Girder Verification LG1 (Wheel Middle)

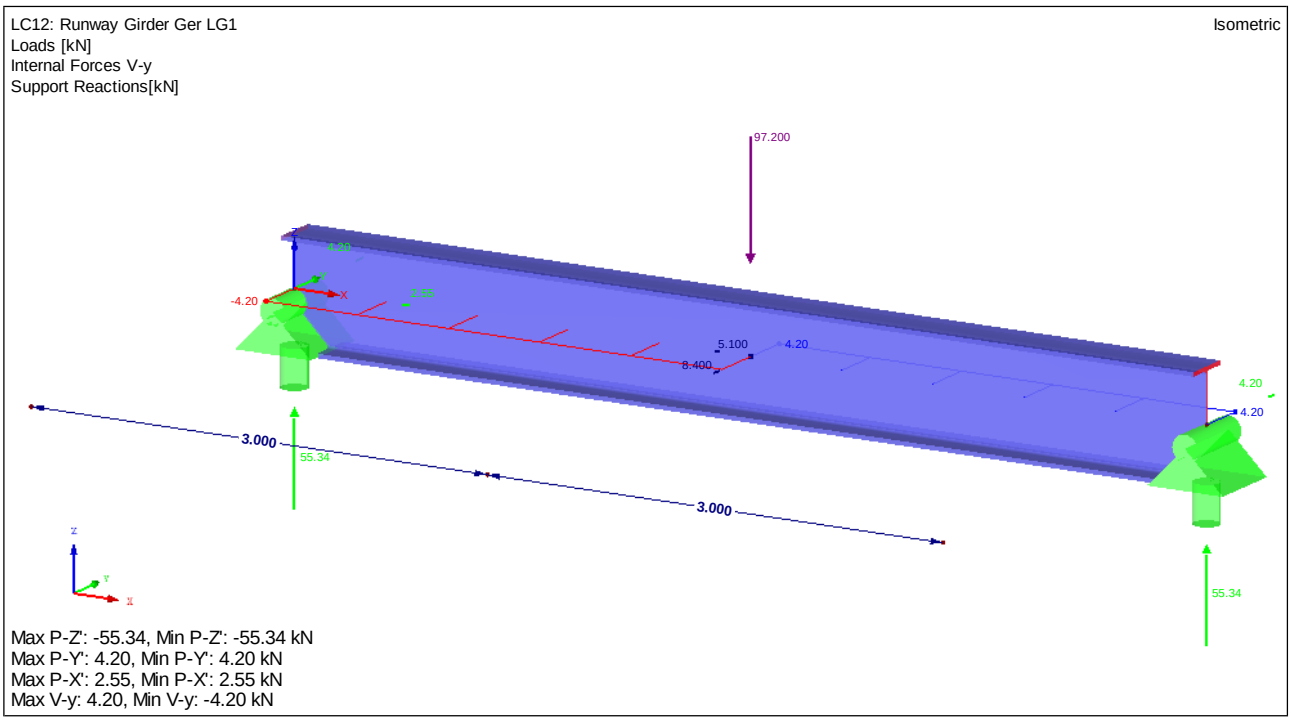

Appendix 12: Shear Force V_y for German Runway Girder Verification LG1 (Wheel Middle)

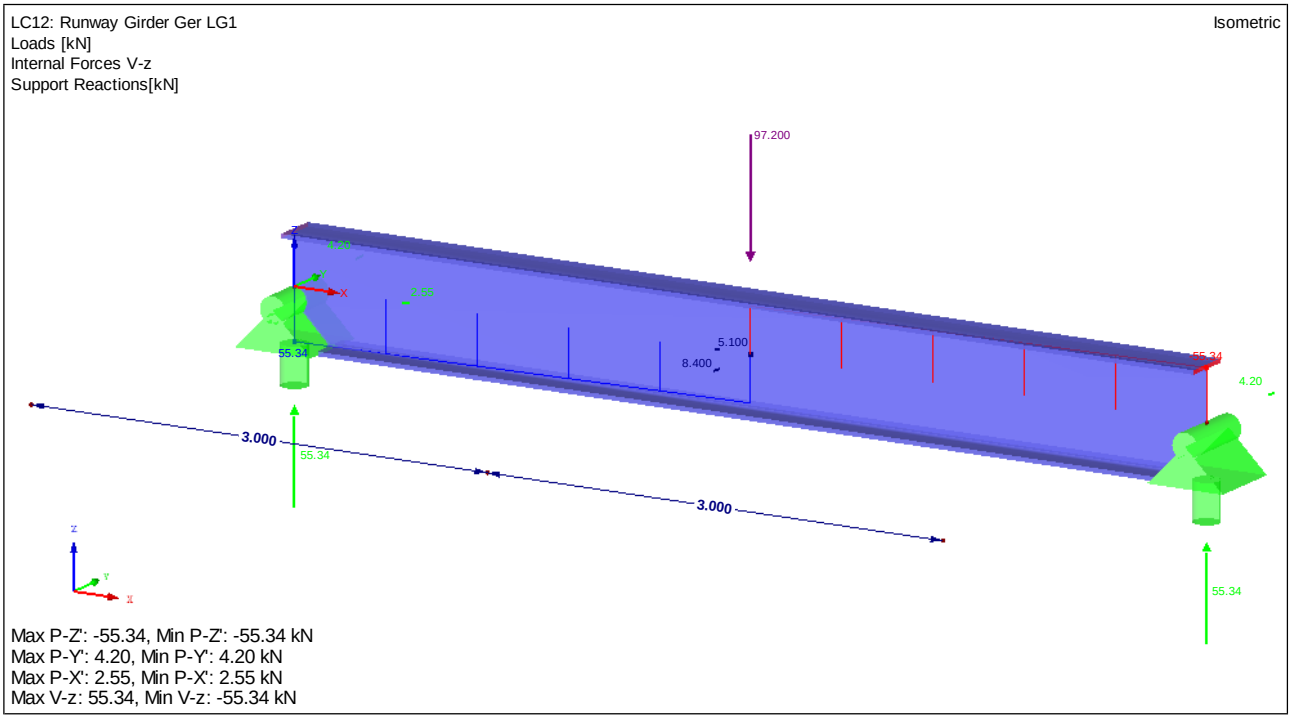

Appendix 13: Shear Force V_z for German Runway Girder Verification LG1 (Wheel Middle)

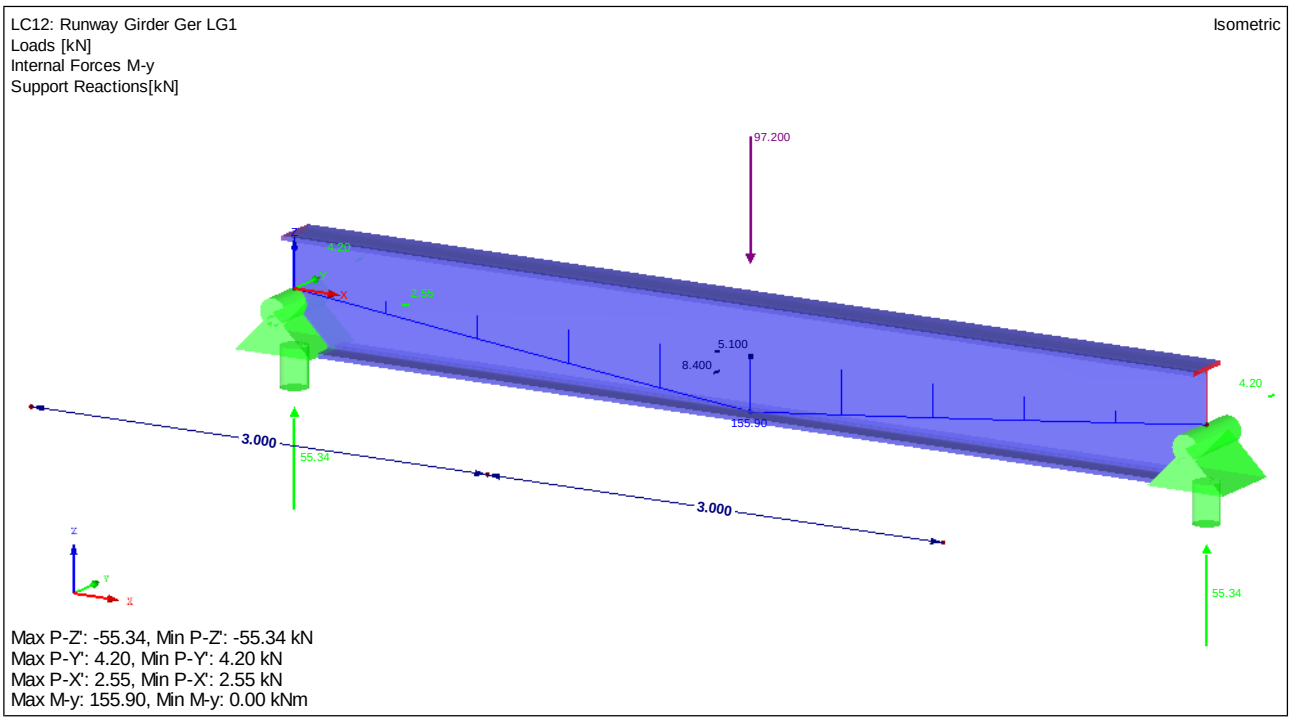

Appendix 14: Moment Force M_y for German Runway Girder Verification LG1 (Wheel Middle)

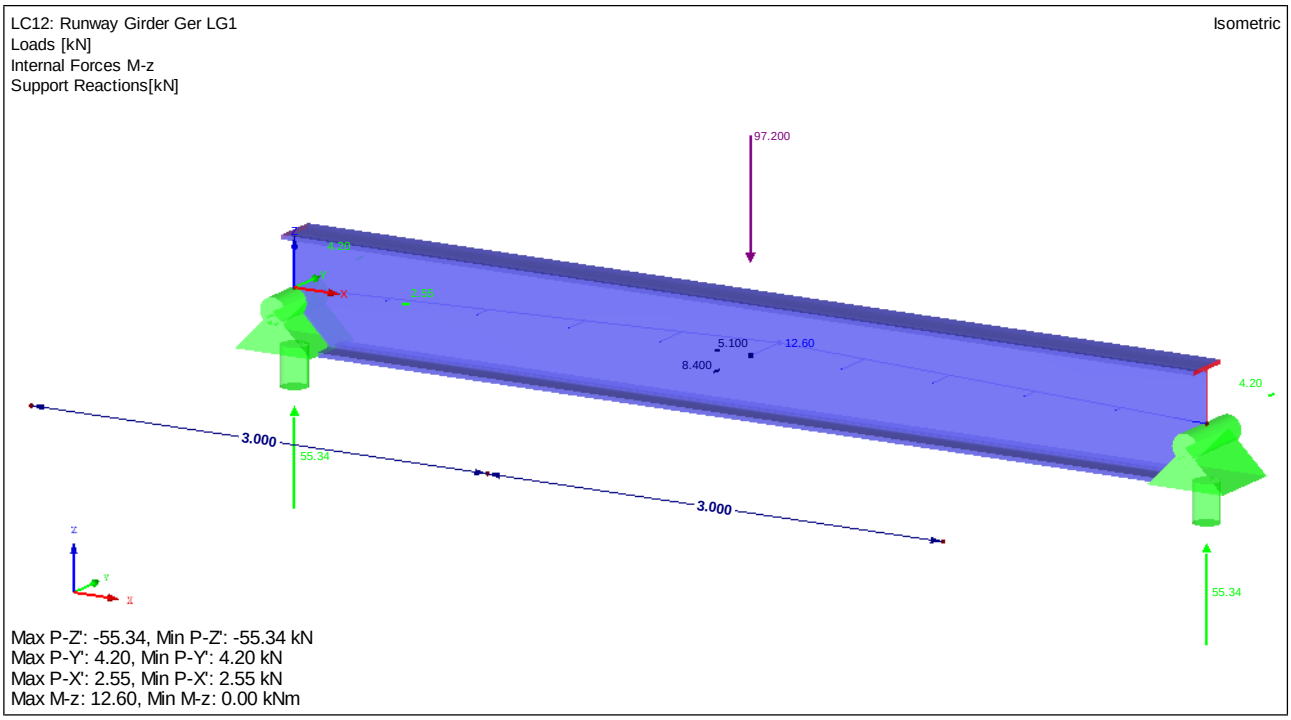

Appendix 15: Moment Force M_z for German Runway Girder Verification LG1 (Wheel Middle)

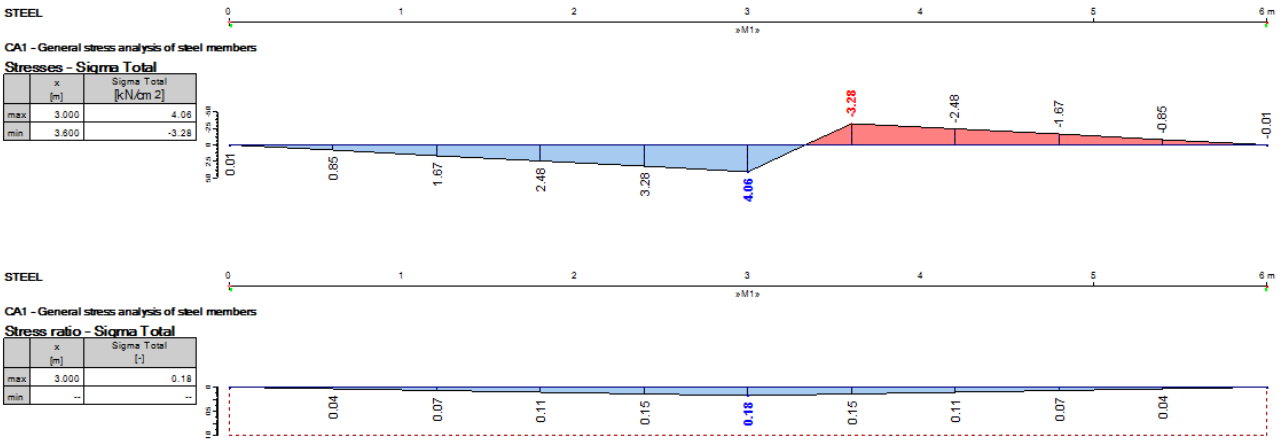

Appendix 16: Stress Ratio of the Runway Girder LG1 (Wheel Middle) for the ASD (German)

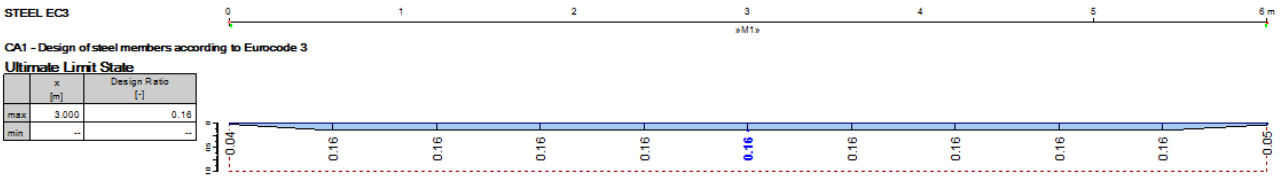

Appendix 17: Design Ratio of the Runway Girder LG1 (Wheel Middle) for the EC-3 (ULS)

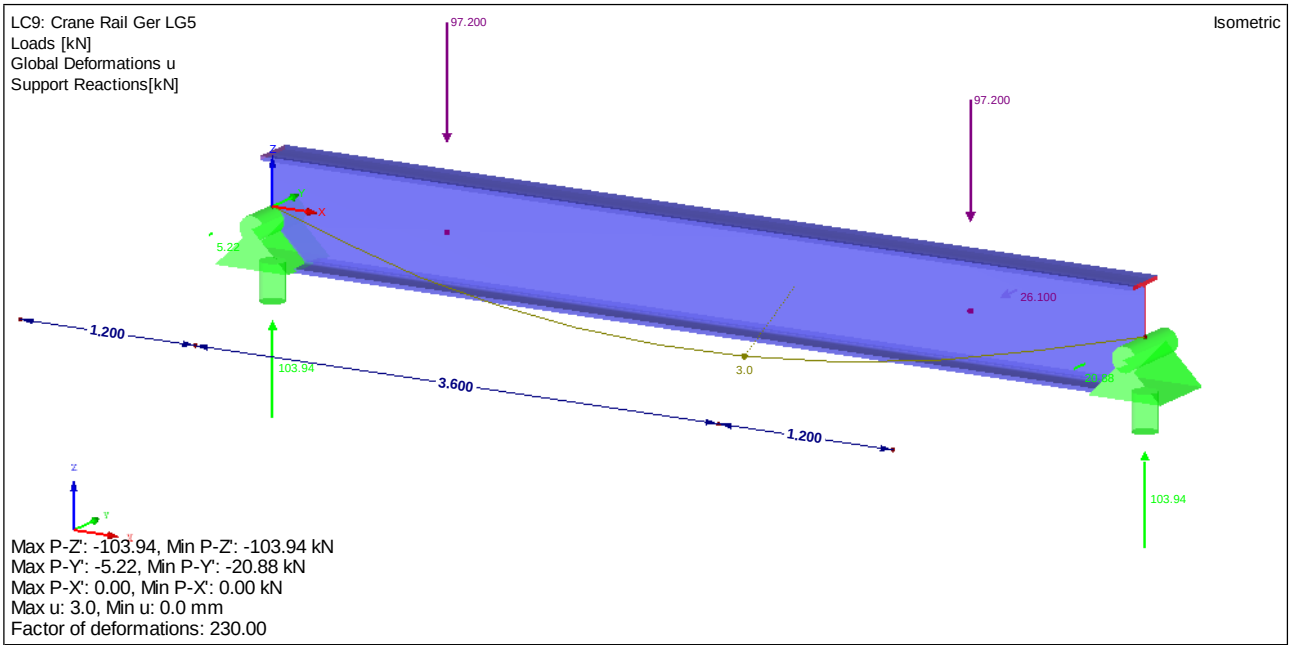

Appendix 18: Deformation for German Runway Girder Verification LG5 (Crane Middle)

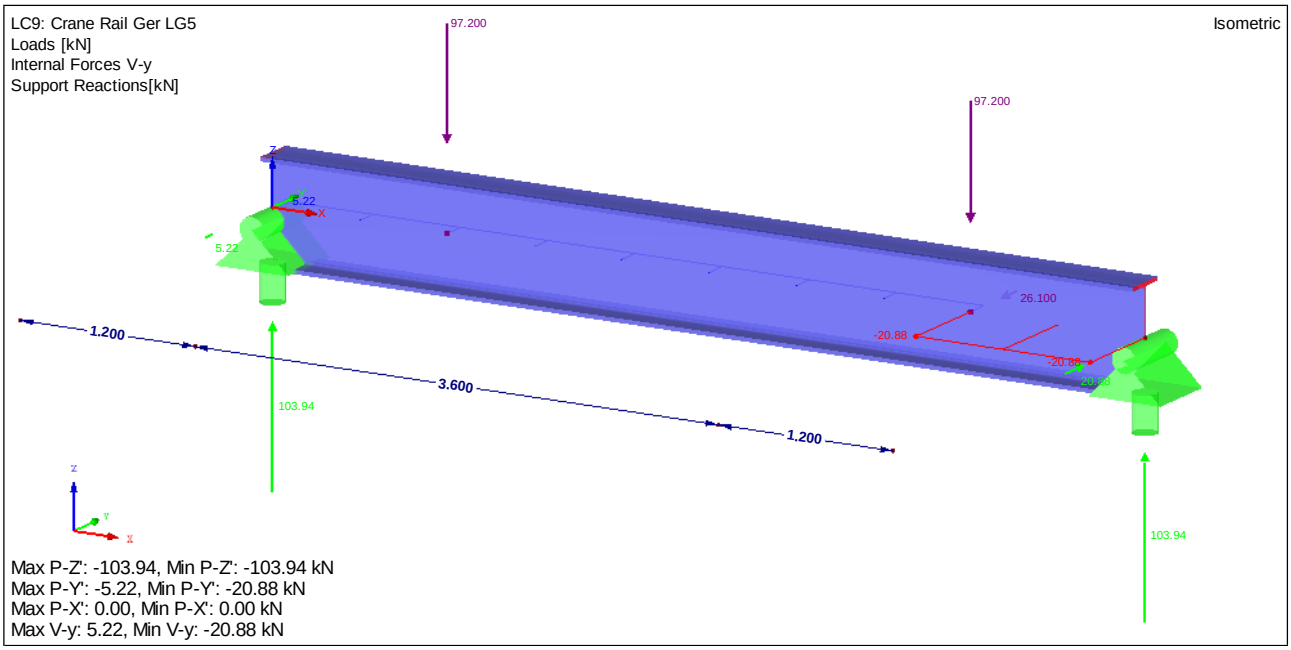

Appendix 19: Shear Force V_y for German Runway Girder Verification LG5 (Crane Middle)

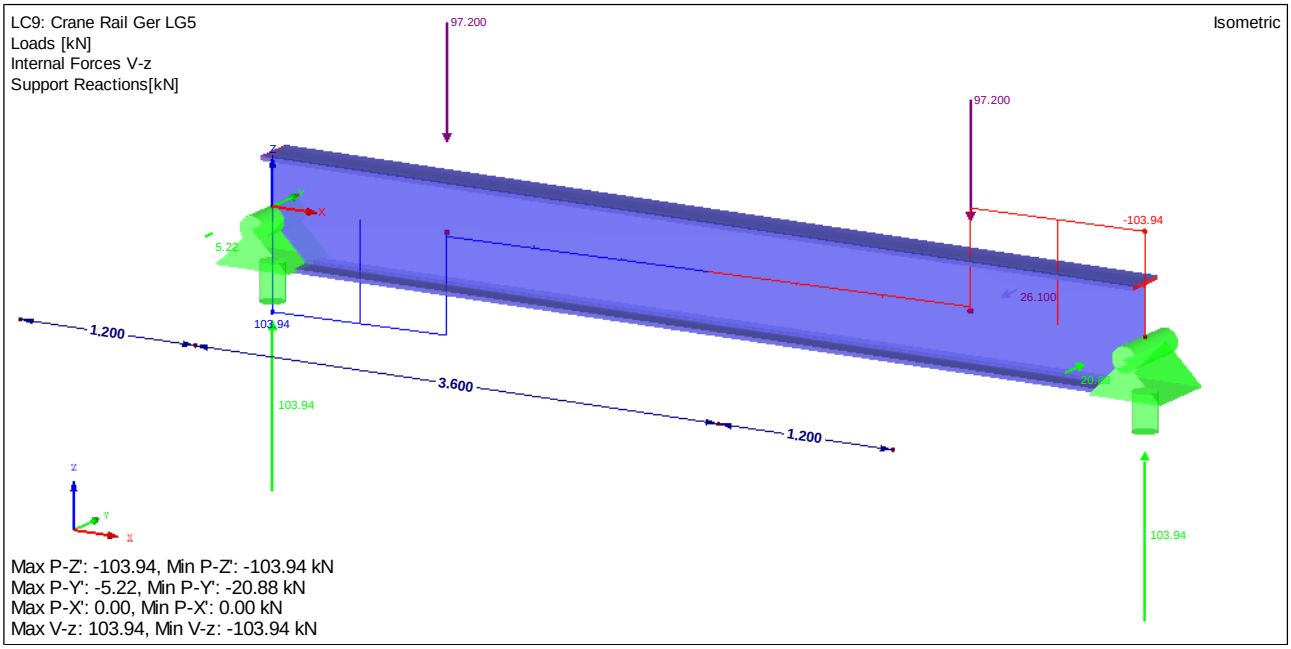

Appendix 20: Shear Force V_z for German Runway Girder Verification LG5 (Crane Middle)

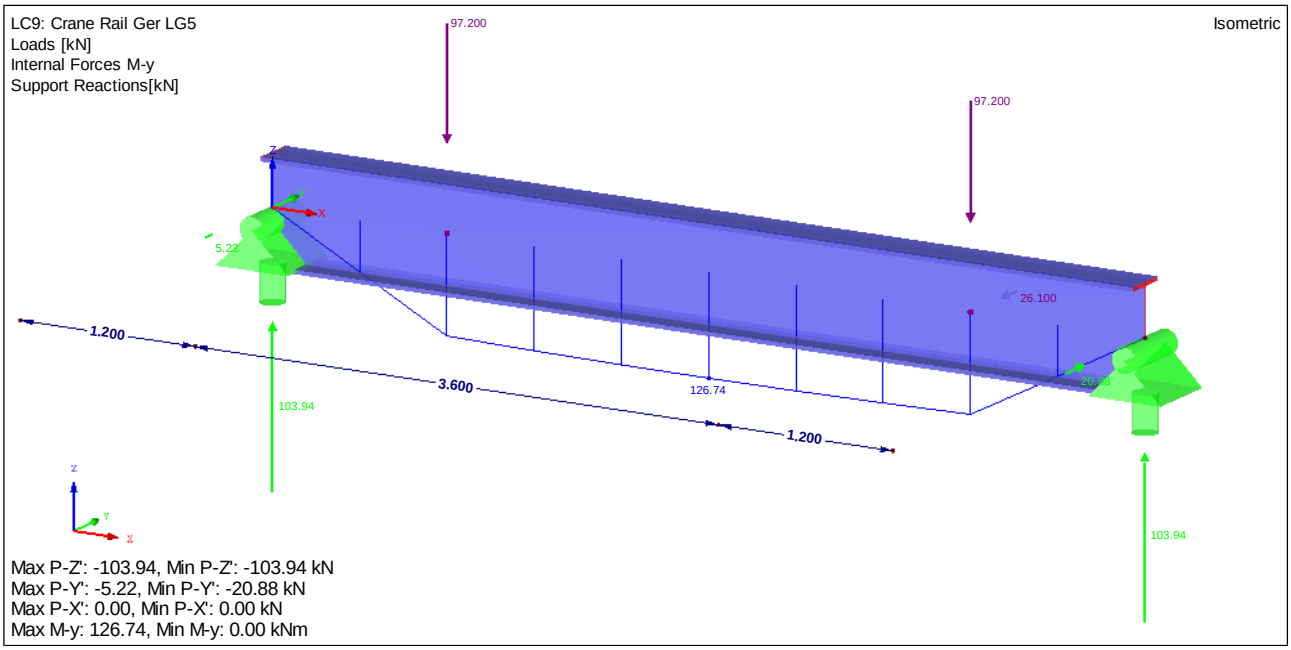

Appendix 21: Moment Force M_y for German Runway Girder Verification LG5 (Crane Middle)

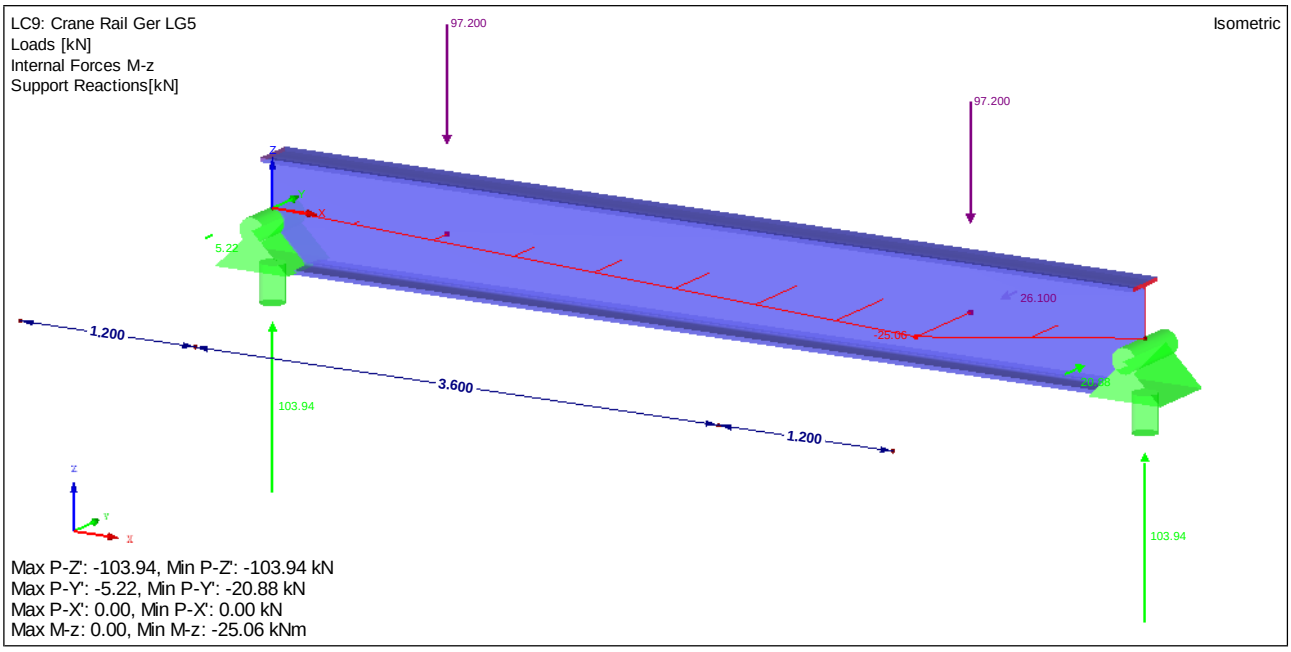

Appendix 22: Moment Force M_z for German Runway Girder Verification LG5 (Crane Middle)

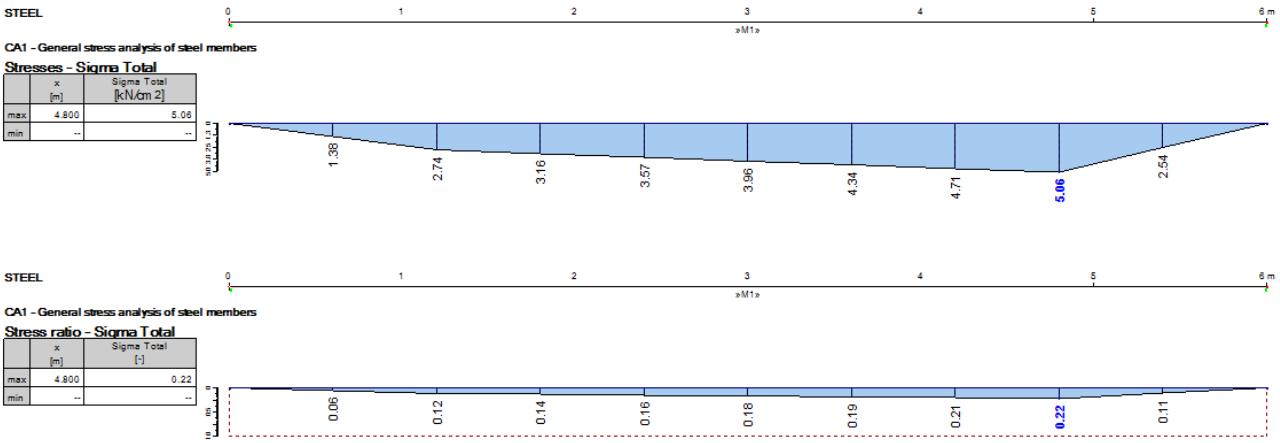

Appendix 23: Stress Ratio of the Runway Girder LG5 (Crane Middle) for the ASD (German)

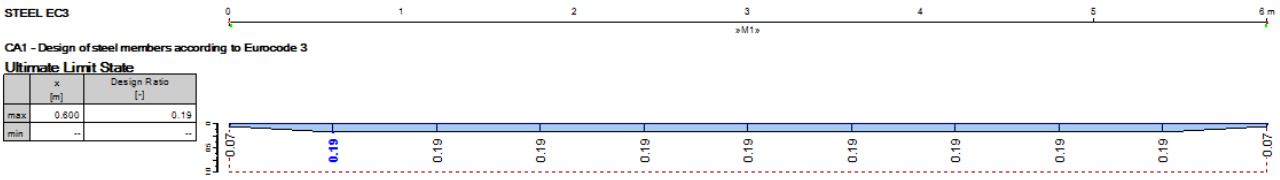

Appendix 24: Design Ratio of the Runway Girder LG5 (Crane Middle) for the EC-3 (ULS)

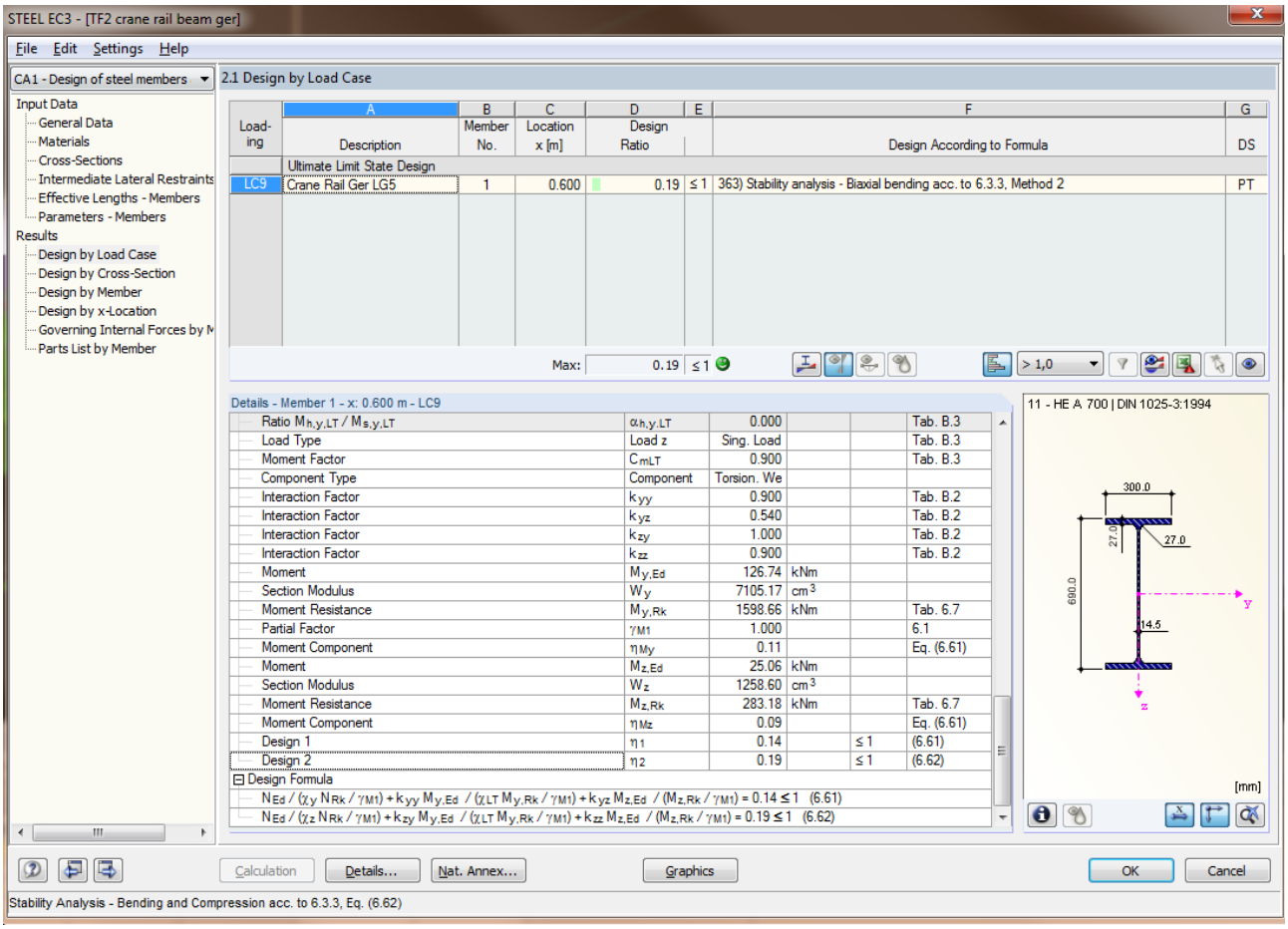

Appendix 25: Demonstration of German Norm Verification (Design Ratio Calculations) for LG5 (Crane Middle)

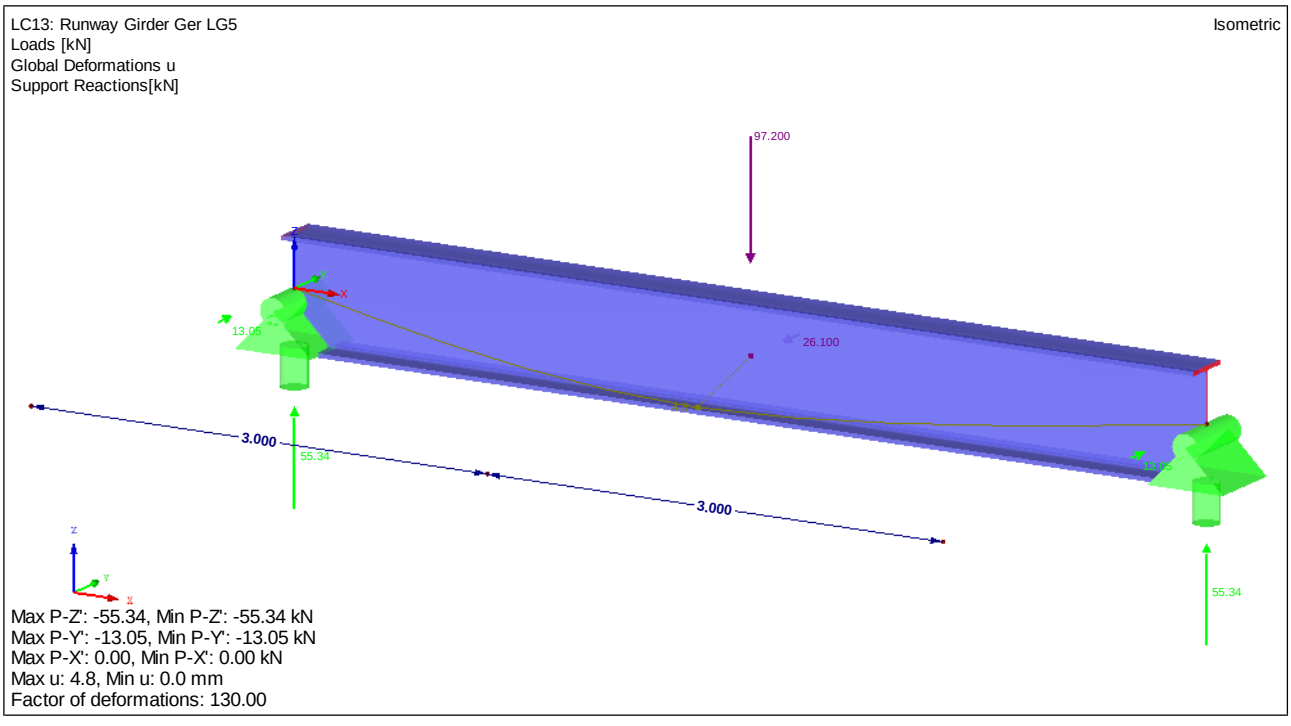

Appendix 26: Deformation for German Runway Girder Verification LG5 (Wheel Middle)

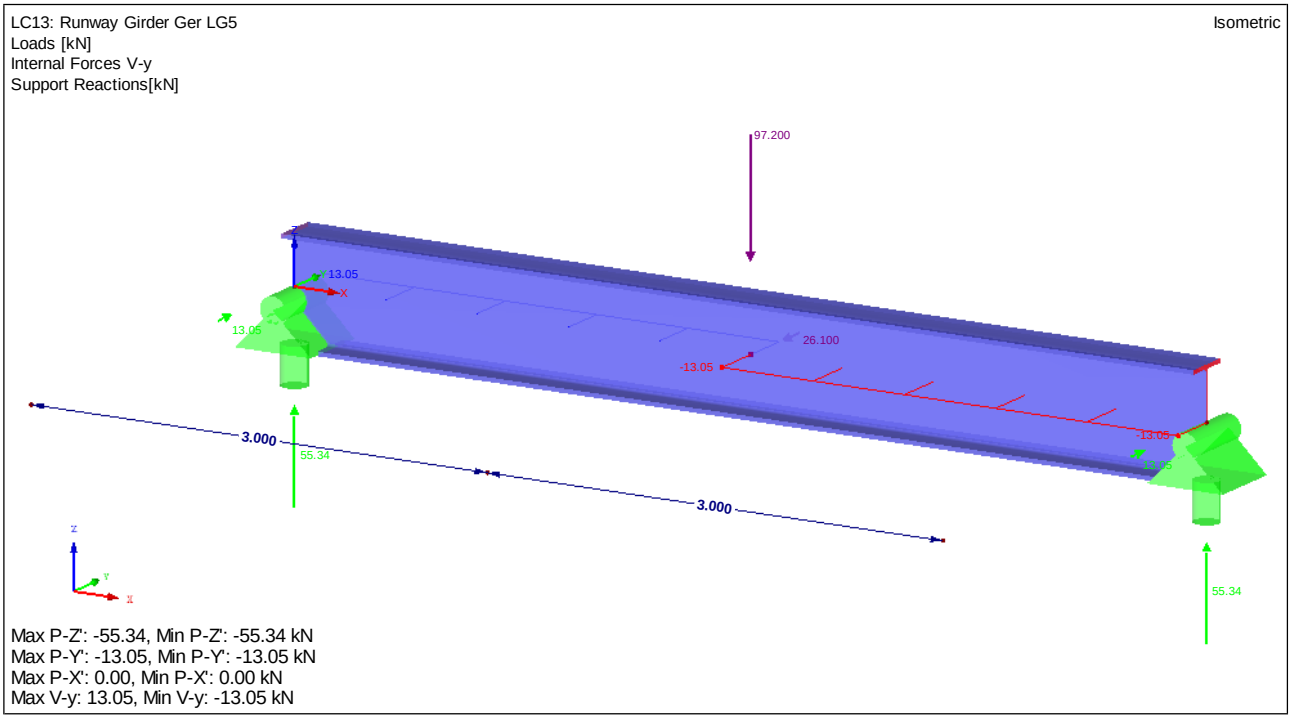

Appendix 27: Shear Force V_y for German Runway Girder Verification LG5 (Wheel Middle)

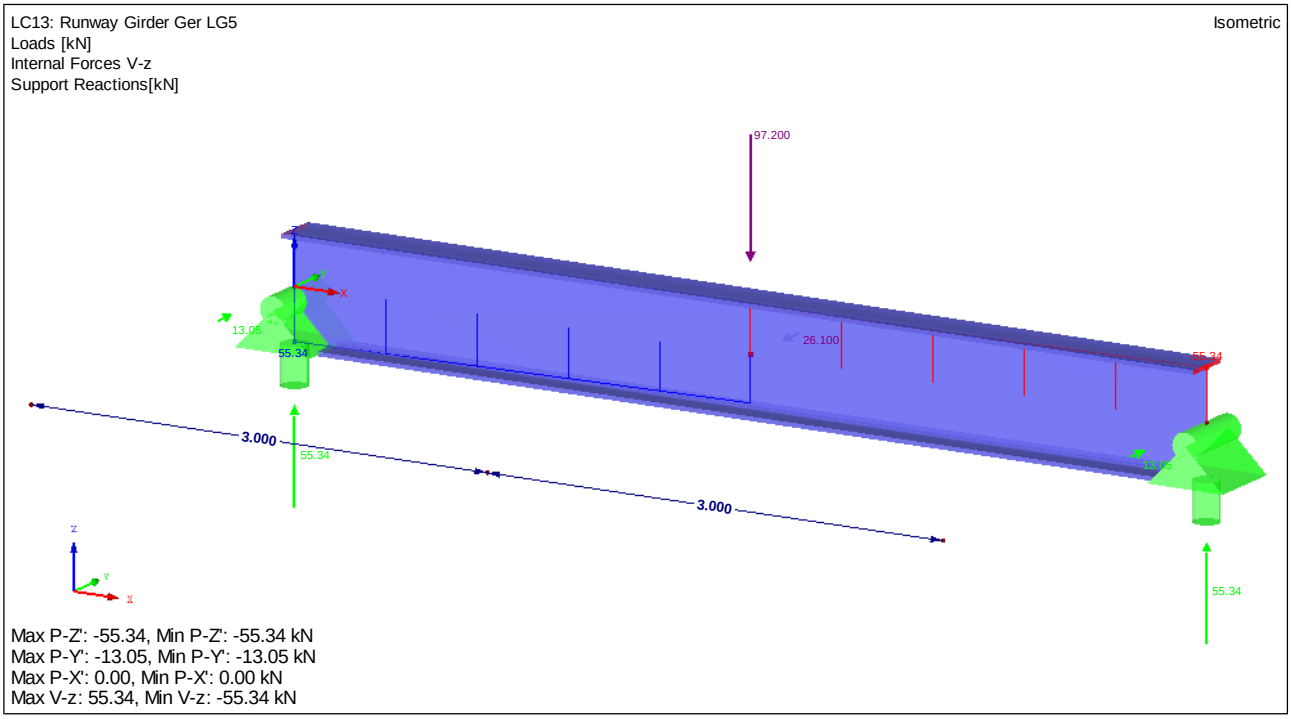

Appendix 28: Shear Force V_z for German Runway Girder Verification LG5 (Wheel Middle)

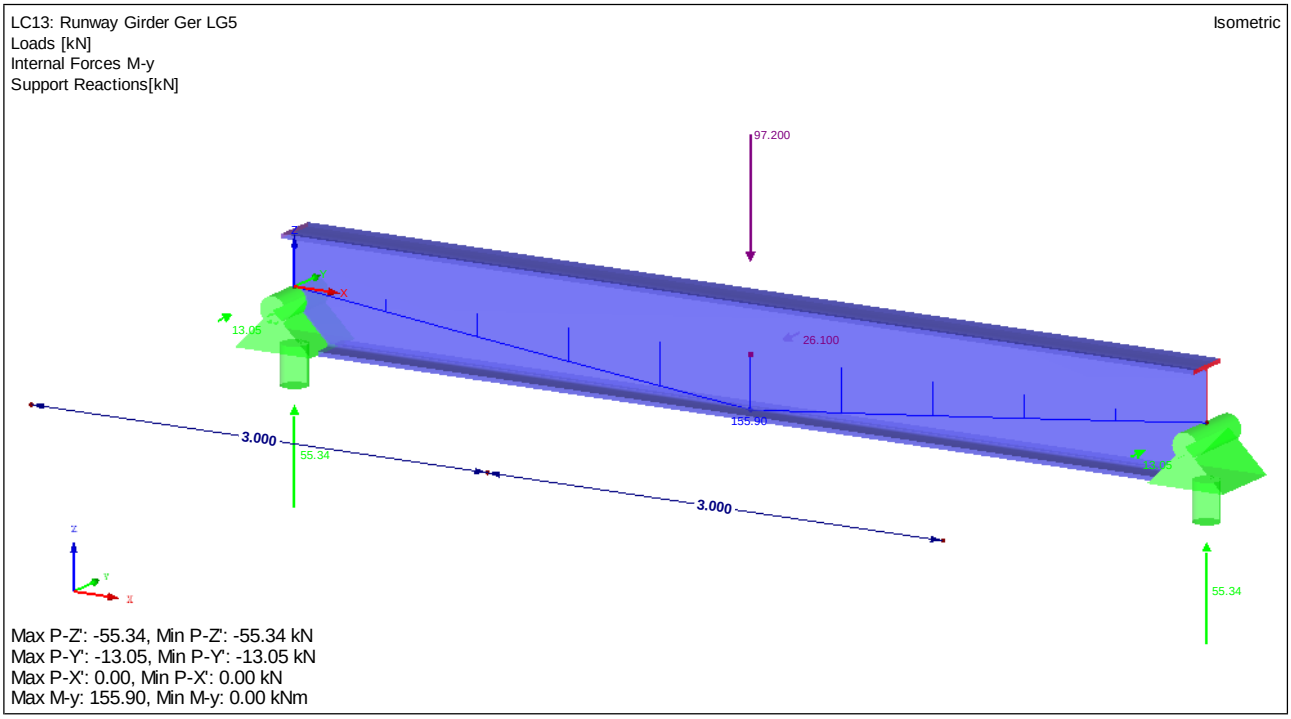

Appendix 29: Moment Force M_y for German Runway Girder Verification LG5 (Wheel Middle)

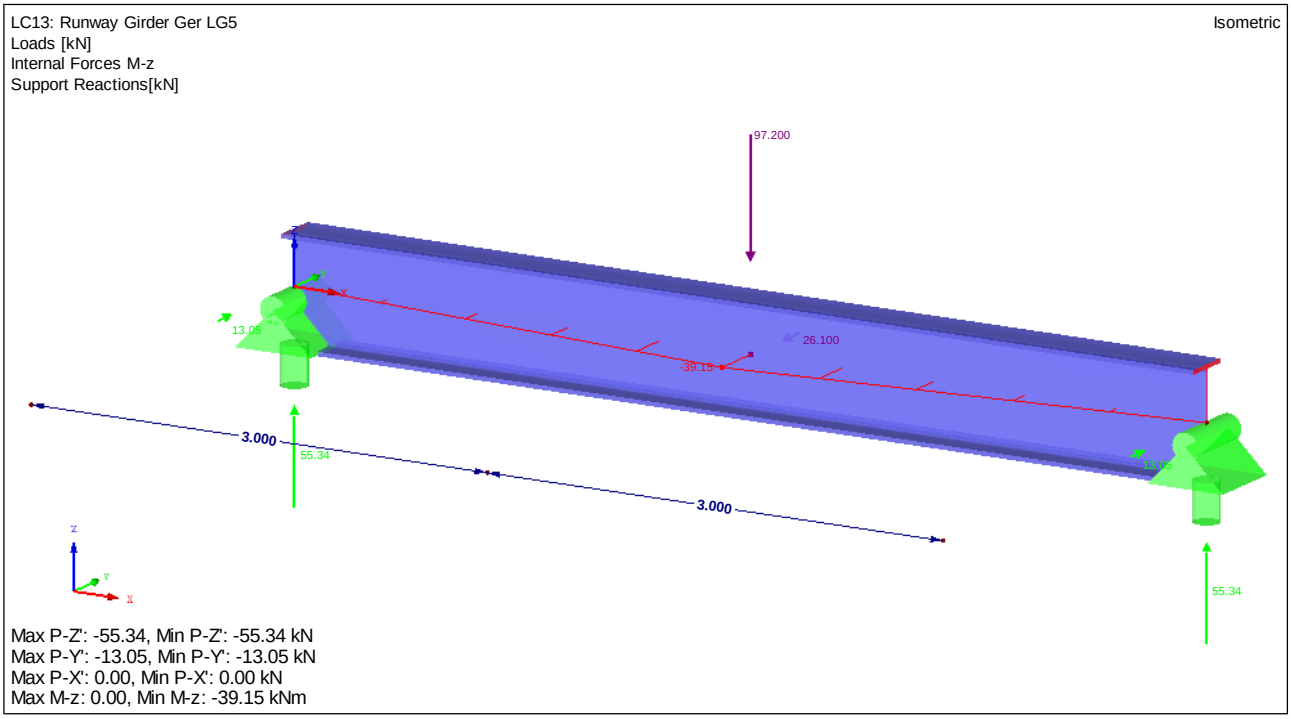

Appendix 30: Moment Force M_z for German Runway Girder Verification LG5 (Wheel Middle)

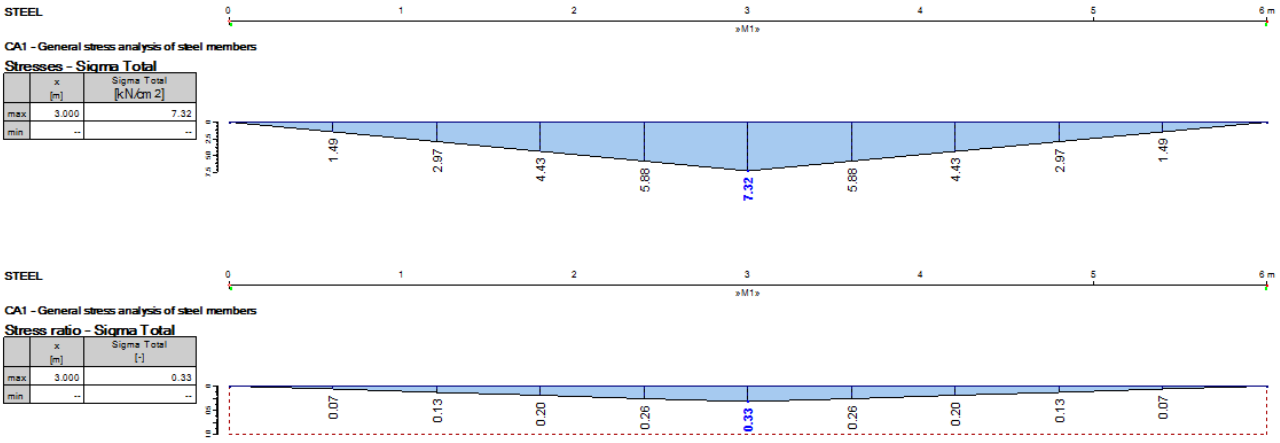

Appendix 31: Stress Ratio of the Runway Girder LG5 (Wheel Middle) for the ASD (German)

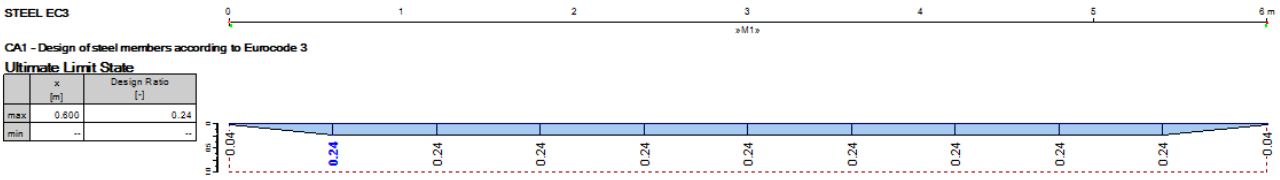

Appendix 32: Design Ratio of the Runway Girder LG5 (Wheel Middle) for the EC-3 (ULS)

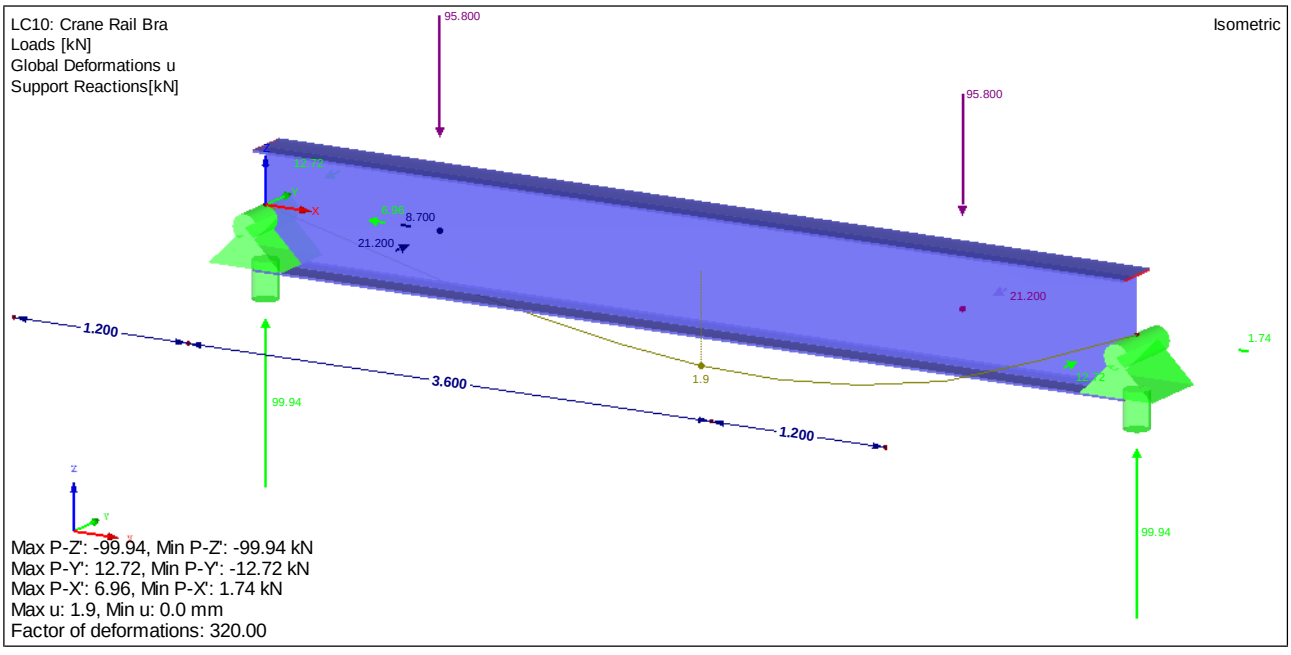

Appendix 33: Deformation for Brazilian Runway Girder Verification (Crane Middle)

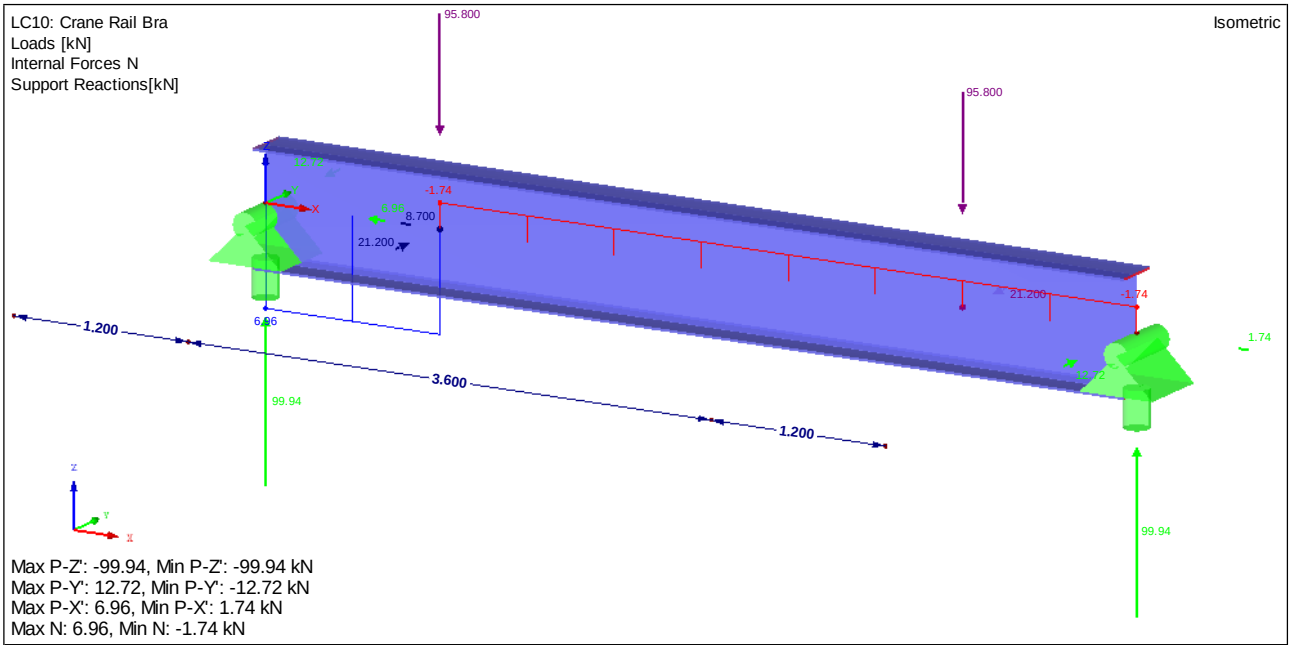

Appendix 34: Normal Force N for Brazilian Runway Girder Verification (Crane Middle)

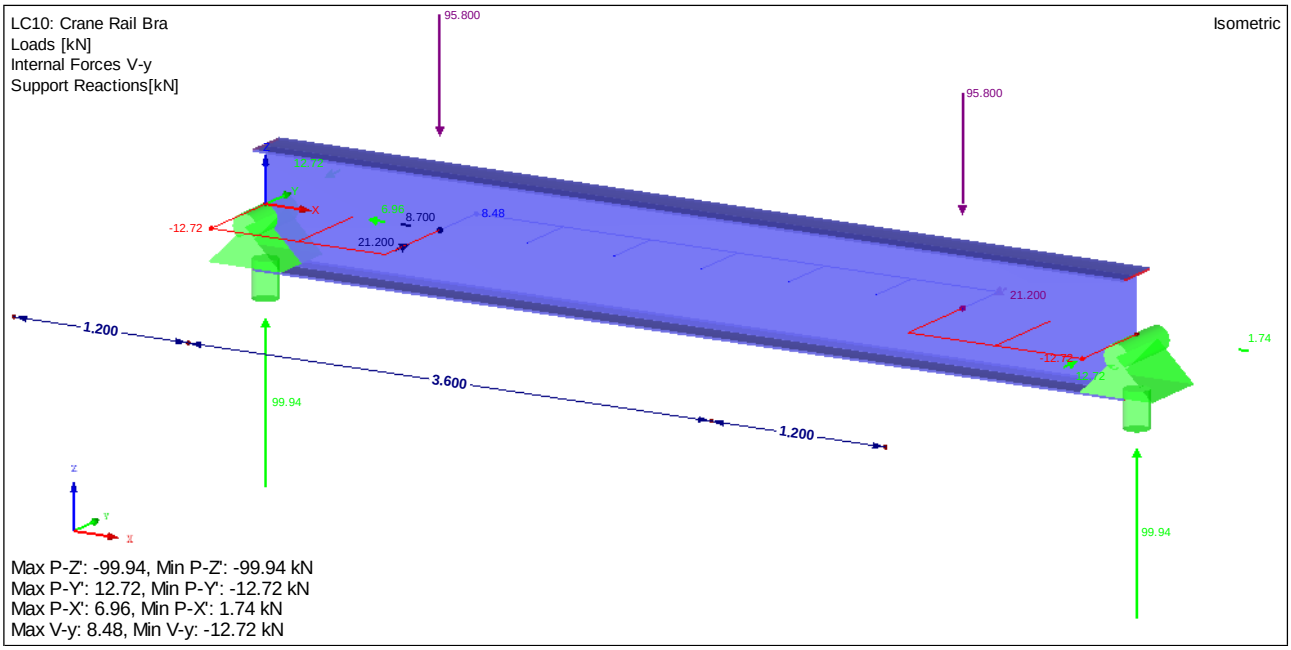

Appendix 35: Shear Force V_y for Brazilian Runway Girder Verification (Crane Middle)

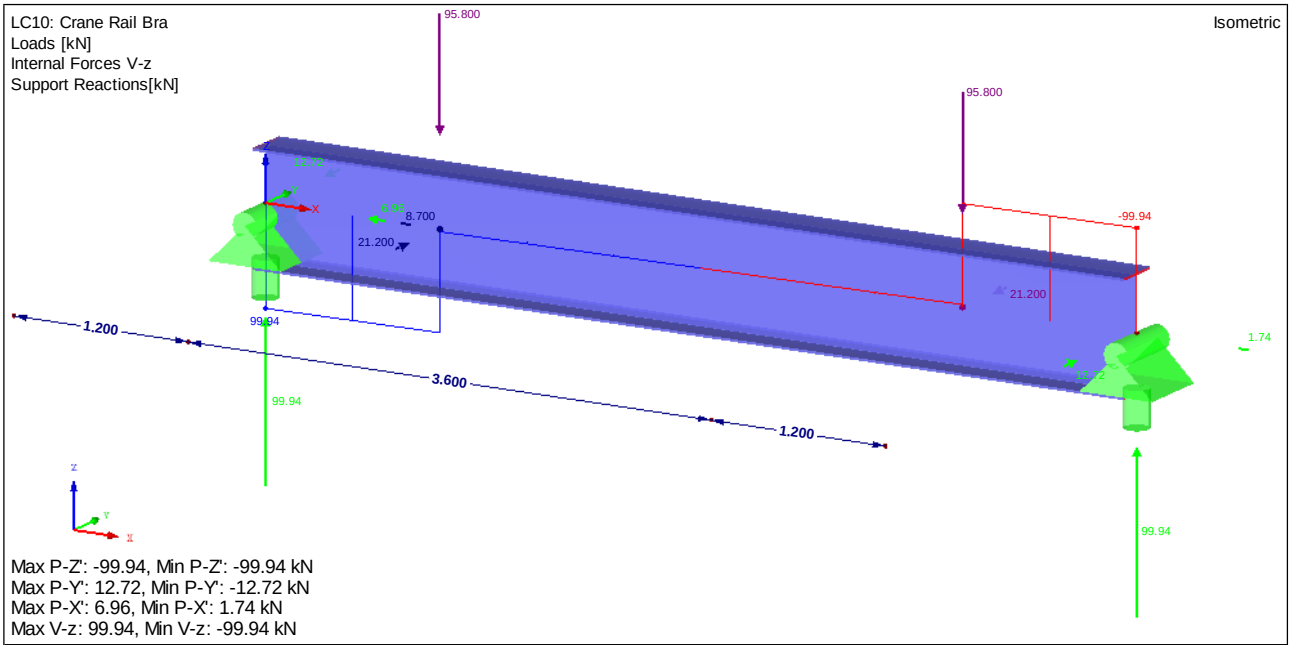

Appendix 36: Shear Force V_z for Brazilian Runway Girder Verification (Crane Middle)

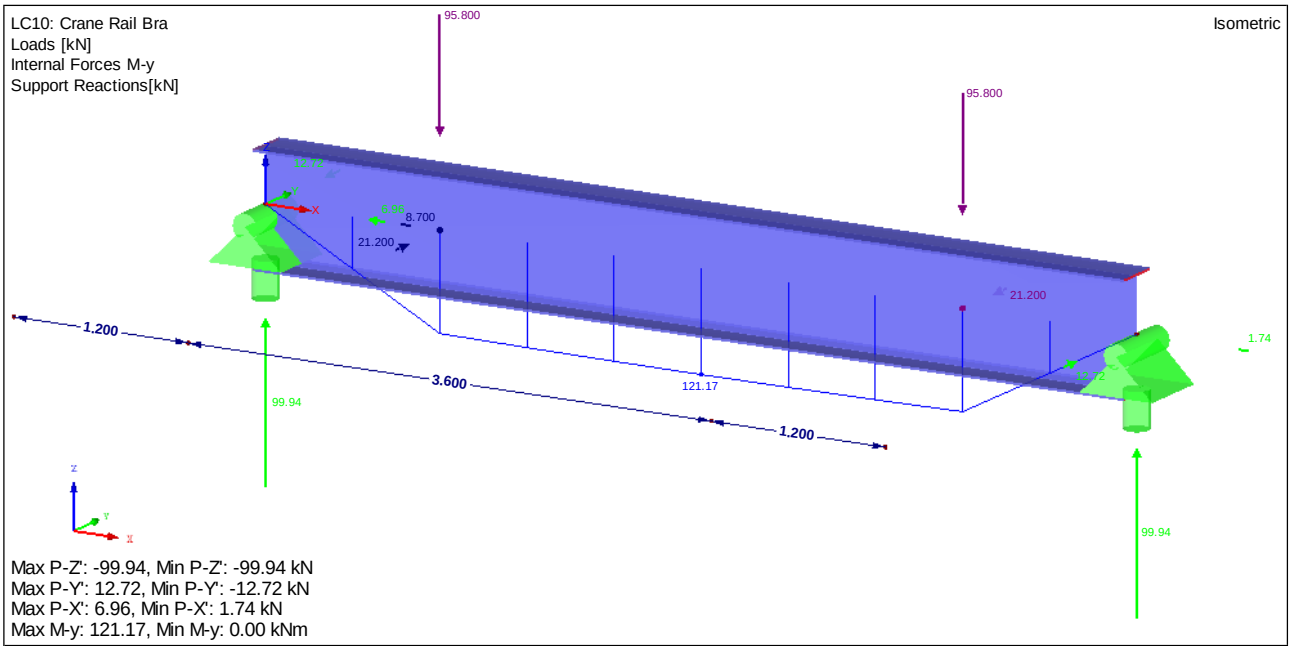

Appendix 37: Moment Force M_y for Brazilian Runway Girder Verification (Crane Middle)

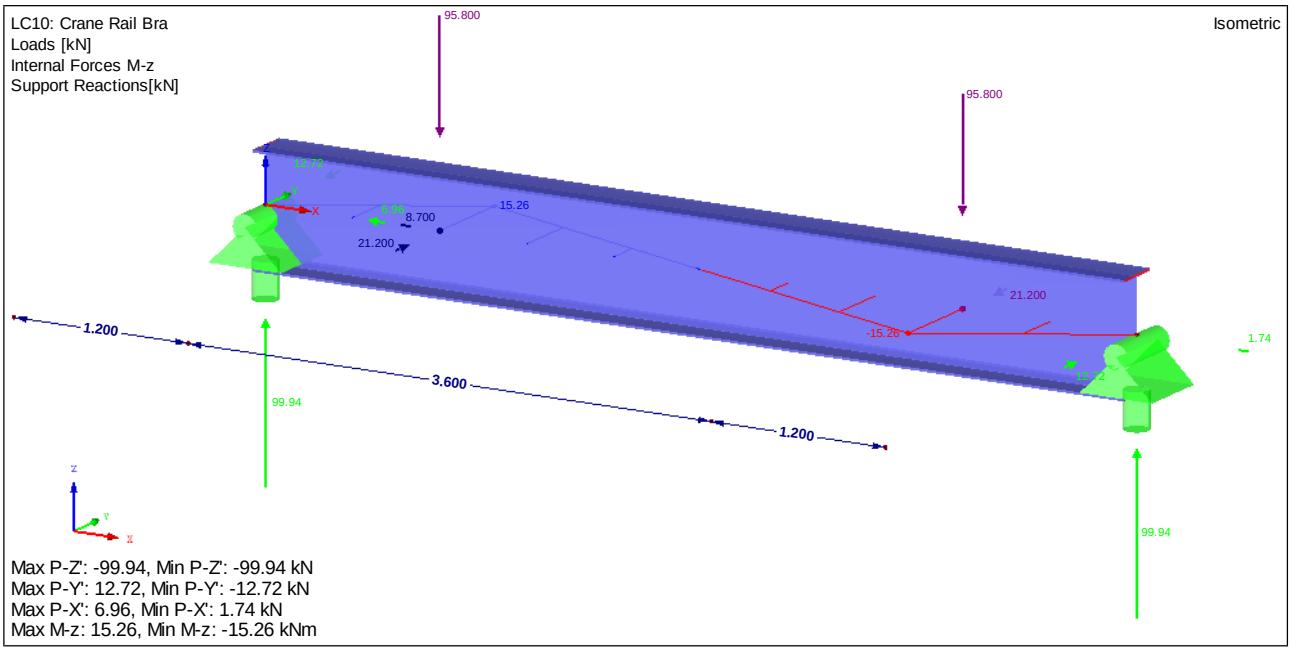

Appendix 38: Moment Force M_z for Brazilian Runway Girder Verification (Crane Middle)

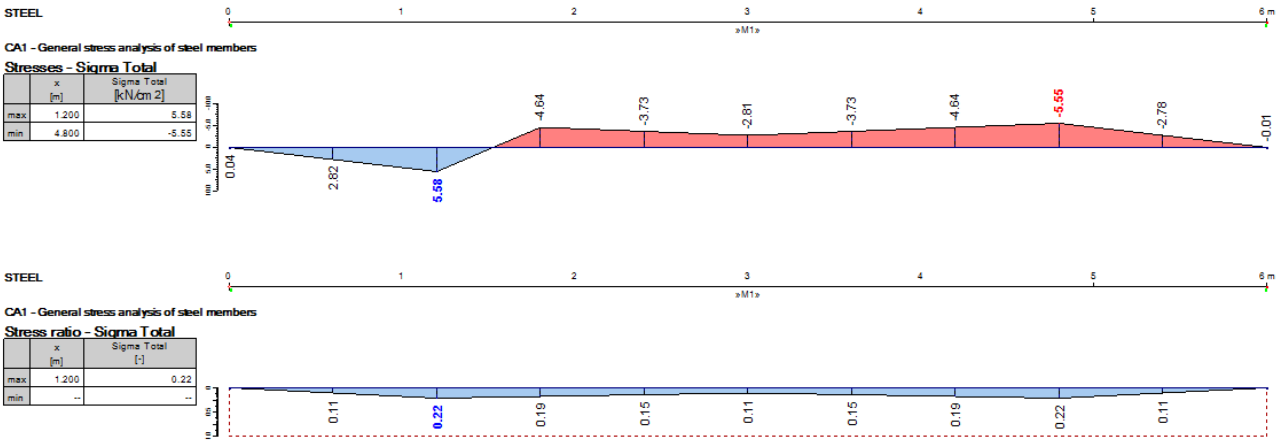

Appendix 39: Stress Ratio of the Runway Girder (Crane Middle) for the ASD (Brazilian)

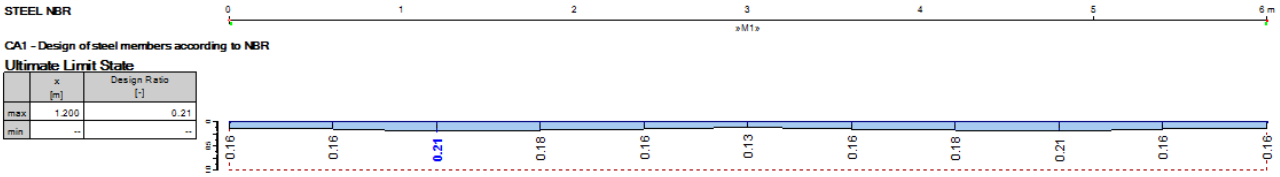

Appendix 40: Design Ratio of the Runway Girder (Crane Middle) for the NBR (ULS)

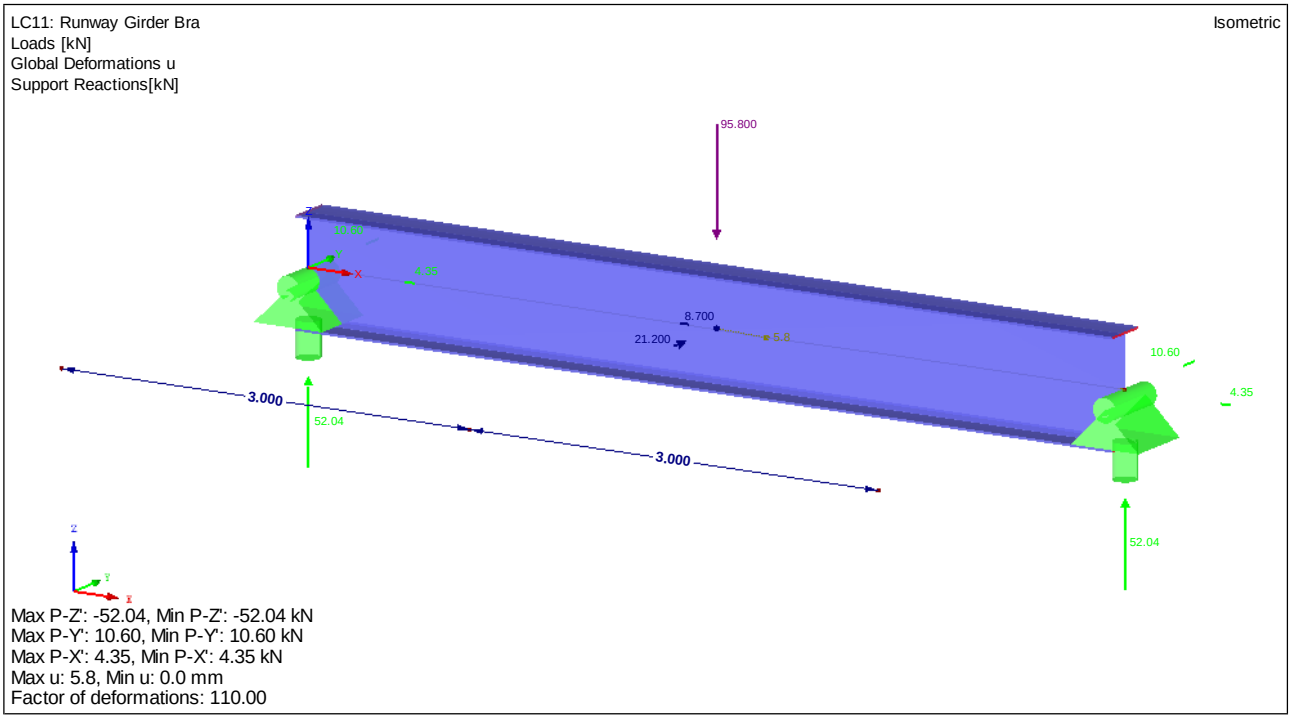

Appendix 41: Deformation for Brazilian Runway Girder Verification (Wheel Middle)

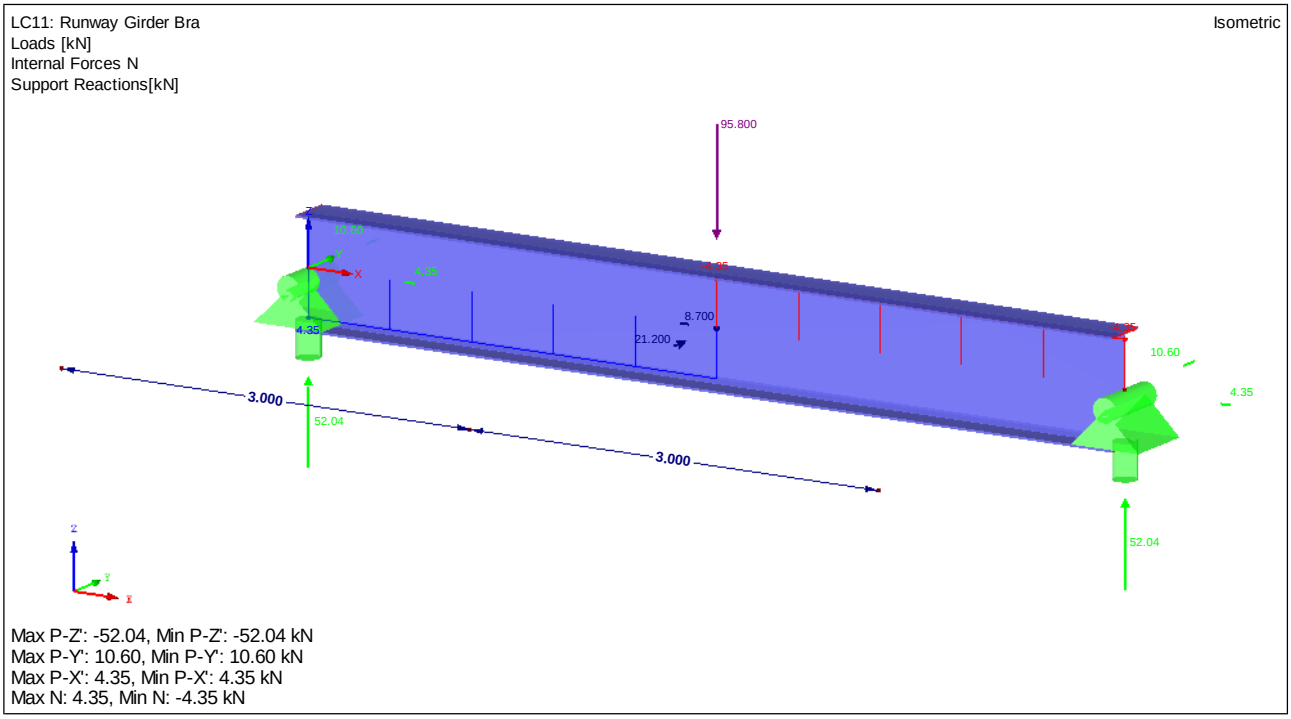

Appendix 42: Normal Force N for Brazilian Runway Girder Verification (Wheel Middle)

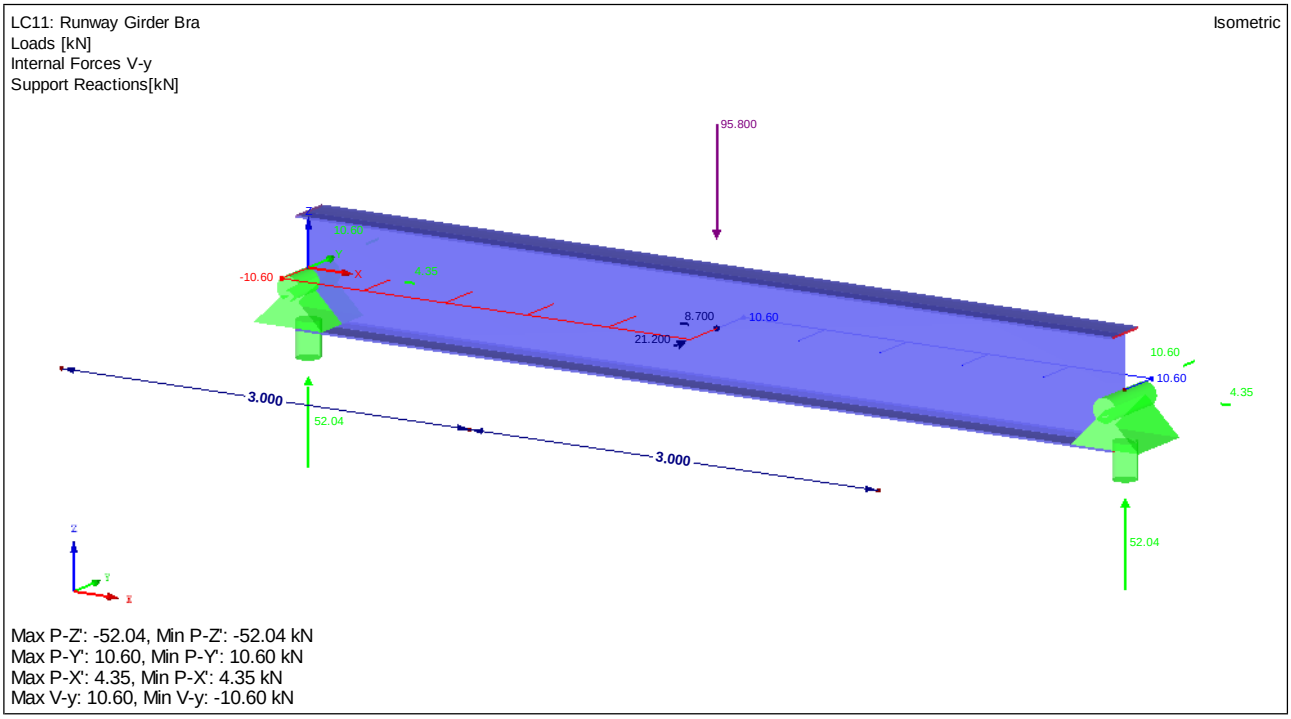

Appendix 43: Shear Force V_y for Brazilian Runway Girder Verification (Wheel Middle)

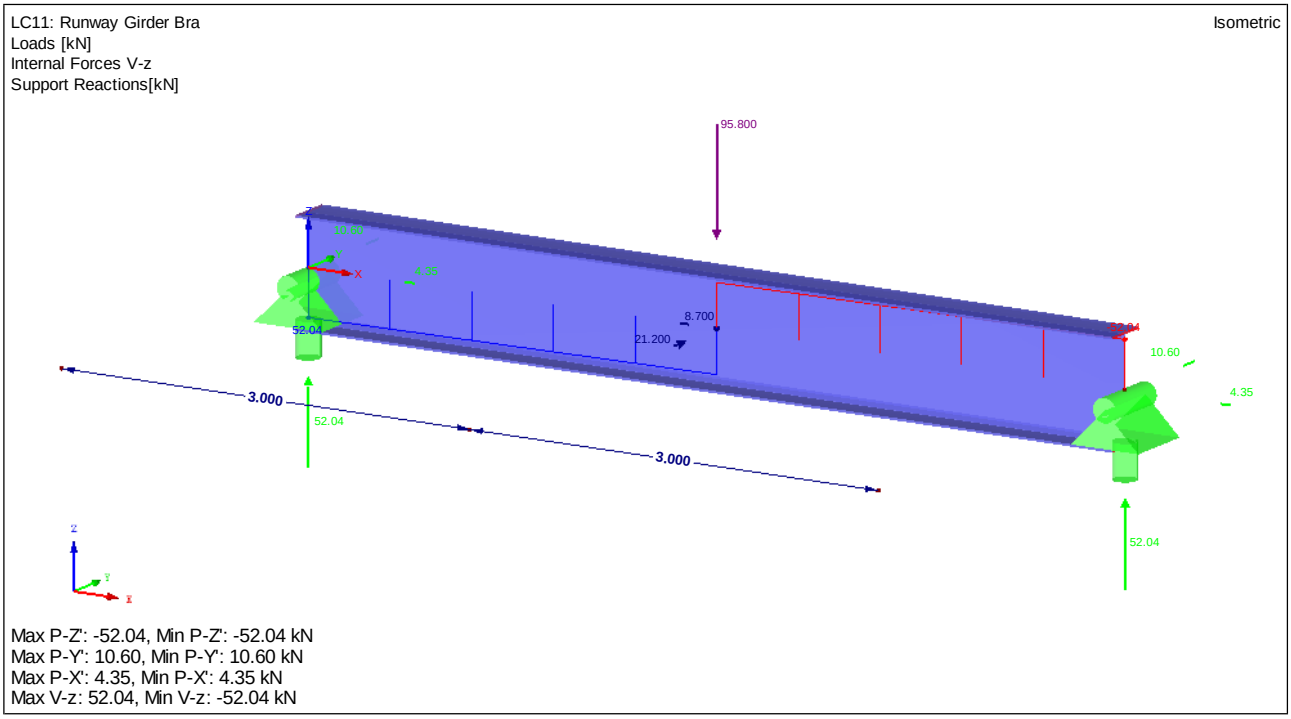

Appendix 44: Shear Force V_z for Brazilian Runway Girder Verification (Wheel Middle)

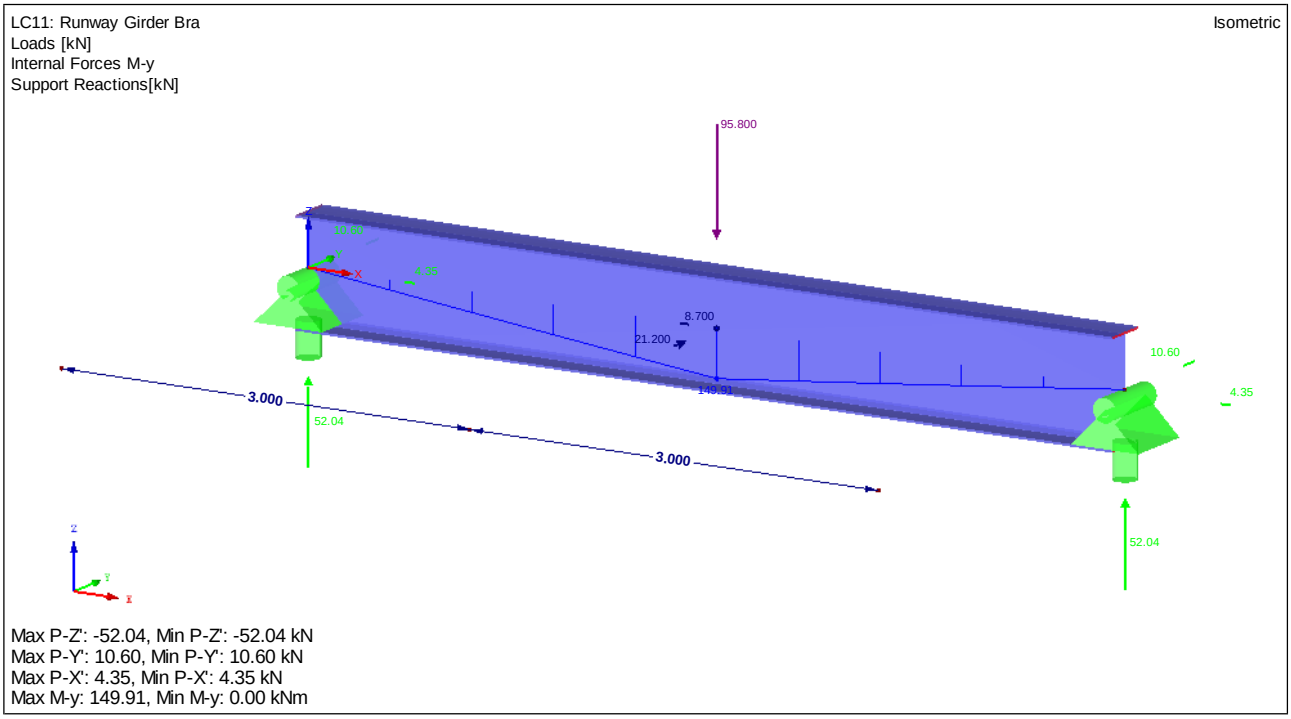

Appendix 45: Moment Force M_y for Brazilian Runway Girder Verification (Wheel Middle)

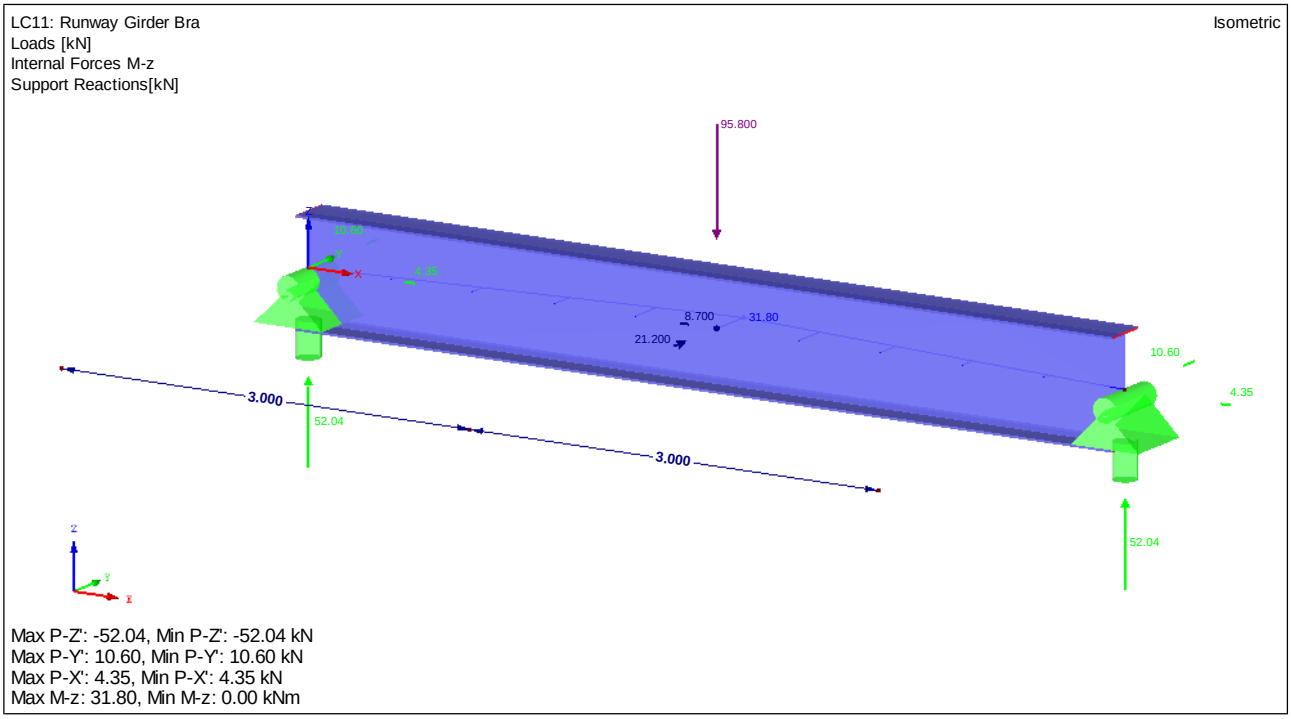

Appendix 46: Moment Force M_z for Brazilian Runway Girder Verification (Wheel Middle)

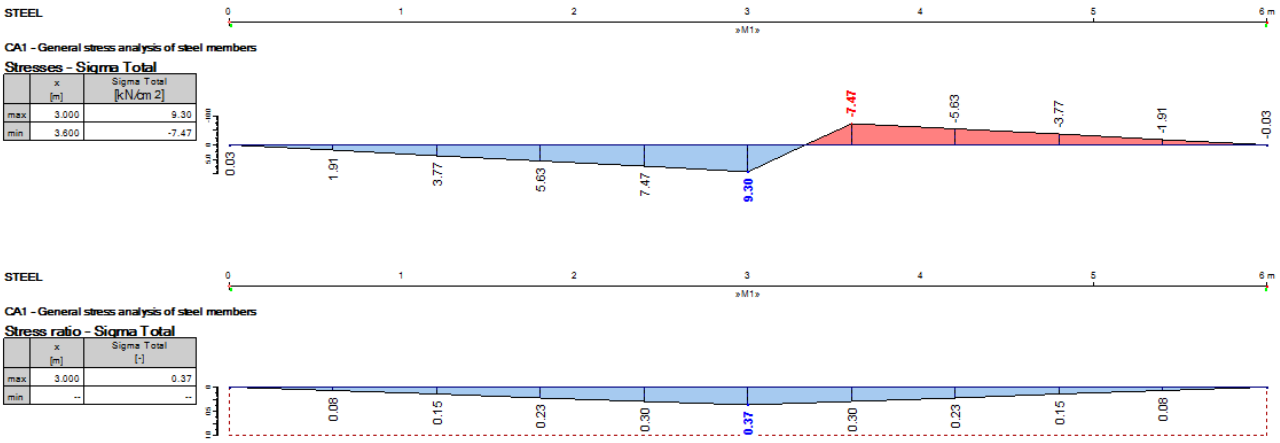

Appendix 47: Stress Ratio of the Runway Girder (Wheel Middle) for the ASD (Brazilian)

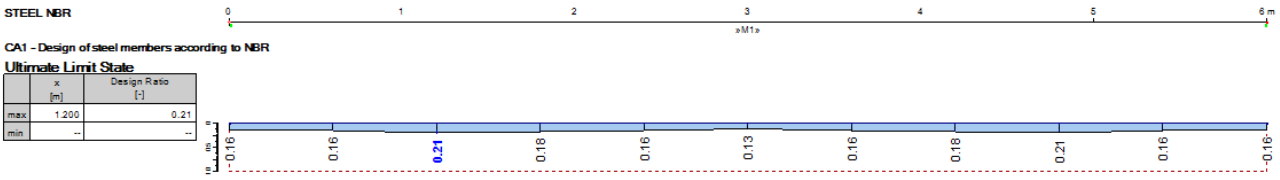

Appendix 48: Design Ratio of the Runway Girder (Wheel Middle) for the NBR (ULS)

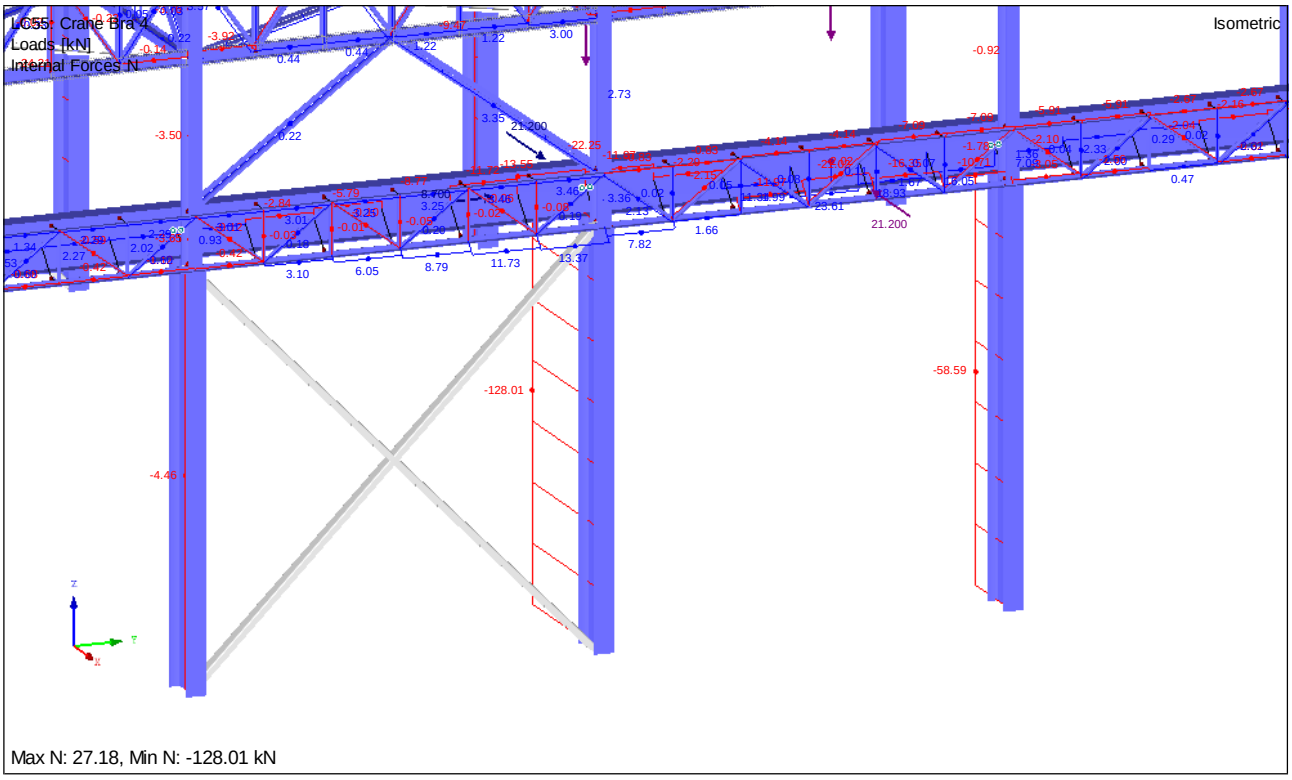

Appendix 49: Results for Wheel Loads with Column Underneath one Wheel (4th Position)

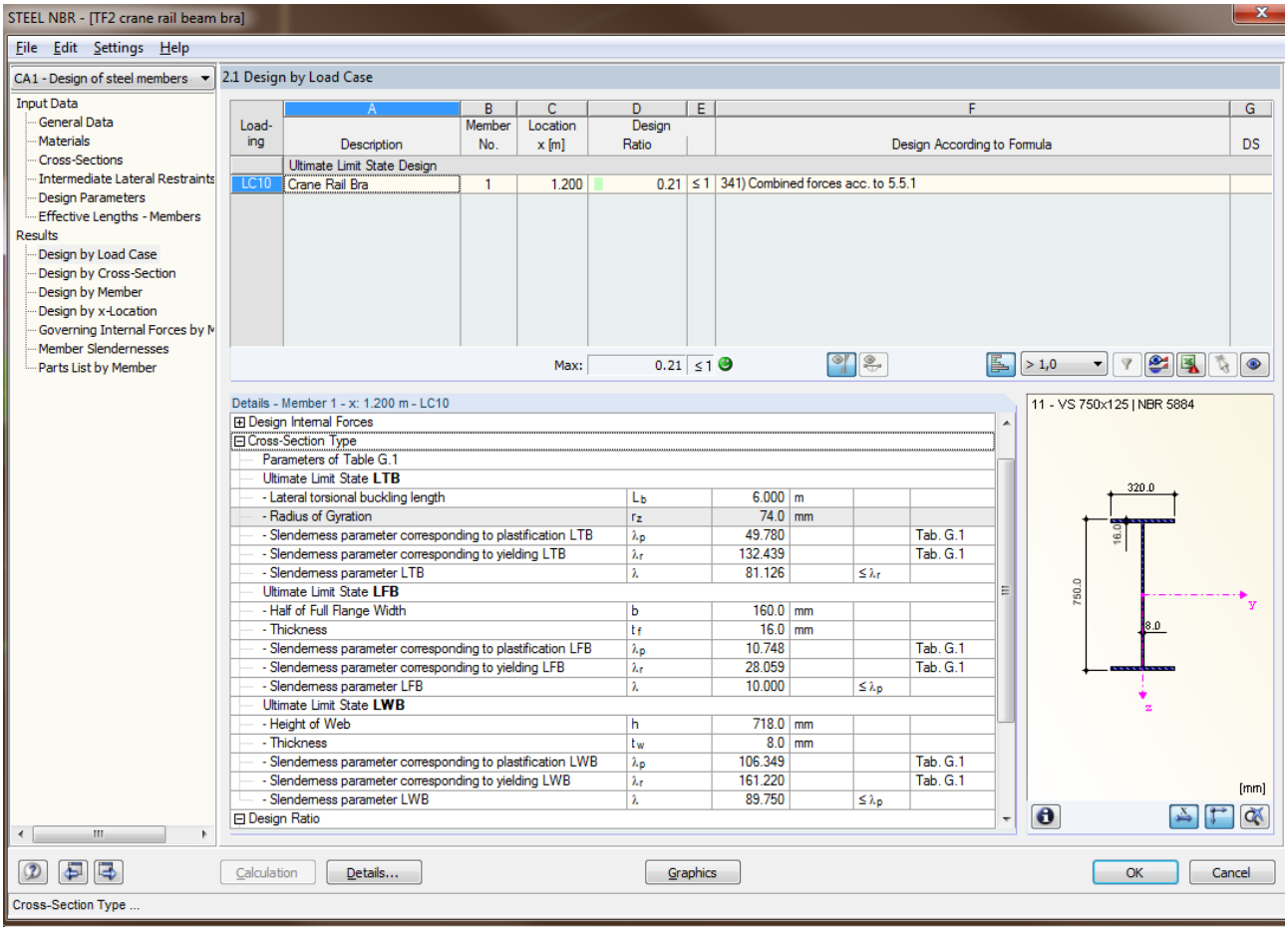

Appendix 50: Demonstration of Brazilian Norm Verification (Parameters of Cross-Section Type)

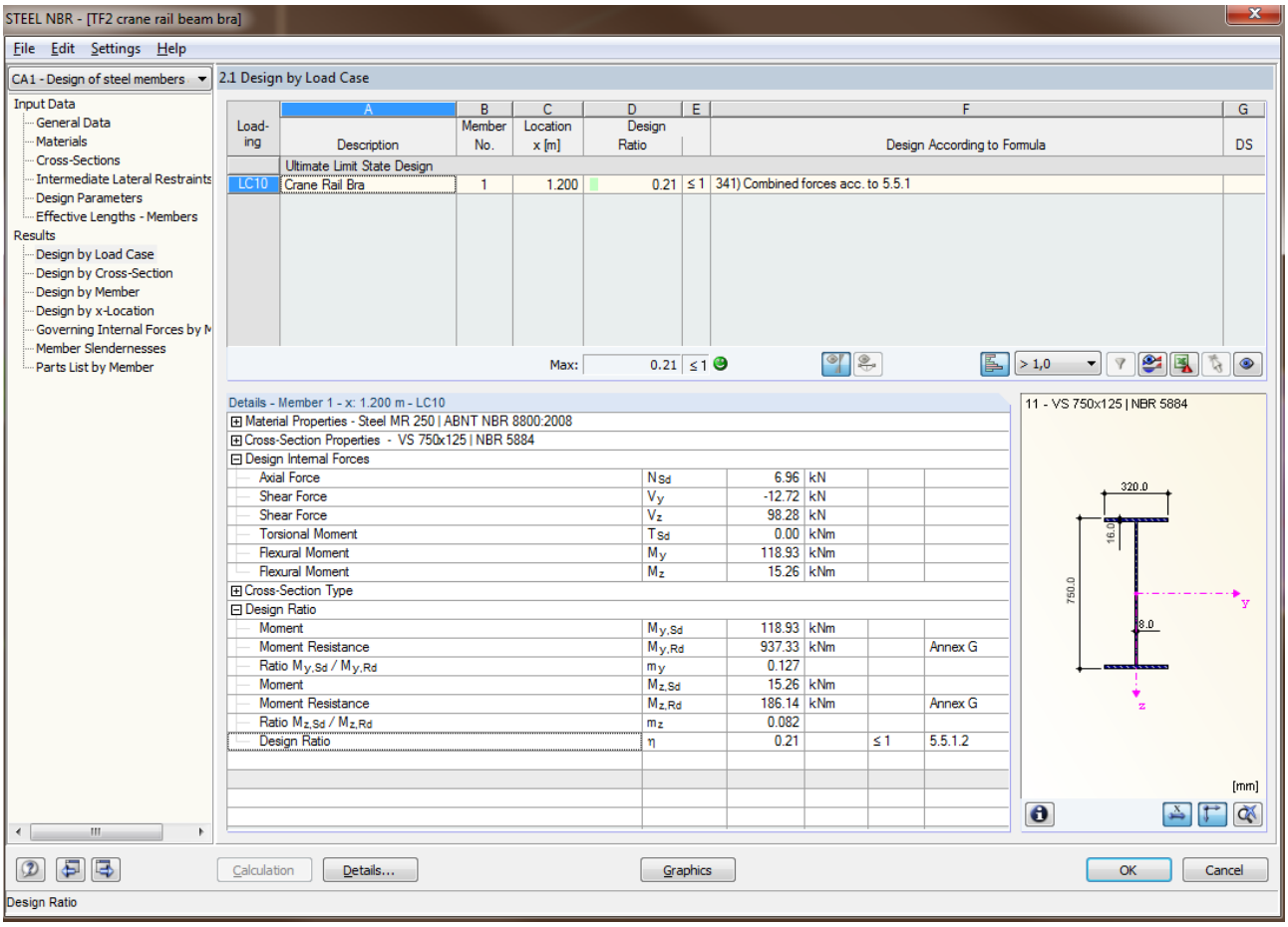

Appendix 51: Demonstration of Brazilian Norm Verification (Internal Forces and Design Ratio Calculations)

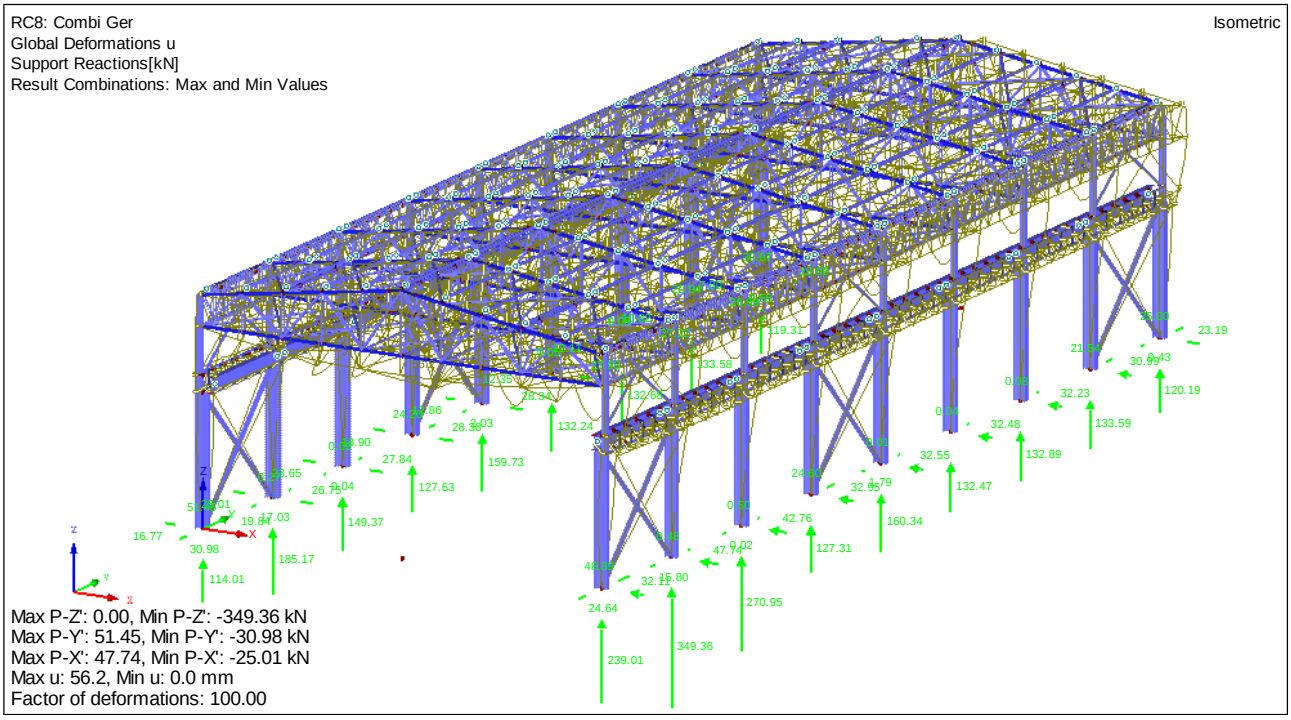

Appendix 52: Global Deformation Results for the German Hall (ULS)

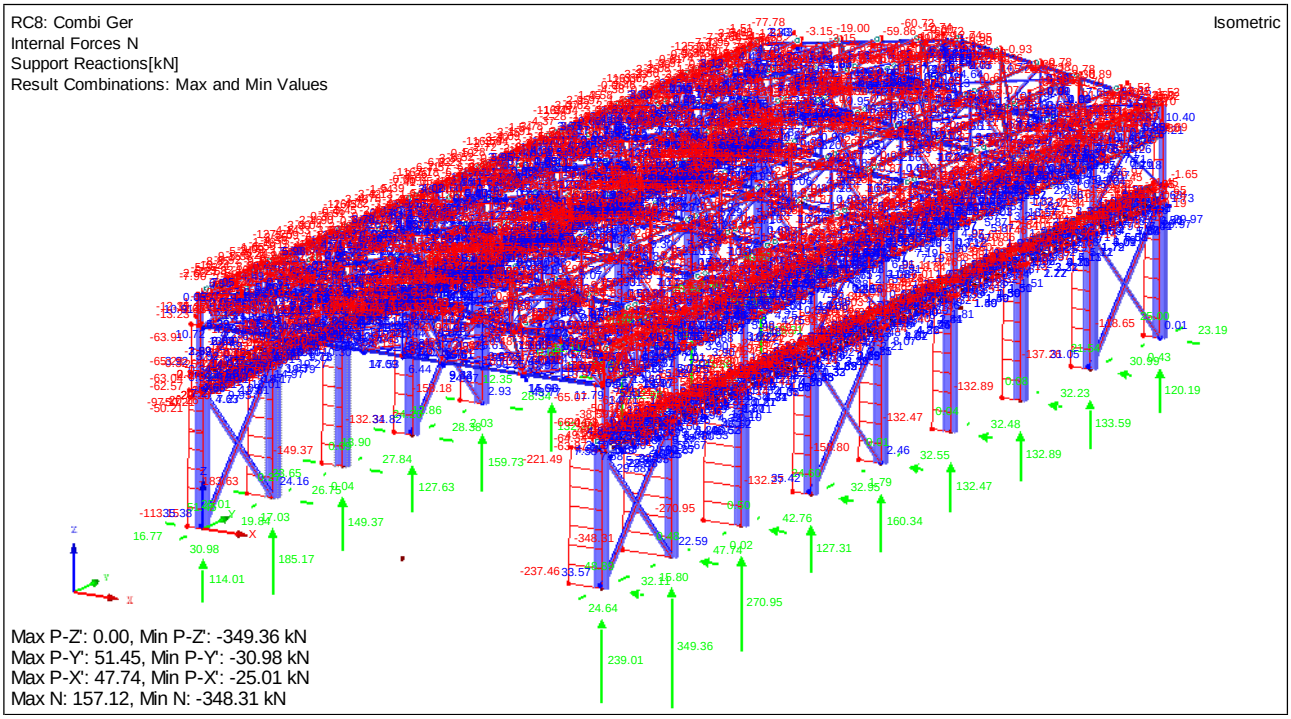

Appendix 53: Normal Forces N for the German Hall (ULS)

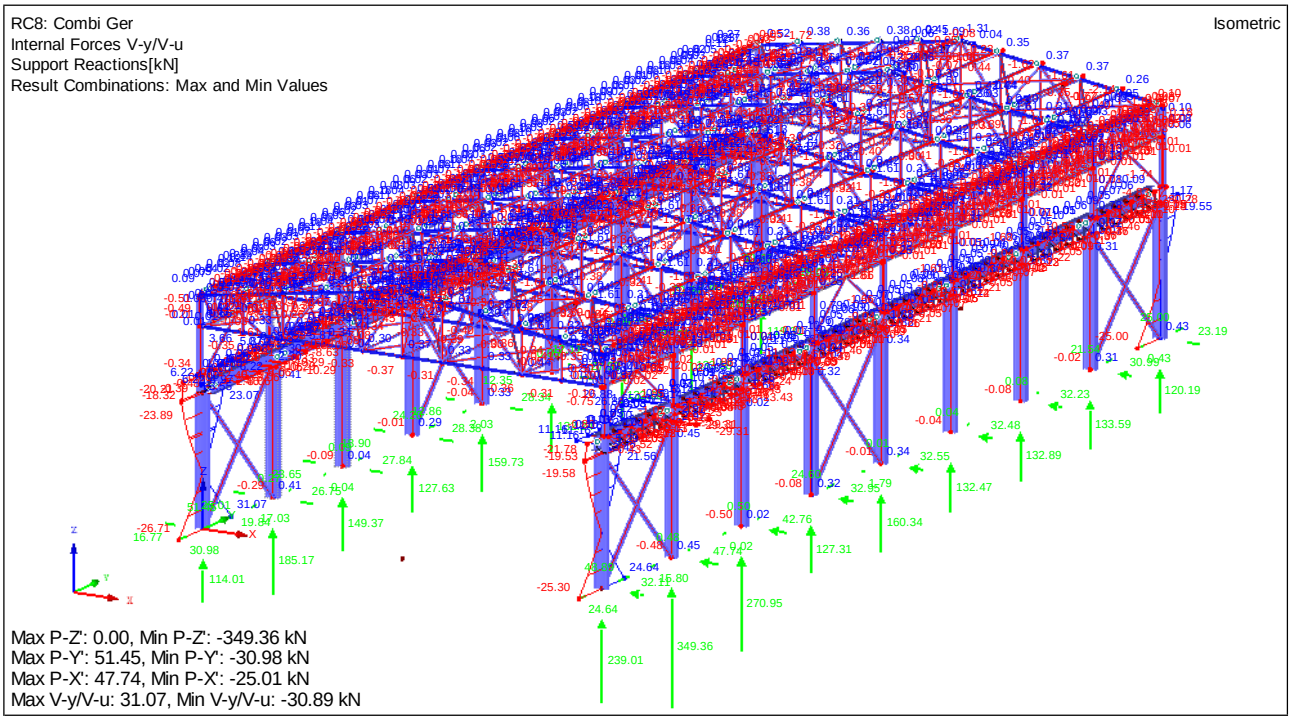

Appendix 54: Shear Forces V_y for the German Hall (ULS)

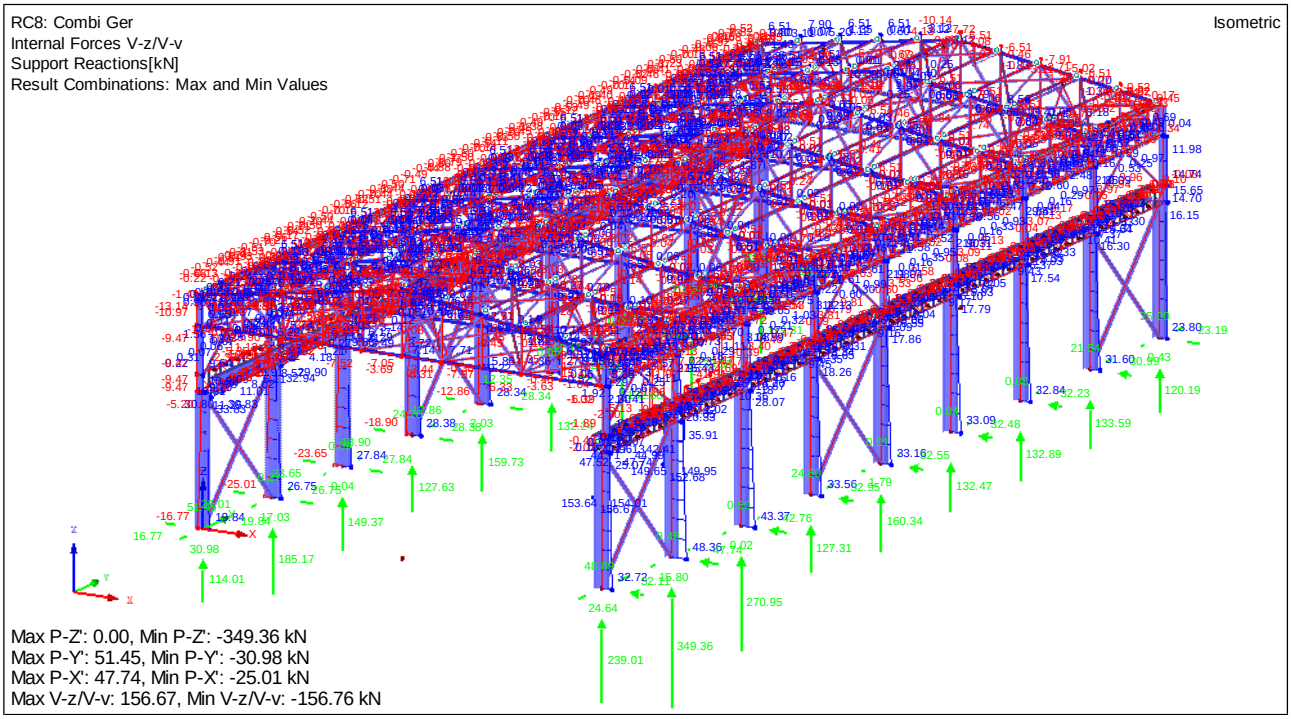

Appendix 55: Shear Forces V_z for the German Hall (ULS)

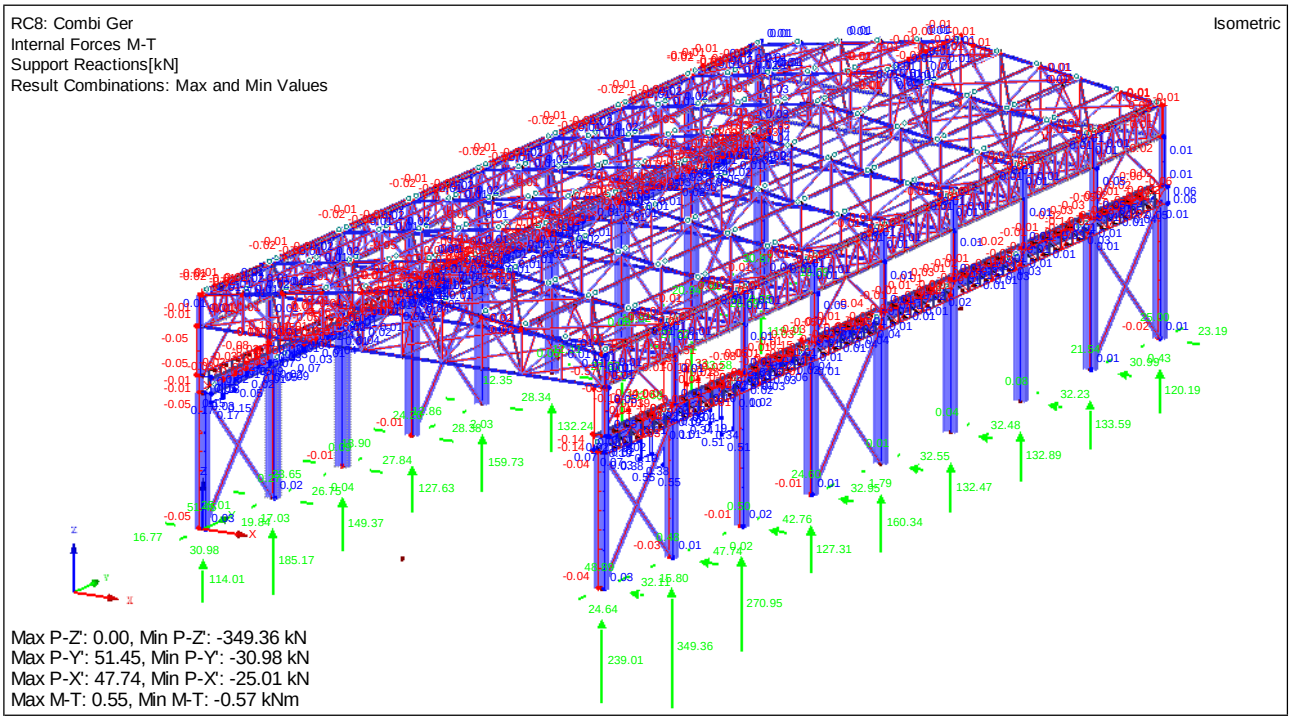

Appendix 56: Torsion Forces M_T for the German Hall (ULS)

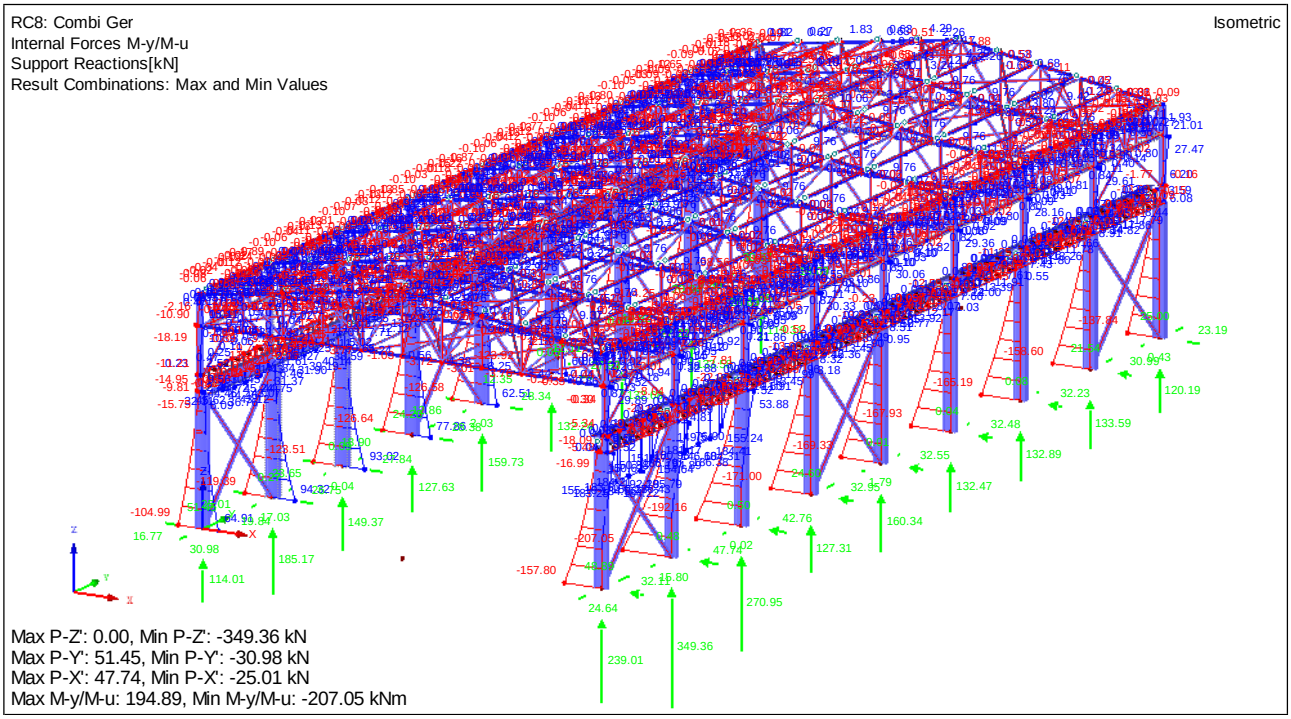

Appendix 57: Moment Forces M_y for the German Hall (ULS)

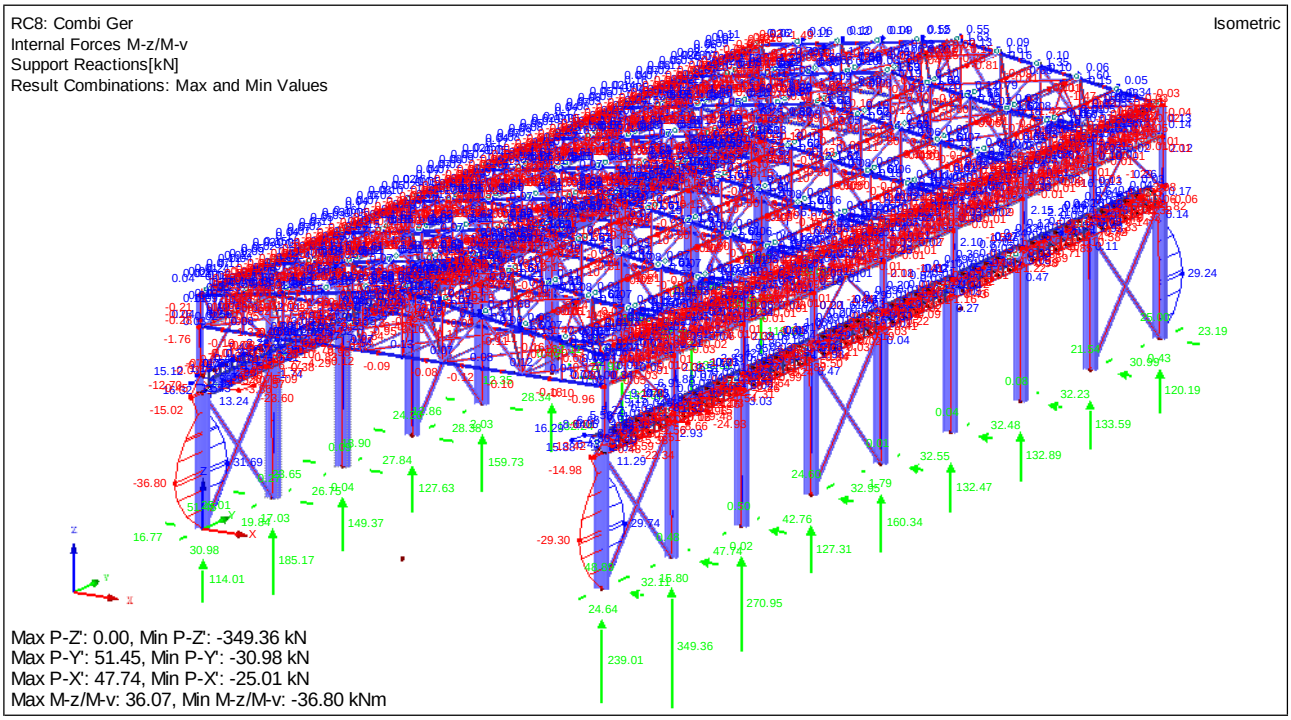

Appendix 58: Moment Forces M_z for the German Hall (ULS)

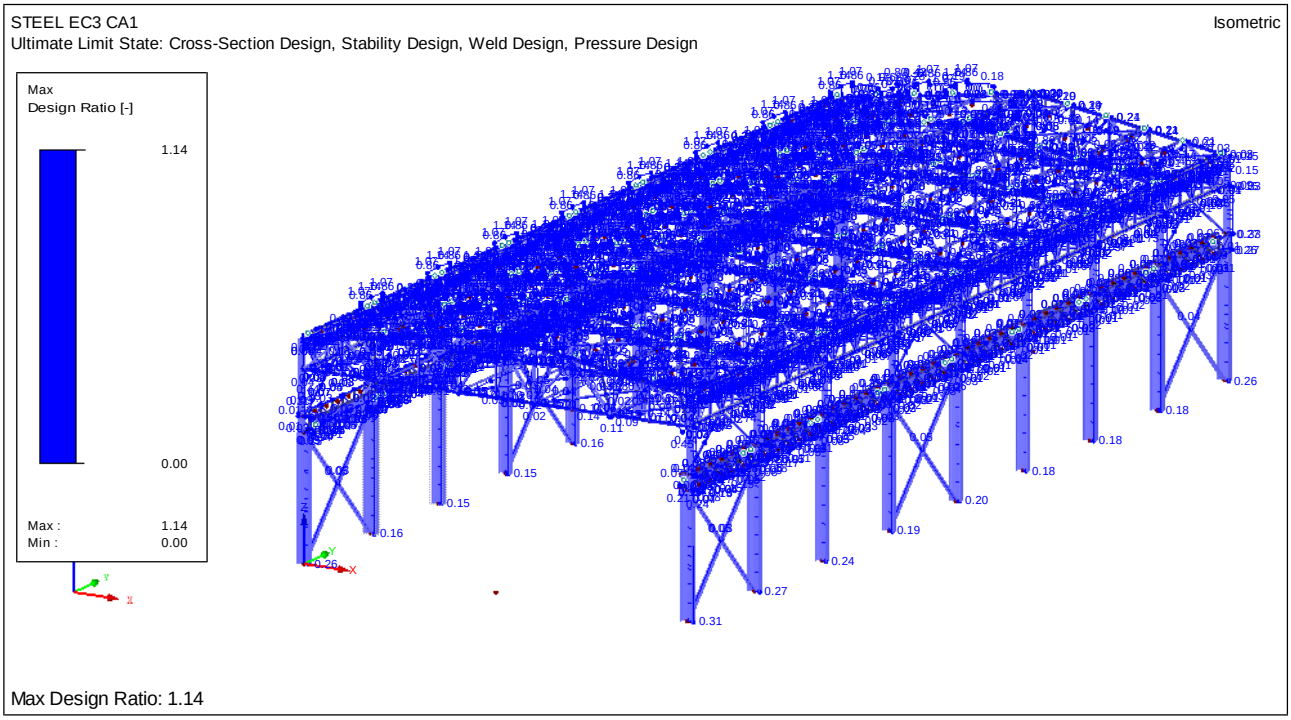

Appendix 59: Design Ratios from the EC-3 for the German Hall (ULS)

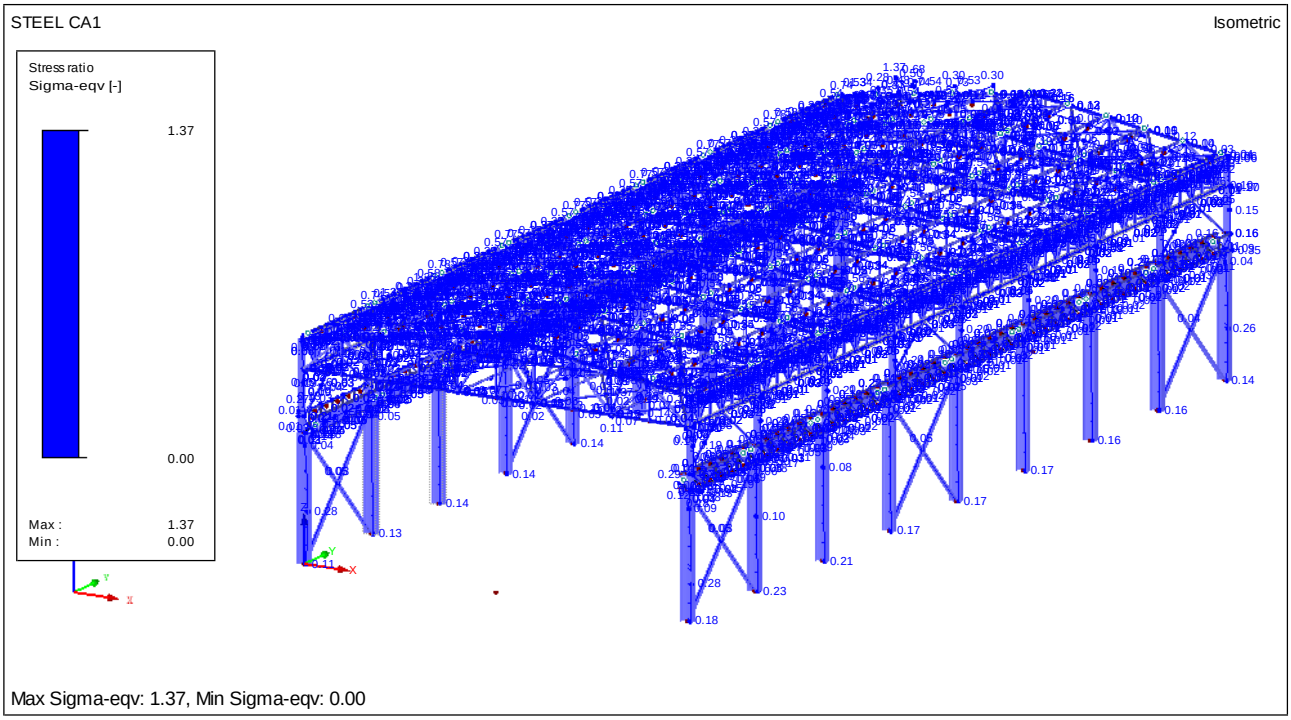

Appendix 60: Stress Ratios from the ASD for the German Hall (ULS)

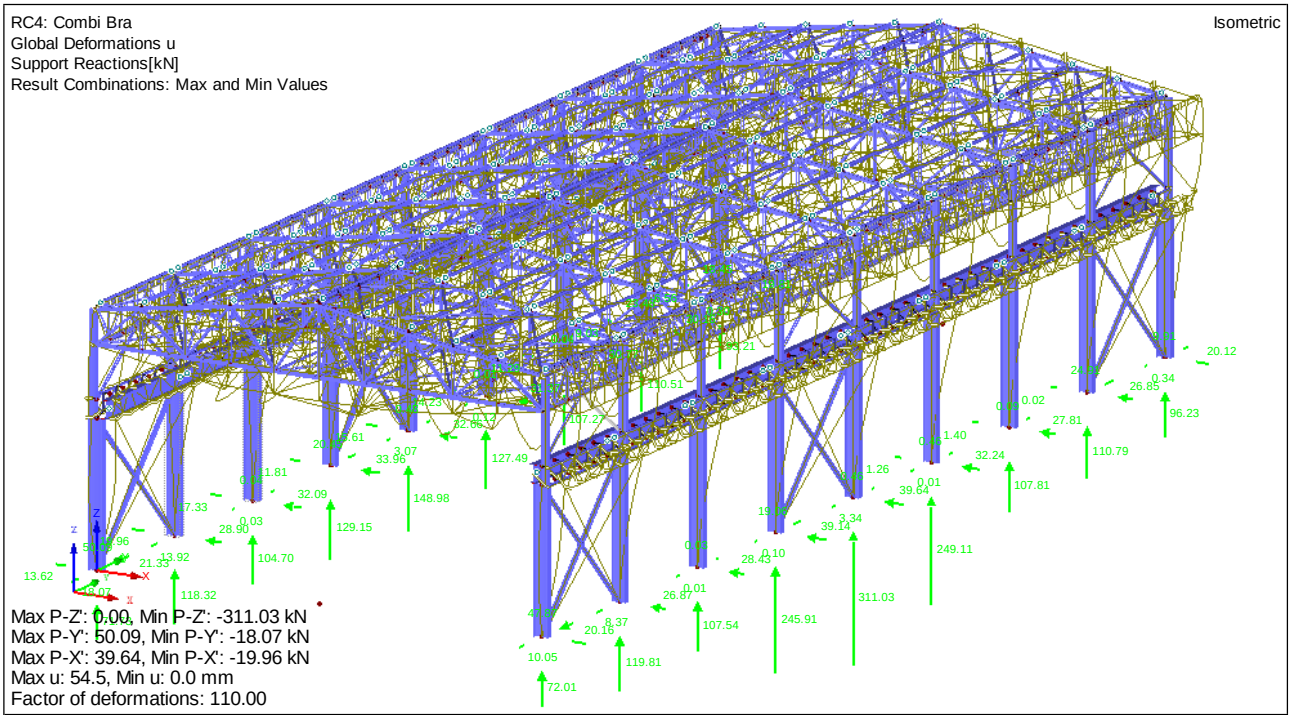

Appendix 61: Global Deformation Results for the Brazilian Hall (ULS)

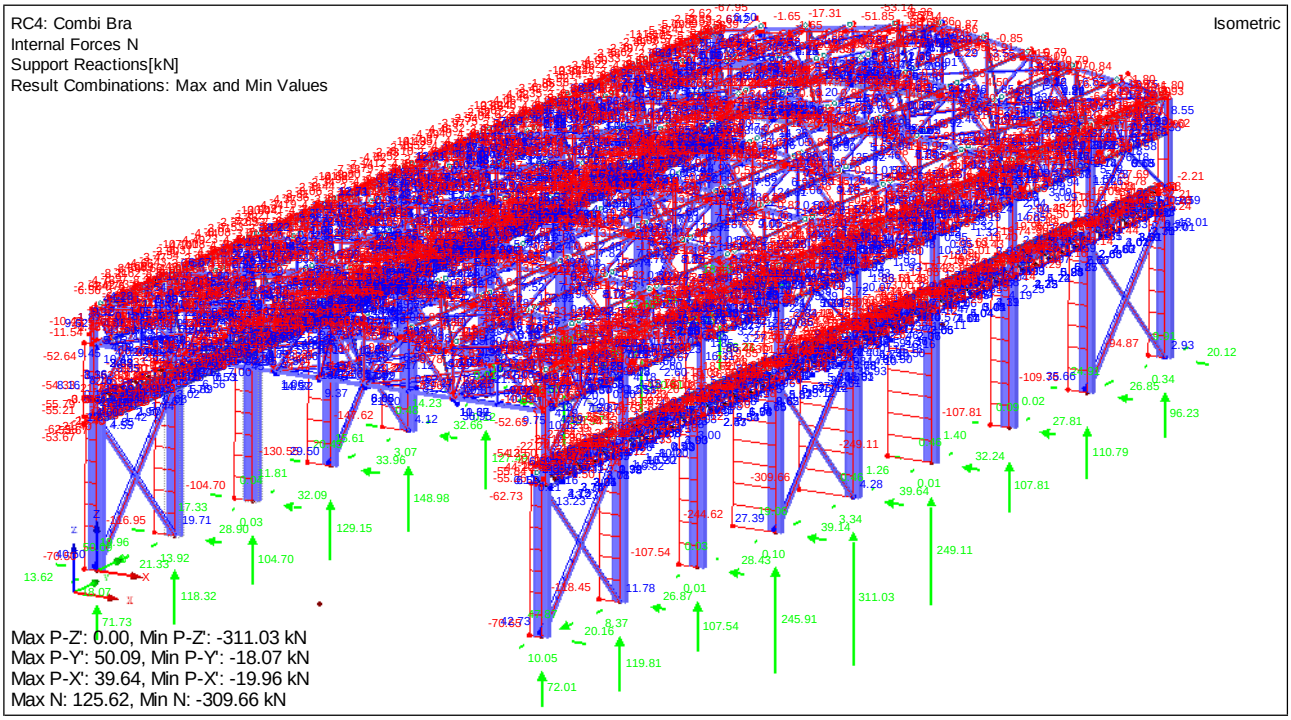

Appendix 62: Normal Forces N for the Brazilian Hall (ULS)

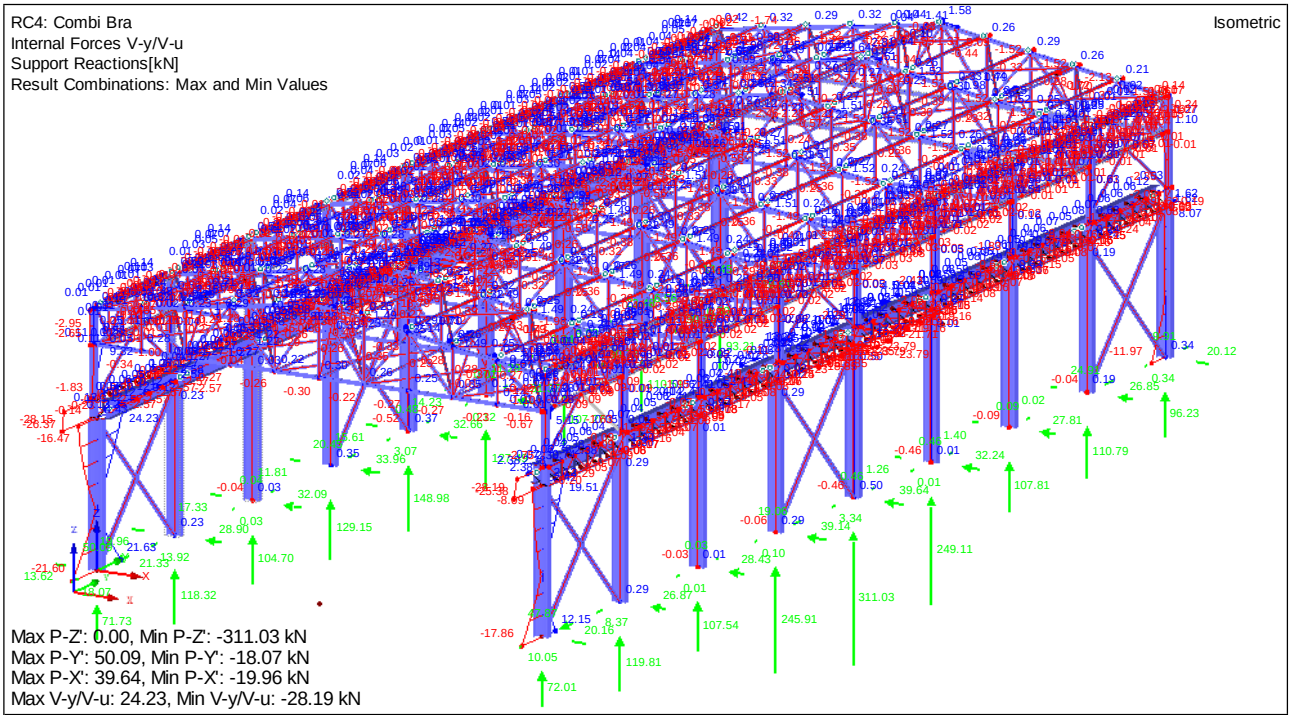

Appendix 63: Shear Forces V_y for the Brazilian Hall (ULS)

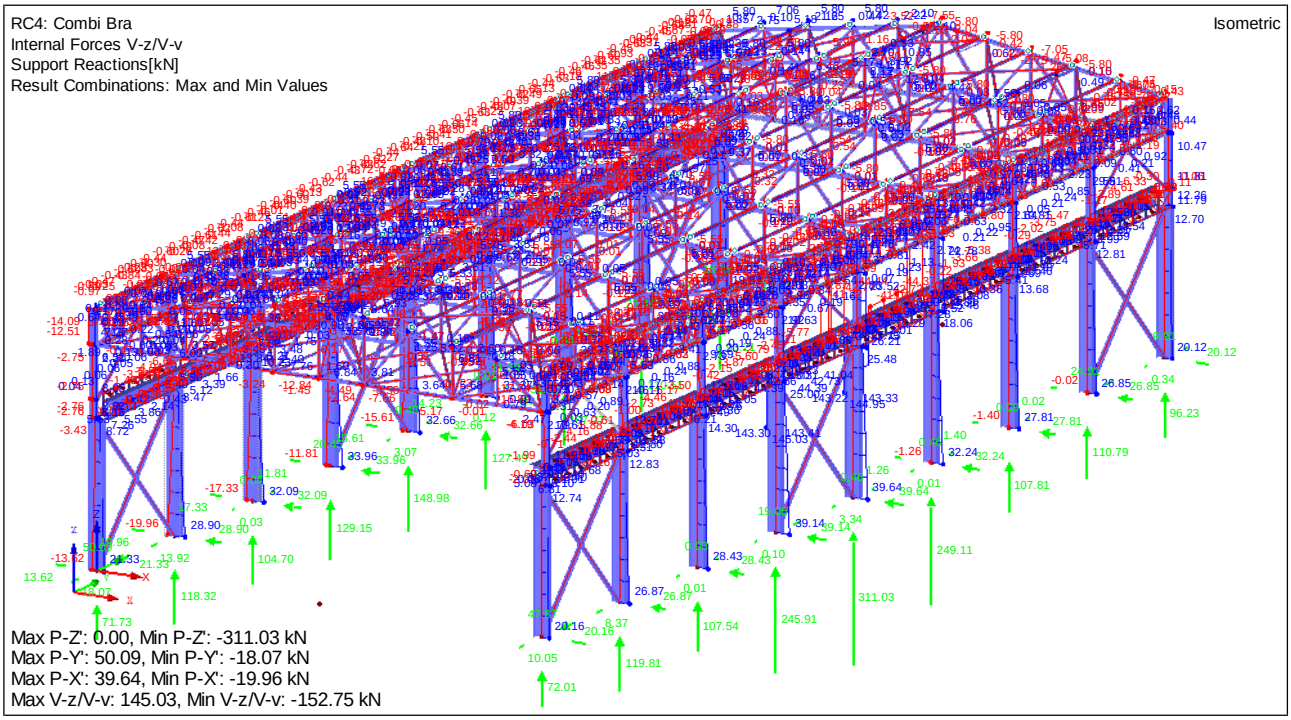

Appendix 64: Shear Forces V_z for the Brazilian Hall (ULS)

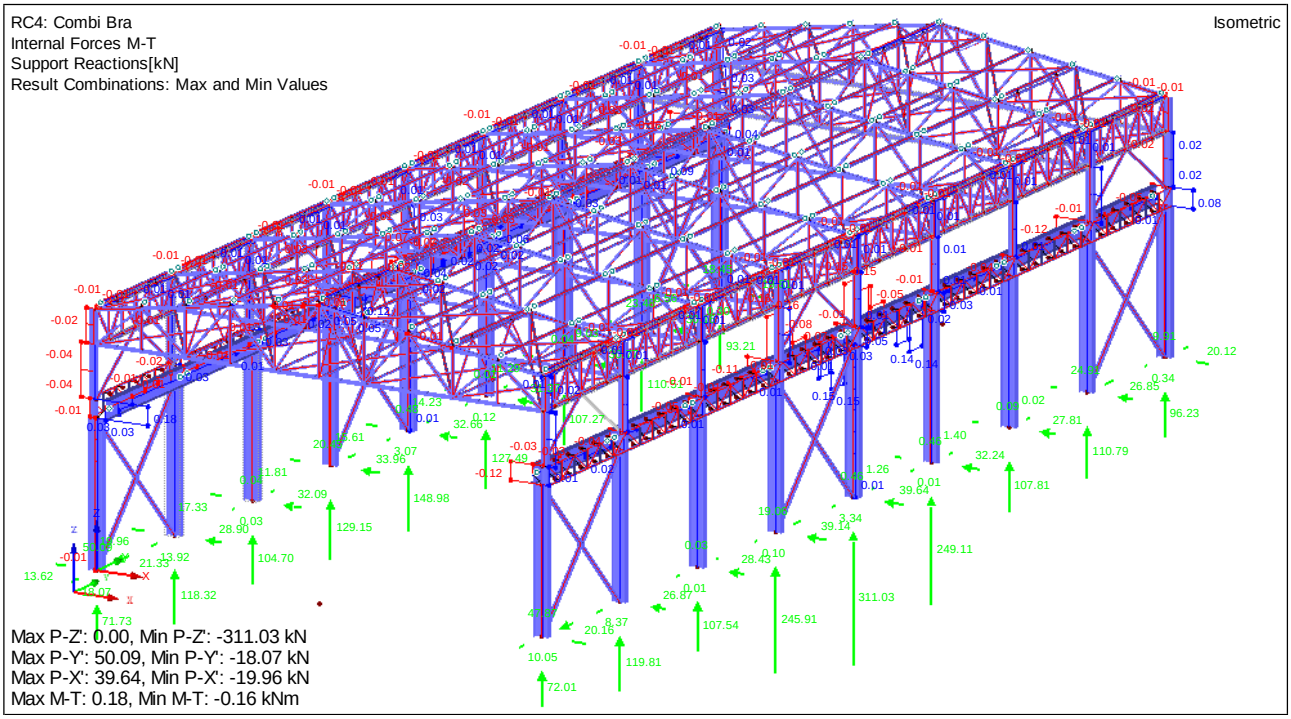

Appendix 65: Torsion Forces M_T for the Brazilian Hall (ULS)

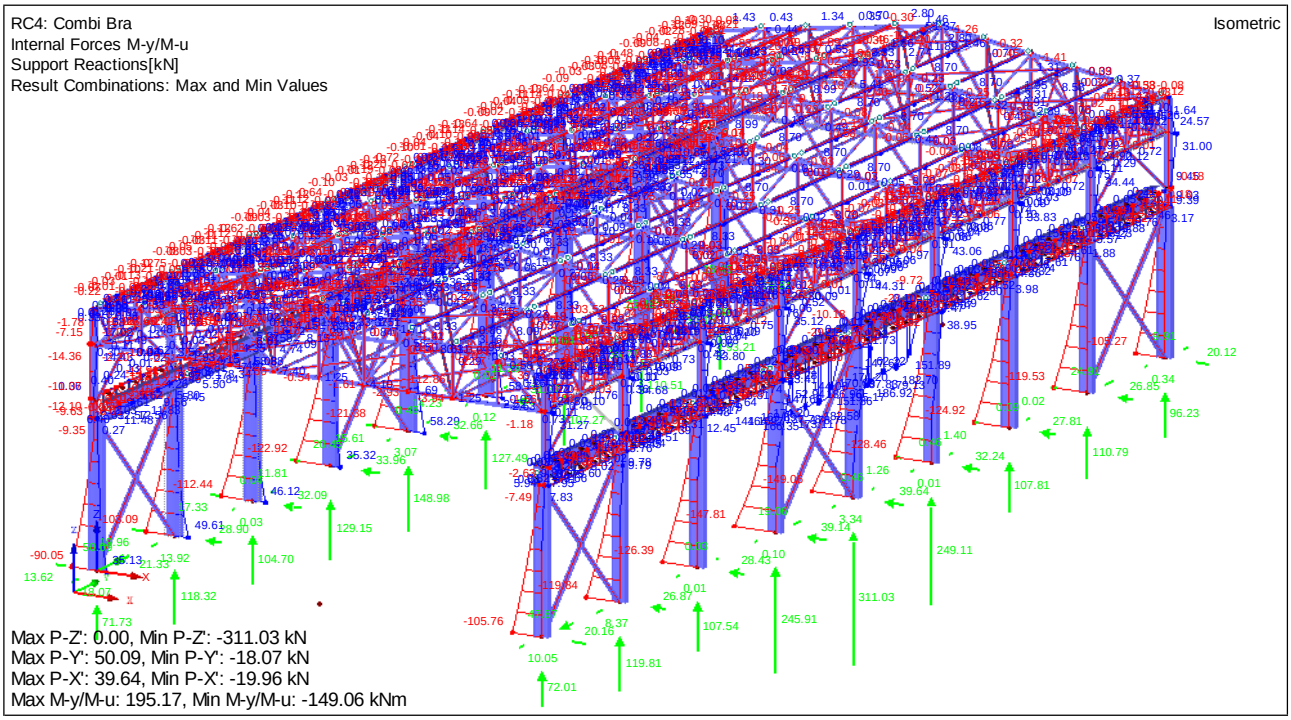

Appendix 66: Moment Forces M_y for the Brazilian Hall (ULS)

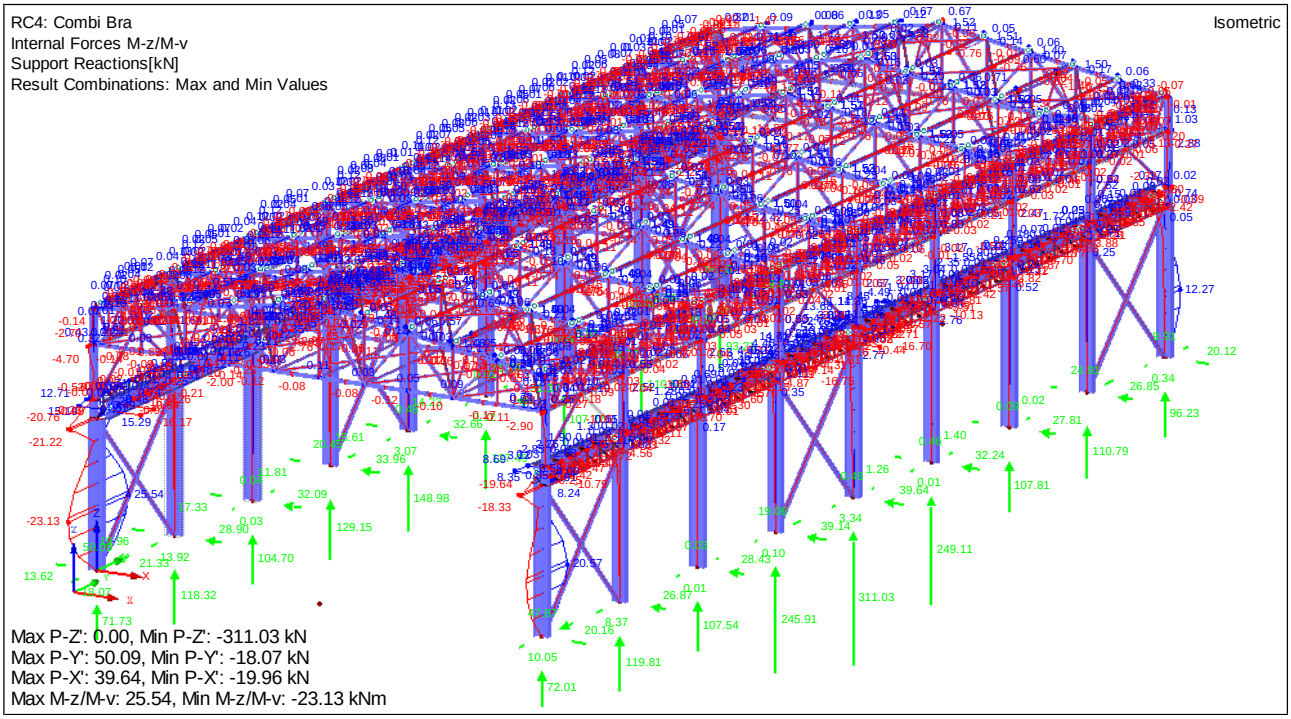

Appendix 67: Moment Forces M_z for the Brazilian Hall (ULS)

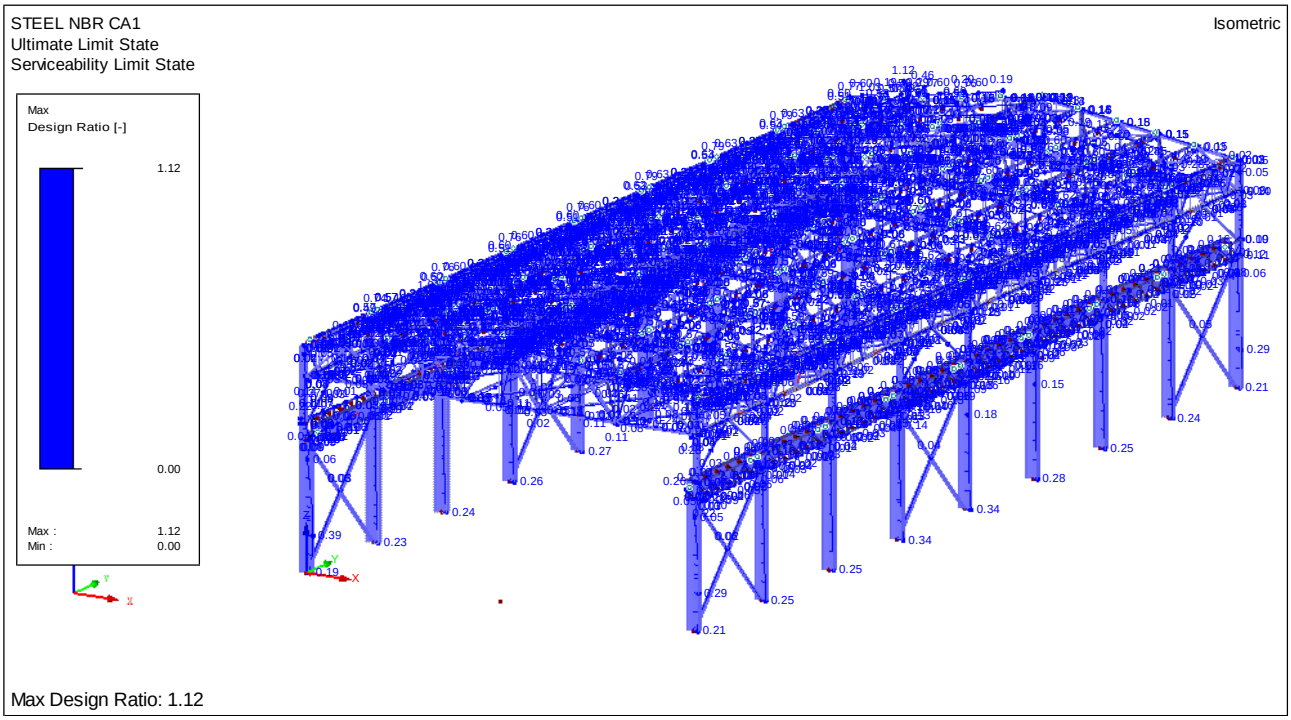

Appendix 68: Design Ratios from the NBR for the Brazilian Hall (ULS)

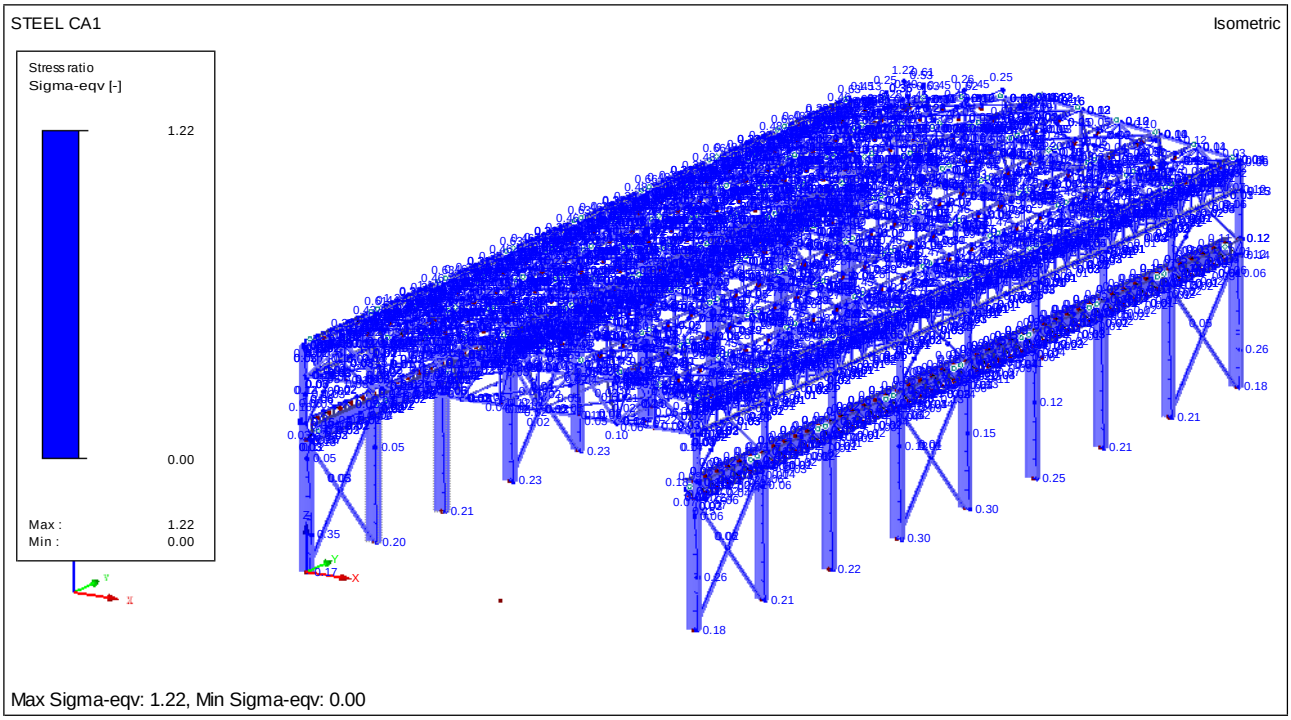

Appendix 69: Stress Ratios from the ASD for the Brazilian Hall (ULS)

RSTAB8

RC4: Combi Bra

Internal forces - N

	x [m]	N [kN]
max	--	--
min	90.000	-309.66

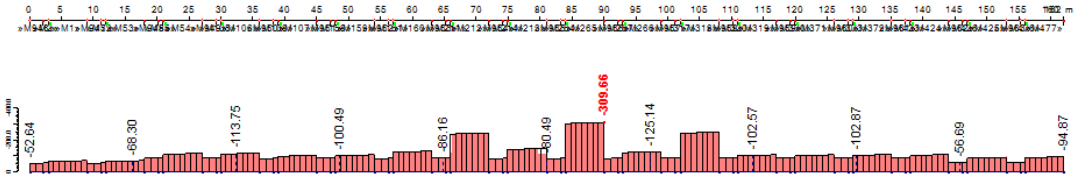

RSTAB8

RC4: Combi Bra

Internal forces - V_Y/V_U

	x [m]	V_Y/V_U [kN]
max	2.936	24.23
min	11.936	-28.19

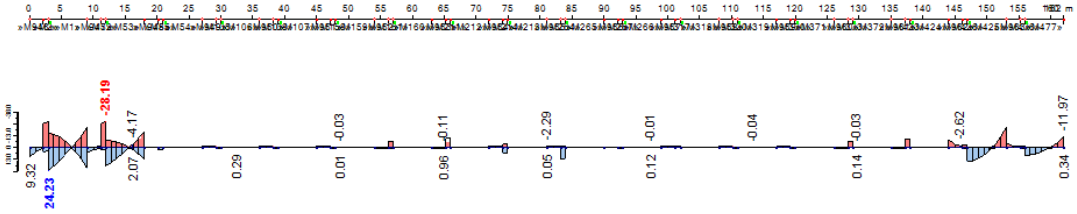

RSTAB8

RC4: Combi Bra

Internal forces - V_Z/V_V

	x [m]	V_Z/V_V [kN]
max	90.000	39.64
min	27.000	-19.96

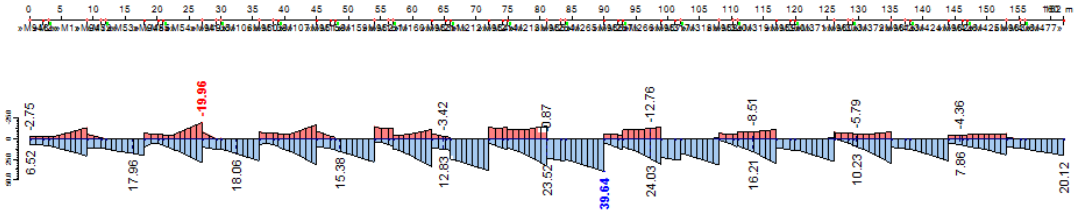

RSTAB8

RC4: Combi Bra

Internal forces - M_T

	x [m]	M_T [kNm]
max	2.186	0.18
min	146.936	-0.16

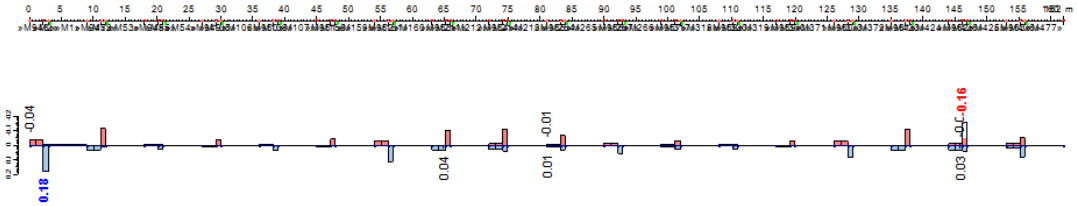

RSTAB8

RC4: Combi Bra

Internal forces - M_Y/M_U

	x [m]	M_Y/M_U [kNm]
max	83.936	62.22
min	90.000	-149.06

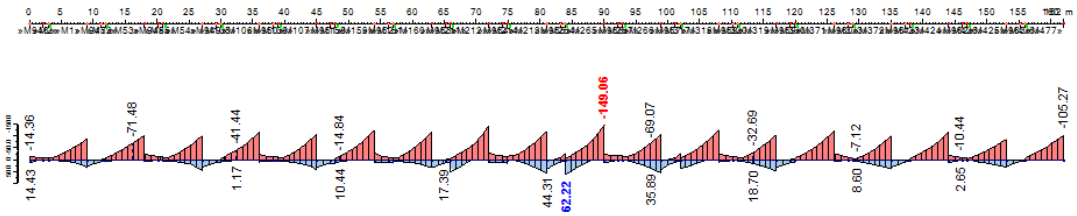

RSTAB8

RC4: Combi Bra

Internal forces - M_Z/M_V

	x [m]	M_Z/M_V [kNm]
max	6.574	25.54
min	6.574	-23.13

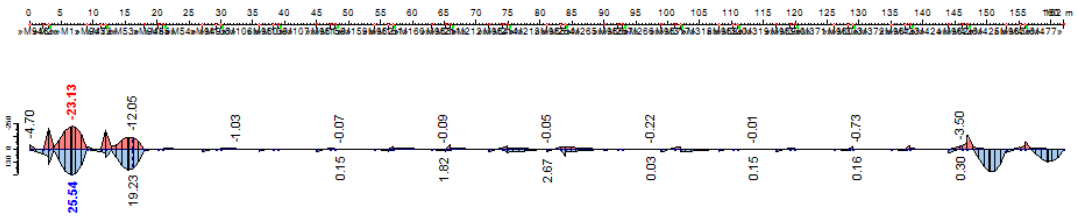

Appendix 70: Column Internal Forces (Brazilian) (ULS)

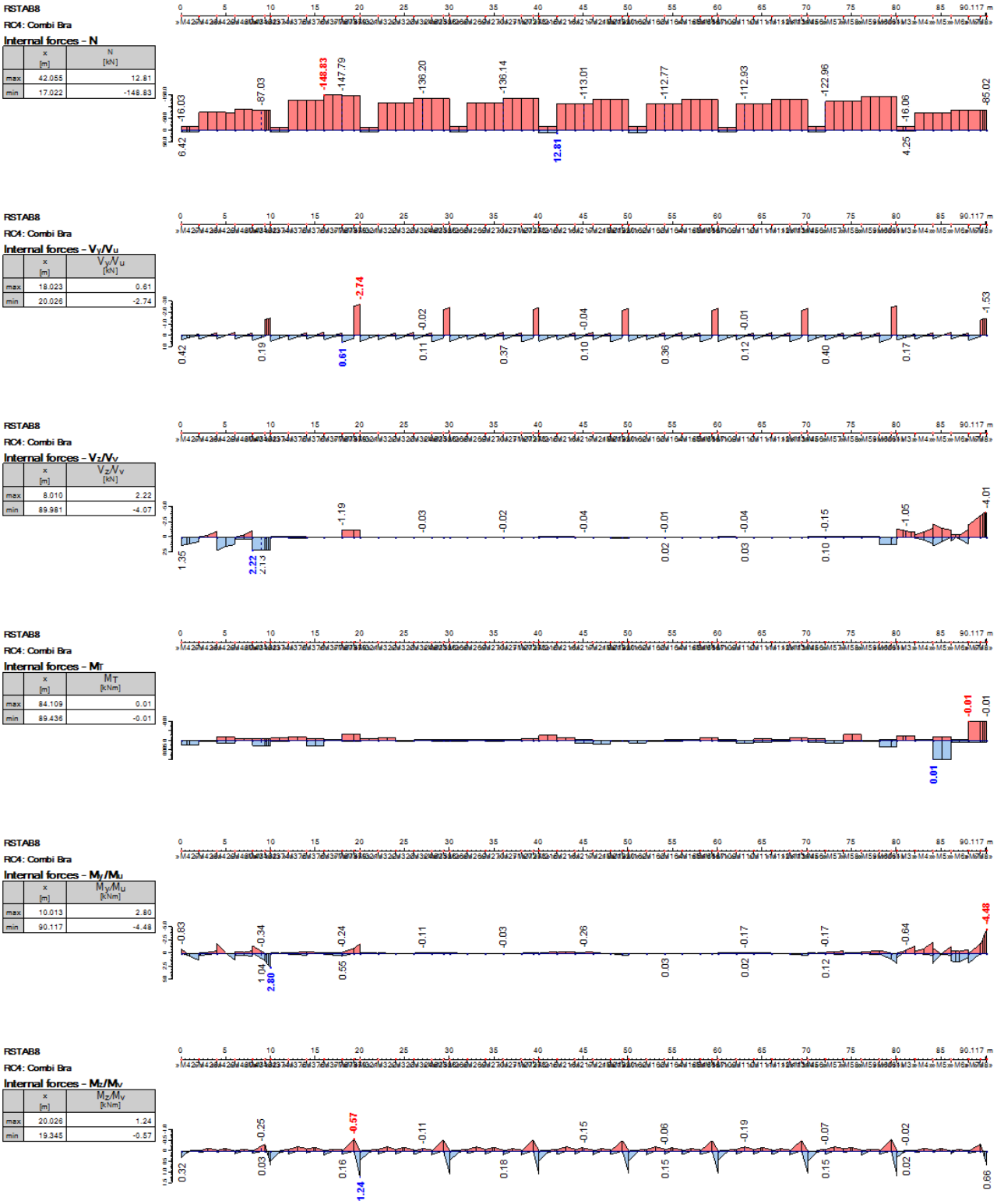

Appendix 71: Upper Left Chords Internal Forces (Brazilian) (ULS)

RSTAB8

RC4: Combi Bra

Internal forces - N

	x [m]	N [kN]
max	48.062	26.28
min	14.018	-148.82

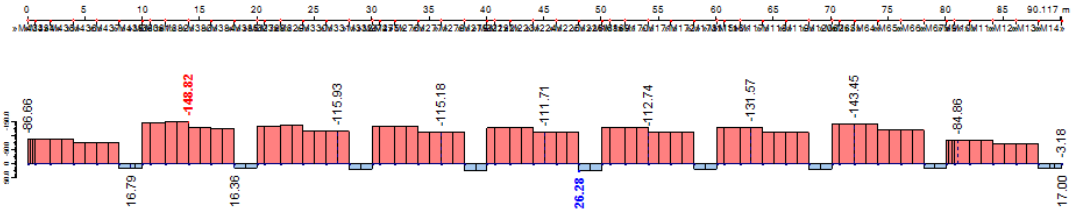

RSTAB8

RC4: Combi Bra

Internal forces - V_Y/V_U

	x [m]	V_Y/V_U [kN]
max	10.013	2.81
min	12.016	-0.60

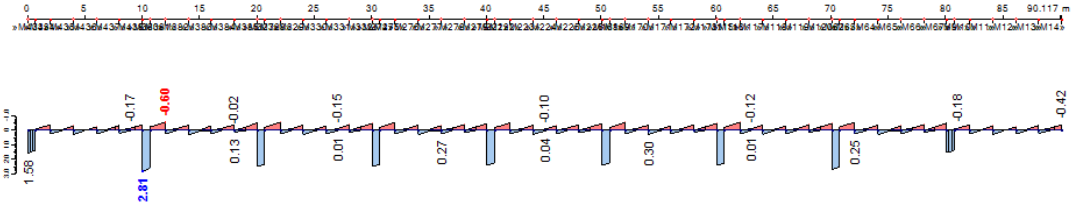

RSTAB8

RC4: Combi Bra

Internal forces - V_Z/V_V

	x [m]	V_Z/V_V [kN]
max	80.236	4.05
min	2.003	-2.04

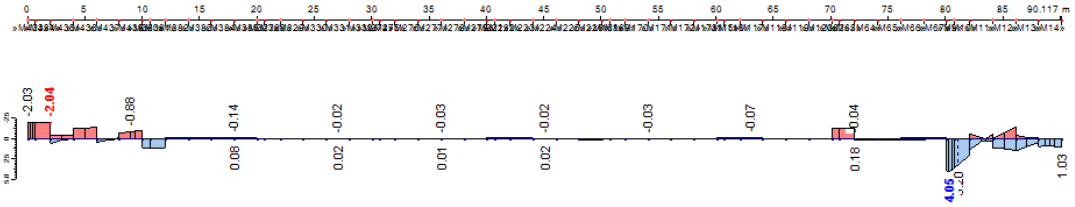

RSTAB8

RC4: Combi Bra

Internal forces - M_T

	x [m]	M_T [kNm]
max	80.104	0.01
min	85.110	-0.01

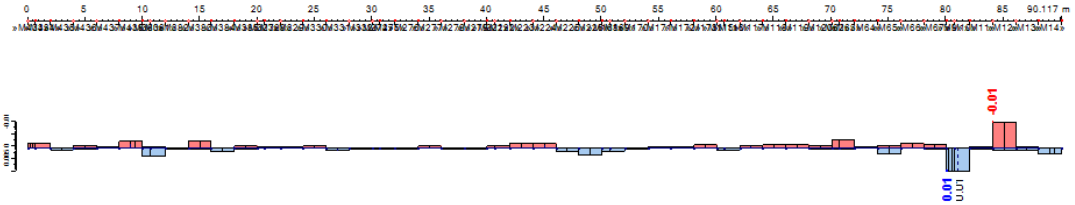

RSTAB8

RC4: Combi Bra

Internal forces - M_y/M_u

	x [m]	M_y/M_u [kNm]
max	0.000	2.80
min	80.321	-4.48

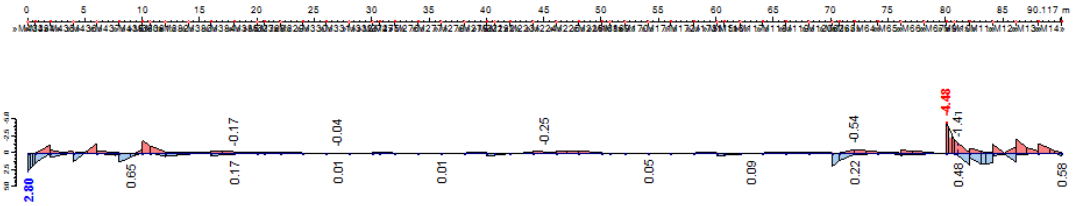

RSTAB8

RC4: Combi Bra

Internal forces - M_z/M_v

	x [m]	M_z/M_v [kNm]
max	10.013	1.24
min	10.674	-0.56

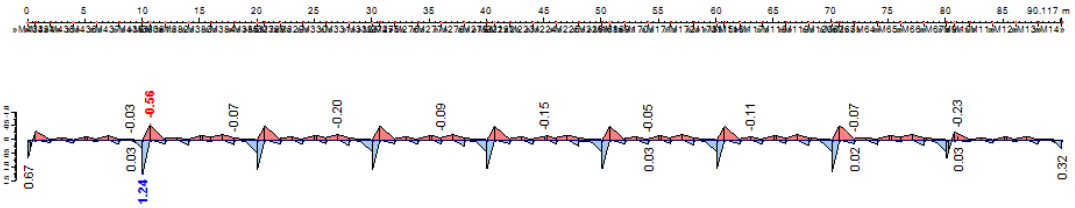

Appendix 72: Upper Right Chords Internal Forces (Brazilian) (ULS)

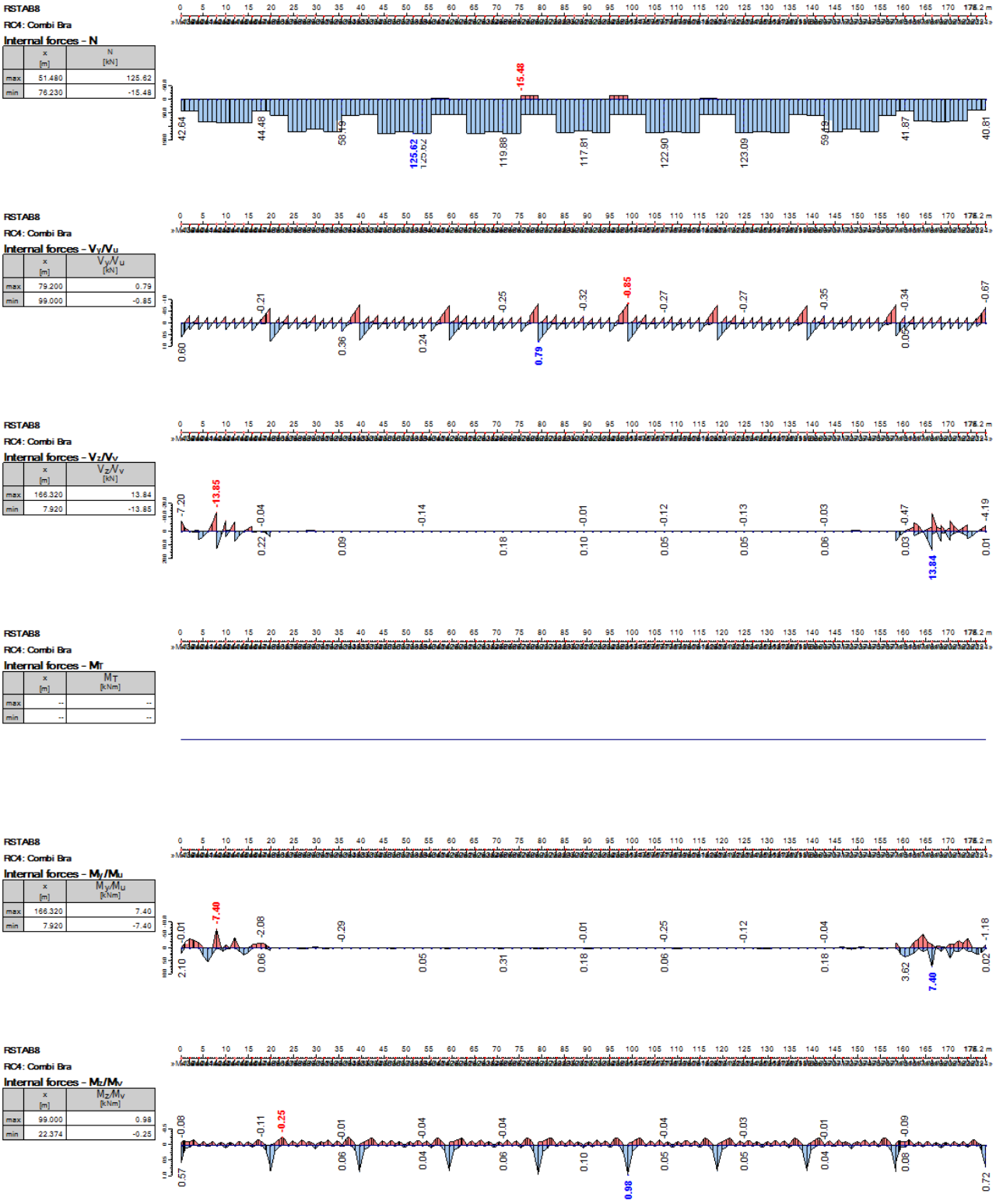

Appendix 73: Lower Chords Internal Forces (Brazilian) (ULS)

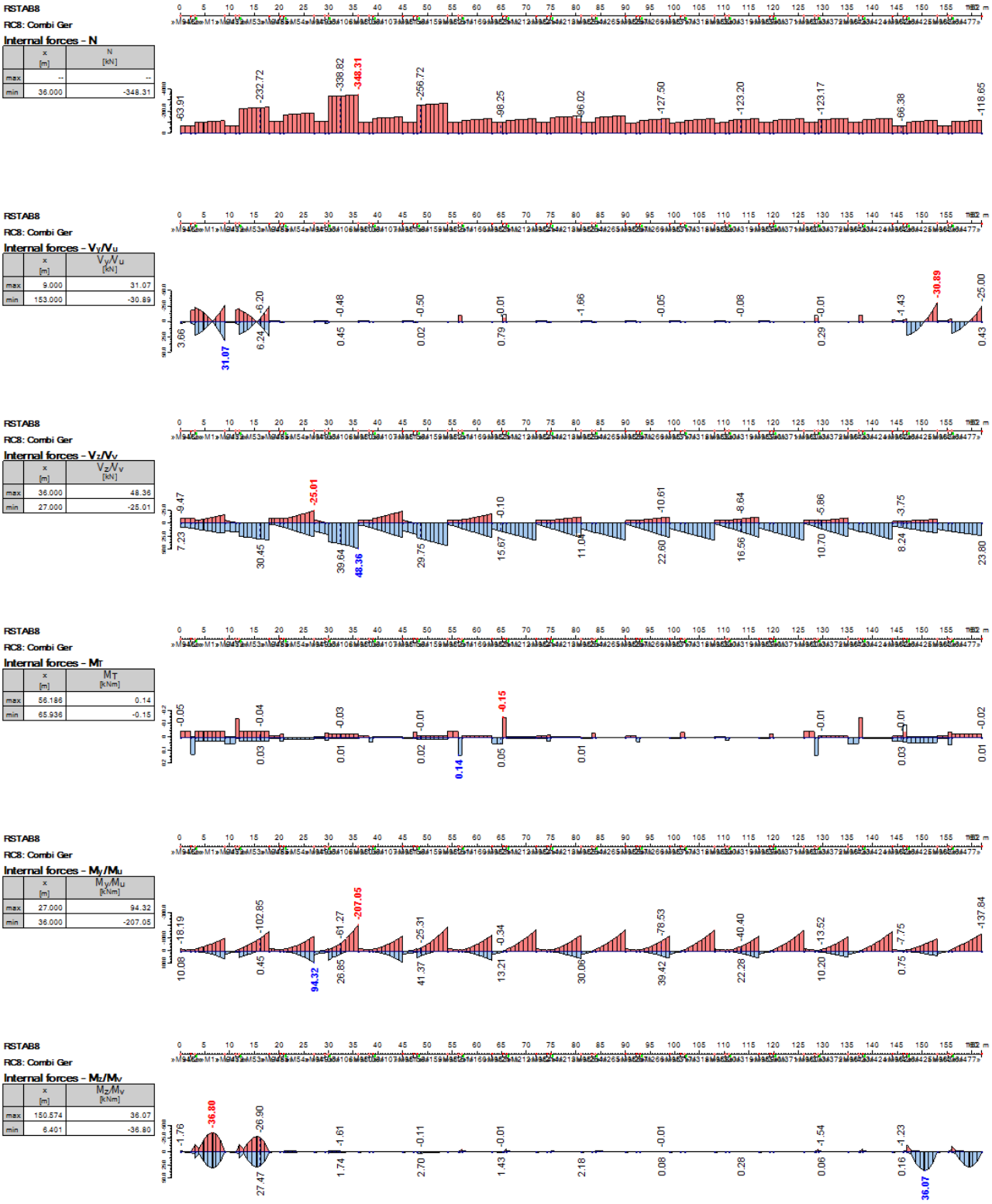

Appendix 74: Column Internal Forces (German) (ULS)

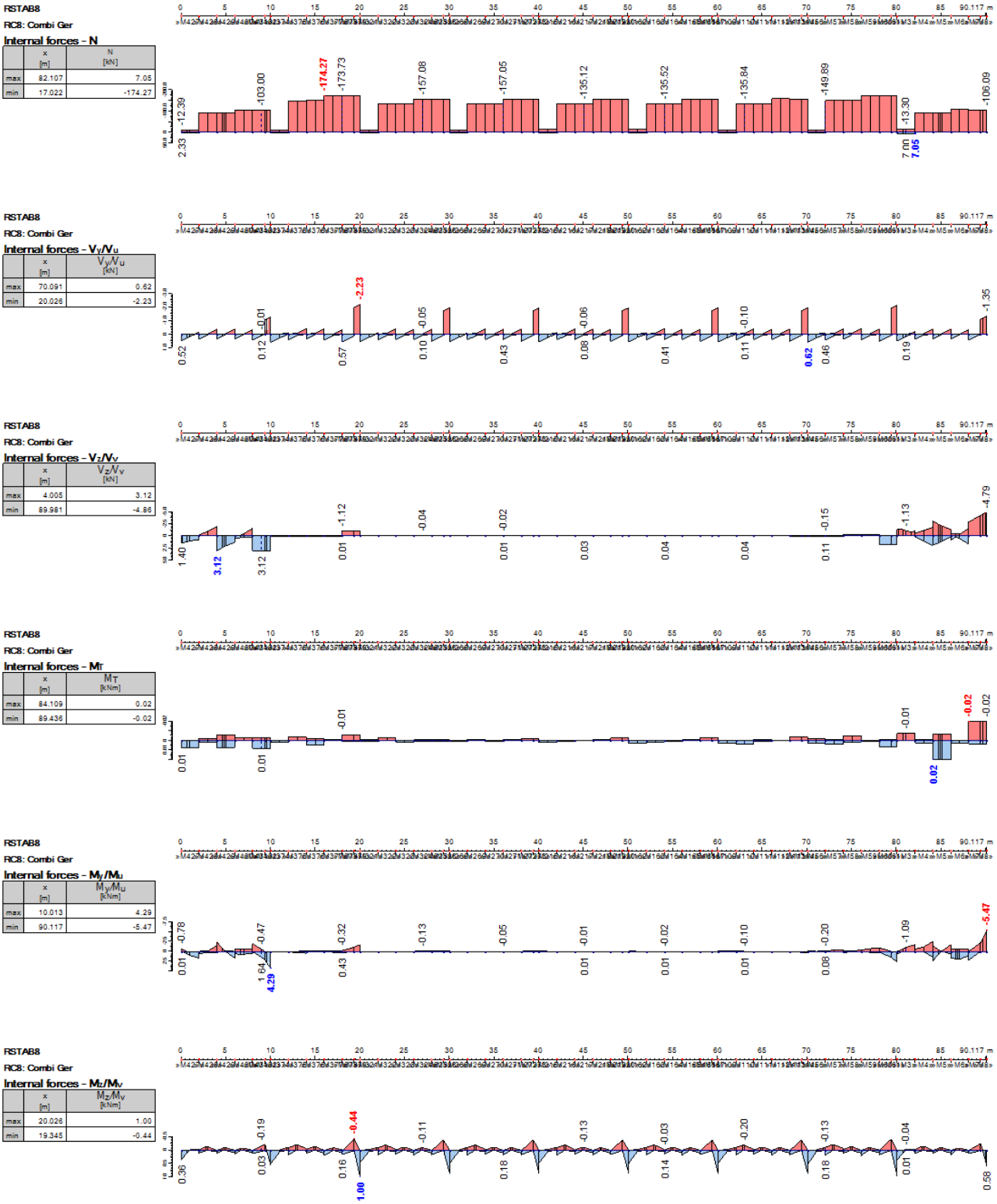

Appendix 75: Upper Left Chords Internal Forces (German) (ULS)

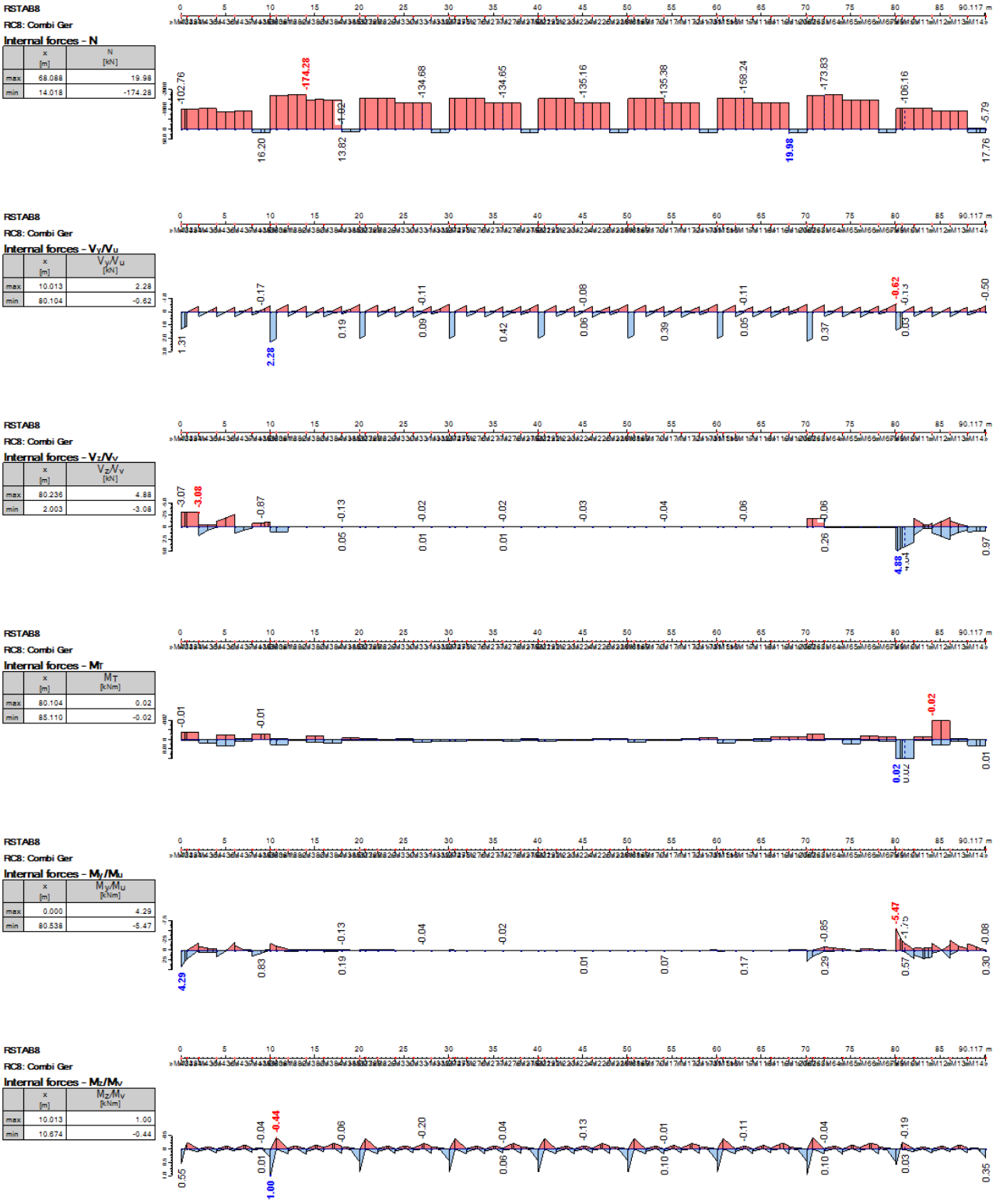

Appendix 76: Upper Right Chords Internal Forces (German) (ULS)

RSTAB8

RC8: Combi Ger

Internal forces - N

	x [m]	N [kN]
max	122.760	157.12
min	--	--

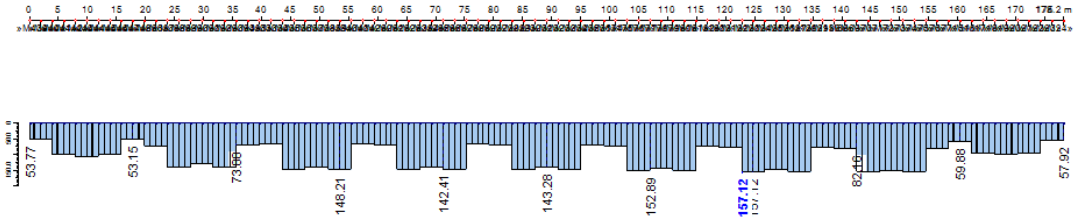

RSTAB8

RC8: Combi Ger

Internal forces - V_y/V_u

	x [m]	V_y/V_u [kN]
max	138.600	0.80
min	158.400	-0.85

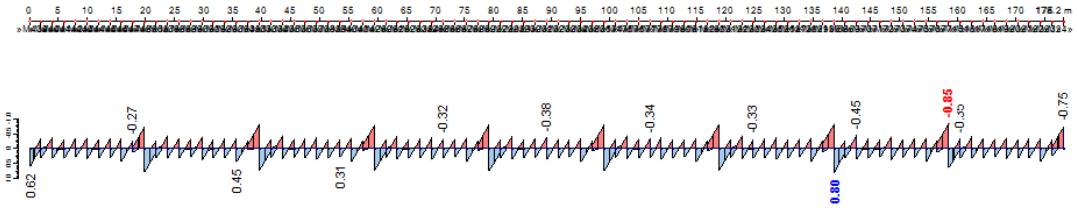

RSTAB8

RC8: Combi Ger

Internal forces - V_z/V_v

	x [m]	V_z/V_v [kN]
max	3.960	10.09
min	163.160	-9.82

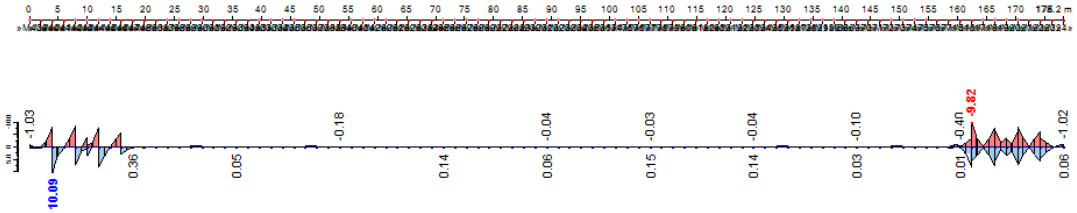

RSTAB8

RC8: Combi Ger

Internal forces - M_T

	x [m]	M_T [kNm]
max	--	--
min	--	--

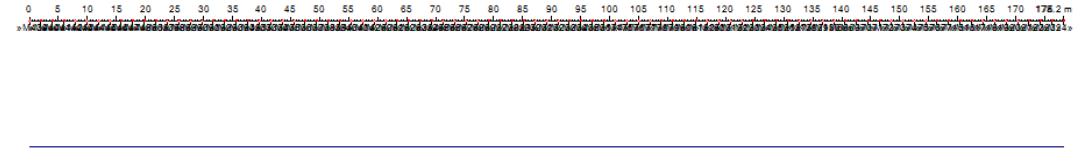

RSTAB8

RC8: Combi Ger

Internal forces - M_y/M_u

	x [m]	M_y/M_u [kNm]
max	162.360	5.21
min	3.960	-5.25

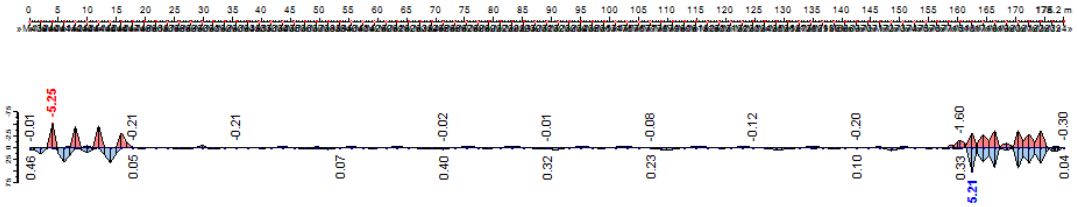

RSTAB8

RC8: Combi Ger

Internal forces - M_z/M_v

	x [m]	M_z/M_v [kNm]
max	158.400	0.87
min	155.826	-0.24

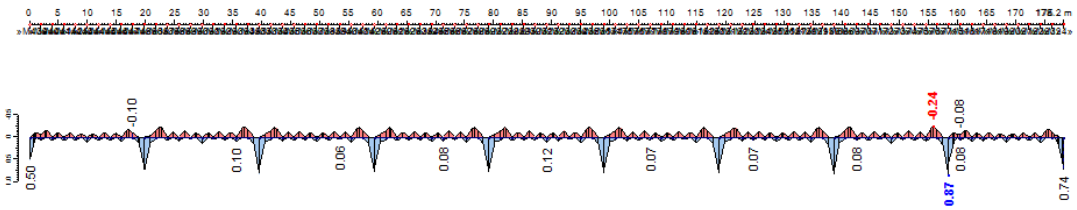

Appendix 77: Lower Chords Internal Forces (German) (ULS)